Imperial College London

STAINLESS STEEL STRUCTURES IN FIRE

A thesis submitted to the University of London for the degree of

Doctor of Philosophy

By

Kee Teong Ng

Department of Civil and Environmental Engineering
Imperial College London
London SW7 2AZ
United Kingdom

January 2007.

ABSTRACT

The initial material cost of structural stainless steel is about four times that of structural carbon steel, due largely to the expense of the alloying elements and the relatively low volume of production. Given broadly similar structural performance, additional areas of benefit need to be identified and exploited in order to establish stainless steel as a viable alternative material for construction. In addition to the familiar benefits of corrosion resistance, low maintenance, high residual value and aesthetics, one such area is fire resistance.

Material properties and their response to elevated temperatures form an essential part of structural fire design. The mechanical and thermal properties of stainless steel differ from those of carbon steel due to variation in chemical composition between the materials. A comparison of these properties for austenitic stainless steel with those for structural carbon steel is presented in this thesis, and implications of the differences explored.

A total of 23 column buckling tests, 6 stub column tests, 5 simply supported beams, 1 continuous beam and 14 temperature development tests have previously been conducted on stainless steel sections in fire. These tests have been replicated numerically using the non-linear finite element package ABAQUS. Following accurate replication of the tests, a series of parametric studies were performed to expand the range of available data.

Based on comparisons between all available test data and the current design rules in Eurocode 3: Part 1.2, together with the findings of the numerical study, a number of revisions to the code have been proposed. They include revised values for the heat transfer coefficient and emissivity, revised buckling curve, consistent strain limits and a new approach to the treatment of cross-section classification and local buckling. These revisions have led to a more accurate determination of temperature development in structural stainless steel, and provide more efficient and more consistent treatment of buckling of stainless steel structures in fire.

1

ACKNOWLEDGEMENTS

CONTENTS

CHAPTER 1 – INTRODUCTION

CHAPTER 2 – LITERATURE REVIEW

CHAPTER 3 – ELEVATED TEMPERATURE MATERIAL PROPERTIES

CHAPTER 4 – TEMPERATURE DEVELOPMENT OF STAINLESS STEEL IN FIRE

CHAPTER 5 – NUMERICAL MODELLING

CHAPTER 6 – DESIGN OF STAINLESS STEEL STRUCTURES IN FIRE

CHAPTER 7 – THERMAL EXPANSION

CHAPTER 8 – CONCLUSIONS AND RECOMMENDATIONS FOR FUTURE WORK

Notation

A_m/V	is the section factor (m^{-1})
$[A_m/V]$	is the familiar section factor
$[A_m/V]_b$	is the box value for the section factor
c_a	is the specific heat of the material
E	is the Young's modulus
f_y	is the material 0.2% proof strength
$f_{0.2p,\theta}$	it the 0.2% proof stress at elevated temperature
$f_{2\%,\theta}$	is the strength at 2% total strain at elevated temperature
$f_{u,\theta}$	is the ultimate strength at elevated temperature
$\dot{h}_{net,c}$	is the net convective heat flux (W/m^2)
$\dot{h}_{net,d}$	is the design value of the net heat flux per unit area (W/m^2 K)
$\dot{h}_{net,r}$	is the net radiative heat flux (W/m^2)
κ_1 and κ_2	are adaptation factors for non-uniform temperature around the cross-section and along the beam length, respectively
k	is the thermal conductivity (W/mK)
$k_{0.2p,\theta}$	is the elevated temperature 0.2% proof strength $f_{0.2p,\theta}$, normalised by the room temperature 0.2% proof strength f_y
$k_{2\%,\theta}$	is the elevated temperature strength at 2% total strain $f_{2\%,\theta}$, normalised by the room temperature 0.2% proof strength f_y
K_{co}	is the stiffness of the column at room temperature
K_s	is the axial stiffness of the frame

k_{sh}	is the correction factor for the shadow effect
l	is the length of the column
q	is the heat flux per unit area (W/m^2)
RHS	is the rectangular hollow section
r_i	is the internal corner radius
SHS	is the square hollow section
t	is the time (minutes) and material thickness
x	is the distance from supported end of the column
α	is the coefficient of thermal expansion and imperfection factor
α_c	is the convective heat transfer coefficient (W/m^{2}K)
α_t	is the relative stiffness (K_s/K_c)
Φ	is the configuration factor (generally taken as unity)
ρ_a	is the material density (kg/m^3)
σ	is the Stefan-Boltzmann constant (= 5.67 × 10^{-8} W/m^{2}K^4)
σ_{cr}	is the elastic critical plate buckling stress
σ_{nom}	is engineering stress
$\sigma_{0.2,v}$	is the 0.2% proof strength of the virgin material
$\dfrac{\partial T}{\partial x}$	is the temperature gradient
ε^{th}	is the thermal elongation at temperature θ
ε_m	is the emissivity of the material
ε_f	is the emissivity of the fire
ε_{nom}	is engineering strain
θ_0	is the room temperature
θ_a	is the steel temperature (°C)
θ_g	is the gas temperature in the furnace (°C)
θ_m	is the surface temperature of the member (°C)
θ_r	is the effective radiation temperature of the fire (°C)
λ_a	is the thermal conductivity of steel (W/mK)
$\bar{\lambda}_0$	is the limiting slenderness
$\bar{\lambda}_\theta$	is the non-dimensional elevated temperature member slenderness
Δl	is the temperature induced expansion
$\Delta\varepsilon_{th}$	is the total free thermal strain

9

$\Delta\varepsilon_{mec}$ is the mechanical strain under constant stress due to change in material property

w_0 is the initial imperfection amplitude

LIST OF FIGURES

LIST OF TABLES

CHAPTER 1

INTRODUCTION

1.1 BACKGROUND

Nowadays fire is considered as a serious hazard that can cause loss of lives and collapse of building structures and fire resistant design has become an integral part of structural engineering. The general cause of deaths is asphyxiation due to inhalation of smoke and gases. Occupants being trapped by collapsed structures would have exposed themselves to additional risks due to time-consuming evacuation, asphyxiation and the effect of heat. Therefore, fire safety design has to ensure public safety rather than to merely safeguard the structure itself, permitting the occupants enough time to escape from the building and to limit the spread of fire. High temperatures caused by fire can lead to the loss of strength and stability of a structure to the extent that structural collapse is possible. This study is primarily focussed on evaluating the fire resistance of stainless steel structures to ensure safe and efficient designs in fire.

Environmental issues should be considered as well, particularly for the feasibility of fires occurring in buildings storing hazardous materials, where pollutants in the smoke and the run-off of water used to fight the fire can cause disproportionate damage to the environment.

An understanding of the behaviour of structures in fire is an important part of structural engineering. Of primary importance in the design of structures for the accidental situation of fire exposure is to preserve the load bearing function of the structure and to avoid premature collapse whilst occupants evacuate and fire-fighters operate. Metallic structures are typically more vulnerable to the effects of fire than timber or reinforced concrete structures, because of the relatively rapid temperature development in the structural members, owing primarily to their high ratio of surface area to volume and the high thermal conductivity of the material. The relatively low probability of the occurrence of fire is reflected by the use of reduced partial safety factors in design.

The subject of steel structures in fire has received increasing attention in recent years. General background information related to the behaviour of steel structures at elevated temperatures and guidance on design for fire safety may be found in Wang (2002) and Buchanan (2001). Notable recent advances in understanding in this area have evolved, in particular, from observations and subsequent analyses of the full-scale Cardington fire tests (Lennon and Moore, 2003), performed in the mid-90s. The importance of structural continuity (Wang, 1997; Liu et al, 2002) and membrane action in composite floors (Bailey, 2004), for example, is now widely accepted. Stainless steel structures in fire have received less attention, principally due to the relatively limited use of stainless steel in structural engineering applications to date.

Bailey (2004) summarised the current methods for structural fire engineering. The prescriptive approach uses nominal fires to generate thermal actions. The performance-based approach, using fire safety engineering, refers to thermal actions based on physical and chemical parameters. The behaviour of the structural system under fire conditions should be considered as an integral part of structural design for engineers. Therefore, new design tools will be produced to allow the performance of the structure to be incorporated within the main design process in the near future. A qualified structural engineer should understand the philosophy behind the prescriptive approaches and have an understanding of the simplest performance-based approach of member design in fire.

Whether fire resistant design is based on a prescriptive approach or a performance based approach, or indeed whether isolated elements or complete structural assemblages are considered, accurate and efficient determination of the temperature development within a structural member upon subjection to fire is paramount. Inaccurate evaluation of temperature

development could lead to an increase in member size or an increase in the required level of fire protection.

The cost of fire protection will vary from project to project, depending on required fire resistance, the size and type of structure and so on, but for multi-storey buildings, the fire protection costs are about 20-30% of the total cost of the steel frame (Ala-Outinen and Oksanen, 1997; Wang, 1998). Although there are some cost savings to be made by reducing the level (thickness) of fire protection, total elimination of the need for fire protection has far more substantial economic incentives. These may include lower construction costs, a shorter construction period, more effective utilisation of interior space and a better working environment. For stainless steel structures, in addition to the economic incentives, exposure of the material surface has particular aesthetic appeal. Although a number of fire protection methods such as intumescent paints, exist that do not impair aesthetics, these are generally at greater expense (Parker et al, 2005).

Thermal expansion is an additional material property of interest for fire design. When a building is subjected to fire, the unexposed building parts remain relatively cool. The fire-affected part of the structure may receive significant restraint from the cooler areas surrounding it. Stainless steel exhibits greater thermal expansion than carbon steel, up to 50% more (as shown in Chapter 3). Greater thermal expansion rates could lead to excessive thermal deformation, higher member forces and may affect the overall stability of a structural frame. Restrained thermal expansion leads to greater forces in the structural member. Many researchers have investigated the effect of thermal expansion; more information can be found in Chapter 2 and Chapter 7.

The determination of the fire resistance of a structural element is a complicated process because of the many variables involved, such as the fire growth and duration, temperature development of the components, alterations in material properties, interaction between the building elements, and the influence of mechanical loads on the structural system. Thus, although the standard test method provides a reasonably simple solution to an otherwise complex problem, it is rather costly and time-consuming. With the rapid increase in computer power and technology, numerical modelling has become the most economic method to simulate the behaviour of structures in fire. The finite element (FE) modelling, ABAQUS, is able to simulate the non-linear response of structures in fire and is employed throughout this study.

The use of stainless steels in structural and architectural applications is increasing due to the materials' attractive appearance, corrosion resistance, ease of maintenance, low life cycle costs and good fire resistance, alongside improved and more widespread design guidance and enhanced product availability. Modern architectural designs to enhance the aesthetic appeal of the façade will further encourage usage of stainless steel in buildings. The biggest challenge remains to shift the prevailing mindset to recognise the merits of stainless steel rather than that of cost alone.

The mechanical and thermal properties of stainless steel differ from those of carbon steel due to variation in chemical composition between the materials. Ala-Outinen and Oksanen (1997) stated that the high levels of nickel and chromium that stainless steel contains can considerably improve the heat resistance of the material. A comparison of these properties for austenitic stainless steel with those for structural carbon steel is presented herein – the austenitic grades of stainless steel being the most widely adopted in structural applications (Gardner, 2005).

1.2 CHEMICAL COMPOSITION AND CLASSIFICATION

Stainless steel is an alloying metal containing a minimum of 10.5% chromium. Chromium is the most important alloying element which makes the steel 'stainless' and provides the stainless steel with good corrosion resistance. The other added elements are nickel and molybdenum. Nickel increases the ductility and toughness of steel. Molybdenum increases the corrosion resistance of steel and also stabilises a ferritic structure. The addition of nitrogen to stainless steel provides a consistent improvement in mechanical properties (Rohrig, 1973), increasing stainless steel yield and tensile strength.

Stainless steel grades fall into four main groups; austenitic, ferritic, martensitic and duplex. The most common grades are austenitic. Stainless steel product forms include plate, sheet, tube, cold-formed structural sections and hot-rolled structural sections. The dominant product form for stainless steel structures is cold-formed hollow sections.

Table 1.1 shows the compositions for three grades of stainless steel: EN 1.4301, EN 1.4401 and EN 1.4462.

Table 1.1: *Chemical compositions for selected stainless steel grades*

	Chemical composition (% by mass)		
	Steel Designation (Number)		
Element	1.4301 (304)	1.4401 (316)	1.4462 (2205)
Carbon (C)	≤ 0.07	≤ 0.07	≤ 0.030
Chromium (Cr)	17.00 to 19.50	16.50 to 18.50	21.00 to 23.00
Nickel (Ni)	8.00 to 10.50	10.00 to 13.00	4.50 to 6.50
Molybdenum (Mo)	-	2.00 to 2.50	2.50 to 3.50
Manganese (Mn)	≤ 2.00	≤ 2.00	≤ 2.00
Silicon (Si)	≤ 1.00	≤ 1.00	≤ 1.00
Phosphorus (P)	≤ 0.045	≤ 0.045	≤ 0.035
Sulphur (S)	≤ 0.015	≤ 0.015	≤ 0.015
Nitrogen (N)	≤ 0.11	≤ 0.11	0.10 to 0.22
Titanium (Ti)	$5 \times C$ to 0.70	$5 \times C$ to 0.70	-
Tungsten (W)	-	-	0.50 to 1.00

1.3 INTRODUCTION TO FIRE SAFETY

The general aims of fire safety in buildings are to:

- Limit the probability of death and injury to people
- Ensure the load bearing capacity of the structure to be adequate for a specified period of time under fire conditions
- Ensure the generation and spread of fire and smoke within the structure are limited
- Ensure the safety of the rescue team is taken into account

Structural designers are generally concerned with ensuring adequate load resistance for the steel members in fire. This is often achieved by preventing the members from heating up excessively and hence loosing strength and stiffness. For many common forms of construction, simplified design tables have been prepared to allow a quick and safe fire design with limited design effort.

However, there are still many more complex structural forms which require more accurate treatment, and design codes often include provisions for these methods in order not to stifle innovative design.

There are currently two basic ways for achieving fire resistance: active and passive measures. Active measures of fire protection, such as automatic detection, use of sprinklers, smoke barriers etc, can improve both life safety and property protection, as they seek to reduce the severity of a fire. Although it is quite efficient in some situations, active fire fighting systems cannot be relied upon fully because the active system could be destroyed by fire or explosion. Passive measures such as fire protection and compartmentation of the structure are to control the effects of a fire once ignition has occurred. Passive fire protection is the primary element of the overall safety strategy to minimise the consequences of a fire.

Compartmentation limits the spread of fire throughout the building. In buildings such as sports halls, shopping malls and factories, compartments are necessarily very large and certain fire protection such as detectors and sprinklers may need to be considered as part of the design concept. In principle, the designer is concerned with determining the amount of fire protection needed to satisfy the required fire resistance for each steel section. Some steel members which support compartments or boundary walls may need special consideration.

1.4 USES OF STAINLESS STEEL IN CONSTRUCTION

The aesthetic of stainless steel has led it to become one of the material preferences for architects and structural engineers. Two early examples of landmark structures that have made use of stainless steel are shown in Figure 1.1 and 1.2: the upper façade of the Chrysler building (1928-30) in New York and the Gateway Arch (1965) in St. Louis.

Figure 1.3 shows a more recent example – the Petronas Towers (1998) in Kuala Lumpur are the world's tallest twin towers. The exterior of the Petronas Twin Towers is organised in horizontal ribbons of vision glass and clad in stainless steel which glint and shimmer in the sun. The enormous height of the Petronas Twin Towers and its attractive appearance has become one of the important landmarks in Malaysia.

24

Figure 1.1: *Chrysler building, New York (1930)*
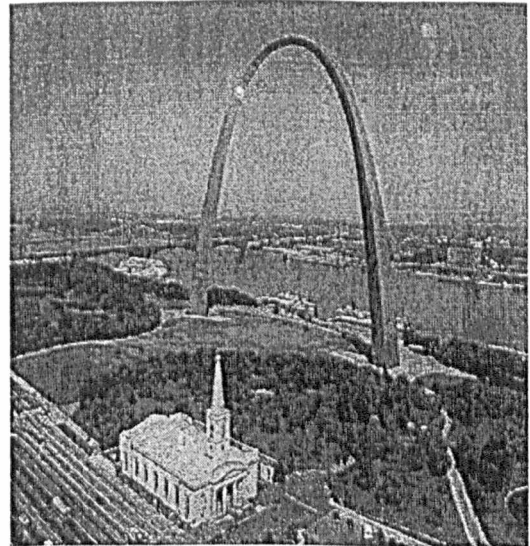
Figure 1.2: *Gateway Arch, St. Louis (1965)*
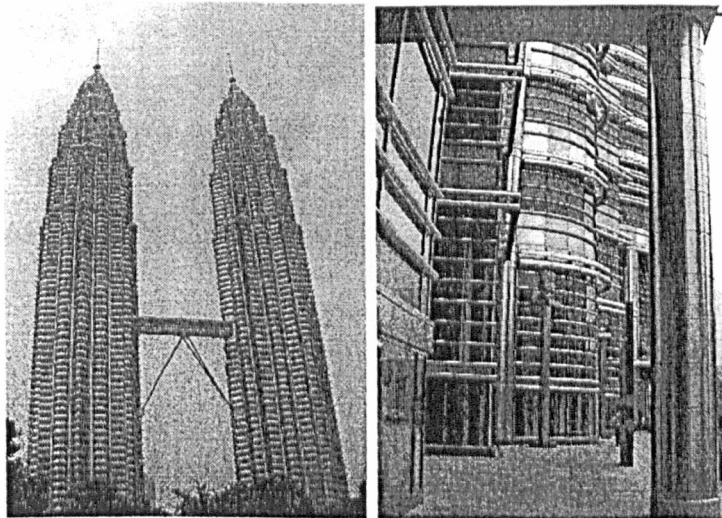
Figure 1.3: *Petronas Twin Towers, Kuala Lumpur (1998)*

1.5 SUMMARY OF HISTORICAL BUILDING FIRE STUDIES

Fire can cause serious damage to buildings and loss of lives. Two topical examples of building fires are given herein.

1.5.1 World Trade Center Towers Collapse, New York

On the 11th September 2001, two passenger planes were hijacked by terrorists and crashed into the twin towers of the World Trade Center (WTC) in New York (Figure 1.4). The impact of the plane caused significant structural damage to both WTC towers. Neither tower collapsed immediately showing that the redundancy of the tube-frame structure enabled the redistribution of the loads from damaged zones to the remaining structure. The multiple floor fires ignited by the jet fuel finally weakened the remaining structures and WTC 1 and WTC 2 collapsed 102 minutes and 56 minutes respectively after the crash.
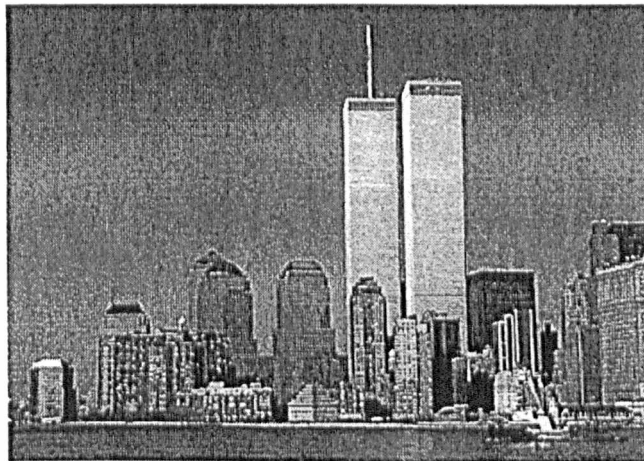
Figure 1.4: *World Trade Center, New York*

1.5.2 First Interstate Bank Fire, Los Angeles

Figure 1.5 shows a fire incident that occurred in a 62 storey office tower in Los Angeles, in 1973. The source of the fire was believed to be electrical in an open-plan office area on the 12th floor. The open-plan floors, with a floor area of over 1600 m^2 and without any internal fire barriers increased the rate of fire growth. In addition, gaps between the external cladding and the floors were not firestopped and the fire could easily spread to floors above.
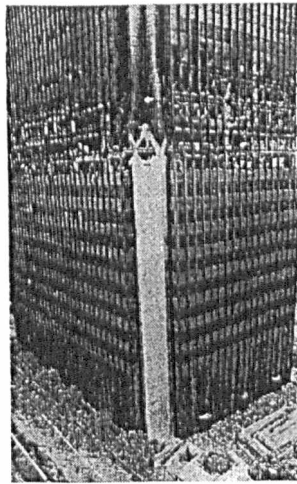
Figure 1.5: *Office tower fire in Los Angeles.*

1.6 INTRODUCTION TO THE CARDINGTON FIRE TESTS

The difference between the behaviour of isolated members and the behaviour of the entire building can have a beneficial or detrimental effect on the overall fire resistance of the building. The UK's Building Research Establishment has carried out a series of full-scale fire tests at Cardington (Figure 1.6) in the United Kingdom. A total of six compartment fire tests, two by BRE (Building Research Establishment) and four by BS (British Steel), were conducted on the frame at various locations throughout the building (Bailey, 2000). The tests have investigated the influence of compartment linings, fire load type and through draft condition on the severity of fully developed, post-flashover fires. The major aim of the tests was to provide quality data to validate and develop computer models, which enable different structural and fire scenarios to be investigated. The Cardington tests highlighted the importance of considering thermal expansion and large deflection behaviour in fire.
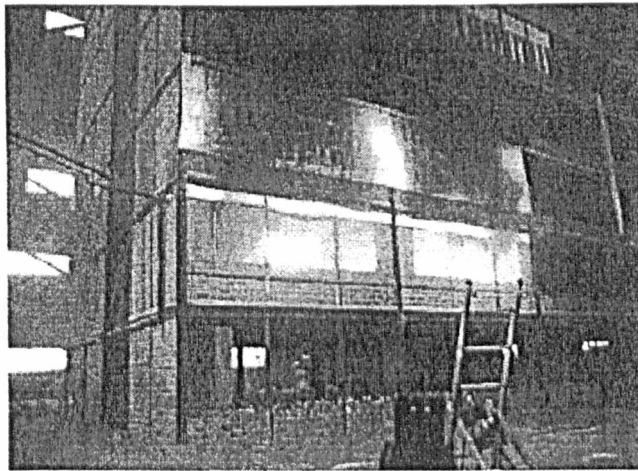
Figure 1.6: *Cardington full-scale fire titest, United Kingdom.*

1.7 OUTLINE OF THESIS

This Chapter provides a brief introduction to fire safety and to the advantages and prospects of stainless steel as a construction material with some examples of stainless steel structural applications.

A broad review of the literature that is relevant to the present research is described in Chapter 2. This subject area has been divided into specific categories to give an overview of important topics that are discussed in necessary details. Further literature is introduced and examined throughout this thesis.

A comparison of mechanical and thermal properties between stainless steel and carbon steel at elevated temperature is reported in Chapter 3. This chapter compares the Eurocode 3 reduction factors of 0.2% proof strength, strength at 2% strain and ultimate strength at elevated temperature for a range of stainless steel grades with results obtained from tests, and proposes rationalising the codified provisions.

In Chapter 4, comparisons of temperature development in structural stainless steel sections are made between existing test results, numerical simulations and the simple calculation model of Eurocode 3: Part 1.2. Based on these comparisons, revised values for the heat transfer coefficient and emissivity of structural stainless steel are proposed.

Chapter 5 presents a numerical modelling programme that was carried out in order to simulate laboratory test results. After validating the numerical models against the test results, a series of parametric studies was conducted to investigate the importance of the key parameters such as material model, initial imperfections, corner material properties and cross-section and member slenderness.

Based on the findings of Chapter 5, a revised buckling curve for stainless steel in fire, consistent strain limits and a modified approach to cross-section classification and the treatment of local buckling are proposed in Chapter 6. These revisions have led to a more efficient and more consistent treatment of buckling of stainless steel columns and beams in fire.

A numerical modelling study was also performed in Chapter 7 to investigate the behaviour of the restrained columns and beams at elevated temperature to assess the importance of the different thermal expansion properties between stainless steel and carbon steel. Parametric studies were conducted to investigate the influence of different levels of axial and rotational restraint for both materials.

Finally Chapter 8 provides a summary of the important findings from the present research project and also offers suggestions for further work.

CHAPTER 2

LITERATURE REVIEW

2.1 INTRODUCTION

This Chapter reviews the general literature that is pertinent to this thesis. More detailed examination and appraisal of previous research is contained within each individual Chapter.

2.2 INTRODUCTION TO STAINLESS STEEL DESIGN STANDARDS

A number of structural stainless steel design codes now exist, a detailed comparison of which has been prepared by Baddoo (2003). Below is a summary of the principal stainless steel design codes. Material grades are generally referred to in accordance with the European designation numbers given in EN 10088-1 (2005). In some cases, where an equivalent European grade is unknown or does not exist.

Eurocode 3 Part 1.2, (EN 1993-1-2, 2005) is the only design code covering the fire resistant design of stainless steel structures. Eurocode 3 Part 1.4 (prEN 1993-1-4, 2003) provides design guidance on several grades of austenitic stainless steel - EN 1.4301 and EN 1.4401 are the most common steel grades, as well as the low carbon grades and stabilised grades, e.g. EN 1.4541

and EN 1.4571 that are popular in some European countries. The duplex grades EN 1.4462 and EN 1.4362 are included. Other stainless steel grades can also be found in the code.

SEI/ASCE (2002), the US design code for stainless steel is confined to cold-formed cross sections, strip, plate, or flat bar stainless steel material. Four grades of austenitic stainless steels, 201, 301, 304 (EN 1.4301) and 316 (EN 1.4401), are covered. Three grades of ferritic stainless steels are included (409, 430 and 439), only in the annealed condition. The standard was extended to cover a further grade UNS S 20400, also known as Nitronic 30, which is an austenitic nitrogen strengthened grade with a 0.2% proof strength between 50 and 100% higher than grade EN 1.4301 and EN 1.4401. The SEI/ASCE Specification does not cover fire resistant design.

The AS/NZS (2001), Australia and New Zealand code covers the design of stainless steel structural members, and is also limited to cold-formed shapes from annealed or temper-rolled sheet, strip, plate or flat bar stainless steels. Mechanical properties are given for the austenitic grades EN 1.4301, EN 1.4401, EN 1.4306, EN 1.4404 and the ferritic grades 409 and 430. The code also includes the duplex alloy EN 1.4462 and the 12% chromium weldable structural steel often referred to as 3CR12 steels or EN 1.4003. The AS/NZS Specification does not cover fire resistant design but an informative appendix describes what guidance is available in ENV 1993-1-4.

In 1995, the Japanese stainless steel structural design standard was issued (SSBJA, 1995). Based largely on the Canadian design standard for carbon steel, the South African structural stainless steel code was published in 1997 (SABS, 1997).

2.3 FIRE RESISTANT DESIGN

Eurocode 3 Part 1.2 (EN 1993-1-2, 2005) is the only design standard available for fire design of stainless steel structures and will be referred to for comparison throughout this study. This section contains an introduction to Eurocode 3 Part 1.2.

2.3.1 Background

In 1975, the Commission of the European Community decided on an action programme in the field of construction. The Commission, with the help of a steering committee with representatives of member states, conducted the development of the Eurocodes programme, which led to the first generation of European codes in the 1980s.

The structural Eurocodes are being written under the guidance of CEN (European Committee for Standardisation) Technical Committee TC250 and cover the design of a wide range of structures. The structural materials covered include: steel, stainless steel, concrete, composite (steel-concrete), timber, masonry and aluminium. Part 1.2 of each of the European design codes for the different structural materials contains guidance on fire design.

2.3.2 Provisions of Eurocode 3 Part 1.2

The European pre-standard ENV 1993-1-2 (1996) was drafted in 1996. Three years later, the ECCS model code (Kruppa et al, 1999) was prepared for the ECCS Technical Committee 3 Fire safety of steel structures by European fire experts. It was recommended that the format of the design guidance for stainless steel structural members should follow the carbon steel guidelines, with appropriate changes in material properties. A number of amendments and modifications were felt to be necessary in order to develop a more realistic and economic standard. The ECCS model code was used extensively during the conversion of ENV 1993-1-2 to the full European Standard EN 1993-1-2 (2005). EN 1993-1-2 covers the design of steel structures for the accidental situation of fire exposure, including methods to determine structural resistances at elevated temperature. Supplementary requirements such as installation and maintenance of sprinkler systems, conditions on occupancy of buildings or fire compartments and the use of approved insulation and coating materials, including their maintenance are not given in the code, as they are subject to specification by the competent authority.

2.4 LABORATORY FIRE TESTING

2.4.1 Introduction

The use of stainless steel in construction is increasing, and hence there is a need for an improved understanding of its structural response. A number of fire tests on material behaviour and member behaviour have been conducted, as summarised in this section. Results from these programmes have enabled the development and publication of design guidance, and are examined in detail in this thesis.

2.4.2 Material tests

Hoke (1977) reported the mechanical properties of stainless steel at elevated temperature. The data on yield strength and ultimate tensile strength is taken from ASTM Data Series DS 5S2 (Smith, 1969) for stainless steel grades 304 (EN 1.4301), 304L (EN 1.4306), 316 (EN 1.4401), 316L (EN 1.4404), 321 (EN 1.4541) and 347 (EN 1.4550).

AISI (1979) provided tables showing typical physical and mechanical properties of eight different stainless steel grades: 410, 430, 304 (EN 1.4301), 309, 310, 316 (EN 1.4401), 321 and 347.

Zhao (2000) reported material tests of five grades of stainless steel: 1.4301, 1.4401, 1.4571, 1.4462 and 1.4403. Three types of tests were carried out:

- Room temperature tests
- Isothermal tests at elevated temperatures
- Anisothermal tests at elevated temperatures

Ala-Outinen et al (2004) reported steady state tensile tests for three cold-worked austenitic stainless steel EN 1.4318, EN 1.4571 and EN 1.4541, and two annealed austenitic stainless steel EN 1.4318 and EN 1.4571. The tests were performed by AvestaPolarit Stainless Oy.

Chen and Young (2006) conducted both steady state and transient tensile coupon tests at different temperatures ranging from approximately 20°C to 1000°C to obtain material properties of stainless steel grades EN 1.4301and EN 1.4462.

The results of all tests are examined in Chapter 3.

Cold-forming increases the strength of stainless steel due to work-hardening. Ala-Outinen (1999) reported material tests for both virgin sheet and cold-formed material for two stainless steel grades (EN 1.4301 and EN 1.4571). Steady-state tensile tests were performed up to 900°C and 950°C respectively. The cold-formed material exhibited about two times the 0.2% proof strength of the virgin sheet at room temperature. Test results (Ala-Outinen, 1996) have indicated that the degradation of strength and stiffness associated with cold-worked material is generally similar to that of annealed material. Strength enhancements associated with cold-work are retained up to about 800°C, beyond which such enhancements disappear.

In Japan, Sakumoto et al (1996) conducted material tests at elevated temperature and compared three grades of stainless steel, EN 1.4301, EN 1.4401 and SUS 304N2* with two grades of conventional carbon steel. From their tests, the tensile strengths and 0.2 % proof stresses of EN 1.4401 were found to be 20-30 N/mm^2 more than EN 1.4301 at 200°C to 800°C. This was explained by the fact that EN 1.4401 contains high levels of molybdenum; this molybdenum increases the austenite ratio at high temperatures to form carbides and thereby improves the elevated temperature mechanical properties of the material.

2.4.3 Member tests

Tests on stainless steel structural members in fire are currently relatively scarce. Table 2.1 provides a summary of the number of tests performed. These tests were reported by Ala-Outinen and Oksanen (1997), Ala-Outinen (1999), Zhao and Blanguernon (2004) and Ala-Outinen (2005) and Gardner and Baddoo (2006), and are described in detail in Chapter 5.

Structural configuration	Number of tests performed			
	RHS	CHS	I-sections	Top hat sections
Stub columns	6	-	-	-
In-plane bending	1	-	3	2
Flexural buckling - pinned	16	3	-	-
Flexural buckling - fixed	3	-	1	-
Beam-columns	6	-	-	-

2.4.4 Temperature development tests

It is important to understand the heating up behaviour of stainless steel for fire design since the evaluation of fire resistance of any structural member requires that the temperature of the member must be known first. Baddoo and Gardner (2000) reported a programme of tests that studied the heating up behaviour of stainless steel members exposed to the standard fire curve ISO 834. Fourteen specimens of different shapes and dimensions were tested and all were unprotected and exposed to fire on all sides. The results are examined in detail in Chapter 4.

2.5 NUMERICAL MODELLING

Fire testing is extremely costly and time-consuming. Numerical modelling has been successfully performed by many researchers and a carefully validated finite element model may be used to expand the pool of available structural performance data. Previous examples of the application of finite element modelling to steel structures in fire are summarised below.

Baddoo and Gardner (2000) reported a finite element study to model the 4 stainless steel column fire tests reported by Baddoo and Burgan (1998). The FE modelling software used was LUSAS, version 13.1. This is able to run non-linear analyses to model the large deformations and non-linear material behaviour of stainless steel in fire. Acceptable agreement between test

and FE model behaviour was achieved. Parametric studies were carried out with variation of load ratio, overall slenderness and cross-section classification.

Feng et al (2002) carried out a finite element modelling study using ABAQUS to model cold-formed thin-walled short carbon steel lipped-channel columns at elevated temperatures. Sensitivity studies on the mesh and initial imperfection were carried out. Three element sizes were employed in these studies: The first element size was the smaller of half lip width or 15 mm; the second element size was twice that of the first one; and the third element size was half that of the first case. The results showed that the first element size gave reasonable results, and whilst the third element size gave slightly more accurate results, with the consideration of reducing computational effort, the first element size was adopted. It was observed that varying imperfections altered the load-axial deformation and load-lateral deflection responses, though the column strength was not significantly affected.

Feng et al (2003) also extended the above study to the modelling of long columns with non-uniform temperature distributions. The FE analyses were performed under steady-state conditions for convenience. The authors developed two simplified temperature distribution profiles and used ABAQUS to simulate model columns of different lengths with different temperature distributions at different fire exposure times. This simplification of non-uniform temperature distributions made it possible to develop hand calculation methods to evaluate column strength.

Yin and Wang (2003) carried out a FE modelling study using ABAQUS to investigate the effects of a number of design factors on the lateral torsional buckling resistance of carbon steel beams with non-uniform temperature distributions. The results were then used to compare with current design methods in BS 5950 Part 8 (1990) and ENV 1993-1-2 (2001). It was found that both methods predict much lower critical temperatures than were predicted by the numerical study, and neither satisfactorily dealt with the effects of non-uniform temperature distributions. The numerical studies showed that to enable both methods to be used, the slenderness of a steel beam must be modified to consider the effects of non-uniform temperature distributions on the elastic critical buckling resistance and on the effective cross-sectional shape of the steel beam.

The above studies have demonstrated the ability of finite element modelling to be applied to the non-linear response of structural elements in fire in a range of loading configurations. Numerical modelling is employed in Chapters 4, 5 and 7 of this thesis to study temperature

development, structural behaviour and the influence of thermal expansion in stainless steel structures.

2.6 THERMAL EXPANSION

Stainless steel expands to a greater extent, up to 50 % more, than carbon steel. Restrained thermal expansion leads to greater forces in structural members. Thus for fire safety design using stainless steel, thermal expansion should be sufficiently taken into account. Currently there are no experiments on stainless steel frames in order to investigate directly the effect of thermal expansion. Therefore numerical modelling has been used to simulate the behaviour of continuous structures at elevated temperature, as described in Chapter 7.

2.6.1 Axial restraint in columns

The level of axial restraint in a steel column will affect its critical temperature. Cabrita Neves et al. (2002) stated that the critical temperature of steel columns under axial compression with thermal restraint is lower than the critical temperature of the same columns free to elongate.

Valente and Cabrita Neves (1999) analysed the influence of the axial elongation and rotation restraints on the critical temperature of columns. Parametric studies on load eccentricity, column slenderness, axial and rotational restraint imposed by the structure have been carried out to cover the great majority of situations to be found in practice. The results showed that axial restraint decreases the critical temperature while rotational restraint increases it. The Eurocode approach was found to be acceptable only for less slender columns with fixed ends and no axial restraint, and also in the cases where the frame provides high rotational restraint to the ends of the column. When the axial restraint is high and the rotational restraint is low, the actual critical temperature of steel columns can be much lower than the critical temperature calculated according to the current design method.

Cabrita Neves et al (2002) carried out further numerical analyses to calculate the critical temperature of several steel columns with pinned ends, fixed ends, free to expand and with restrained thermal elongation and different load ratios. Based on the results, a proposal was made to correct the value of the critical temperature of axially loaded steel columns free to

elongate, in order to take into account the restraint effect of the structure to which they belong in a practical situation.

A total of 168 tests on pin-ended bars were performed by Correia Rodrigues et al. (2000). Four different slenderness values, two eccentricities and six levels of axial restraint were considered. The test results and the results of finite element simulations showed that neglecting the effect of thermal axial restraint may result in overestimation of the fire resistance of columns. It was further stated that the restraint to thermal elongation of centrally compressed elements having slenderness higher than 80, can lead to reductions in their critical temperature by up to 200°C. If the loading is eccentric and the eccentricity is high, the restraint to the elongation does not cause such significant variation in the critical temperature. The authors remarked that load transfer from the heated column to the cold surrounding elements can be accepted as long as these elements are capable of supporting it without producing the collapse of the structure; this behaviour was observed at Cardington, when one heated column squashed but no global structural collapse occurred.

Ali and O'Connor (2001) carried out a parametric experimental investigation on the performance of rotationally restrained steel columns in fire. The paper presented a method of estimating the effective length of a fixed end column tested under fire. It was observed that the addition of rotational restraint had a relatively minor effect on the level of generated restraint forces but failure temperatures were greatly increased under the same load.

Wang and Davies (2003) performed two series of fire tests on non-sway loaded steel columns, rotationally restrained by two loaded steel beams, subjected to fire. The objectives were to evaluate how bending moments in restrained columns would change and how these changes might affect the column failure temperatures. It was found that for columns with high initial bending moments, the direction of bending moments change near failure whilst those with low initial bending moments change direction at a much earlier stage. The column failure temperatures were mainly dependent on the total applied load, with some influence from the type of connection and the level of unbalanced loads in the restraining beams.

2.6.2 Restrained beams

In general, a steel beam exposed to a local fire in the interior of a multi-bay floor will be subjected to higher axial forces due to the high degree of axial restraint provided by neighbouring members than for the same beam near the edge of the floor. Different axial restraining conditions may induce significantly different design actions due to thermal restraint. These axial forces generated in the steel beams in fire due to the end restraining actions by adjacent members could be so significant that buckling failure may occur. The current design approach of using the plastic bending moment resistance or lateral torsional buckling bending resistance of the beam at small deflections will have a relatively low critical temperature and would require fire protection. However, catenary action that occurs at large deflections will allow the beam to achieve higher load carrying resistance.

Tests on restrained steel beams in fire performed by Liu et al (2002), and subsequently modelled by Yin and Wang (2003), are replicated numerically in Chapter 7 of this thesis. The relative performance of restrained carbon steel and stainless steel beams is examined.

2.6.3 Frames

Wang and Moore (1995) presented a finite element modelling to study of the structural behaviour of steel frames at elevated temperature. The results showed that the behaviour of an individual member in fire is different from that of the same member active as part of a frame. The authors suggested that the fire resistance of unprotected steel members can be improved by placing the concrete floor within the depth of the beam and reducing the area of the steel section exposed to fire.

Wang et al (1994) described a comprehensive parametric study to investigate various aspects of steel frame behaviour under fire conditions. It was noted that if a column is designed to reach its limiting temperature in fire, the fire safety design of a connected beam may be performed by assuming pinned support from the column and that if the additional axial load generated in the column due to the change in length from thermal expansion may be expressed as:

$$\Delta P = \left(\frac{\alpha_t}{1+\alpha_t}\right) K_{co} \left(\Delta \varepsilon_{th} - \Delta \varepsilon_{mec}\right) L \qquad (2.1)$$

where α_t is the relative stiffness (K_s/K_{co}), K_{co} is the axial stiffness of the column and K_s is the axial stiffness of the frame. $\Delta\varepsilon_{th}$ is the total free thermal strain and $\Delta\varepsilon_{mec}$ is the mechanical strain under constant stress due to change in material property. L is the length of the column.

2.7 DISCUSSION

This chapter has provided an overview of the subjects that are investigated within this thesis. The review has shown that numerous studies on stainless steel material behaviour at elevated temperature have been carried out and a number of temperature development tests and member tests have been conducted. All of the temperature development tests are simulated numerically in Chapter 4 and the majority of the member tests in Chapter 5. Following validation of the numerical models, a range of sensitivity and parametric studies are presented.

All test results, together with insight acquired from the numerical study are employed in Chapter 6 to propose modified design rules for stainless steel structural components in fire.

On the basis of previous experimental (Rodrigues et al, 2000; Wang and Davies, 2003 and Liu et al, 2002) and numerical studies (Valente and Cabrita Neves, 1999; Correia Rodrigues et al, 2000; Neves et al, 2002; Franssen, 2000; Wong, 2005 and Yin and Wang, 2004) of restrained carbon steel elements in fire, numerical studies of the response of restrained stainless steel elements in fire are performed in Chapter 7.

CHAPTER 3

ELEVATED TEMPERATURE MATERIAL PROPERTIES

3.1 INTRODUCTION

Material properties and their response to elevated temperatures form an essential part of structural fire design. Of primary importance is the stress-strain characteristics, but other properties including thermal expansion, thermal conductivity and specific heat are also important. The four principal families of stainless steel are austenitic, ferritic, martensitic and duplex. It is the austenitic grades (such as 1.4301 and 1.4401) that are the most commonly adopted in structures. This chapter focuses primarily on austenitic stainless steel material properties at elevated temperature, and makes comparisons between Eurocode 3 Part 1.2 and all available laboratory test data.

3.2 ROOM TEMPERATURE PROPERTIES

Figure 3.1 compares representative stress-strain curves for stainless steel and carbon steel at room temperature. Carbon steel exhibits initially linear elastic material behaviour, with a sharply defined yield point, followed by a plastic yield plateau. For stainless steel, though, there

is rounded stress-strain behaviour, no sharply defined yield point and substantial strain hardening is possible. For materials such as stainless steel that do not exhibit a definite yield point, the yield stress is generally approximated by a proof stress. This is a stress that causes a specified small, permanent extension of the material. Commonly the stress to produce 0.2% plastic strain is employed. Since fire design allows the use of a higher strain limit (2%), the high degree of strain hardening that stainless steel displays is beneficial. Fire design allows use of the 2% strain limit since deformation under fire conditions is less of a concern.
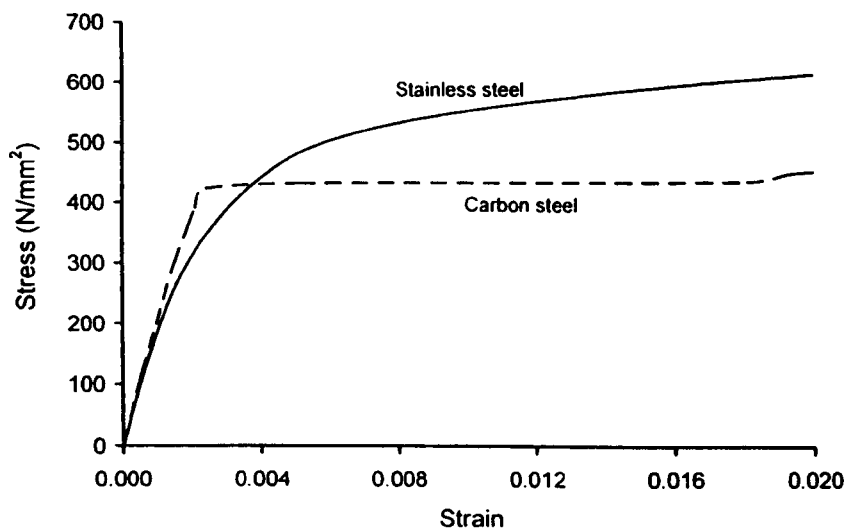
Figure 3.1: *Stress-strain curve of stainless steel and carbon steel at room temperature*

Table 3.1 compares the yield strength f_y and ultimate strength f_u of common grades of austenitic stainless steel and carbon steel; values are taken from Eurocode 3. The table shows that the common grades of carbon steel possess higher yield strength f_y than those of austenitic stainless steel though the ultimate strengths of the stainless steel grades are higher.

Table 3.1: *The nominal values of the yield strength f_y and the ultimate tensile strength f_u for common grades of stainless steel and carbon steel.*

Type of steel	Grade	f_y (N/mm^2)	f_u (N/mm^2)
Austenitic Stainless Steel	1.4301	230	540
	1.4401	240	530
Carbon Steel	S 235	235	360
	S 275	275	430
	S 355	355	510

3.3 MATERIAL PROPERTIES AT ELEVATED TEMPERATURE

3.3.1 Comparison of Eurocode 3 properties for stainless steel and carbon steel

The ability of a material to retain strength and stiffness at elevated temperature is paramount for achieving fire resistant structures. At elevated temperatures, stainless steel offers better retention of strength and stiffness than carbon steel, due to the beneficial effects of the alloying elements. A comparison of the elevated temperature performance of stainless steel and structural carbon steel is presented in Figure 3.2 and 3.3; the data are given in EN 1993-1-2 (2005) and the Euro Inox/SCI Design Manual for Structural Stainless Steel (2002). Neither the US nor the Australia/New Zealand structural stainless steel design standards, which are amongst the most sophisticated, currently cover fire design. The strength reduction factors shown in Figure 3.2 are for grade 1.4301 (304) austenitic stainless steel (EN 10088-1, 2005), the most widely adopted grade for structural applications, whereas the stiffness reduction factors are common to all grades (austenitic, ferritic and duplex) included in the design guidance. The strength reduction factor $k_{y,\theta}$ is defined as the elevated temperature strength at 2% total strain $f_{2\%,\theta}$, normalised by the room temperature 0.2% proof strength $f_{0.2\%}$. The stiffness reduction factor $k_{E,\theta}$ is defined as the elevated temperature initial tangent modulus normalised by that at room temperature E. It should be noted that the minimum specified room temperature 0.2% proof strength for the most common structural grades of austenitic stainless steel typically ranges between 210 and 240 N/mm^2, whilst Young's modulus is 200000 N/mm^2 (EN 10088-2, 2005).

The comparison demonstrates that carbon steel and stainless steel display distinctly different behaviour at elevated temperature. From Figure 3.2, it can be seen that carbon steel retains its full (room temperature) strength up to about 450°C whereupon it drops rapidly to only about 10% of its room temperature strength at 800°C. At low temperatures, stainless steel has a reduction factor of greater than unity due to use of the 2% strain limit at elevated temperatures and the substantial strain hardening that stainless steel exhibits. By 200°C stainless steel retains around 90% of its room temperature strength, falling to around 75% at 500°C. The curves show that above 500°C which is the important temperature region for structural fire design, stainless steel has better retention of strength than carbon steel. For a fire resistance of 30 minutes, material will be exposed to temperatures in excess of 700°C, following the standard fire curve of ISO 834-1 (1999) and EN 1991-1-2 (2002).
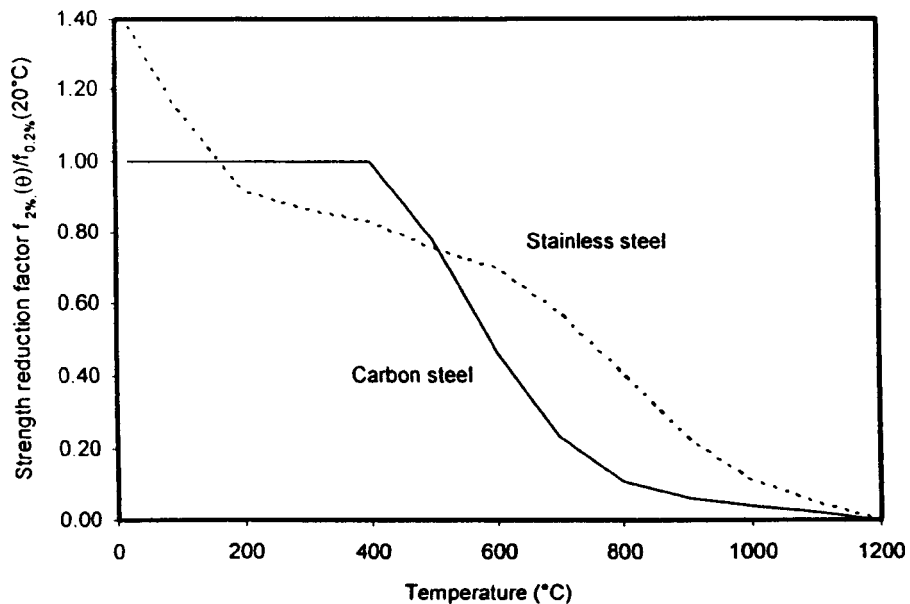
Figure 3.2: *Comparison of 2% strength reduction factors at elevated temperature for stainless steel and carbon steel*

Figure 3.3 compares the elevated temperature stiffness retention of stainless steel and carbon steel. For stainless steel, the stiffness reduces approximately linearly with temperature up to 700C, at which point it retains 70% of its room temperature stiffness before falling away more rapidly at higher temperatures. The elevated temperatures stiffness of carbon steel degrades far more significantly, reducing to only 13% of its room temperature value at 700°C. Both converge to zero stiffness at 1200°C.
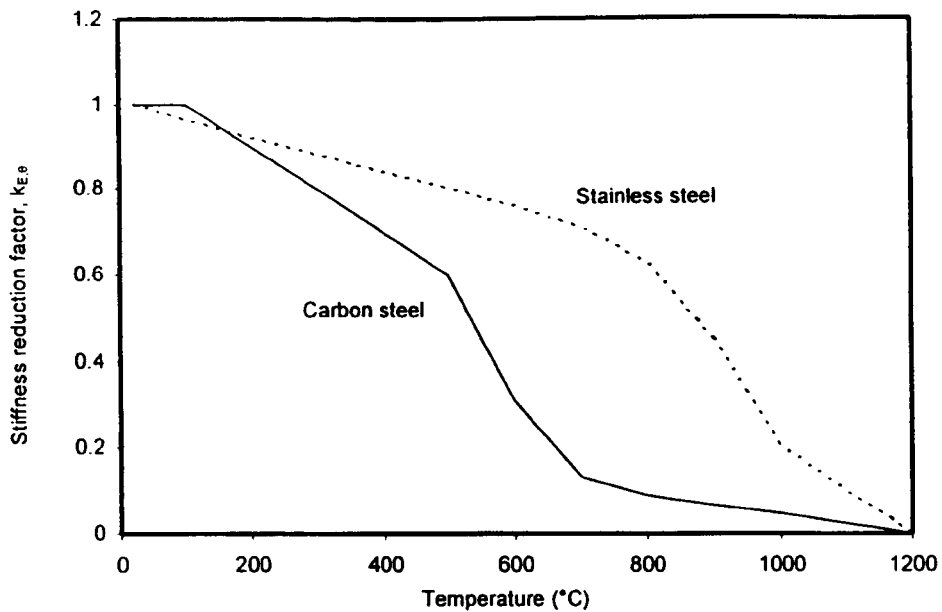
Figure 3.3: *Variation of Young's Modulus with temperature for stainless steel and carbon steel*

The key differences between stainless steel and carbon steel material behaviour at elevated temperature may be summarised as follows:

- Allowance of a higher (2%) strain limit at Fire Limit State is advantageous to stainless steel (see Figure 3.1)

- Stainless steel has better stiffness retention than carbon steel at elevated temperatures (up to 5 times more at around 700°C).

- Stainless steel has better strength retention above 500°C (up to 2 times more than carbon steel)

3.3.1.1 Thermal expansion

All metals expand when heated. Typically during component tests in fire, structural members will be free to expand against the applied load, and thus no additional load is induced due to this expansion. However, in structural frames, where continuity exists between members and often fire is relatively localised, thermal expansion may be restrained by other (stiffer) parts of the

45

structure, resulting in additional member loading. Further consequences of thermal expansion may include higher axial and lateral member deformations and increased member forces and moments due to second-order effects. Further details are given in Chapter 7 and Figure 7.1 compares the thermal expansion of carbon steel and stainless steel.

3.3.1.2 Specific heat

Specific heat (or specific heat capacity) is the amount of heat per unit mass of a material required to raise the temperature by 1 °C, and is clearly an important property in controlling the temperature development in a structural member. Figure 3.4 compares the specific heat of stainless steel and carbon steel at varying temperatures. The figure shows that the specific heat of stainless steel increases steadily with temperature and shows no marked discontinuities (due to the absence of any phase change). The specific heat C_a (J/kg K) of stainless steel may be determined from Equation (3.1) from Eurocode 3: Part 1.2 (2005), where θ_a is the steel temperature (°C).

$$C_a = 450 + 0.280 \times \theta_a - 2.91 \times 10^{-4}\theta_a^2 + 1.34 \times 10^{-7}\theta_a^3 \quad \text{(J/kgK)} \tag{3.1}$$

The specific heat of carbon steel is, on average, slightly higher than stainless steel, and shows the latent heat of a phase change in the region on 723°C. On average, the specific heat of carbon steel is approximately 600 J/kg K, as compared with approximately 550 J/kg K for stainless steel. The higher the specific heat of a material, the more slowly it tends to heat up.
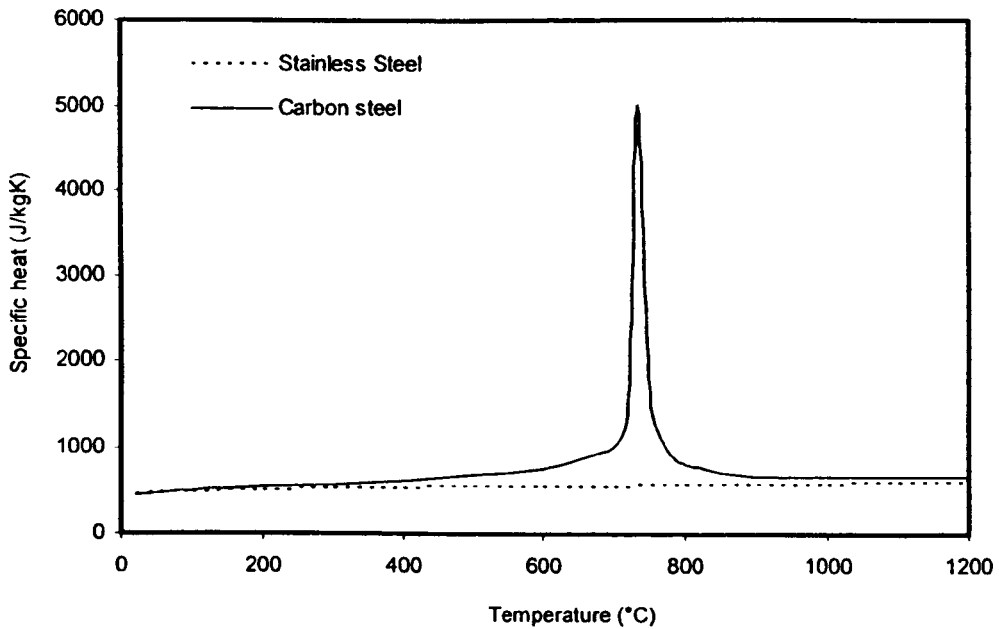
Figure 3.4: *Specific heat of stainless steel and carbon steel as a function of temperature*

3.3.1.3 Thermal conductivity

The variation of thermal conductivity with temperature is distinctly different for stainless steel as compared with carbon steel, as illustrated in Figure 3.5. The thermal conductivity of stainless steel from Eurocode 3: Part 1.2 is defined by the following equation:

$$\lambda_a = 14.6 + 1.27 \times 10^{-2} \theta_a \ (W/mK) \tag{3.2}$$

where θ_a is the steel temperature (°C)

The thermal conductivity of carbon steel is about 53 W/m K at room temperature and reduces steadily with temperature to a value of 27 W/m K by approximately 800°C. In this temperature region (723°C) a phase transformation occurs and the thermal conductivity subsequently remains constant. Stainless steel displays the opposite tendency, with increasing thermal conductivity with time. The relationship is continuous with temperature since no phase transformation occurs in austenitic stainless steel upon heating, increasing from about 15 W/m K at room temperature to a value of about 30 W/m K at 1200°C. For carbon steel, the equation to determine its specific heat can be found in Eurocode 3: Part 1.2.

For temperatures below about 1000°C, the thermal conductivity of stainless steel is lower than that of carbon steel; at low temperatures the difference is significant, whilst above about 700°C, the difference is small. The effect of lower thermal conductivity will be to cause more localised temperature development in a steel frame, though it is not believed that the differences in thermal conductivity between stainless steel and carbon steel has any significant influence on the general fire performance of a structure.
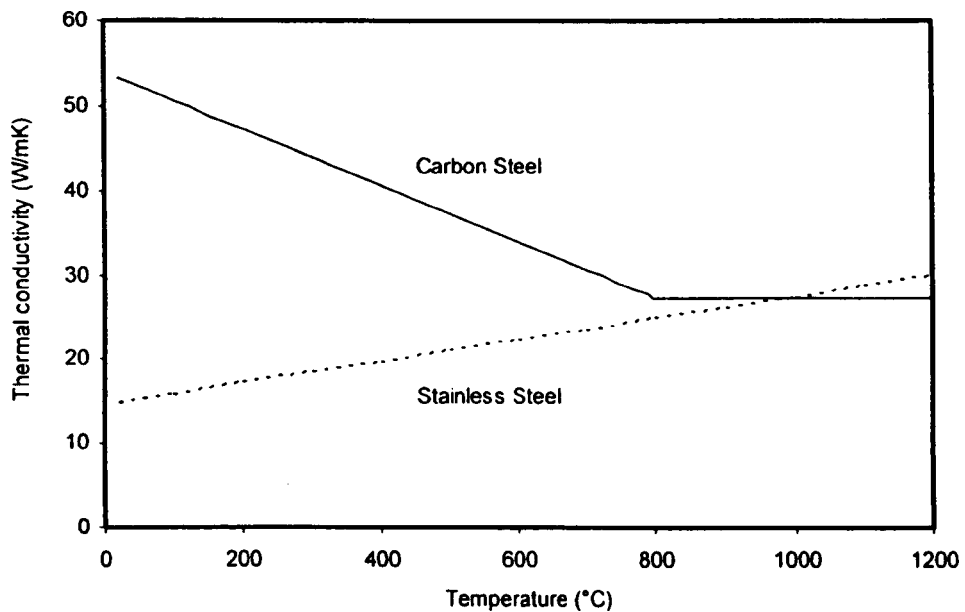
Figure 3.5: *Thermal conductivity of stainless steel and carbon steel as a function of temperature*

3.4 MATERIAL TESTS AT ELEVATED TEMPERATURE

Two distinct types of elevated temperature material test may be employed:

- Isothermal tests
- Anisothermal tests

3.4.1 Testing techniques

3.4.1.1 Isothermal tests

Isothermal tests, also known as steady state tests, describe the procedure whereby a test specimen is heated up to a particular test temperature θ_{test} and then a tensile test is conducted until the failure stress σ_u is reached. Figure 3.6 illustrates the isothermal test procedure diagrammatically.
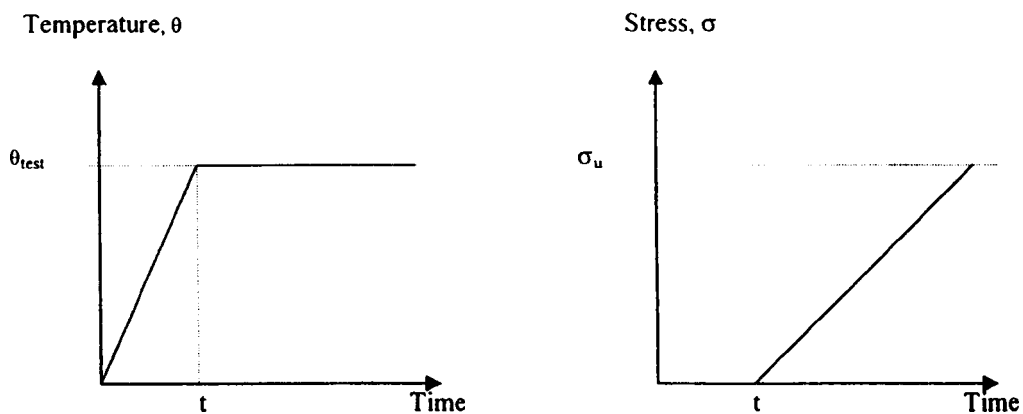
Figure 3.6: *Temperature and applied load varied in time in isothermal tests*

3.4.1.2 Anisothermal tests

Anisothermal tests, also known as transient state tests, describe the procedure whereby a test specimen is firstly loaded to a particular stress level σ_{test}, then subjected to an increasing temperature until the failure temperature θ_u is reached. This type of test is more representative of a real fire situation, but the data is less amenable to incorporation into numerical models. Figure 3.7 illustrates the anisothermal test procedure diagrammatically.
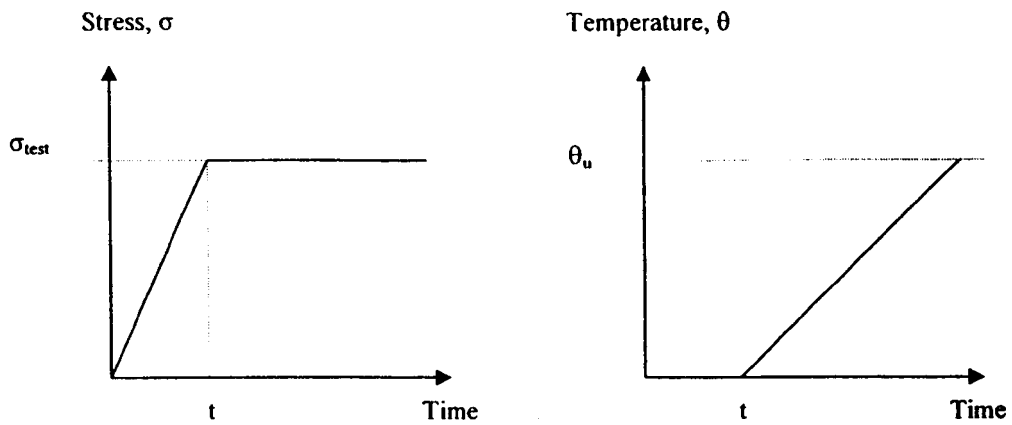
Figure 3.7: *Temperature and applied load varied in time in anisothermal tests*

3.5 COMPARISON OF EUROCODE 3 STAINLESS STEEL PROPERTIES WITH TESTS

This section compares all available material test results on the two most widely adopted grades of stainless steel for structural applications (EN 1.4301 and EN 1.4401), with the codified values of Eurocode 3. More grades are presented in Section 3.6.

The following properties are examined:

- Elevated temperature 0.2% proof stress $f_{0.2p,\theta}$

- Elevated temperature strength at 2% total strain $f_{2\%,\theta}$

- Elevated temperature ultimate strength $f_{u,\theta}$

- Elevated temperature Young's modulus $E(\theta)$

- Thermal elongation

3.5.1 Strength at 0.2% proof stress $f_{0.2p,\theta}$

Figure 3.8 compares the 0.2% proof strength reduction factor of stainless steel grade EN 1.4301 of Eurocode 3 with tests at elevated temperature. Test results were obtained from AISI (1979),

Ala-Outinen and Oksanen (1997), Hoke (1977), Zhao (2000) and Chen and Young (2006). The comparison shows good average agreement between Eurocode 3 and test results, but there is a relatively high degree of scatter.
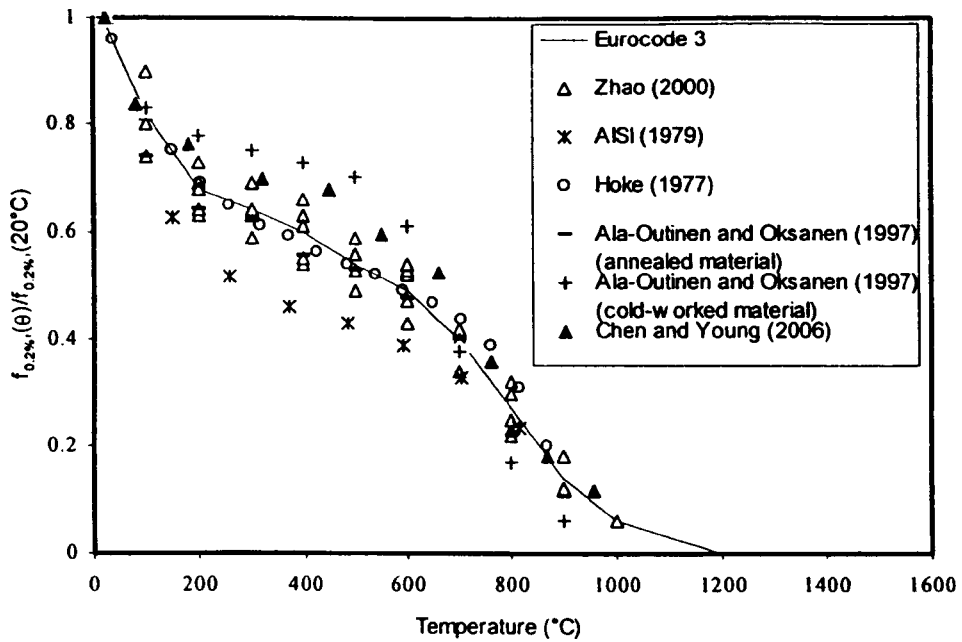
Figure 3.8: *0.2% proof strength of stainless steel grade EN 1.4301 at elevated temperature*

Figure 3.9 compares test results for 0.2% proof strength reduction factors of stainless steel grade EN 1.4401 at elevated temperature with Eurocode 3. Test results were obtained from Zhao (2000), AISI (1979) and Hoke (1977). As for grade EN 1.4301, there is good average agreement between test results and Eurocode 3, but there is still a relatively high degree of scatter.
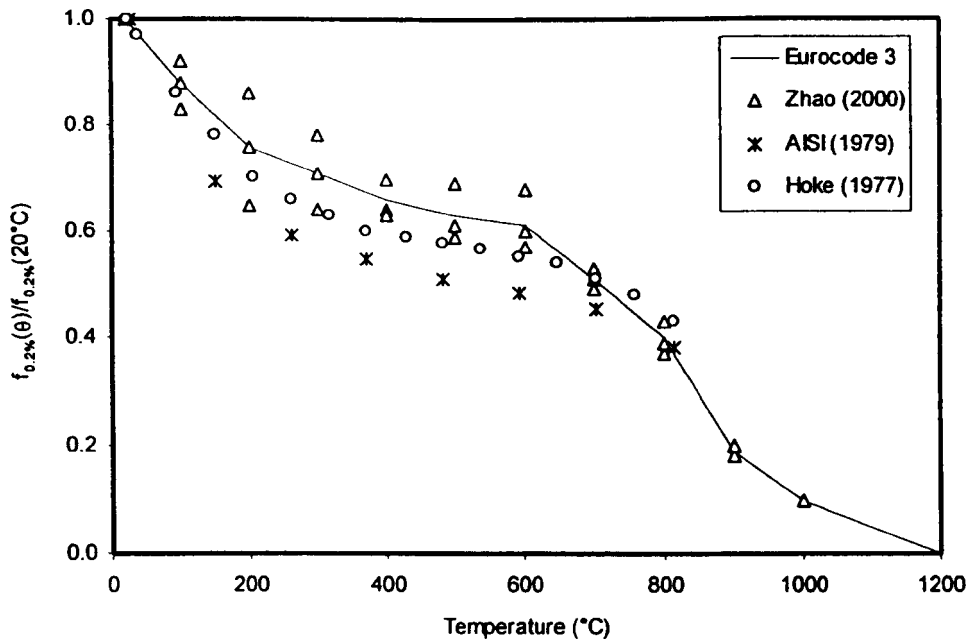
Figure 3.9: *0.2% proof strength of stainless steel grade EN 1.4401 at elevated temperature*

3.5.2 Strength at 2% strain $f_{2\%,\theta}$

Figure 3.10 compares the Eurocode 3 reduction factors for strength at 2% strain $f_{2\%,\theta}$ for stainless steel grade EN 1.4301, with tests from Chen and Young (2006) and Ala-Outinen and Oksanen (1997). Tests were conducted on flat annealed material and cold-worked material. The test results generally fall slightly below the Eurocode 3 curve. The main difference in mechanical properties between the flat annealed and cold-worked is that the flat annealed had a 0.2% proof stress of 291 N/mm² whereas the cold-worked material had about two times the 0.2% proof stress of flat annealed material (592 N/mm²) at room temperature.
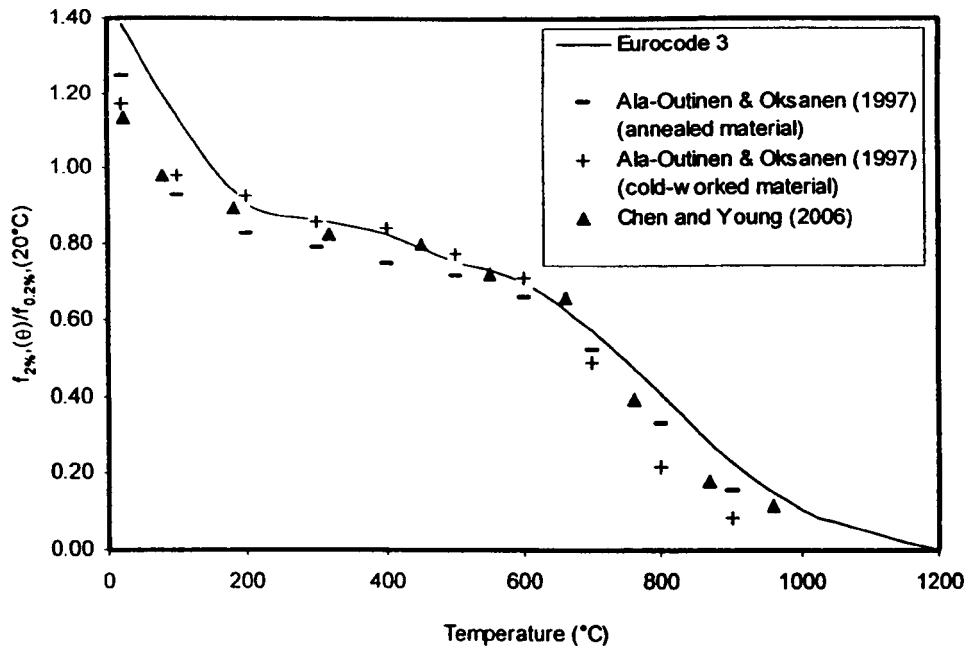
Figure 3.10: *Strength at 2% strain of stainless steel grade EN 1.4301 at elevated temperature*

3.5.3 Ultimate strength $f_{u,\theta}$

Figure 3.11 compares the ultimate strength reduction factors at elevated temperatures for stainless steel grade EN 1.4301 obtained from tests by Zhao (2000), AISI (1979), Hoke (1977) and Chen and Young (2006) with Eurocode 3 Part 1.2. Overall there is a good agreement between Eurocode 3 and the test results.
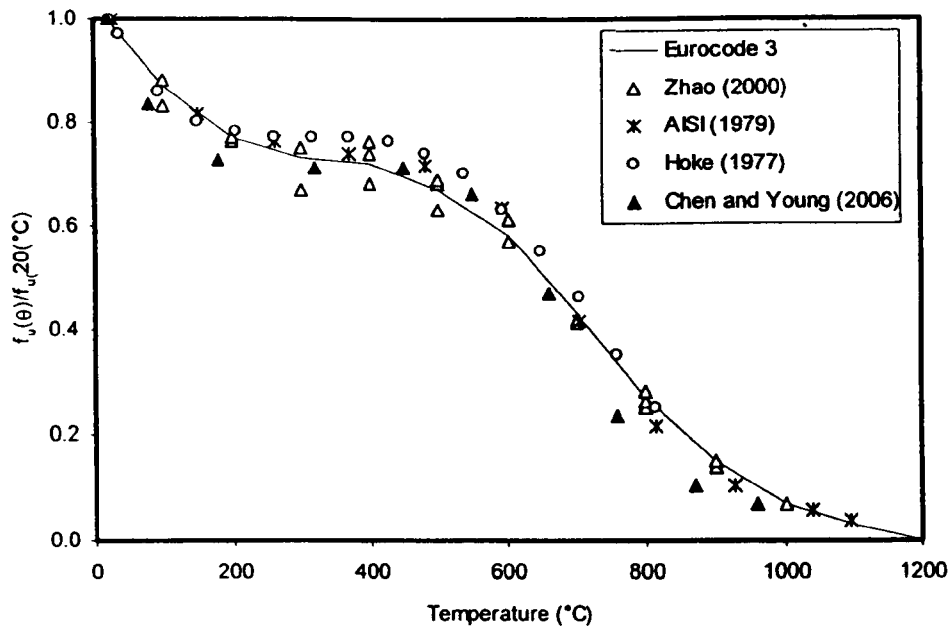
Figure 3.11: *Ultimate strength reduction factor for stainless steel grade EN 1.4301 at elevated temperature*

3.5.3.2 Stainless steel grade EN 1.4401

Figure 3.12 compares the ultimate strength reduction factors at elevated temperature of stainless steel grade EN 1.4401 obtained from tests by Zhao (2000), AISI (1979), Hoke (1977) with Eurocode 3. The test results are distributed satisfactory around the Eurocode 3 curve, though greater scatter exists than for the grade EN 1.4301 results.
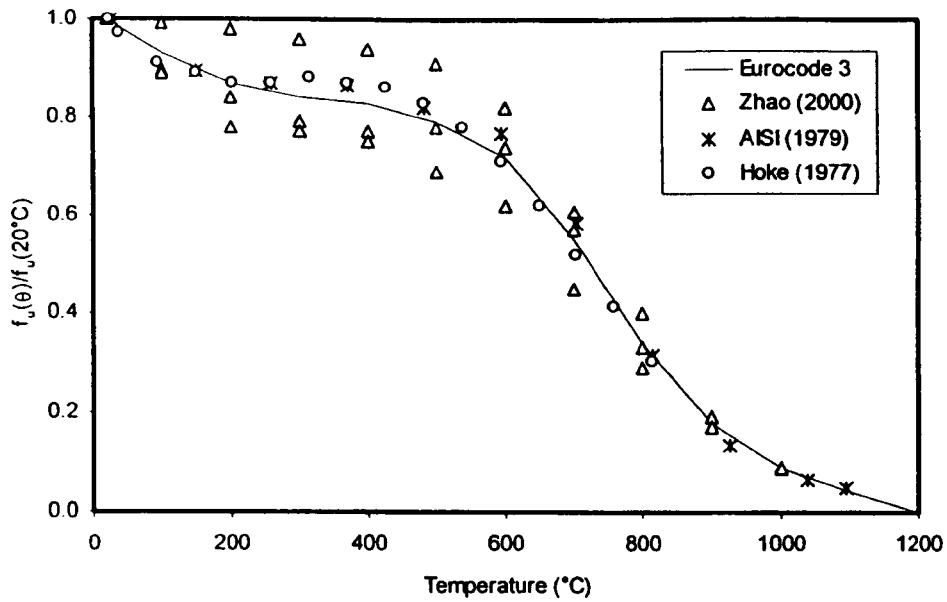
Figure 3.12: *Ultimate strength reduction factor for stainless steel grade EN 1.4401 at elevated temperature*

3.5.4 Young's modulus E(θ)

Figure 3.13 shows the Eurocode 3 reduction factors for Young's modulus of stainless steel compared with tests on Grade 1.4301 material by Ala-Outinen and Oksanen (1997), Zhao (2000), AISI (1979), Hoke (1977) and Chen and Young (2006). The Ala-Outinen and Oksanen (1997) test results (annealed material and cold-worked material) are much lower than the Eurocode 3 curve. The Zhao (2000) test results are also lower than the Eurocode 3 curve, but closer, whilst the AISI (1979) test results are slightly higher than the Eurocode 3 curve. Chen and Young's (2006) test results show unexpected reduction factor of greater than unity at 80°C and 320°C. Other than the Ala-Outinen and Oksanen tests (1997), the Eurocode 3 reduction factors generally reflect the test results.
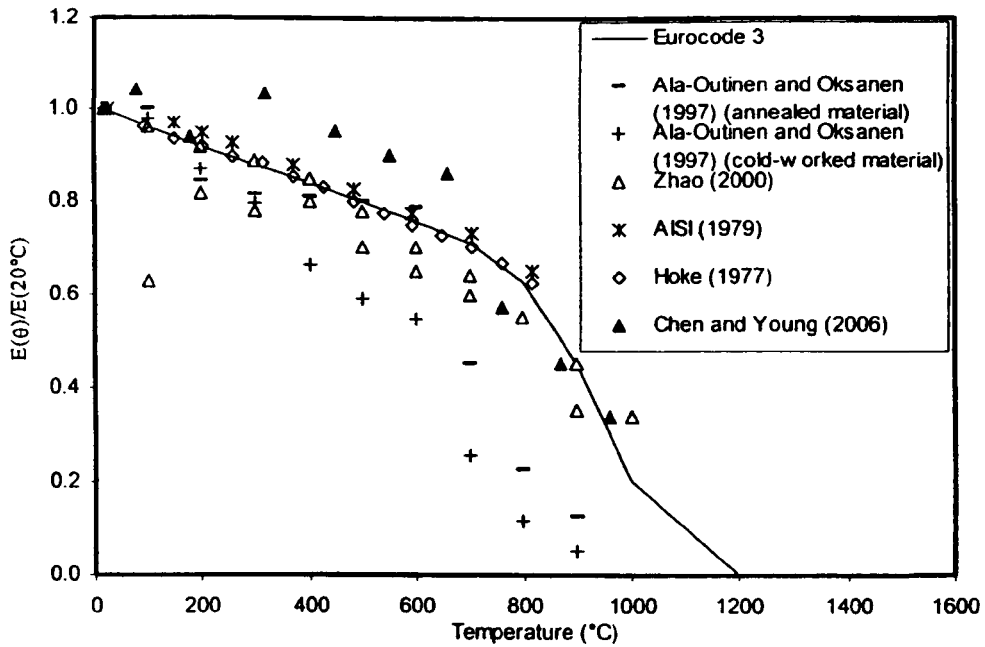
Figure 3.13: *Reduction factor of Young's modulus of stainless steel grade EN 1.4301 at elevated temperature*

As mentioned in section 3.3.1, stiffness reduction factors given in Eurocode 3 are identical for all stainless grades. Test results (e.g. Hoke, 1977) showed that values of elevated temperature Young's modulus of stainless steel grade EN 1.4401 are very similar (maximum percentage of 4% difference) to EN 1.4301, thus a single set of reduction factors can be used to represent many grades of stainless steel.

3.5.5 Thermal elongation

The thermal elongation of austenitic stainless steel from EN 1993-1-2 (2005) is given by the following equation:

$$\Delta l/l = (16 + 4.79 \times 10^{-3}\theta_a - 1.243 \times 10^{-6}\theta_a^2) \times (\theta_a - 20)\, 10^{-6} \tag{3.3}$$

where l is the length at 20°C, Δl is the temperature induced expansion and θ_a is the steel temperature (°C)

Figure 3.14 compares the thermal elongation for stainless steel grade EN 1.4301 as defined by Eurocode 3 with tests conducted by Sakumoto et al. (1996) and Ala-Outinen and Oksanen (1997). The test results show good agreement with Eurocode 3.
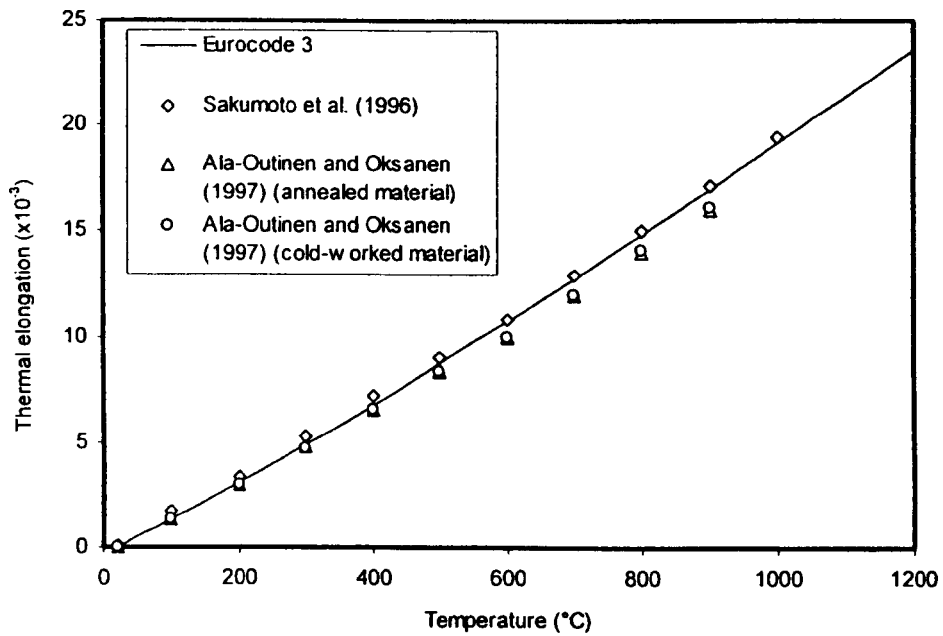
Figure 3.14: *Thermal elongation for stainless steel grade EN 1.4301*

3.6 RATIONALISATION OF STRENGTH REDUCTION FACTORS

EN 1993-1-2 (2005) has proposed a single series of strength reduction factors at elevated temperature for all grades of carbon steel. However a total of eight series of strength reduction factors are given in EN 1993-1-2 (Table C1) and the Euro-Inox/SCI Design Manual for Structural Stainless Steel (2006) for nine different grades of stainless steel. Reducing the number of sets of reduction factors will be more practical for structural engineers.

Chen and Young (2006) proposed a general equation for strength at different levels of strain. However this equation was very conservative as compared to the test results and the predictions from the other design guidance.

Figures 3.15 to 3.17 compare the strength reduction factors at 0.2% proof strain, 2% total strain and for ultimate strength respectively for nine different stainless steel grades given in EN 1993-

1-2 and the Euro-Inox/SCI Design Manual (2006). It is proposed herein that these nine sets of strength reduction factors given in EN 1993-1-2 and the Euro-Inox/SCI Design Manual (2006) be divided into four groups: duplex (EN 1.4462), ferritic (EN 1.4003) and 2 groups of austenitic (Group 1: EN 1.4301, EN 1.4318 C850 and EN 1.4318 and Group 2: EN 1.4401/ EN 1.4404, EN 1.4571 and EN 1.4571 C850). In Eurocode 3, the strength reduction factors of EN 1.4404 are the same as EN 1.4401, since there have been no material tests conducted for steel grade EN 1.4404. Therefore in the following sections, EN 1.4401 and EN 1.4404 will be plotted in the same graph for simplicity.
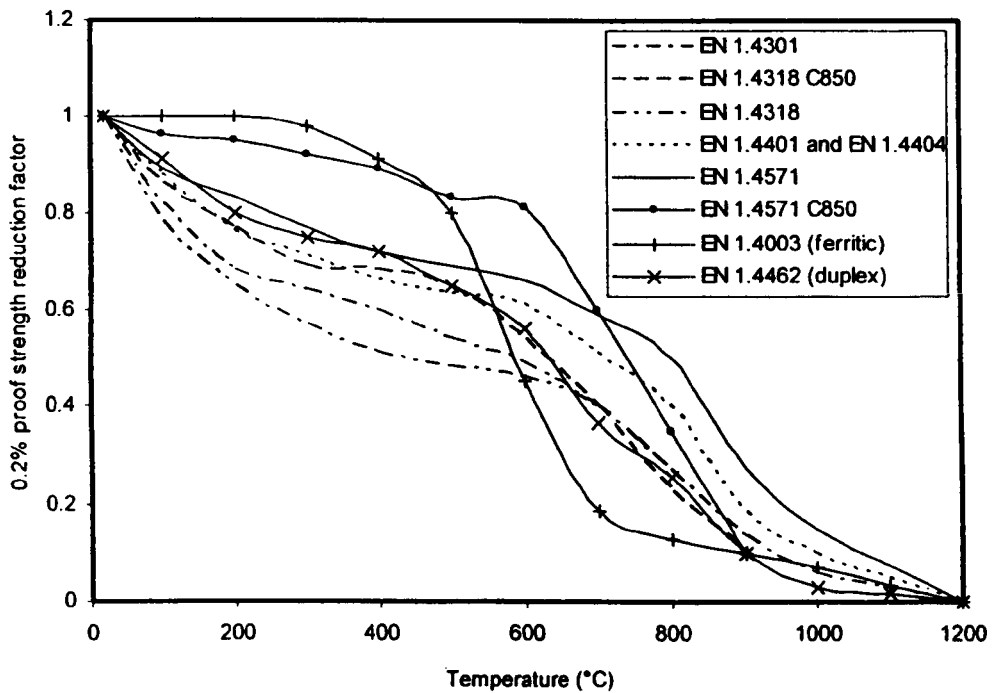
Figure 3.15: *Comparison of 0.2% proof strength reduction factor for 9 different stainless steel grades*
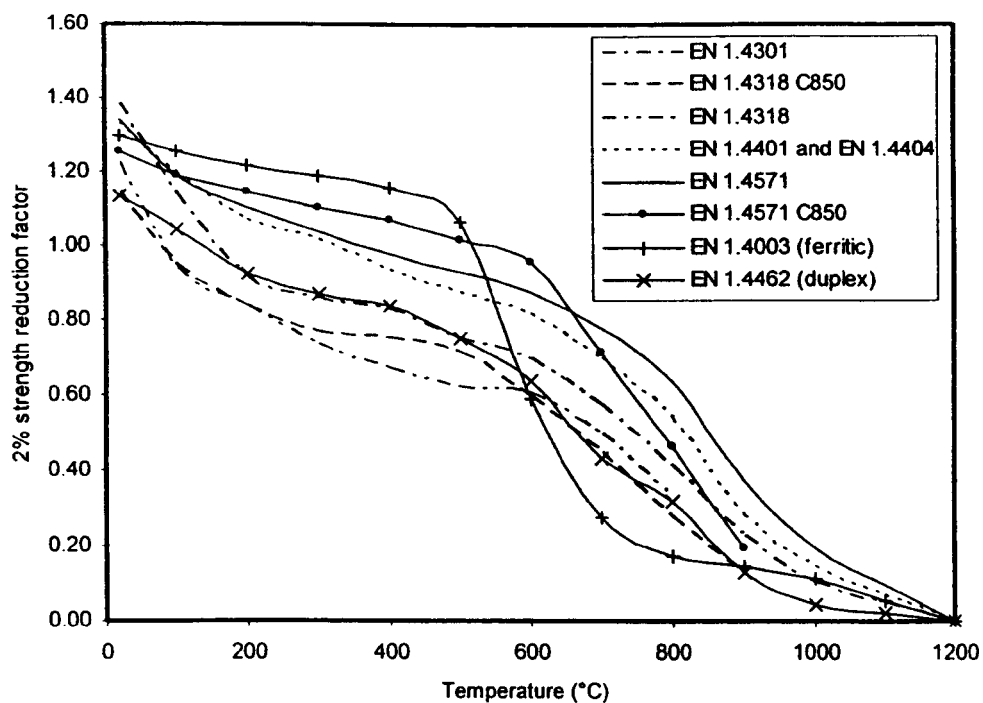
Figure 3.16: *Comparison of 2% strength reduction factor for 9 different stainless steel grades*
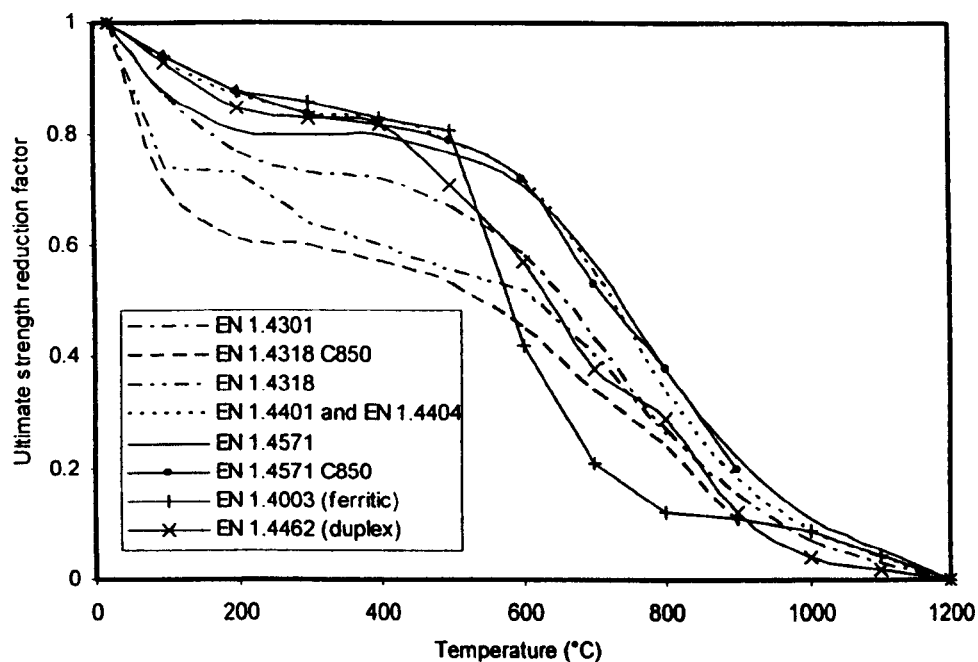
Figure 3.17: *Comparison of ultimate strength reduction factor for 9 different stainless steel grades*

In order to determine the elevated temperature strength at 2% total strain $f_{2\%,\theta}$, EN 1993-1-2 (2005) provides Eq. (3.4). Eq. (3.4) ensures that $f_{2\%,\theta}$ will lie between $f_{0.2p,\theta}$ and $f_{u,\theta}$, and requires the definition of the parameter $k_{2\%,\theta}$.

$$f_{2\%,\theta} = f_{0.2p,\theta} + k_{2\%,\theta} \left(f_{u,\theta} - f_{0.2p,\theta} \right) \qquad (3.4)$$

Since different stainless steel grades have different yield strengths and ultimate strengths, the $k_{2\%,\theta}$ factors for each group were derived indirectly by considering the $k_{0.2p,\theta}$ and $k_{u,\theta}$ factors from EN 1993-1-2 (2005).

3.6.1 Proposed curve on 0.2% strength reduction factors

Figures 3.18 to 3.23 compare the proposed grouped curves with the Eurocode 3 curves and tests for different stainless steel grades. Figures 3.18 to 3.20 and Figures 3.21 to Figure 3.23 have been categorized as Group 1 and Group 2 respectively. The proposed curve was defined as the mean curve from Eurocode 3 predictions in Group 1. However for Group 2, the strength reduction factors curve of grade EN 1.4571 C850 is very high, is only based on one test series, and shows a large discrepancy with EN 1.4401/ EN 1.4404 and EN 1.4571. The mean curve of Group 2 would therefore give unsafe predictions for grades EN 1.4401/ EN 1.4404 and EN 1.4571. It is proposed to use Eurocode 3 stainless steel grade EN 1.4401/ EN 1.4404 as the new curve for Group 2.

Figure 3.18: *Comparison of 0.2% proof strength reduction factor of proposed curve against the current design guidance and test results for EN 1.4301(Austenitic Group 1)*
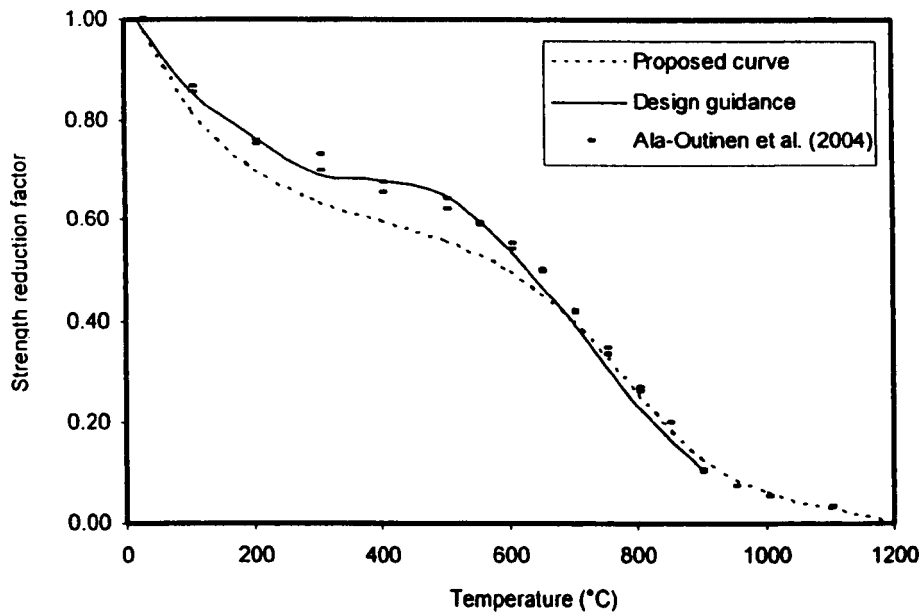
Figure 3.19: *Comparison of 0.2% proof strength reduction factor of proposed curve against the current design guidance and test results for EN 1.4318 C850 (Austenitic Group 1)*

61
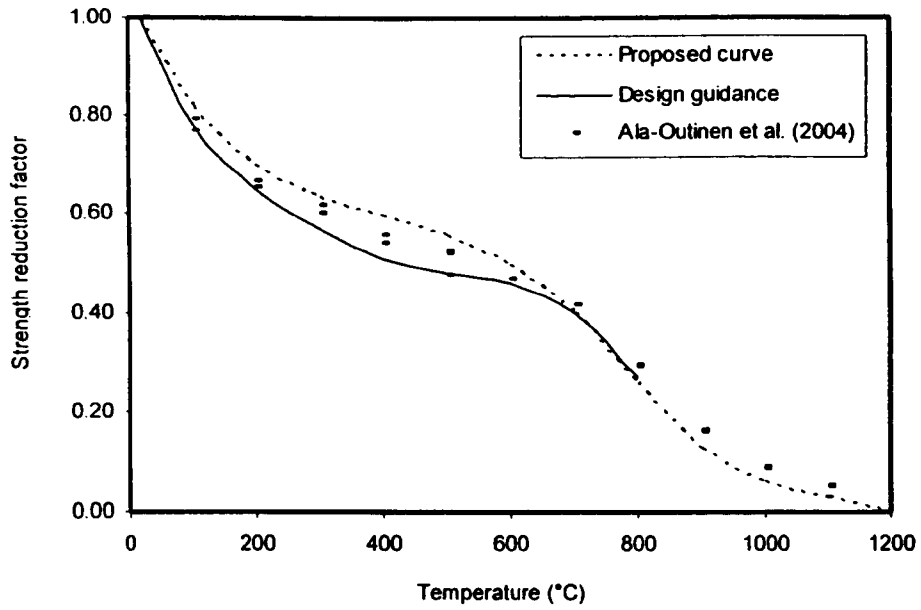
Figure 3.20: *Comparison of 0.2% proof strength reduction factor of proposed curve against the current design guidance and test results for EN 1.4318(Austenitic Group 1)*
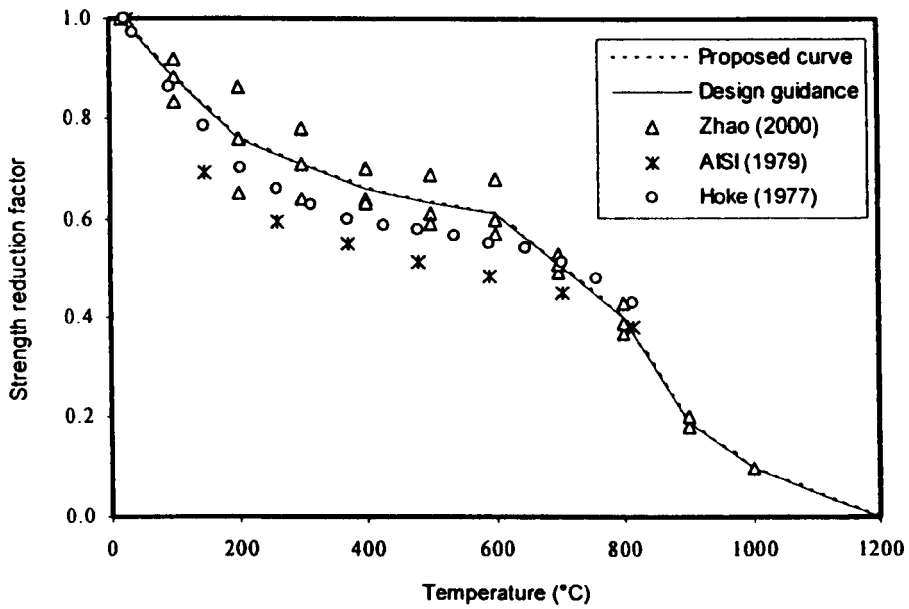
Figure 3.21: *Comparison of 0.2% proof strength reduction factor of proposed curve against the current design guidance and test results for EN 1.4401/ EN 1.4404 (Austenitic Group 2)*
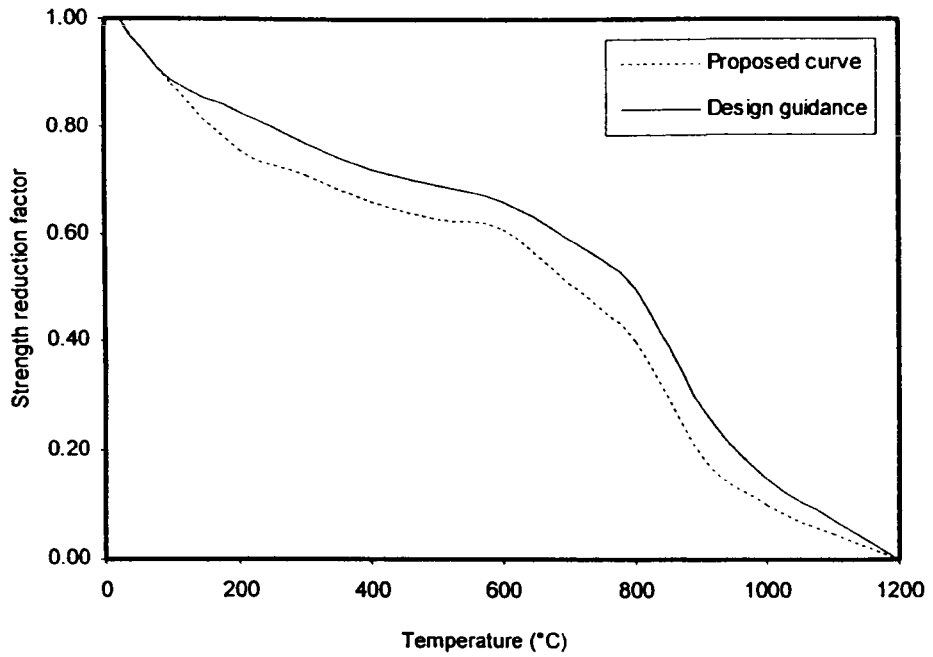
Figure 3.22: *Comparison of 0.2% proof strength reduction factor of proposed curve against the current design guidance for EN 1.4571 (Austenitic Group 2)*
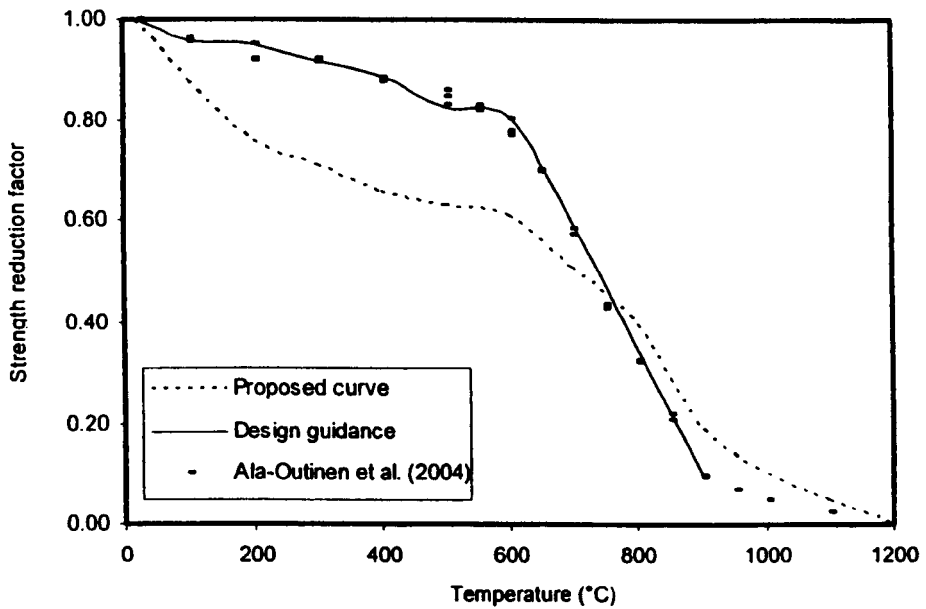
Figure 3.23: *Comparison of 0.2% proof strength reduction factor of proposed curve against the current design guidance and test results for EN 1.4571 C850 (Austenitic Group 2)*

In Group 1, Figure 3.18 shows that for Grade 1.4301 the proposed curve predicts the strength reduction factors accurately as compared to tests and existing design guidance. Figure 3.19 and 3.20 show some, but not significant, disparity between the proposed curve and existing tests and design guidance.

In Group 2, the proposed curve gave accurate prediction against the tests in Figure 3.21 for Grade 1.4401, but lower strength reduction factors for stainless steel grade EN 1.4571 and EN 1.4571 C850 (Figures 3.22 and 3.23). The discrepancy is greatest for Grade 1.4571 C850 at low temperature. The current design guidance curve was based on only one series of available test results. It is believed that if more test data can be provided, the discrepancy of Eurocode 3 curve and proposed curve will be smaller.

Tables 3.2 and 3.3 show the comparisons of the proposed values of strength reduction factors with EN 1993-1-2 (2005) and Euro-Inox (2006) for Group 1 and 2.

Table 3.2: *Comparisons of 0.2% proof strength reduction factor of the proposed values with predictions from EN 1993-1-2 and Euro-Inox/SCI Design Manual (Austenitic Group 1)*

Temperature (°C)	Proposed	EN 1.4318 C850	EN 1.4318	EN 1.4301
20	1.00	1.00	1.00	1.00
100	0.82	0.86	0.78	0.82
200	0.70	0.77	0.65	0.68
300	0.63	0.69	0.57	0.64
400	0.60	0.68	0.51	0.6
500	0.56	0.65	0.48	0.54
600	0.50	0.54	0.46	0.49
700	0.40	0.40	0.40	0.40
800	0.26	0.23	0.27	0.27
900	0.13	0.11		0.14
1000	0.06			0.06
1100	0.03			0.03
1200	0.00			0.00

Temperature (°C)	Proposed	EN 1.4401/1.4404	EN 1.4571	EN 1.4571 C850
20	1.00	1.00	1.00	1.00
100	0.88	0.88	0.89	0.96
200	0.76	0.76	0.83	0.95
300	0.71	0.71	0.77	0.92
400	0.66	0.66	0.72	0.89
500	0.63	0.63	0.69	0.83
600	0.61	0.61	0.66	0.81
700	0.51	0.51	0.59	0.60
800	0.40	0.40	0.50	0.35
900	0.19	0.19	0.28	0.10
1000	0.10	0.10	0.15	
1100	0.05	0.05	0.08	
1200	0.00	0.00	0.00	

3.6.2 Proposed curve on ultimate strength reduction factors

The same approach was applied to determine rationalised curves for ultimate strength reduction factors. Figures 3.24 to 3.29 compare the proposed curve with the design guidance and tests for different stainless steel grades. The same groups were retained and Figures 3.24 to 3.26 show Group 1 whilst Figures 3.27 to Figure 3.29 show Group 2. The proposed curves were defined as the mean curve from EN 1993-1-2 and Euro-Inox/SCI Design Manual predictions for both groups.

For Group 1, the proposed ultimate strength reduction factors marginally underpredict test results for Grade 1.4301 and marginally over predict test results for Grade 1.4318 C850. Grade 1.4318 test results are accurately represented by the proposed Group 1 curve.

In Group 2, the proposed curve gives good agreement with the design guidance curve and test results for all four stainless steel grades: EN 1.4401/ EN 1.4404, EN 1.4571 and EN 1.4571 C850, as shown in Figure 3.27 to 3.29.
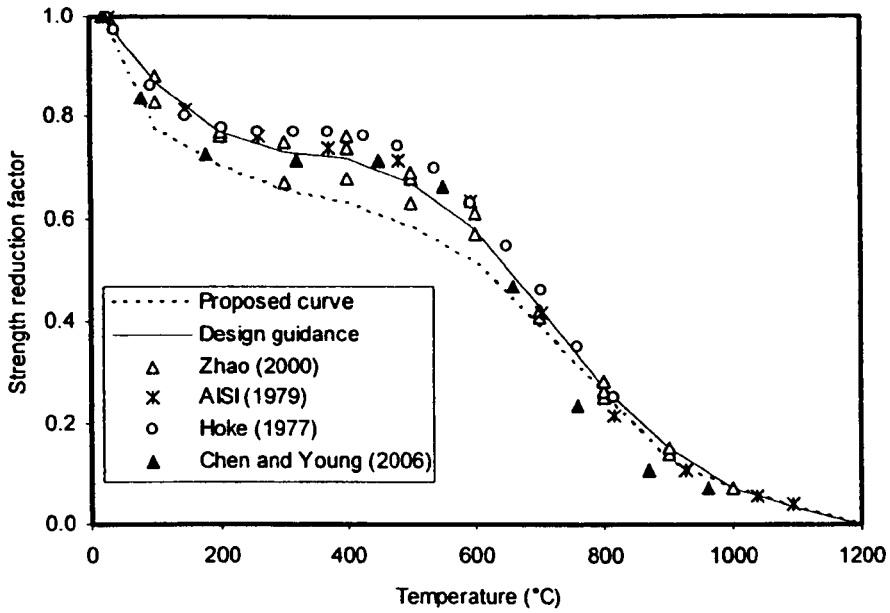
Figure 3.24: *Comparison of ultimate strength reduction factor of proposed curve against the current design guidance and test results for EN 1.4301(Austenitic Group 1)*
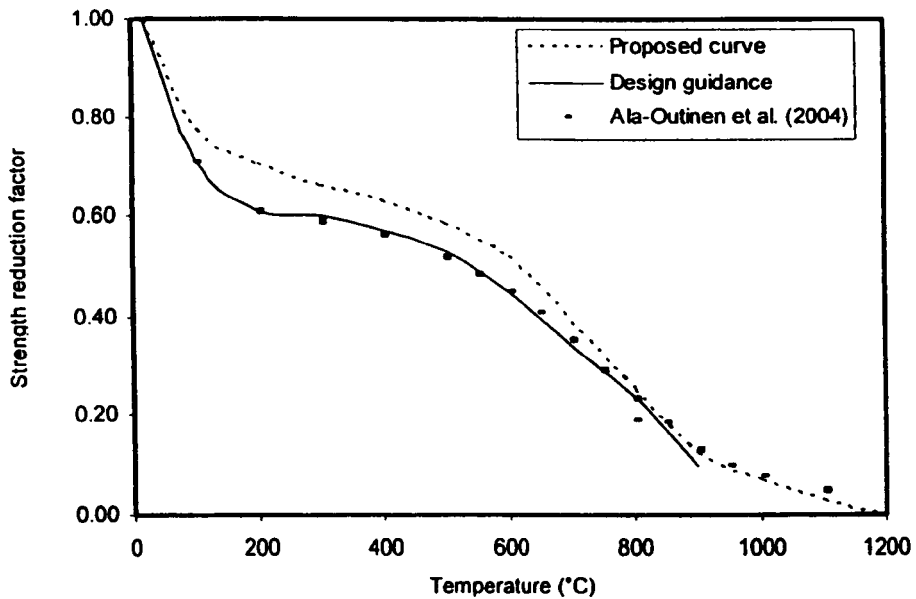
Figure 3.25: *Comparison of ultimate strength reduction factor of proposed curve against the current design guidance and test results for EN 1.4318 C850 (Austenitic Group 1)*
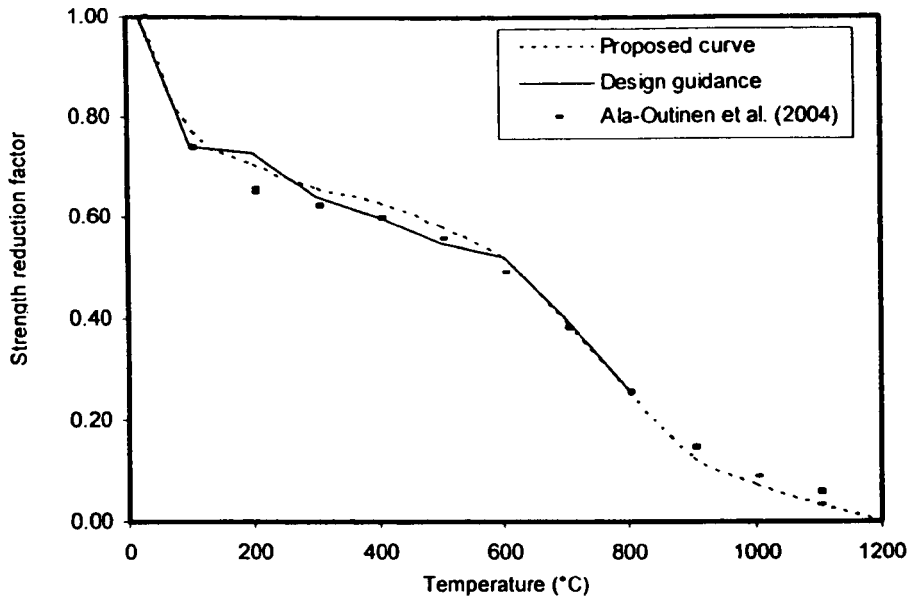
Figure 3.26: *Comparison of ultimate strength reduction factor of proposed curve against the current design guidance and test results for EN 1.4318 (Austenitic Group 1)*
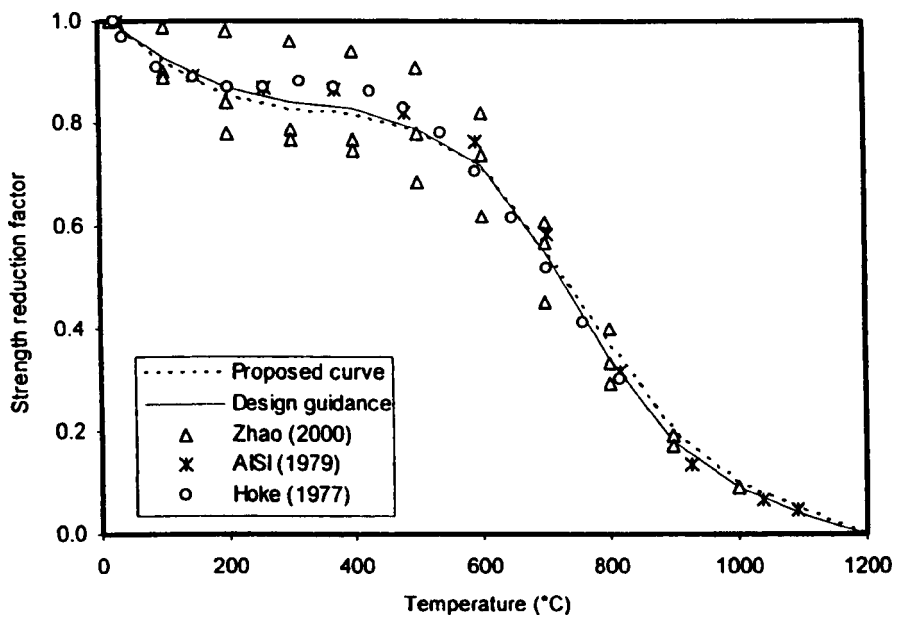
Figure 3.27: *Comparison of ultimate strength reduction factor of proposed curve against the current design guidance and test results for EN 1.4401/ EN 1.4404 (Austenitic Group 2)*
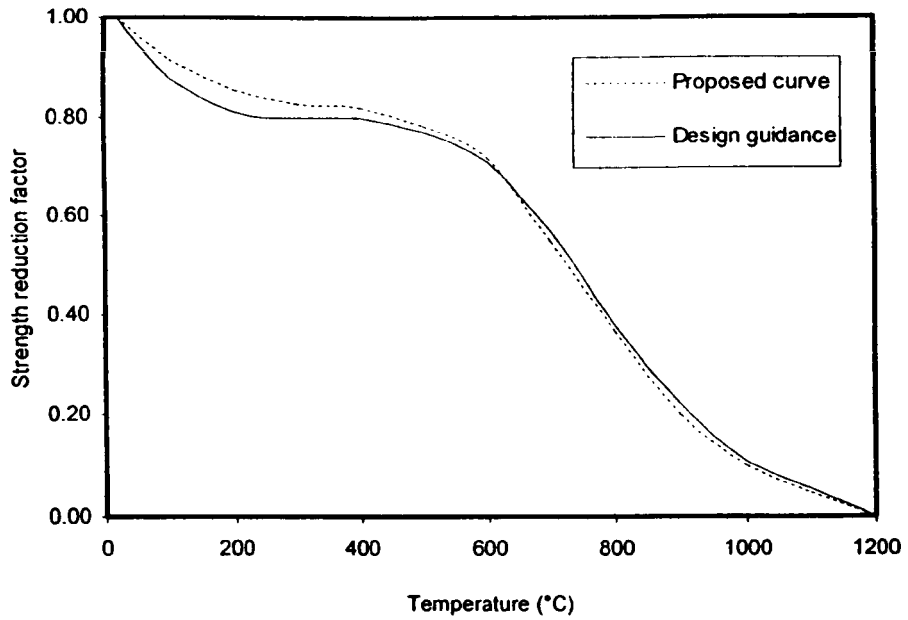
Figure 3.28: *Comparison of ultimate strength reduction factor of proposed curve against the current design guidance for EN 1.4571 (Austenitic Group 2)*
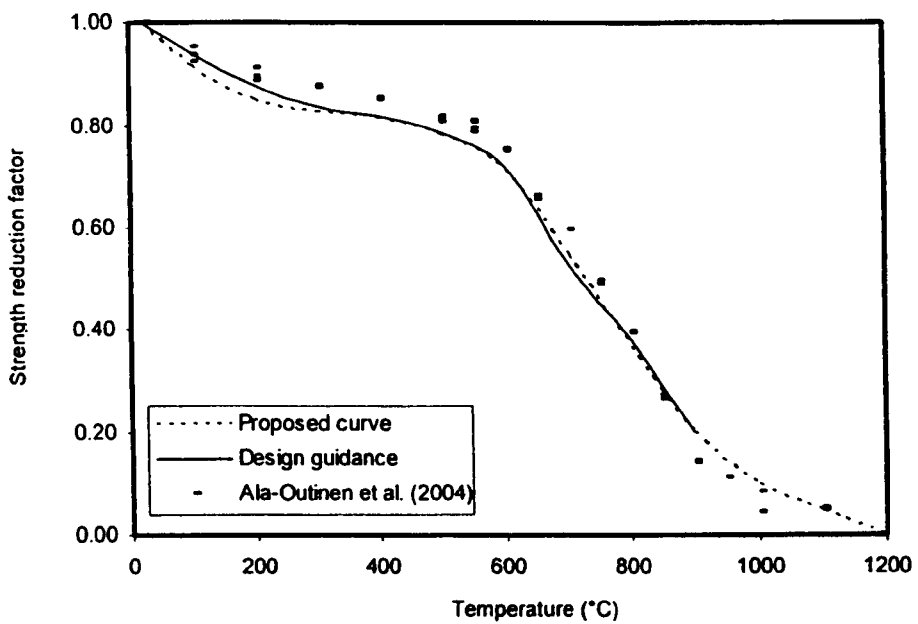
Figure 3.29: *Comparison of ultimate strength reduction factor of proposed curve against the current design guidance and test results for EN 1.4571 C850 (Austenitic Group 2)*

Tables 3.4 and 3.5 show the comparisons of the proposed (mean) values of strength reduction factors with EN 1993-1-2 (2005) and Euro-Inox/SCI Design Manual (2006) for Groups 1 and 2.

Table 3.4: *Comparisons of ultimate strength reduction factor of the proposed values with predictions from EN 1993-1-2 and Euro-Inox/SCI Design Manual (Austenitic Group 1)*

Temperature (°C)	Proposed	EN 1.4318 C850	EN 1.4318	EN 1.4301
20	1.00	1.00	1.00	1.00
100	0.77	0.71	0.74	0.87
200	0.70	0.61	0.73	0.77
300	0.66	0.60	0.64	0.73
400	0.63	0.57	0.60	0.72
500	0.58	0.53	0.55	0.67
600	0.52	0.45	0.52	0.58
700	0.39	0.34	0.40	0.43
800	0.26	0.24	0.26	0.27
900	0.13	0.10		0.15
1000	0.07			0.07
1100	0.03			0.03
1200	0.00			0.00

Table 3.5: *Comparisons of ultimate strength reduction factor of the proposed values with predictions from EN 1993-1-2 and Euro-Inox/SCI Design Manual (Austenitic Group 2)*

Temperature (°C)	Proposed	EN 1.4401/1.4404	EN 1.4571	EN 1.4571 C850
20	1.00	1.00	1.00	1.00
100	0.92	0.93	0.88	0.94
200	0.85	0.87	0.81	0.88
300	0.83	0.84	0.8	0.84
400	0.82	0.83	0.8	0.82
500	0.78	0.79	0.77	0.79
600	0.72	0.72	0.71	0.72
700	0.55	0.55	0.57	0.53
800	0.37	0.34	0.38	0.38
900	0.20	0.18	0.22	0.20
1000	0.10	0.09	0.11	
1100	0.05	0.04	0.06	
1200	0.00	0.00	0.00	

3.6.3 Proposed curves for 2% strength reduction factors

The strength at 2% strain is determined through Eq. (3.4), and is a function of $f_{0.2p,\theta}$ and $f_{u,\theta}$. The values of $f_{0.2p,\theta}$ and $f_{u,\theta}$ can be determined on the basis of the proposed reduction factors in Tables 3.2 to 3.5 and by multiplying by the appropriate yield strength and ultimate strength for the different stainless steel grades. Values of $k_{2\%,\theta}$ are adjusted to achieve agreement with test results and existing design guidance.

Tables 3.6 and 3.7 compare the proposed values of 2% strength reduction factors those obtained from Eurocode 3 and the Euro-Inox Design Manual for Stainless Steel.

Table 3.6: *Comparison of 2% strength reduction factor of proposed method with the current design guidance (Austenitic Group 1)*

Temperature (°C)	Proposed $k_{2\%,\theta}$	$f_y = 500$ N/mm², $f_u = 850$ N/mm²		$f_y = 330$ N/mm², $f_u = 630$ N/mm²		$f_y = 210$ N/mm², $f_u = 520$ N/mm²	
		1.4318 C850	Proposed $f_{2\%,\theta}$	1.4318	Proposed $f_{2\%,\theta}$	1.4301	Proposed $f_{2\%,\theta}$
20	0.24	1.15	1.17	1.23	1.22	1.38	1.35
100	0.26	0.94	0.95	0.94	0.94	1.14	1.10
200	0.24	0.84	0.82	0.84	0.86	0.91	0.95
300	0.21	0.77	0.73	0.73	0.79	0.86	0.84
400	0.21	0.75	0.70	0.67	0.76	0.82	0.80
500	0.21	0.71	0.65	0.62	0.70	0.75	0.74
600	0.24	0.60	0.59	0.60	0.63	0.70	0.68
700	0.26	0.45	0.47	0.50	0.48	0.57	0.55
800	0.27	0.27	0.30	0.33	0.32	0.41	0.36
900	0.28	0.13	0.15		0.16	0.23	0.18
1000	0.35		0.08		0.10	0.11	0.10
1100	0.20		0.03		0.04	0.05	0.04
1200	0.00		0.00		0.00		0.00

Table 3.7: *Comparison of 2% strength reduction factor of proposed method with the current design guidance (Austenitic Group 2)*

Temperature (°C)	Proposed $k_{2\%,\theta}$	$f_y = 220$ N/mm², $f_u = 520$ N/mm² Proposed $f_{2\%,\theta}$ 1.4401/1.4404	$f_y = 220$ N/mm², $f_u = 520$ N/mm² Proposed $f_{2\%,\theta}$ 1.4571	$f_y = 500$ N/mm² 1.4571 C850	$f_u = 850$ N/mm² Proposed $f_{2\%,\theta}$
20	0.24	1.33	1.34	1.25	1.20
100	0.27	1.20	1.19	1.19	1.09
200	0.31	1.07	1.10	1.15	1.01
300	0.30	1.02	1.04	1.10	0.96
400	0.29	0.93	0.98	1.07	0.91
500	0.28	0.88	0.93	1.01	0.86
600	0.28	0.82	0.87	0.96	0.81
700	0.30	0.70	0.78	0.71	0.66
800	0.37	0.54	0.64	0.47	0.48
900	0.17	0.28	0.37	0.20	0.24
1000	0.26	0.15	0.19		0.14
1100	0.25	0.07	0.10		0.07
1200	0.00	0.00	0.00		0.00

For Group 1, Figures 3.30 to 3.32 show that the proposed curve gives good agreement with the Eurocode 3 curve and test results.

For Group 2, the proposed curve predicts higher strength reduction factor than current design guidance, for Grades 1.4401/ 1.4404 and 1.4571 as shown in Figure 3.33 and 3.34. The proposed curve is conservative at low temperature for Grade 1.4571 C850, as shown in Figure 3.35.
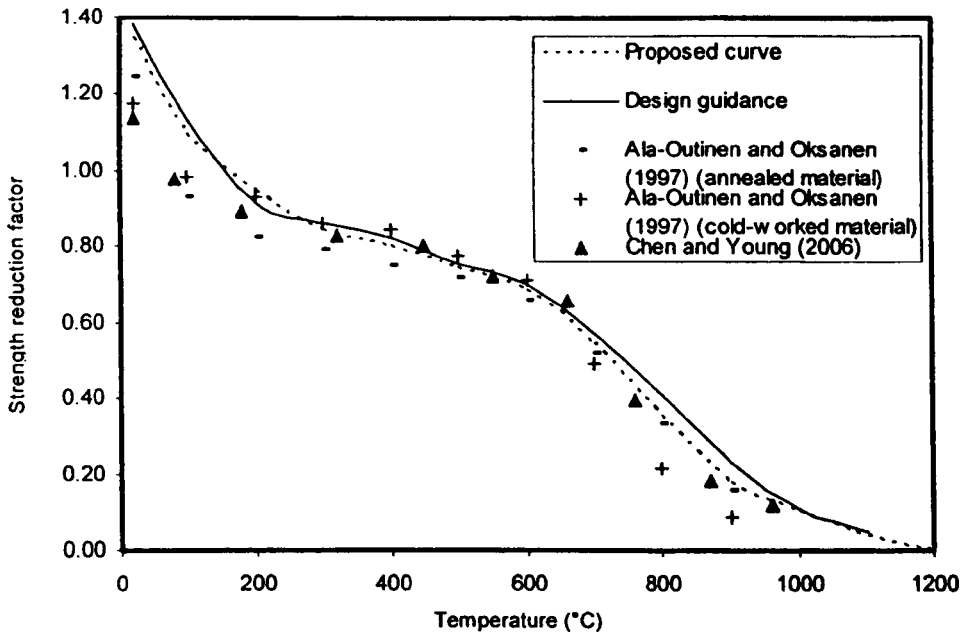
Figure 3.30: *Comparison of 2% strength reduction factor of proposed curve against the current design guidance and test results for EN 1.4301 (Austenitic Group 1)*
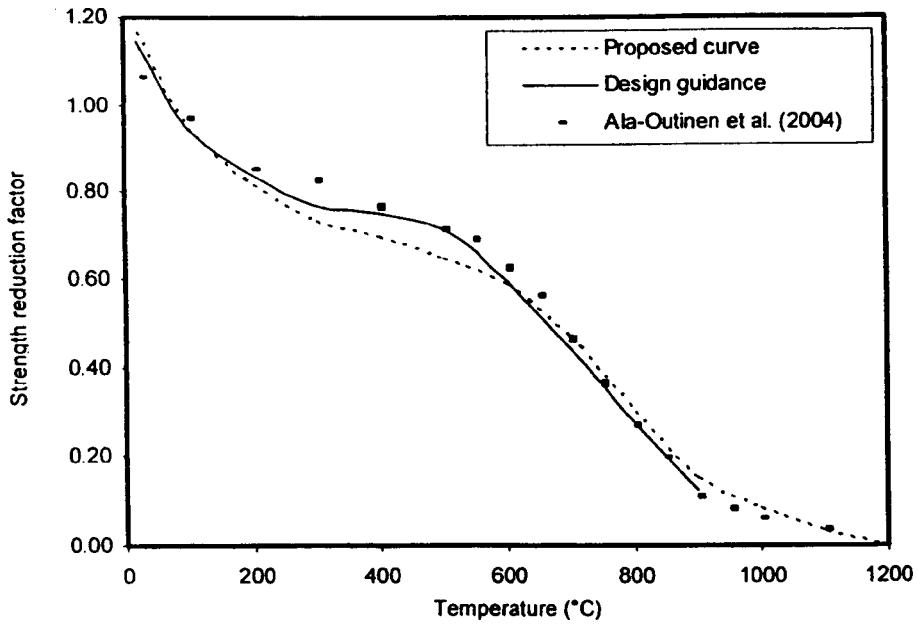
Figure 3.31: *Comparison of 2% strength reduction factor of proposed curve against the current design guidance and test results for EN 1.4318 C850 (Austenitic Group 1)*
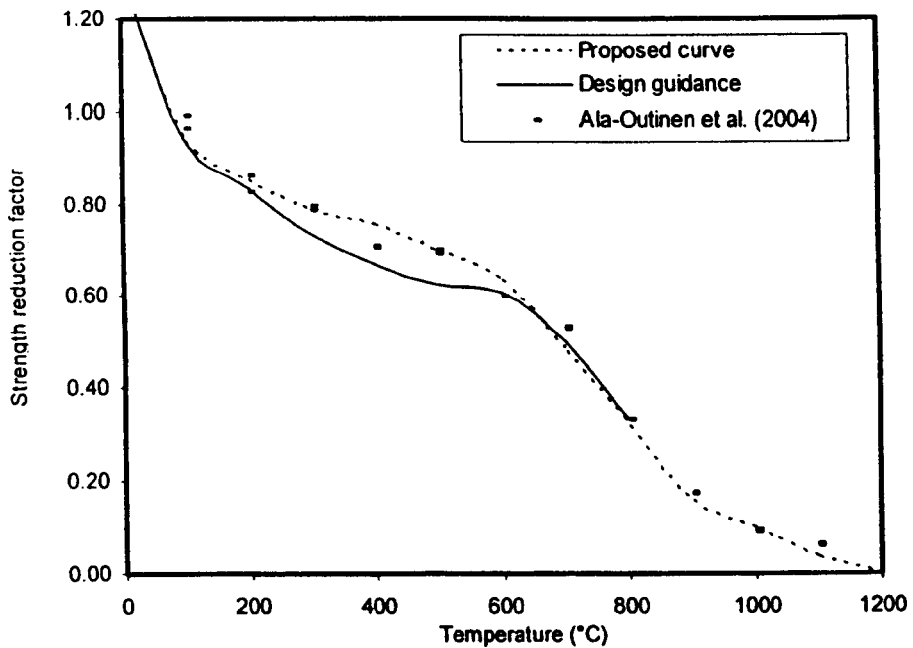
Figure 3.32: *Comparison of 2% strength reduction factor of proposed curve against the current design guidance and test results for EN 1.4318 (Austenitic Group 1)*
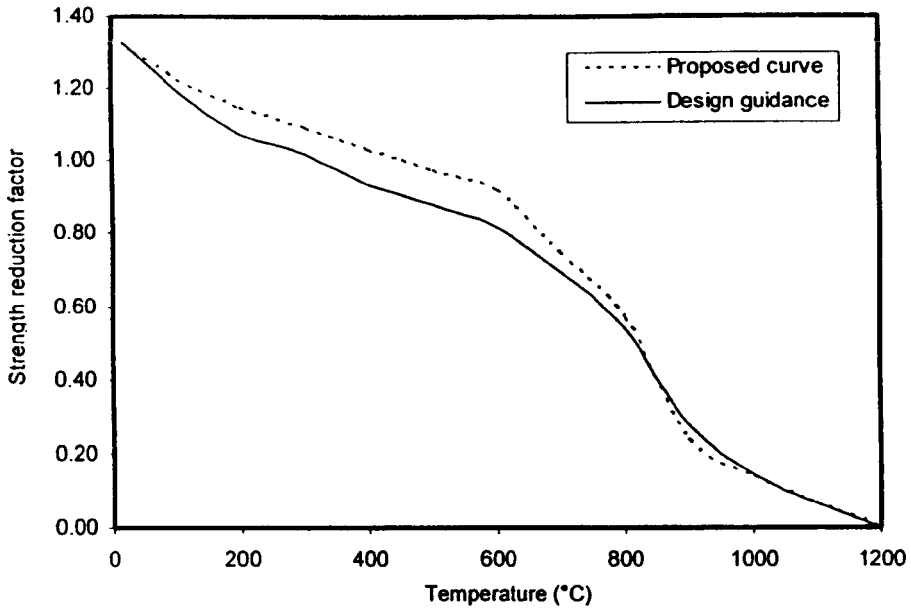
Figure 3.33: *Comparison of 2% strength reduction factor of proposed curve against the current design guidance for EN 1.4401/ EN 1.4404 (Austenitic Group 2)*
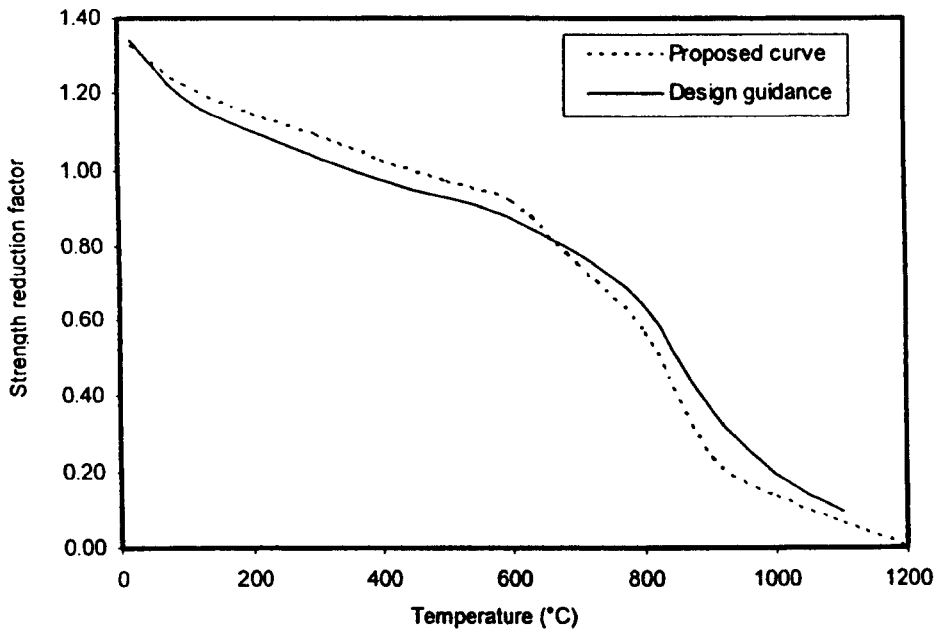
Figure 3.34: *Comparison of 2% strength reduction factor of proposed curve against the current design guidance for EN 1.4571 (Austenitic Group 2)*
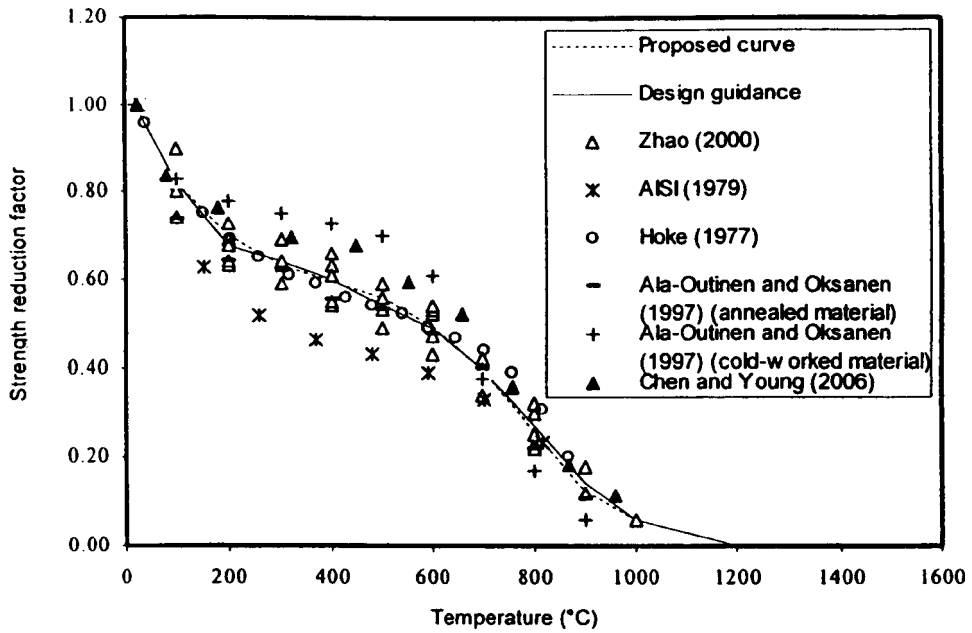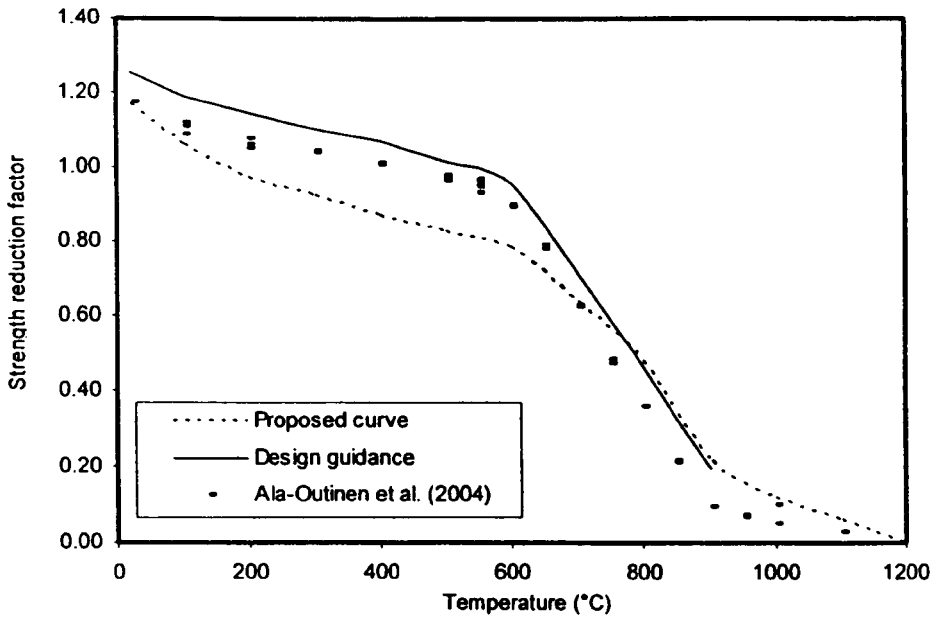
Figure 3.35: *Comparison of 2% strength reduction factor of proposed curve against the current design guidance and test results for EN 1.4571 C850 (Austenitic Group 2)*

3.7 INFLUENCE OF NITROGEN ADDITION

As stated by Rohrig (1973), the addition of nitrogen to stainless steels provides a consistent improvement in mechanical properties, increasing stainless steel yield and tensile strength at elevated temperature. The nitrogen content in grades EN 1.4301 and EN 1.4401 at elevated temperature ranges between 0.10 to 0.16 percent.

3.8 CONCLUDING COMMENTS

Stainless steel displays superior behaviour to carbon steel in terms of strength and stiffness retention at elevated temperature. At 700°C, Grade 1.4301 stainless steel retains 5 times the Young's Modulus of carbon steel (see Figure 3.2). Use of the 2% strain limit at fire limit states benefits stainless steel because of its high level of strain hardening.

EN 1993-1-2 (2005) provides a single series of strength reduction factor for carbon steel. However there are in total of eight sets of strength reduction factors for nine different stainless

76

steel grades given in EN 1993-1-2 (2005) and Euro-Inox/SCI Design Manual (2006), which is not practical for structural engineers. Section 3.6 reported in detail that these nine stainless steel grades can be divided into 4 groups: duplex (EN 1.4462), ferritic (EN 1.4003) and 2 groups of austenitic (Group 1: EN 1.4301, EN 1.4318 C850 and EN 1.4318 and Group 2: EN 1.4401/ EN 1.4404, EN 1.4571 and EN 1.4571 C850).

Revised strength reduction factors for these four groups, based on all available test data, have been proposed. Based on the comparisons shown in Section 3.6, the proposed curves give good agreement with the current design guidance and the test results. Further elevated temperature material tests would be valuable.

CHAPTER 4

TEMPERATURE DEVELOPMENT OF STAINLESS STEEL IN FIRE

4.1 INTRODUCTION

With heightened emphasis now being placed on the performance of structures at elevated temperatures (Bailey, 2004), and an increasing trend towards the use of bare steelwork (Wong et al., 1998), a number of recent studies of the response of unprotected stainless steel structural members exposed to fire have been performed (Ala-Outinen and Oksanen, 1997; Baddoo and Burgan, 1998; Baddoo and Gardner, 2000; Gardner and Baddoo, 2006).

The mechanical and thermal properties of stainless steel differ from those of carbon steel due to variation in chemical composition between the materials. A comparison of these properties for austenitic stainless steel with those for structural carbon steel is presented in Chapter 3. In addition to the mechanical and thermal properties of a material, the two key parameters for the determination of temperature development in structural members are the convective heat transfer coefficient and the emissivity (absorptivity). Both of these are a function of a range of factors including surface geometry and are therefore not material constants (Drysdale, 1985); these factors are discussed later in more detail.

This Chapter examines the temperature development in structural stainless steel sections and has been reported by Gardner and Ng (2006). Comparisons of temperature development in structural stainless steel sections are made between existing test results, numerical simulations (using the non-linear finite element package ABAQUS) and the simple calculation model of EN 1993-1-2 (2005). Based on these comparisons, revised values for the heat transfer coefficient and emissivity of stainless steel members exposed to fire are proposed. The significance of such revisions to the fire resistance and critical temperature of structural stainless steel members is assessed.

4.2 HEAT TRANSFER

4.2.1 Introduction

The rate of temperature development in heated objects is controlled by the three mechanisms of heat transfer, namely conduction, convection and radiation. Heat transfer is thermal energy in transit due to a temperature difference. When two objects with different temperatures come close enough together to affect each other thermally, heat transfer occurs with the hotter object transferring energy to the cooler object.

4.2.2 Conduction

When a temperature gradient exists in a stationary medium, which may be a solid or a fluid, conduction is the heat transfer that will occur across the medium. High temperatures are associated with higher molecular energies and conduction may be viewed as the transfer of energy from the more energetic to the less energetic particles of a substance due to interactions between the particles.

The amount of energy being transferred per unit time by heat conduction can be calculated by:

$$q = -k \frac{\partial T}{\partial x} \qquad (4.1)$$
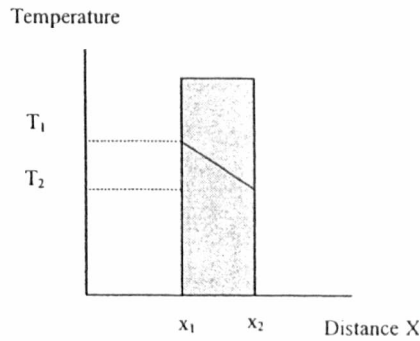
Figure 4.1: *One-Dimensional heat transfer by conduction*

where, $\dfrac{\partial T}{\partial x}$ is the temperature gradient, k is the thermal conductivity (W/mK) and q is the heat flux per unit area (W/m^2).

The negative sign in (4.1) is a consequence of the fact that heat is transferred in the direction of decreasing temperature.

Figure 4.1 shows the temperature distribution is linear under the steady-state conditions. The temperature gradient may be expressed as:

$$\frac{\partial T}{\partial x} = \frac{T_2 - T_1}{x_2 - x_1} \tag{4.2}$$

thus, heat flux is
$$q = -k\frac{T_2 - T_1}{x_2 - x_1} \tag{4.3}$$

4.2.3 Convection

The convective heat transfer coefficient is not a material constant, but is known to be a function of the fluid properties, the flow parameters and the geometry of the surface of the heated object (Drysdale, 1985). The convective heat transfer coefficient is also a function of temperature, and although convection will occur at all stages of a fire, it is particularly important at low temperatures where radiation levels are low.

Heat flux on a surface due to convection is governed by:

$$\dot{h}_{net,c} = \alpha_c \left(\theta_g - \theta_m \right) \qquad (4.4)$$

where $\dot{h}_{net,c}$ is the net convective heat flux (W/m^2), α_c is the convective heat transfer coefficient (W/m^{2}K), θ_g is the gas temperature in the furnace (°C) and θ_m is the surface temperature of the member (°C).

For use with the standard temperature-time curve, EN 1991-1-2 recommends a single convective heat transfer coefficient α_c of 25 W/m^{2}K. In EN 1993-1-2, this value is not dependent on material, though alternative values are provided for different temperature-time curves (the hydrocarbon curve). In the following sections, the sensitivity of the temperature development in the stainless steel cross-sections to variation in the convective heat transfer coefficient α_c is accessed numerically; based on experimental and numerical results, a modified value of α_c is proposed for use in the temperature development model of EN 1993-1-2 (2005).

4.2.4 Radiation

Radiation energy is transferred by electromagnetic waves, which can occur in a vacuum as well as in a medium. Experimental evidence indicates that radiant heat transfer is proportional to the fourth power of the absolute temperature. The rate of radiation heat transfer from the surface can be expressed as below:

$$\dot{h}_{net,r} = \Phi \, \varepsilon_m \, \varepsilon_f \, \sigma \left[(\theta_r + 273)^4 - (\theta_m + 273)^4 \right] \qquad (4.5)$$

where $\dot{h}_{net,r}$ is the net radiative heat flux (W/m^2), Φ is the configuration factor (generally taken as unity), ε_m is the emissivity of the material, ε_f is the emissivity of the fire, σ is the Stefan-Boltzmann constant ($= 5.67 \times 10^{-8}$ W/m^{2}K^4), θ_r is the effective radiation temperature of the fire (°C) and θ_m is the surface temperature of the member (°C).

Radiative heat transfer is controlled by resultant emissivity. Emissivity is a dimensionless property that ranges between zero and unity, and depends on factors such as temperature,

emission angle and wavelength. A common engineering assumption which is adopted in EN 1991-1-2 (2002) is that a surface's spectral emissivity does not depend on wavelength, and thus is taken as a constant. According to Kirchhoff's law of thermal radiation, the emissivity of a surface is also equal to its absorptivity. Thus, an emissivity equal to zero corresponds to all radiation being reflected and an emissivity of unity corresponds to all radiation being absorbed; the lower the emissivity, the more slowly the material heats up.

Tabulated emissivities for materials are widely available in the literature, but show substantial variation depending, in particular, on the condition of the surface. In general, the emissivity of a polished metallic surface is very low, whilst the emissivity of dull, oxidised material approaches unity. EN 1993-1-2 (2005) adopts an emissivity ε_m of 0.7 for carbon steel and 0.4 for stainless steel. This study examines the suitability of the adopted emissivity for stainless steel, based on the results of temperature development tests on structural stainless steel sections, and a supporting numerical programme.

The temperature development of a specimen in a furnace depends on both the emissivity of the material ε_m and the emissivity of the fire (furnace) ε_f, and thus the relative sizes and position of the specimen in the furnace are important (Kay et al., 1996). Both of these features are incorporated into resultant emissivity ε_r, which is commonly approximated as the product of the emissivity of the material ε_m and the emissivity of the fire ε_f. If a specimen is small relative to the dimensions of the furnace and only a negligible amount of emitted radiation is reflected back from the furnace walls, the resultant emissivity will be equal to the emissivity of the material. In EN 1991-1-2 (2002) and EN 1993-1-2 (2005), the emissivity of the fire is taken in general as unity; in the remainder of the present study, the emissivity of the fire will also be assumed as unity.

4.3 REVIEW OF TEMPERATURE DEVELOPMENT TESTS

All temperature development test data for unprotected austenitic stainless steel sections exposed to fire have been collated. In total, 20 specimens exposed to fire on all four sides and three specimens exposed on three sides (with a concrete slab on the fourth side), have been tested. All specimens were subjected to the standard fire curve defined by ISO 834-1 (1999).

Fourteen specimens, tested solely to investigate the temperature development characteristics of stainless steel sections and exposed to fire on all four sides, were reported by Baddoo and Gardner (2000). Other temperature development data were acquired from full scale member tests conducted to determine the fire resistance of structural stainless steel components (Ala-Outinen and Oksanen, 1997; Baddoo and Burgan, 1998; Baddoo and Gardner, 2000; Gardner and Baddoo, 2006; Ala-Outinen, 1999). The deformation of the specimens during testing was assumed not to affect their temperature development.

Tables 4.1 and 4.2 summarise the details of the temperature development tests, including section type, nominal dimensions, A_m/V ratio and correction factor k_{sh} (defined in Section 4.4). Table 4.1 contains specimens exposed to fire on all four sides, while Table 4.2 contains specimens exposed to fire on three sides, with a concrete slab on the fourth side.

In all tests, the gas temperature in the furnace was controlled to achieve the standard temperature-time relationship specified in ISO 834-1 (1999) and EN 1991-1-2 (2002), and given by Eq. (4.6). The relationship of Eq. (4.6) is often referred to as the cellulosic heating rate, and although it does not correspond to an actual fire, it provides a standard basis upon which the fire performance of structural elements may be evaluated.

$$\theta_g = 20 + 345 \log_{10}(8t + 1) \tag{4.6}$$

where θ_g is the gas temperature in the furnace (°C) and t is the time (minutes).

However, although the furnace temperatures were controlled to follow the standard fire curve, this was not achieved exactly in all cases. Furthermore, even with precise control of the furnace, there are still some factors such as differences in furnace construction, fuel used and mode of operation that can cause variation in the effective heat flux at the surface of the test specimen (Thomas and Preston, 1996).

Table 4.1: *Summary of temperature development test specimens exposed to fire on 4 sides*
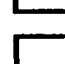
Reported by	Section shape	Dimensions of the section (mm)	Section factor A_m/V (m^{-1})	k_{sb}
Baddoo and Gardner (2000)		20×20, t=3	720.7	0.854
		100×100, t=10	210.5	0.854
		30×15, t_w=4, t_f=4	538.5	0.804
		160×65, t_w=7.5, t_f=10.5	234.7	0.805
		25×25, t=4	543.5	0.739
		100×100, t=10	210.5	0.765
		80×40, t_w=4.5, t_f=5.2	426.5	0.695
		120×64, t_w=7.5, t_f=7	284.4	0.689
		160×82, t_w=10,t_f=12	188.7	0.694
		100×50, t=4	264.1	1.0
		120×60, t=5	211.8	1.0
		250×100, t=4	255.8	1.0
		100×100, t=4	260.4	1.0
		200×200, t=4	255.1	1.0
		100×100, t=4, r=8	258.6	1.0
Baddoo and Burgan (1998)		150×100, t=6, r=4.5	167.4	1.0
		150×75, t=6, r=4.5	168.2	1.0
		100×75, t=6, r=4.5	171.2	1.0
		200×150, t=6, r=4.5	234.7	0.646
Ala-Outinen (1999)		40×40, t=4, r=4	273.5	1.0

Table 4.2: *Summary of temperature development test specimens exposed to fire on 3 sides*

Reported by	Section shape	Dimensions of the section (mm)	Section factor A_m/V (m^{-1})
Baddoo and Burgan (1998)		200×125, t=6, r=4.5	163.9
		200×150, t=6, r=4.5	169.5
Baddoo and Gardner (2000)		120×64, t_w=7.9, t_f=7.3	271.8

4.4 NUMERICAL MODELLING

4.4.1 Background

Numerical models, using the general purpose finite element package ABAQUS (2003), were developed in order to simulate the temperature development of the test specimens. Initially, values for the heat transfer coefficient and emissivity were taken as those recommended in EN 1991-1-2 (2002) and EN 1993-1-2 (2005). Parametric studies were subsequently carried out to investigate the suitability of these values.

The heat transfer analyses adopted in this study utilise heat conduction with general, temperature-dependent conductivity, internal energy (including latent heat effects where appropriate), and general convection and radiation boundary conditions. The analyses do not consider the stress or deformation of the member; instead only the temperature field is calculated. However, the analyses are non-linear because the material properties are temperature dependent, though the non-linearity is mild because the properties do not change rapidly with temperature (Wang, 1995). A number of previous studies have demonstrated the applicability of ABAQUS to the modelling heat transfer problems in structural fire engineering (Feng et al., 2003; Yin and Wang, 2004).

4.4.2 Development of models

Temperature development is controlled by combined convective and radiative heat transfer. The net heat flux h_{net} (W/m^2) is therefore given as the sum of the heat flux due to convection $h_{net,c}$ (Eq. (4.4)) and that due to radiation $h_{net,r}$ (Eq. (4.5)).

Thermal conductivity and specific heat are both temperature dependent. For this study, their values have been determined from EN 1993-1-2 (2005), and are as given in Figures. 3.4 and 3.5. The density of stainless steel may be considered to be independent of temperature and has been taken as $\rho_a = 7850$ kg/m^3. The heat transfer analyses do not consider deformation of the sections, thus material stress-strain properties are not required. The heat transfer shell elements DS4 were adopted throughout the study (ABAQUS, 2003).

4.4.3 Specimens exposed to measured furnace temperature on all four sides

The temperature development of each of the twenty tests outlined in Table 4.2 was modelled numerically, adopting the heat transfer coefficient proposed in EN 1991-1-2 ($\alpha_c = 25$ W/m^{2}K), the emissivity proposed in EN 1993-1-2 ($\varepsilon_m = 0.4$) and the measured furnace temperature-time relationships. A sample of the finite element models is shown in Figure 4.2, and comparisons between test and finite element results are made in Figure 4.3.
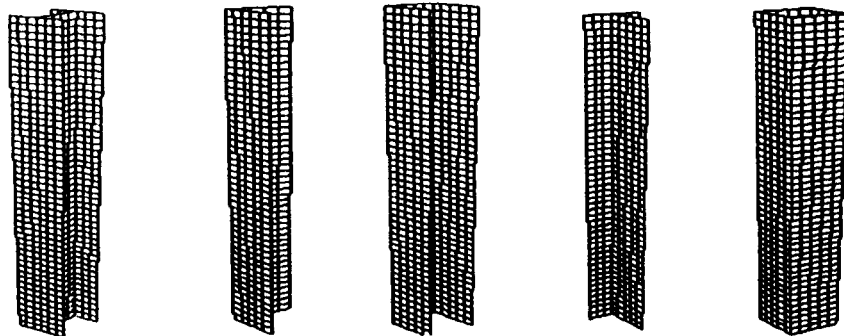
Figure 4.2: *Sample of finite element models*
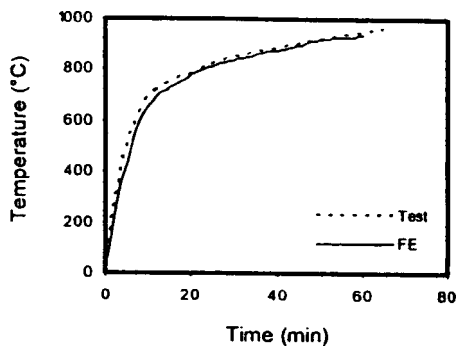
(a): L20x20
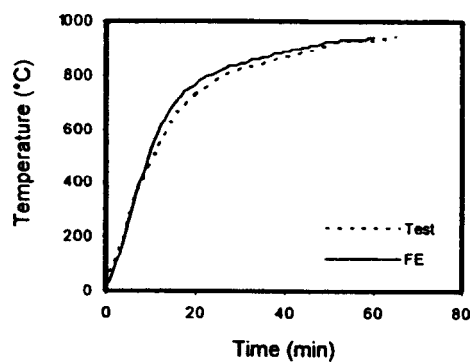
(b): L100x100
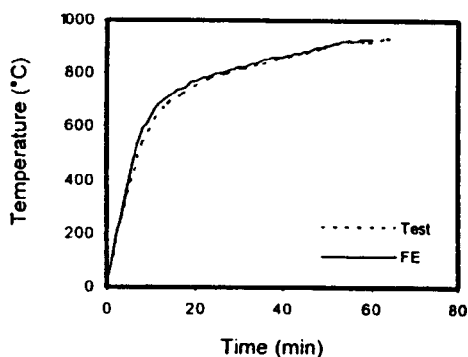
(c): U30x15
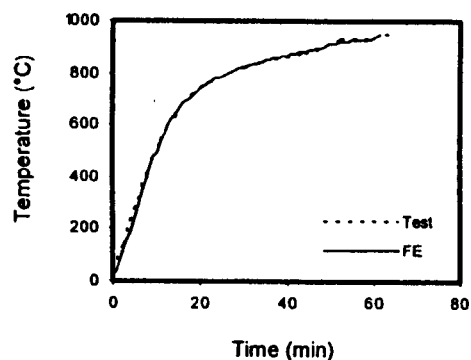
(d): U160x65
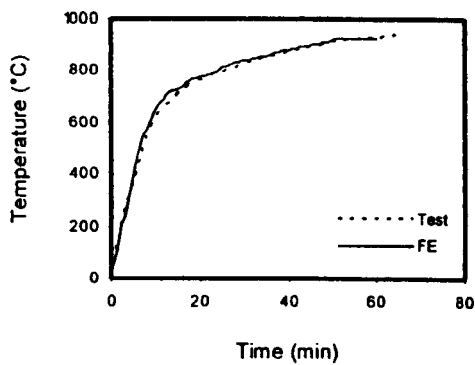
(e): T25x25
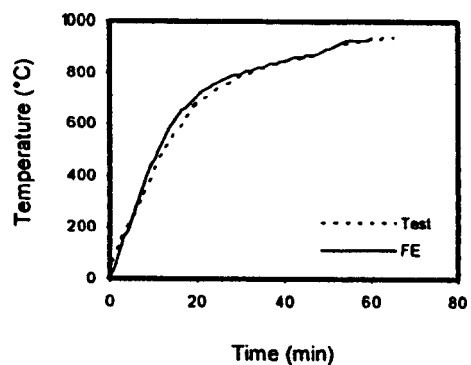
(f): T100x100
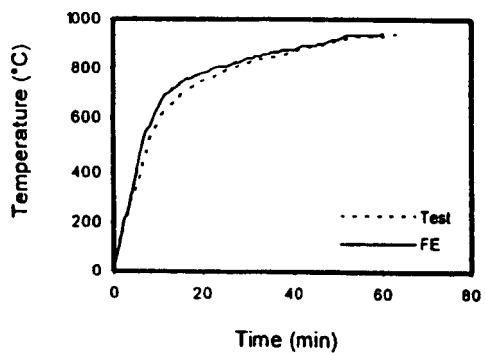
(g): I80x40
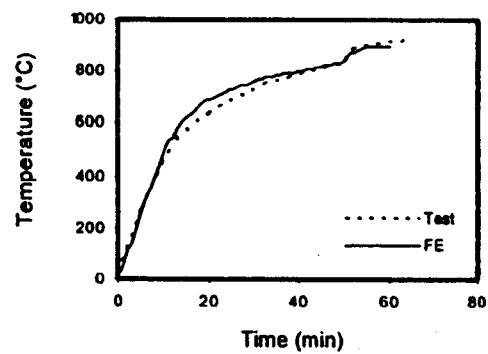
(h): I120x64
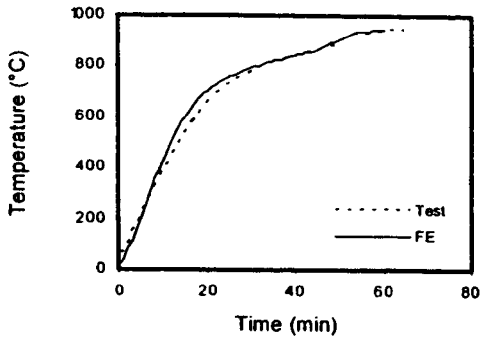
(i): I60x82
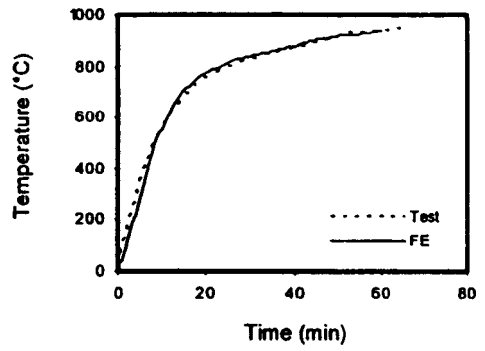
(j): RHS100x50
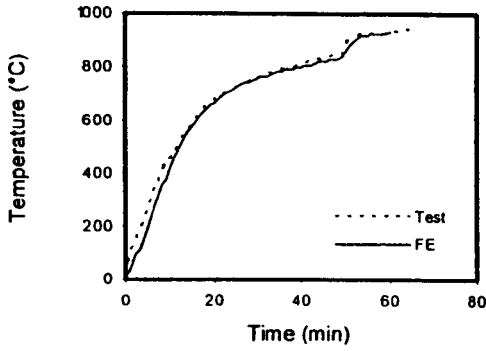
(k): RHS120x60
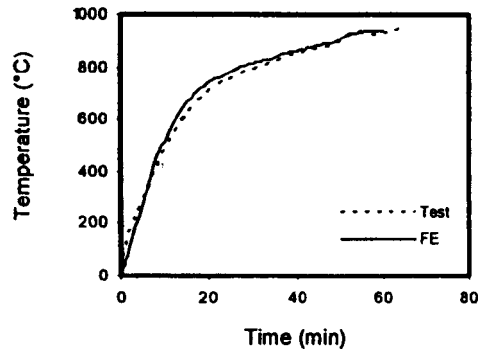
(l): RHS250x100
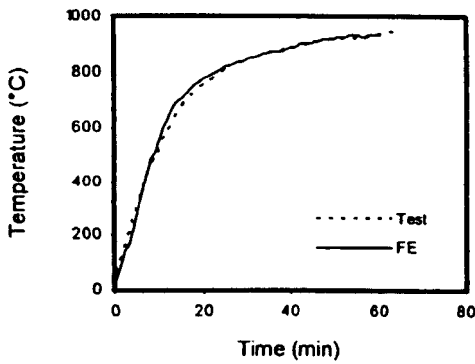
(m):RHS100x100
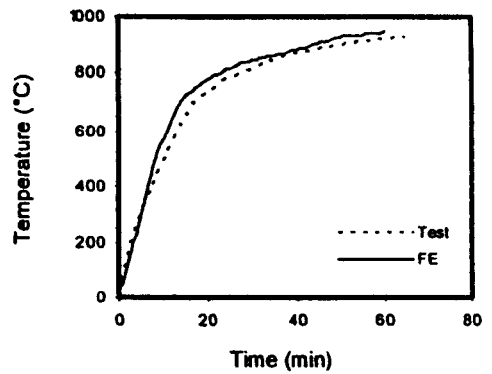
(n): RHS200x200
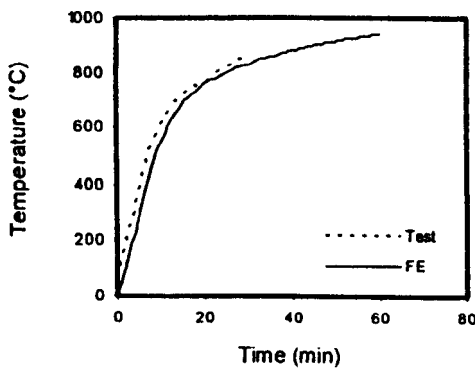
(o): RHS100x100 (CTICM)

(p): RHS150x100

(q): RHS150x75

(r): RHS100x75

(s): I200x150
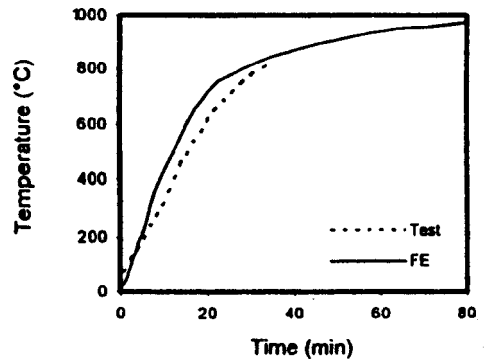
(t): RHS 40x40
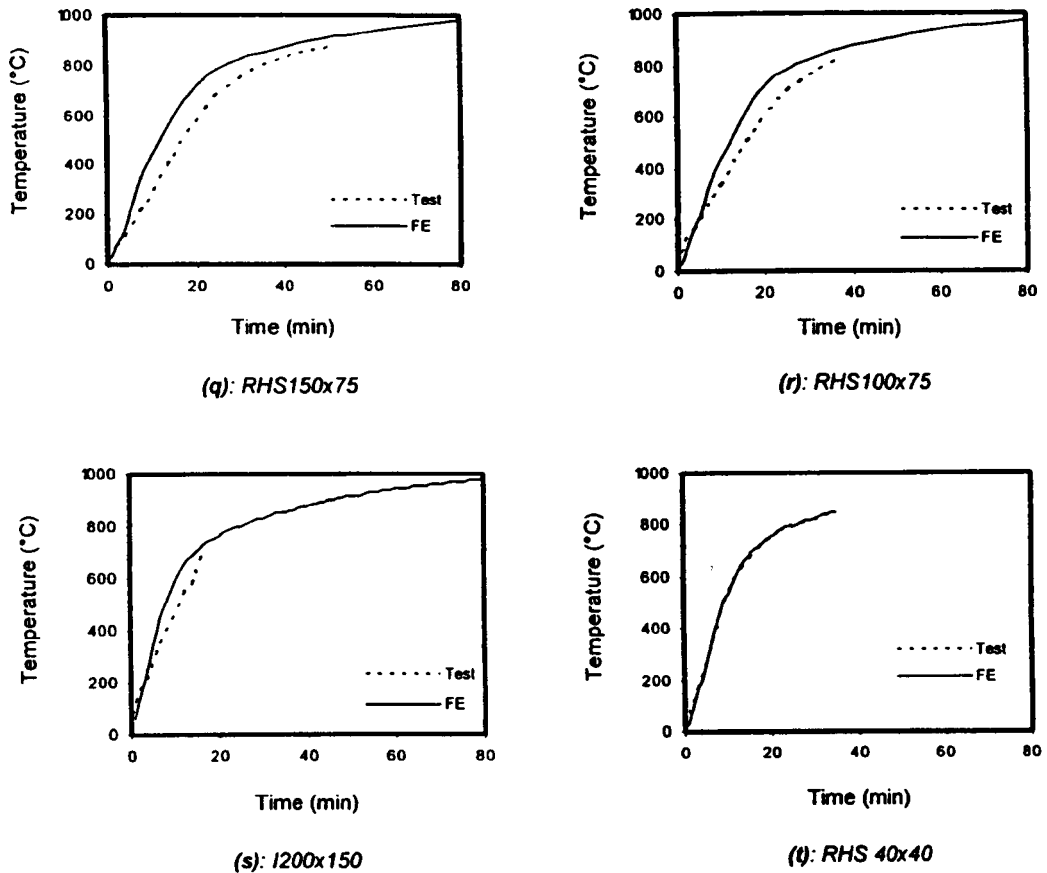
Figure 4.3: *Comparison between test and FE (without shadow effect) temperature development in sections exposed to fire on four sides.*

The measured furnace temperature-time curves were initially adopted in the finite element models in preference to that specified in ISO 834-1 (Eq. (4.6)) to minimise disparities between test and model behaviour due to differences in the basic fire curve. The comparisons of Figures 4.3(h) and 4.3(k) indicate the validity of this proposal, where the rapid increase in steel temperature observed in the test at around 850°C in response to a sharp increase in furnace temperature was also picked up by the finite element model.

Comparisons between test and FE results for each of the twenty specimens exposed to fire on all four sides are shown in Figures 4.3(a) to 4.3(t). In the finite element models, the measured furnace temperatures were applied directly to the surfaces of the models, and no account was made for shadow effects. The shadow effect refers to the reduced heat flux that inner surfaces of flanged sections receive due to their partial obscurity from the direct action of the fire. Cross-

sections with a convex profile (such as structural hollow sections) are therefore not subject to such effects. It is not straightforward to incorporate shadow effects directly into finite element models because of the uncertainty in specifying suitable reduced values for emissivity and the heat transfer coefficient in the partially obscured areas of the sections. It was therefore decided to allow for shadow effects indirectly by modifying the finite element results by means of the correction factor k_{sh} which is included in the calculation model (Eq. (4.9)) set out in EN 1993-1-2. The finite element temperatures were reduced by a proportion obtained from the calculation model temperatures determined with and without shadow effects. The correction factor k_{sh} introduces the concept of a box value for the section factor $[A_m/V]_b$ defined as the ratio between the exposed surface area of a notional bounding box to the section and the volume of steel (EN 1993-1-2, 2005), and may be determined from Eq. (4.7) for an I-section and from Eq. (4.8) in all other cases. Comparison between test and modified FE results with shadow effects is shown in Table 4.3.

$$k_{sh} = 0.9 [A_m/V]_b / [A_m/V] \qquad (4.7)$$

$$k_{sh} = [A_m/V]_b / [A_m/V] \qquad (4.8)$$

where $[A_m/V]_b$ is the box value for the section factor defined above and $[A_m/V]$ is the familiar section factor. The closer the box value of the section factor to the general section factor, the lesser the influence of the shadow effect – consequently, for hollow sections, the correction factor for the shadow effect k_{sh} equals unity. Values of k_{sh} for the twenty tested (and modelled) sections have been included in Table 4.1. Figure 4.4 demonstrates the significance of the shadow effect on temperature development for varying k_{sh} and varying A_m/V at 20 minutes exposure time to ISO-834-1. The graph shows that, in general, the shadow effect is relatively small (given typical values of k_{sh} and A_m/V, such as those in Table 4.1), but becomes more significant at low values A_m/V.
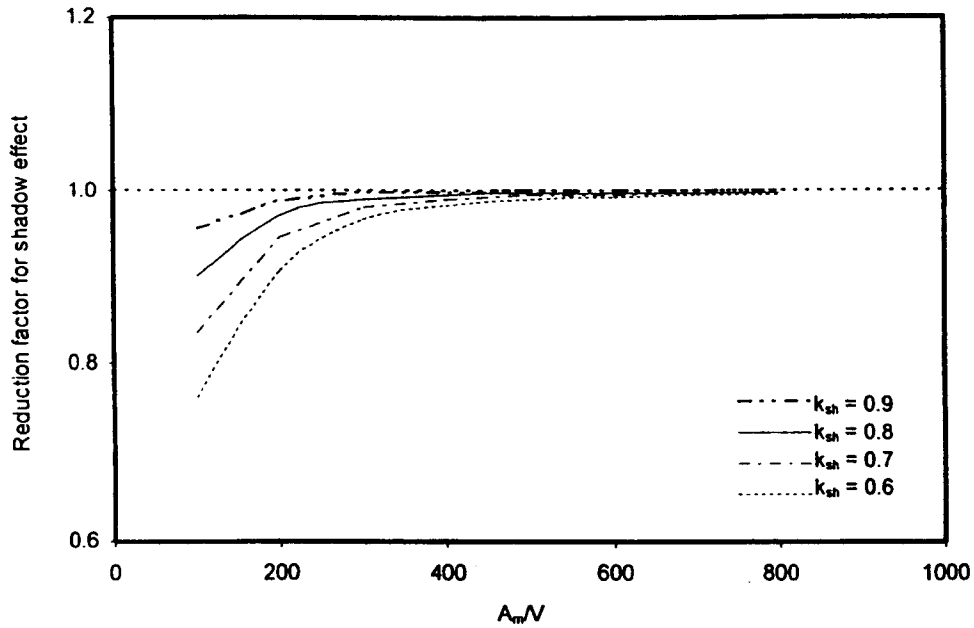
Figure 4.4: *Significance of shadow effect on temperature development for varying k_{sh} and A_m/V ratio at 20 minutes exposure time to ISO-834*

Table 4.3 compares the results of the modified finite element analyses including shadow effects (taking $\varepsilon_m = 0.4$ and $\alpha_c = 25$ W/m^{2}K) with those from the tests. The results show that the temperature development is over-predicted for all fire exposure times (between 10 and 60 minutes) using the recommended values for ε_m and α_c. Ignoring shadow effects led to a slightly greater over-prediction. A parametric study is conducted in the following section with the aim of investigating the sensitivity of temperature development in stainless steel sections to variation in ε_m and α_c and of identifying more appropriate values. It should be noted that the influence of the shadow effect on the results was very small, but it has been included to ensure that conservative values of ε_m and α_c were derived.

Table 4.3: *Comparison of FE/test temperatures for all structural stainless steel temperature development tests with $\alpha_c = 25 \ W/m^2K$ and $\varepsilon_m = 0.4$*

Specimens	FE/Test temperatures ($\alpha_c = 25 \ W/m^2K$, $\varepsilon_m = 0.4$) Time (mins)					
	10	20	30	40	50	60
L20x20x3	0.93	0.98	0.98	0.99	1.00	0.99
L100x100x10	0.96	1.03	1.02	1.02	1.01	1.01
U30x15x4	1.04	1.02	1.01	1.01	1.00	1.01
U160x65	0.86	0.97	1.00	1.00	1.00	0.99
T25x25x4	0.99	1.01	1.01	1.01	1.01	1.00
T100x100x10	0.92	1.01	1.01	1.00	1.00	1.00
I80x40	1.04	1.04	1.02	1.01	1.01	1.01
I120x64	0.93	1.06	1.04	1.01	1.00	0.99
I160x82	0.88	1.01	1.00	1.00	1.01	1.01
RHS 100x50x4	1.02	1.03	1.01	1.01	1.00	1.01
RHS 120x60x5	0.92	1.00	1.00	0.99	0.99	1.00
RHS 250x100x4	1.09	1.05	1.03	1.02	1.01	1.01
RHS 100x100x4	1.08	1.03	1.01	1.01	1.01	1.00
RHS 200x200x4	1.18	1.07	1.03	1.02	1.03	1.03
RHS 150x100x6	1.25	1.16	1.09	-	-	-
RHS 150x75x6	1.54	1.24	1.10	1.06	1.04	-
RHS 100x75x6	1.32	1.19	1.08	-	-	-
I200x150x6	1.02	1.32	-	-	-	-
RHS 40x40x4	1.02	1.01	1.01	-	-	-
RHS 100x100x4	0.89	0.99	0.97	-	-	-
Mean	1.04	1.06	1.02	1.01	1.01	1.00
Overall mean			1.03			
COV	0.162	0.088	0.034	0.015	0.014	0.010

4.4.4 Specimens exposed to measured furnace temperature on three sides (beams)

The temperature development of the three beam tests outlined in Table 4.2 (where the specimens were exposed to fire on three sides, with a concrete slab on the fourth) was modelled numerically, also adopting the heat transfer coefficient proposed in EN 1991-1-2 (α_c = 25 W/m^{2}K), the emissivity proposed in EN 1993-1-2 (ε_m = 0.4) and the measured furnace temperature-time relationships. Thermal actions were not applied to the top side of the upper flanges, which were protected by the concrete slab. Initially, no account was made for shadow effects or for the heat sink effect of the concrete slab.

In all three beam tests, thermocouples were peened into the surface of the specimens to measure the temperature development around the cross-section and along the length of the members. Temperatures were relatively uniform along the lengths of the member, but displayed more significant variation around the cross-sections. The positions of the thermocouples around the cross-sections and the corresponding measured temperature-time relationships are shown in Figures 4.5 to 4.7.

As anticipated, with no account for shadow effects or for the heat sink effect of the concrete slab, the observed temperature rises in the lower flanges of the beam were well predicted numerically, but there is less good correlation for other parts of the cross-section, particularly towards the concrete slab. In the following section, parametric studies are performed on the three stainless steel beams to improve the correlation between finite element and test behaviour.
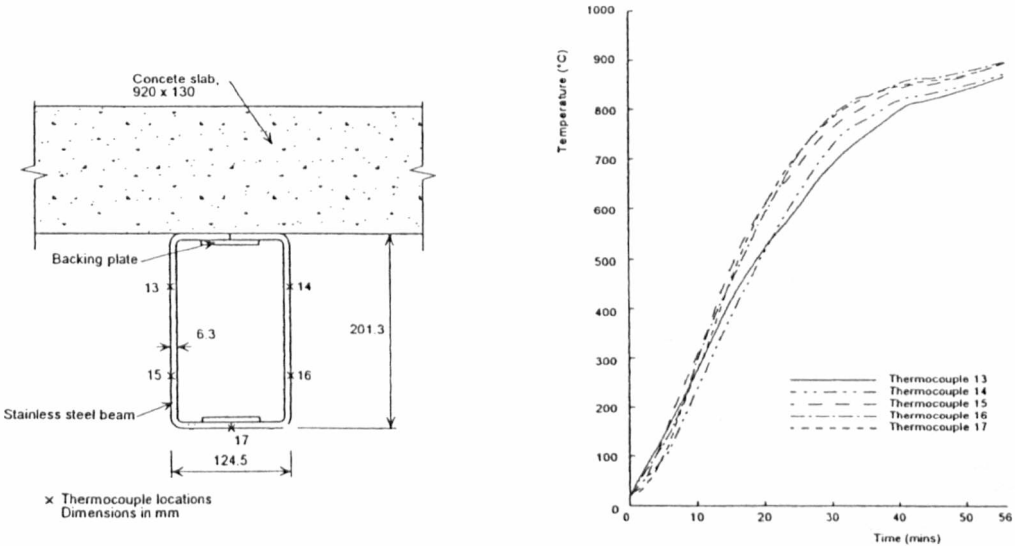
Figure 4.5: *Location of thermocouples and temperature development in 200×125×6.0 RHS beam*
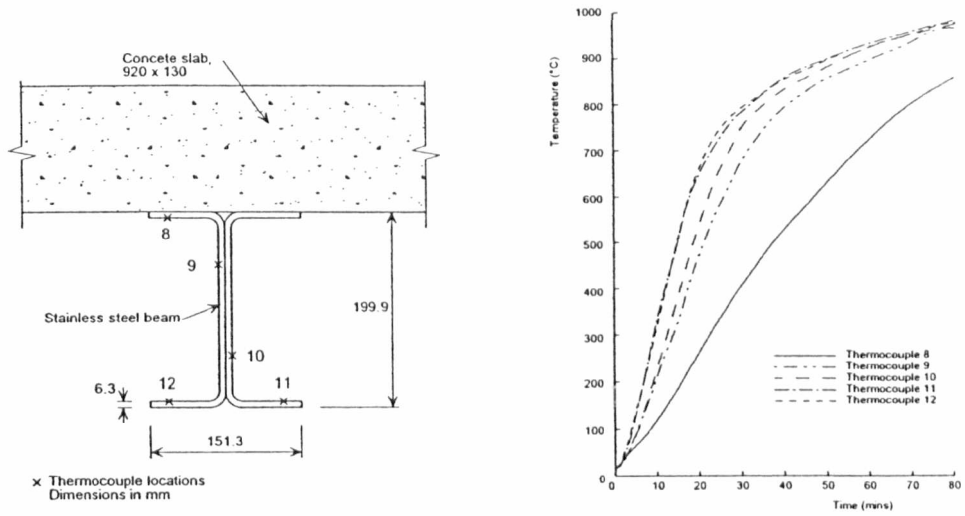
Figure 4.6: *Location of thermocouples and temperature development in 200×150×6 I-section beam*
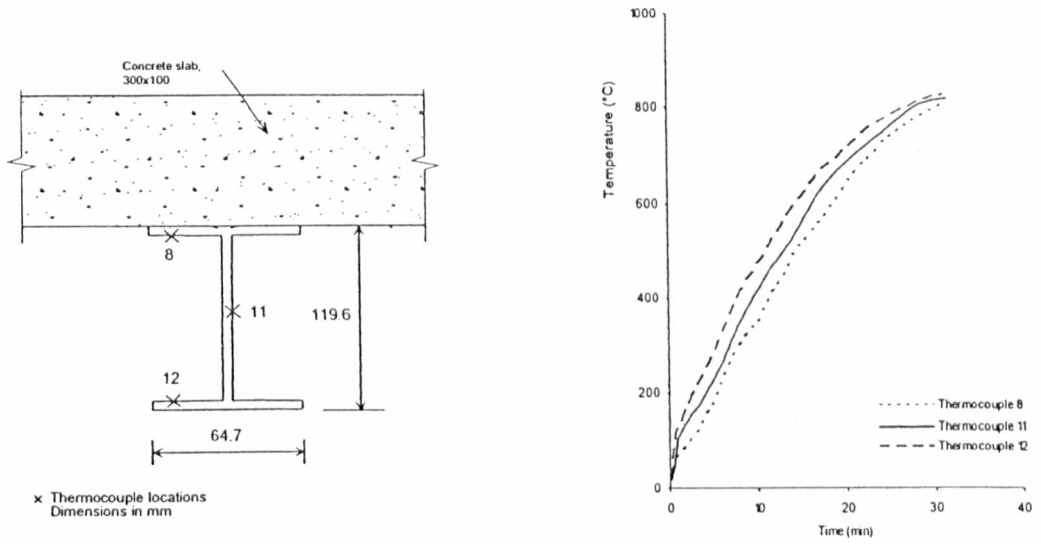
Figure 4.7: *Location of thermocouples and temperature development in 120×64 CTICM I-section beam*

94

4.5 PARAMETRIC NUMERICAL STUDIES

4.5.1 Specimens exposed to fire on all four sides

In this section, the sensitivity of the models to variation in heat transfer coefficient and emissivity is assessed. As an illustration of sensitivity, Figures 4.8 and 4.9 show numerically generated temperature-time curves for the RHS $150 \times 75 \times 6$ $(A_m/V = 168.2 \text{ m}^{-1})$ with varying values of heat transfer coefficient and emissivity. In Figure 4.8, emissivity is held constant $(\varepsilon_m = 0.4)$ and the heat transfer coefficient is varied between $\alpha_c = 1$ W/m^2K and $\alpha_c = 40$ W/m^2K. In Figure 4.9, the heat transfer coefficient is held constant $(\alpha_c = 25$ $W/m^2K)$ and emissivity is varied between 0.1 and 0.4. The Figures demonstrate, as expected, that lower values of both heat transfer coefficient and emissivity lead to slower temperature development, and that heat transfer by convection (controlled by the heat transfer coefficient) is more significant at low temperatures, whereas heat transfer by radiation (controlled by emissivity) is dominant at higher temperatures.
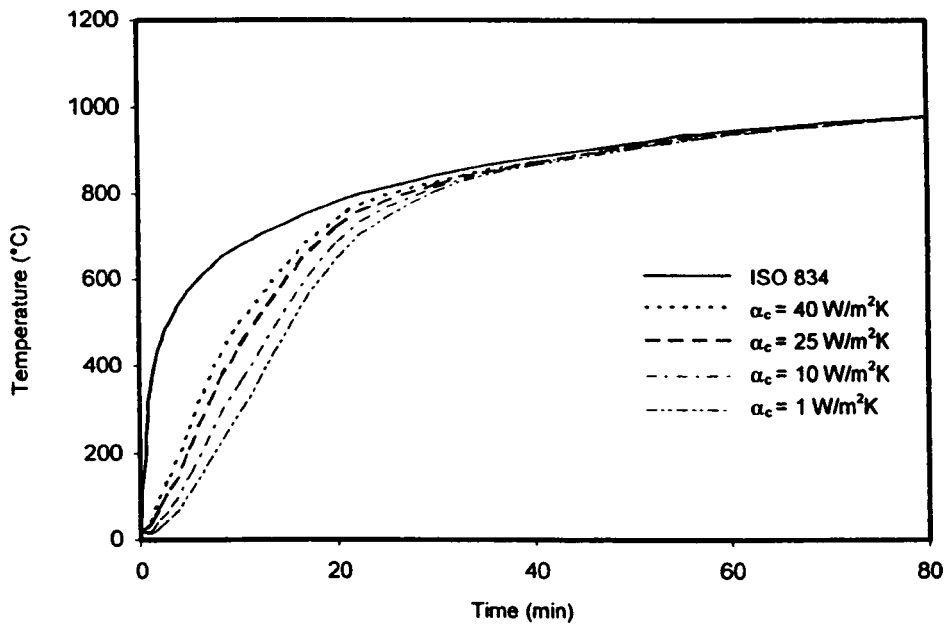
Figure 4.8: *Comparison of temperature development in RHS $150 \times 75 \times 6$ with constant emissivity ($\varepsilon_m = 0.4$) and varying heat transfer coefficient*
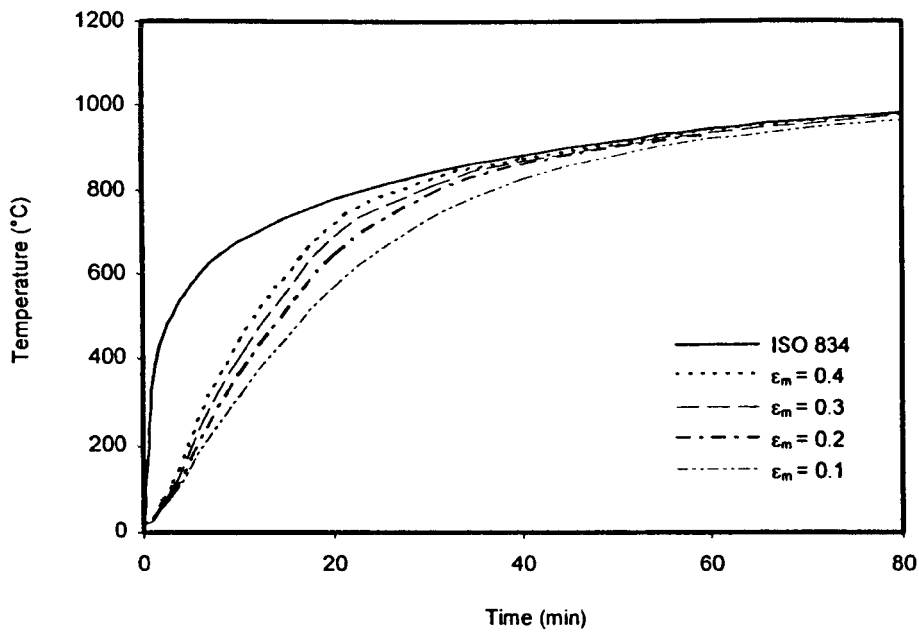
Figure 4.9: *Comparison of temperature development in RHS 150×75×6 with constant heat transfer coefficient (α_c = 25 W/m²K) and varying emissivity*

Figures 4.10 to 4.12 compare all test results with numerical predictions of varying heat transfer coefficient and emissivity. On the vertical axes, the temperature predicted by the FE model is divided by the temperature recorded in the test; thus a factor greater than unity indicates that the model is heating up more rapidly than the test. In general, it may be seen that temperature development is most sensitive to variation in both the heat transfer coefficient and emissivity at short exposure times – less than about 30 minutes - (i.e. at low temperatures). It may also be observed that the proposed codified values (ε_m = 0.4 and α_c = 25 W/m²K) result in a consistent over-prediction of the rate of temperature development; this is confirmed in Table 4.3 where comparisons for the individual test specimens are given.
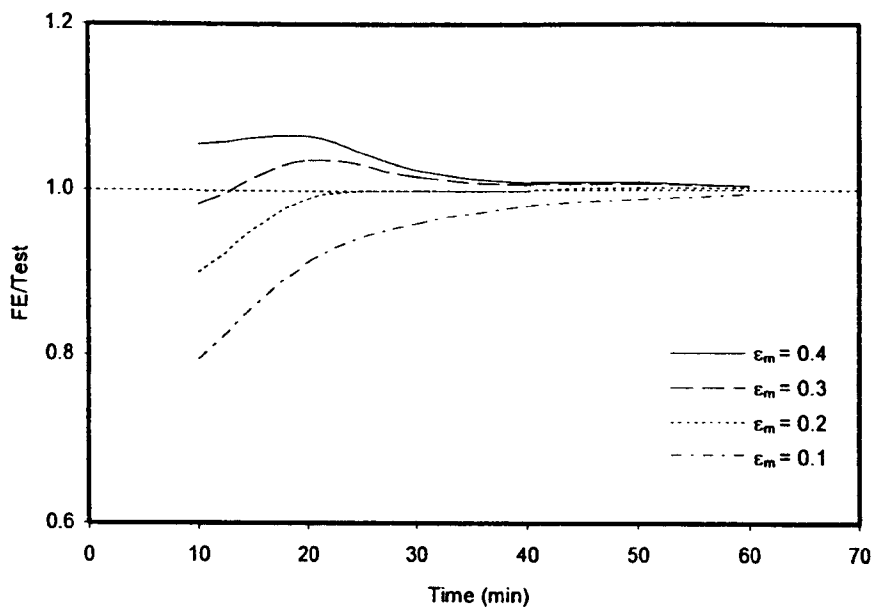
Figure 4.10: *Comparison of FE/test temperature for $\alpha_c = 25 \ W/m^2 K$ and varying emissivity*
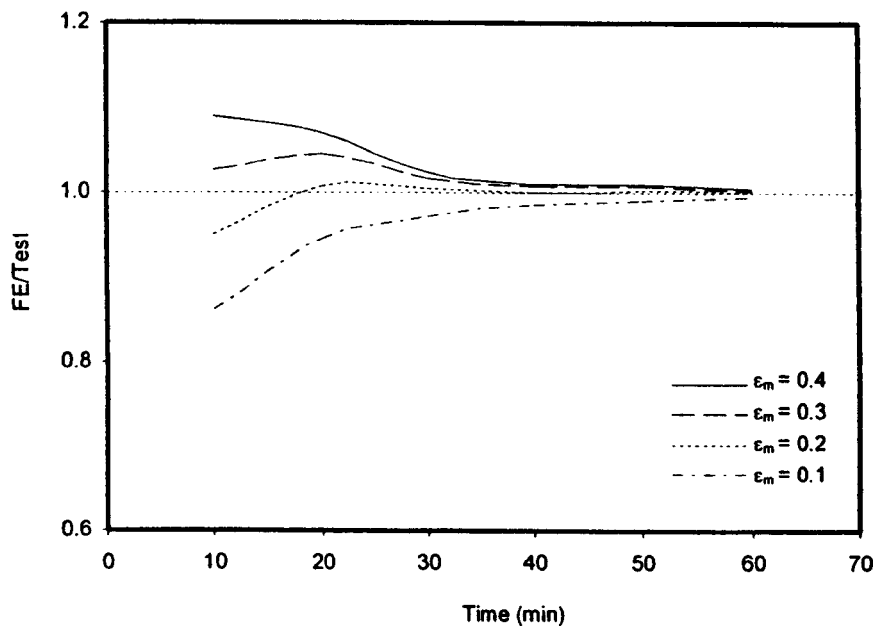
Figure 4.11: *Comparison of FE/test temperature for $\alpha_c = 30 \ W/m^2 K$ and varying emissivity*
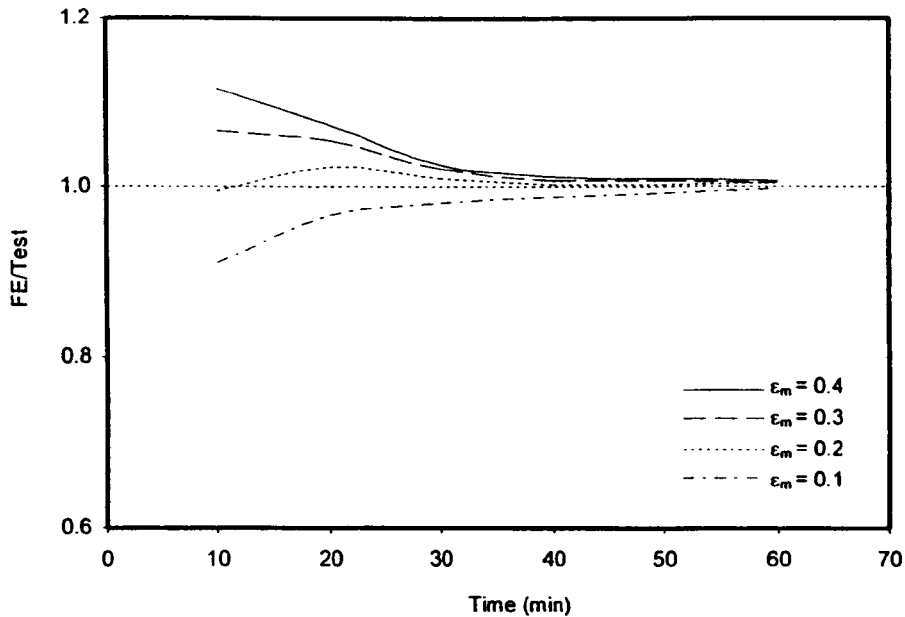
Figure 4.12: *Comparison of FE/test temperature for* $\alpha_c = 35$ W/m^{2}K *and varying emissivity*

Tables 4.4 to 4.6 present the mean predicted (FE) divided by test temperatures for the twenty test specimens at ten minute intervals of fire exposure time, along with the corresponding coefficient of variation of the predictions. The parametric studies show that the temperature development of structural stainless steel sections exposed to fire on all four sides is best predicted by taking emissivity $\varepsilon_m = 0.2$ and the heat transfer coefficient $\alpha_c = 35$ W/m^2 K. These values produce a predicted-to-test temperature ratio of unity and exhibit the minimum of scatter, and it is therefore proposed that these be adopted in place of those currently recommended in EN 1991-1-2 and EN 1993-1-2. The influence of adopting the proposed coefficients on the fire resistance of structural members is assessed in a following section.

Table 4.4: *Mean FE/test temperature values from table 4.3 for* $\alpha_c = 25\ W/m^2 K$ *and varying emissivity* ε_m

Time (mins)	FE/Test, $\alpha_c = 25$ W/m^2 K			
	$\varepsilon_m = 0.4$	$\varepsilon_m = 0.3$	$\varepsilon_m = 0.2$	$\varepsilon_m = 0.1$
10	1.06	0.98	0.90	0.80
20	1.06	1.04	0.98	0.91
30	1.02	1.02	1.00	0.96
40	1.01	1.01	1.00	0.98
50	1.01	1.01	1.00	0.99
60	1.01	1.00	1.00	0.99
Mean	1.03	1.01	0.98	0.94
COV	0.025	0.017	0.041	0.081

Table 4.5: *Mean FE/test temperature values from table 4.3 for* $\alpha_c = 30\ W/m^2 K$ *and varying emissivity* ε_m

Time (mins)	FE/Test, $\alpha_c = 30$ W/m^{2}K			
	$\varepsilon_m = 0.4$	$\varepsilon_m = 0.3$	$\varepsilon_m = 0.2$	$\varepsilon_m = 0.1$
10	1.09	1.03	0.95	0.86
20	1.07	1.05	1.01	0.94
30	1.03	1.02	1.00	0.97
40	1.01	1.01	1.00	0.99
50	1.01	1.01	1.00	0.99
60	1.01	1.00	1.00	1.00
Mean	1.04	1.02	0.99	0.96
COV	0.035	0.016	0.022	0.054

Table 4.6: Mean FE/test temperature values from table 4.3 for $\alpha_c = 35$ W/m²K and varying emissivity ε_m

Time (mins)	FE/Test, $\alpha_c = 35$ W/m² K			
	$\varepsilon_m = 0.4$	$\varepsilon_m = 0.3$	$\varepsilon_m = 0.2$	$\varepsilon_m = 0.1$
10	1.12	1.07	1.00	0.91
20	1.07	1.05	1.02	0.97
30	1.03	1.02	1.01	0.98
40	1.01	1.01	1.00	0.99
50	1.01	1.01	1.00	0.99
60	1.01	1.01	1.00	1.00
Mean	1.04	1.03	1.01	0.97
COV	0.043	0.026	0.009	0.034

4.5.2 Specimens exposed to fire on three sides

The temperature development in three stainless steel beams exposed to fire on three sides and supporting a concrete slab on the fourth was recorded experimentally, as described in the previous section, and initially modelled numerically ignoring shadow effects and the heat sink effect of the concrete. Large discrepancies between test and model behaviour and indicate the importance of the influence of the concrete slab.

Modelling of the heat transfer between a structural steel section and an adjoining concrete slab and indeed within the concrete slab itself is complex, because of the large number of uncertainties that exist. These include details of the interface between the materials, the conductivity, density and specific heat of the concrete slab, the moisture content of the concrete and values of emissivity and heat transfer coefficients. Given the scarcity in test results on stainless steel beams supporting concrete slabs, and uncertainties in many of the above parameters, it was not deemed appropriate to conduct an extensive numerical analysis of the beam tests. Detailed numerical heat transfer analyses of composite slabs in fire, including thorough parametric studies have been performed by Lamont et al. (2001). Nonetheless, improved correlation between the test results and numerical results was sought using assumed values for the required parameters.

The density of the concrete slabs in the three tests was calculated based on the reported self-weights and nominal dimensions (Baddoo and Gardner, 2000) to be approximately 2000 kg/m^3. The thermal conductivity and specific heat of the concrete slab were assumed to be 0.7 W/mK and 700 J/kgK, respectively, based on values adopted by Lamont et al. (2001). The heat transfer coefficients for the top and bottom of the concrete slab were taken as 10 and 5 W/m^2 K, respectively, whilst the emissivity of the concrete was taken as 0.6, all based on the reference values of Lamont et al. (2001). Values for the emissivity and heat transfer coefficient for the fully exposed lower flanges of the beams, and the webs of the RHS beam, were taken as those generated in the present study for stainless steel sections exposed to fire on all four sides (ε_m = 0.2 and α_c = 35 W/m^2 K). For the partially obscured web and upper flange of the I-sections beams, values of emissivity and heat transfer were adjusted in order to improve the fit with test results, a technique adopted by Wang (1995). Reasonable agreement was achieved with the adoption of the values given in Table 4.7, as shown in Figures 4.13 to 4.15.

Table 4.7: *Distribution of α_c and ε_m from parametric study on beams*

Component	α_c (W/m^{2}K)	ε_m
Concrete slab (bottom)	5	0.6
Concrete slab (top)	10	0.6
Beam (I-section web)	10	0.2
Beam (lower flange and RHS web)	35	0.2
Beam (I-section upper flange)	10	0.2
Beam (I-section lower flange)	35	0.2
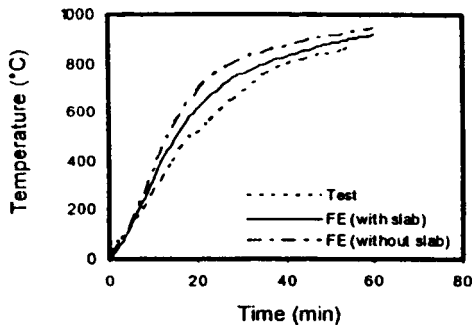
(a): Thermocouple 13
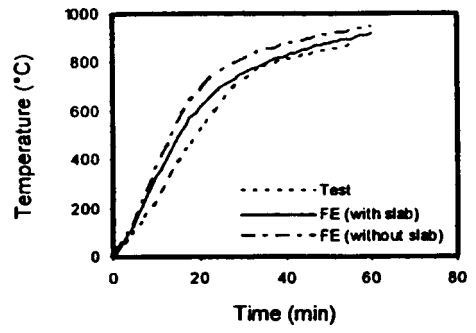
(b): Thermocouple 14
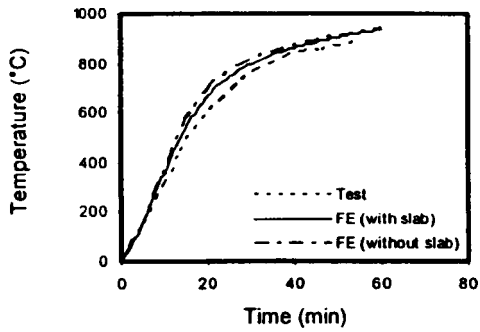
(c): Thermocouple 15
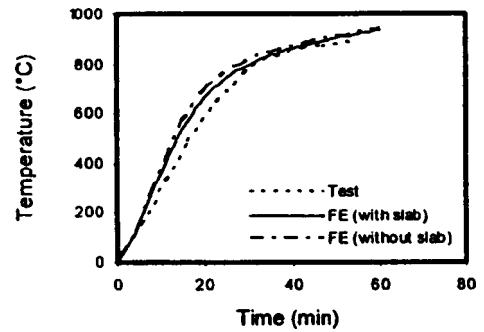
(d): Thermocouple 16
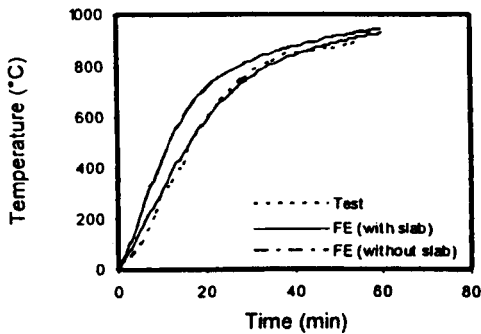
(e): Thermocouple 17

Figure 4.13: *Comparison between FE and test temperature development in 200x125x6.0 RHS beam section at different thermocouple locations*
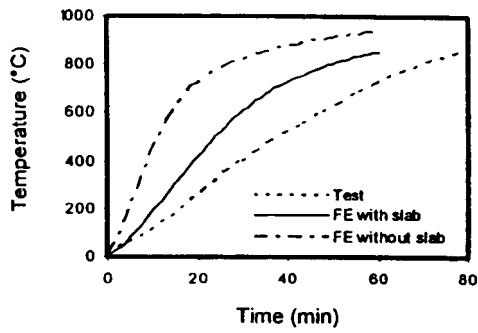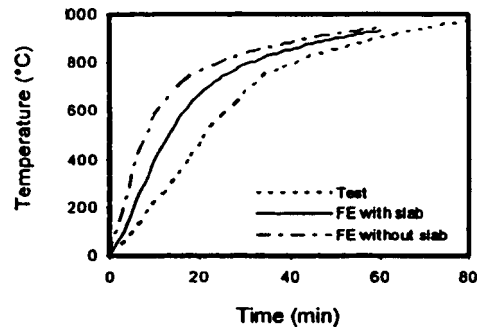
(a): Thermocouple 8

(b): Thermocouple 9
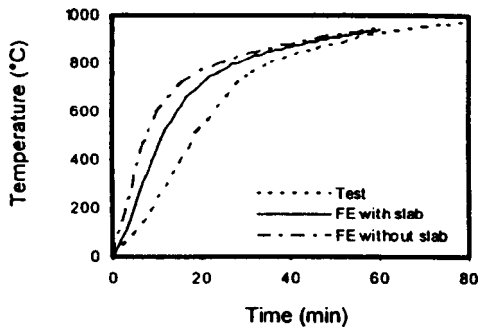
(c): Thermocouple 10
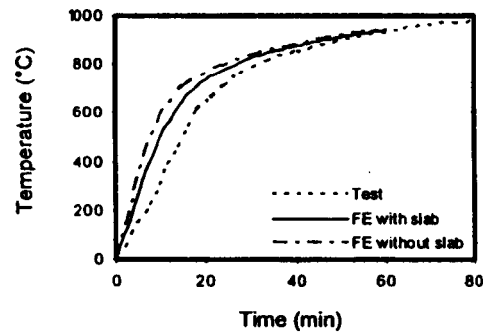
(d): Thermocouple 11
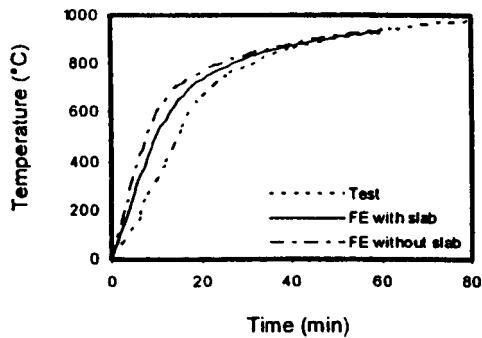
(e): Thermocouple 12

Figure 4.14: *Comparison between FE and test temperature development in 200X150X6 I-section beam at different thermocouple locations*
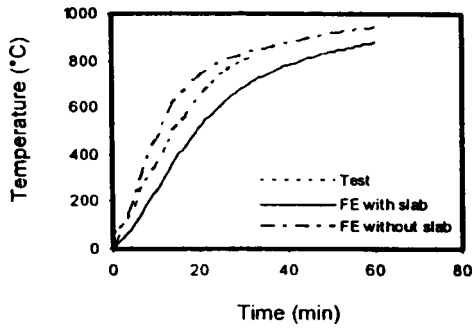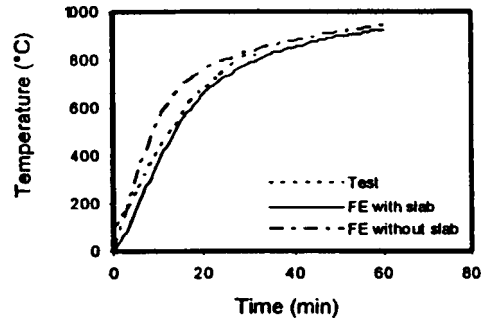
(a): Thermocouple 8

(b): Thermocouple 11
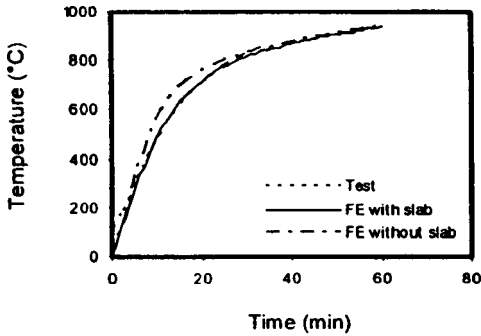
(c): Thermocouple 12

Figure 4.15: *Comparison between FE and test temperature development in 120x64 CTICM I-section beam at different thermocouple locations*

Despite reasonable agreement between finite element and test behaviour, the results of the beam analyses are not included in the determination of suitable values for emissivity and the heat transfer coefficient, due primarily to the uncertainties surrounding the properties of the concrete slab and the limited number of test results. The influence of a concrete slab on the temperature development of a structural stainless steel section would not be expected to be significantly different from its influence on a carbon steel section. It is therefore considered that the carbon steel current practice of employing the adaptation factor κ_1 to allow for non-uniform temperature in the calculation of member resistances may be equally applicable to stainless steel beams supporting a concrete or composite slab.

4.6 Calculation Model

Temperature development in unprotected and uniformly heated steelwork is determined in EN 1993-1-2 (2005) using the simple calculation model of Eq. 4.9, in which $\Delta\theta_{a,t}$ is the increase in temperature (°C) in a time increment Δt (in seconds).

$$\Delta\theta_{a,t} \quad = \quad k_{sh} \frac{A_m/V}{c_a \rho_a} \dot{h}_{net,d} \Delta t \tag{4.9}$$

where k_{sh} is the correction factor for the shadow effect, A_m/V is the section factor (m^{-1}), c_a is the specific heat of the material, ρ_a is the material density (kg/m^3), and $\dot{h}_{net,d}$ is the design value of the net heat flux per unit area (W/m^2 K).

Calibration of the calculation model (i.e. selection of suitable values for emissivity and the heat transfer coefficient to determine the net heat flux) for structural carbon steel was originally conducted during the development of ENV 1991-1-2 (Kay et al, 1996) and was re-evaluated for the conversion to EN 1991-1-2 (Kirby, 2004). The calculation model would not be expected to yield exactly the same results as the FE model because of the simplification of using the A_m/V ratio to represent the profile of the section, and assuming uniform temperature throughout the section (despite elements of different form and thickness). However, for common geometries the errors will be very small.

It is difficult to validate the calculation model directly against the tests, because the furnace temperatures did not always exactly follow the standard fire curve, and the measured furnace temperature cannot be used easily in the calculation model because there is no simple formulation to describe the measured furnace temperature, as there is with ISO 834-1 (Eq. (4.6)). However, having validated the numerical model against the test data, it is possible to compare the calculation model against the test results where the measured furnace temperature closely followed ISO 834-1 and against finite element results generated with the ISO 834-1 fire curve. An example of this comparison, using the proposed values for emissivity ($\varepsilon_m = 0.2$) and the heat transfer coefficient ($\alpha_c = 35$ W/m^{2}K) is shown in Figure 4.16. The resultant temperature-time curves from the finite element model and the calculation model coincide.

(a): L20x20

(b): L100x100

(c): T25x25
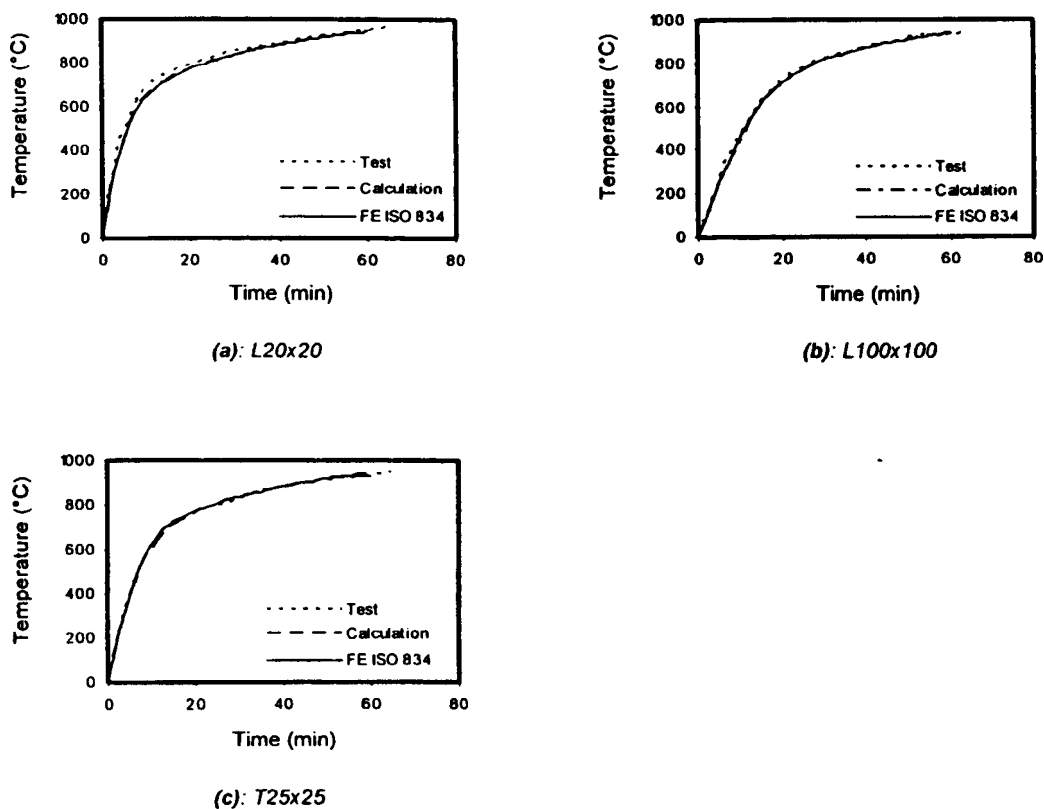
Figure 4.16: *Comparison between FE, calculation model and test temperature development*

4.7 INFLUENCE OF MODIFIED COEFFICIENTS ON FIRE RESISTANCE OF STRUCTURAL MEMBERS

Based on comparisons with all available test data, revised values for the heat transfer coefficient and emissivity of structural stainless steel sections have been proposed. Figure 4.17 compares the temperature development in a structural section (A_m/V = 200 m^{-1}) made of stainless steel (with the current and proposed values for the emissivity and heat transfer coefficient) and of carbon steel. For carbon steel, the emissivity and heat transfer coefficient were taken as 0.7 (as recommended by EN 1993-1-2) and 25 W/m^{2}K (as recommended by EN 1991-1-2), respectively, and the mechanical and thermal properties were taken as described previously in this thesis. The two curves were generated using the calculation model of Eq. (4.9). The comparison shows the effect of the proposed values for emissivity and the heat transfer coefficient on the temperature development in structural stainless steel sections, and indicated

106

generally that a stainless steel section heats up slightly less rapidly than a similar carbon steel section.
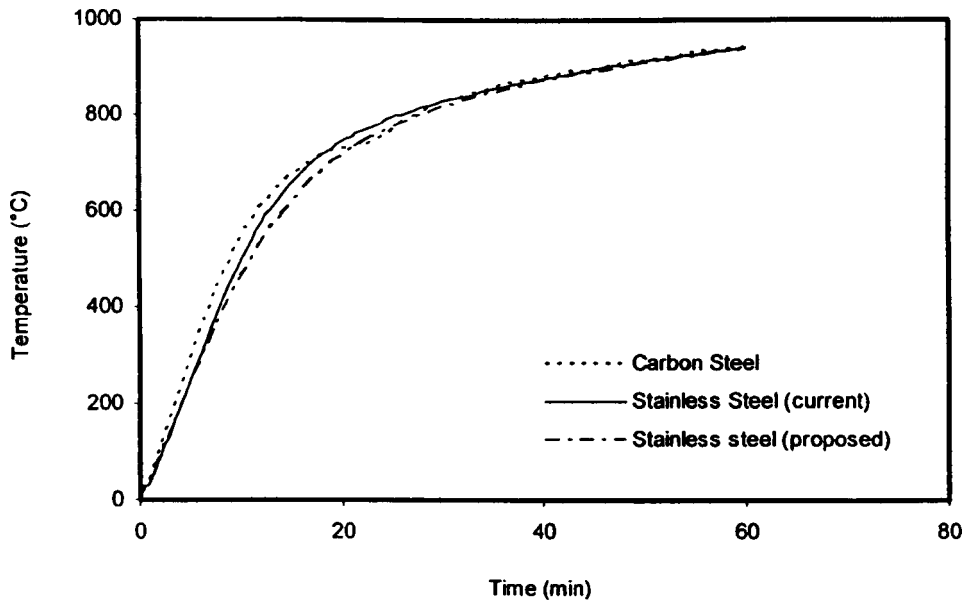
Figure 4.17: *Temperature development of stainless steel and carbon steel*

In the remainder of this section, the significance of the proposed modified values for emissivity and the heat transfer coefficient on the fire resistance of structural members is assessed. The critical temperature and fire resistance of six stainless steel columns (Baddoo and Gardner, 2000; Gardner and Baddoo, 2006) are predicted using the design method of EN 1993-1-2, adopting the emissivity and the heat transfer coefficient recommended in the Code, and those proposed in the present study. The results are given in Table 4.8, and demonstrate that for all of the members considered, use of the proposed coefficients yields improved predictions of test performance. Critical temperatures vary with the use of different values for emissivity and heat transfer coefficient simply because of the requirement to present fire resistance to the nearest minute. Average enhancements in fire resistance of 10% are achieved.

Nominal Section Size of Column	Critical temperature (°C)			Fire Resistance (minutes)		
	Test	Eurocode[a]	Proposed[b]	Test	Eurocode[a]	Proposed[b]
150x100x6 RHS	801	731	737	32	20	23
150x75x6 RHS	883	851	851	51	35	37
100x75x6 RHS	806	759	763	36	22	25
200x150x6][	571	392	377	14	7	7
100x100x4 SHS	835	778	783	27	22	24
200x200x4 SHS	820	513	523	24	9	10

Notes: [a] $\varepsilon_m = 0.4$, $\alpha_c = 25$ W/m^{2}K (as recommended by EN 1993-1-2 and EN 1991-1-2, respectively)

[b] $\varepsilon_m = 0.2$, $\alpha_c = 35$ W/m^{2}K (proposed herein)

4.8 CONCLUDING COMMENTS

Whether fire resistant design is based on a prescriptive approach or a performance based approach, or indeed whether isolated elements or complete structural assemblages are considered, accurate and efficient determination of the temperature development within a structural member upon subjection to fire is paramount. The physical properties of stainless steel that influence temperature development have been discussed and the suitability of the emissivity and heat transfer coefficient currently recommended in the structural Eurocodes has been examined. Following analysis of all available test data on structural stainless steel sections and numerically generated results, revised values for the emissivity and heat transfer coefficient of structural stainless steel members exposed to fire are proposed. In the temperature development calculation model of EN 1993-1-2, it is proposed that emissivity be taken as 0.2 (in place of 0.4) and the heat transfer coefficient be taken as 35 W/m^{2}K (in place of 25 W/m^{2}K). This achieves better correlation between predicted and measured temperature development in structural stainless steel sections and results in average enhancements of 10% in fire resistance.

CHAPTER 5

NUMERICAL MODELLING

5.1 INTRODUCTION

This chapter examines existing test results and presents the results of a numerical parametric study, using ABAQUS on stainless steel columns in fire. Sensitivity to local and global initial geometric imperfections, enhancement of corner strength due to cold-work and partial protection of the column ends is assessed. Parametric studies to explore the influence of variation in local cross-section slenderness, global member slenderness and load level are described.

At elevated temperatures, stainless steel offers better retention of strength and stiffness than structural carbon steel, due to the beneficial effects of the alloying elements. This behaviour is reflected in EN 1993-1-2 (2005), as shown in Figures 5.1 and 3.3. The strength reduction factors shown in Figure 5.1 are for grade 1.4301 (304) austenitic stainless steel, the most widely adopted grade for structural applications, whereas the stiffness reduction factors of Figure 3.3 are common to all grades. Strength reduction factors are defined at two strain levels: $k_{2\%,\theta}$ is the elevated temperature strength at 2% total strain $f_{2\%,\theta}$, normalised by the room temperature 0.2% proof strength f_y, whilst $k_{0.2p,\theta}$ is the elevated temperature 0.2% proof strength $f_{0.2p,\theta}$, normalised

by the room temperature 0.2% proof strength f_y. The stiffness reduction factor $k_{E,\theta}$ is defined as the elevated temperature initial tangent modulus E_θ, normalised by the initial tangent modulus at room temperature E_a. Other thermal properties, including those which influence temperature development are discussed in Chapters 3, 4 and 7. It is worth noting that the minimum specified room temperature 0.2% proof strength f_y for the most common structural grades of austenitic stainless steel typically ranges between 210 and 240 N/mm^2, whilst the Young's modulus is 200000 N/mm^2 (EN 10088-2, 2005).
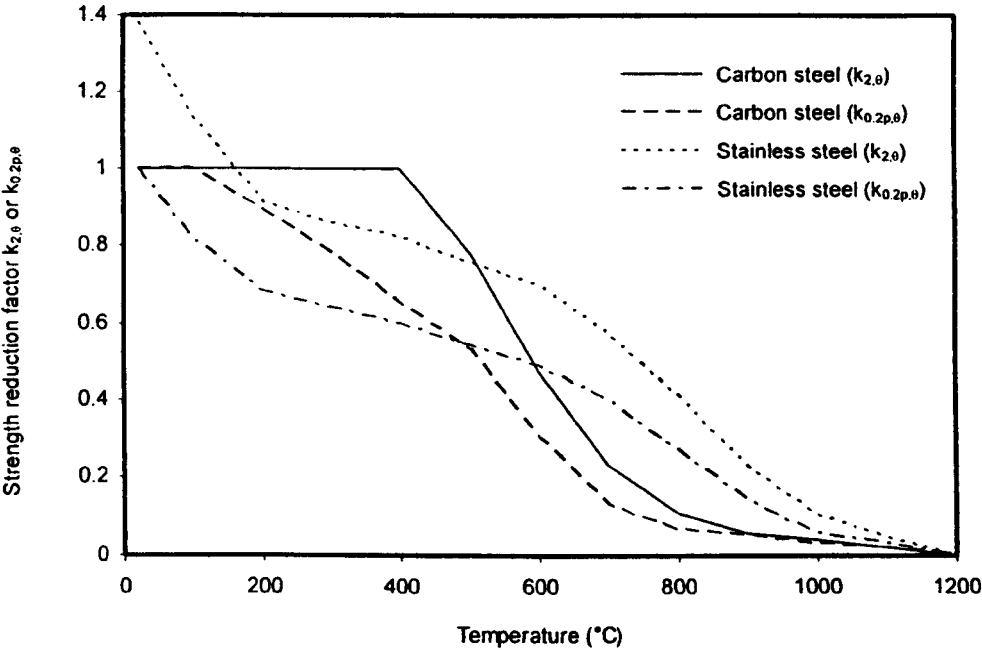
Figure 5.1: *Comparison of strength reduction at elevated temperatures*

5.2 REVIEW OF FIRE TESTS ON STRUCTURAL STAINLESS STEEL MEMBERS

A number of recent experimental studies of the response of unprotected stainless steel structural members exposed to fire have been performed. All tests are summarised in this section, and utilised in Chapter 6 for comparison with existing design methods and for the development of revised design provisions. A selection of the tests is replicated numerically in section 5.3 of this Chapter, forming the basis for parametric studies.

Fire tests on a total of 23 austenitic stainless steel columns (Baddoo and Gardner, 2000; Gardner and Baddoo, 2006; Ala-Outinen and Oksanen, 1997; Ala-Outinen, 1999; Zhao and Blanguernon, 2004) (where failure was by flexural buckling) and 6 stub columns (Ala-Outinen, 2005) have been reported. A summary of the tests is provided in Tables 5.1 and 5.2. Nominal section sizes, cross-section classifications, boundary conditions, applied loads and critical temperatures have been tabulated. Those tests in Table 5.1 marked with superscript 'a' or 'b' were reported in most detail and together with those of Table 5.2, have been used to validate the numerical models, as described in the following section of this chapter.

Of the 23 column buckling tests detailed in Table 5.1, four had fixed boundary conditions whilst the remainder were pin-ended. All column buckling tests were performed on hollow sections (19 rectangular hollow sections (RHS) and 3 circular hollow sections (CHS)) with the exception of one I-section, made up of a pair of channel sections welded back-to-back. The 6 stub column tests given in Table 5.2 were all Class 4 rectangular hollow sections. All tests were anisothermal, whereby the load was held at a constant level and the temperature was increased (generally following the standard fire curve of ISO 834-1 (1999)) until failure.

Table 5.1: *Summary of tests conducted on structural stainless steel columns*

Nominal section size (mm)	Cross-section classification	Boundary conditions	$\overline{\lambda}$	Applied load (kN)	Critical temperature (°C)
RHS 150×100×6[a]	Class 1	Fixed	0.49	268	801
RHS 150×75×6[a]	Class 1	Fixed	0.65	140	883
RHS 100×75×6[a]	Class 1	Fixed	0.65	156	806
][200×150×6[a]	Class 4	Fixed	0.66	413	571
RHS 100×100×4[a]	Class 2	Pinned	1.27	80	835
RHS 200×200×4[a]	Class 4	Pinned	0.51	230	820
RHS 40×40×4 (T1)[b]	Class 1	Pinned	1.07	45	873
RHS 40×40×4 (T2)[b]	Class 1	Pinned	1.07	129	579
RHS 40×40×4 (T3)[b]	Class 1	Pinned	1.07	114	649
RHS 40×40×4 (T4)[b]	Class 1	Pinned	1.07	95	710
RHS 40×40×4 (T5)[b]	Class 1	Pinned	1.07	55	832
RHS 40×40×4 (T7)[b]	Class 1	Pinned	1.07	75	766
RHS 40×40×4[c]	Class 1	Pinned	1.02	102	720
RHS 40×40×4[c]	Class 1	Pinned	1.02	73	834
RHS 40×40×4[c]	Class 1	Pinned	1.02	63	873
RHS 30×30×3[c]	Class 1	Pinned	1.40	41	610
RHS 30×30×3[c]	Class 1	Pinned	1.40	33	693
RHS 30×30×3[c]	Class 1	Pinned	1.40	21	810
CHS 33.7×2[c]	Class 1	Pinned	1.26	26	668
CHS 33.7×2[c]	Class 1	Pinned	1.26	12	850
CHS 33.7×2[c]	Class 1	Pinned	1.26	20	716
RHS 100×100×3[d]	Class 4	Pinned	1.02	52	835
RHS 100×100×3[d]	Class 4	Pinned	1.20	52	880

Notes: [a] Tests reported in Baddoo and Gardner (2000) and Gardner and Baddoo (2006) and replicated numerically in section 5.3

[b] Tests reported in Ala-Outinen and Oksanen (1997) and replicated numerically in section 5.3

[c] Tests reported in Ala-Outinen (1999)

[d] Tests reported in Zhao and Blanguernon (2004)

Table 5.2: *Summary of tests conducted on structural stainless steel stub columns*

Nominal section size (mm)	Cross-section classification	Boundary conditions	Applied load (kN)	Critical temperature (°C)
RHS 200×200×5	Class 4	Fixed	694	609
RHS 200×200×5	Class 4	Fixed	567	685
RHS 200×200×5	Class 4	Fixed	463	768
RHS 150×150×3	Class 4	Fixed	248	590
RHS 150×150×3	Class 4	Fixed	203	678
RHS 150×150×3	Class 4	Fixed	165	720

5.3 DEVELOPMENT OF NUMERICAL MODELS

5.3.1 General

A numerical modelling study was performed to gain further insight into the buckling response of stainless steel compression members in fire, and to investigate the influence of key parameters. The finite element software package ABAQUS (2003) was employed throughout the study. Analyses were conducted to simulate 12 column buckling fire tests (as indicated in Table 5.1): 4 fixed-ended and 2 pin-ended columns reported in Baddoo and Gardner (2000) and Gardner and Baddoo (2006), and 6 pin-ended columns reported in Ala-Outinen and Oksanen (1997), and six stub column fire tests reported by Ala-Outinen (2005). Numerical modelling of the column buckling tests is described in Section 5.3.2 to 5.3.6, whilst stub column modelling is covered in Section 5.3.7. Subsequent sensitivity studies were performed to investigate the influence of local and global initial geometric imperfections, cold-worked corner material properties and partial protection of the column ends. Parametric studies were conducted to assess variation in local cross-section slenderness, global member slenderness and load level, and are described in Section 5.3.8.

The stainless steel members were modelled using the shell elements S4R, which have four corner nodes, each with six degrees of freedom, and are suitable for thick or thin shell applications (ABAQUS, 2003). These elements have been demonstrated to perform well in similar applications, as reported by Feng et al. (2003). A mesh convergence study was

performed to identify an appropriate mesh density to achieve suitably accurate results whilst maintaining practical computation times. Models with a range of mesh sizes from two to ten elements across the cross-section width yielded very similar results. Five elements across each plate width and an aspect ratio of close to unity (defining mesh size in the length direction) were adopted. Test boundary conditions were replicated by restraining suitable displacement and rotation degrees of freedom at the column ends, and through the use of constraint equations. A typical finite element fixed-ended column model is shown in Figure 5.2.

Figure 5.2: *Undeformed shape of finite element column model*

The fire tests described in section 5.2 were performed anisothermally. This was reflected in the numerical modelling by performing the analyses in two steps: in the first step, load was applied to the column at room temperature, and in the second step, temperature was increased following the measured temperature-time relationships until failure. It should be noted that the RHS 40×40×4 test specimens reported in Ala-Outinen and Oksanen (1997) did not follow the standard fire curve of ISO 834-1 (1999); instead, a bespoke, bi-linear temperature-time relationship was used – this relationship was also included in the numerical study by employing the measured temperature-time data (Ala-Outinen and Oksanen, 1997).

5.3.2 Material modelling

Material modelling represents one of the most important aspects of a FE simulation. Inappropriate definition of material behaviour will significantly hinder the ability of a model to replicate observed structural response. In the present study, material modelling was based on a multi-linear fit to measured elevated temperature stress-strain data. The measured stress-strain curves of Ala-Outinen and Oksanen (1997) were rather erratic, particularly at low strains, with regions where increasing strain was met with increasing stiffness. Thus in order to smooth the stress-strain relationship, a compound Ramberg-Osgood formulation was used to represent the experimental data. The adopted compound Ramberg-Osgood model has been shown to be capable of very accurately representing measured stress-strain data of similar form (Gardner and Ashraf, 2006). The measured stress-strain data and corresponding compound Ramberg-Osgood curves for 200°C and 600°C are shown in Figure 5.3.
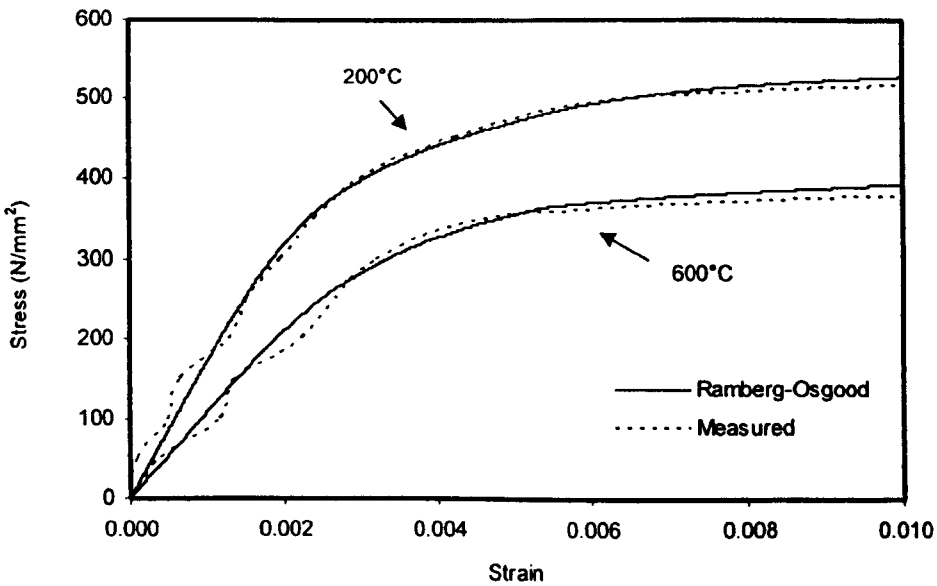
Figure 5.3: *Stress-strain curves using compound Ramberg-Osgood formulation at elevated temperatures*

ABAQUS (2003) requires that the material stress-strain relationship is defined in terms of true stress σ_{true} and log plastic strain ε_{ln}^{pl}, as defined by Eqs. (5.1) and (5.2), where σ_{nom} and ε_{nom} are engineering stress and strain, respectively and E is Young's modulus.

$$\sigma_{true} = \sigma_{nom}(1 + \varepsilon_{nom})$$

(5.1)

$$\varepsilon_{ln}^{pl} = \ln(1 + \varepsilon_{nom}) - \frac{\sigma_{true}}{E} \qquad (5.2)$$

The material coefficient of thermal expansion was taken from EN 1993-1-2 (2005) for all models. The models described in this chapter were free to expand against the load (as in the tests); restrained members are investigated numerically in Chapter 7.

5.3.3 Corner material properties

The mechanical properties of stainless steel are sensitive to the level of cold-work, resulting in the corner regions of cold-formed sections having 0.2% proof strengths significantly higher than the 0.2% proof strengths of the flat regions. Failure to allow for these enhanced strength regions in numerical modelling and design leads to under-prediction of load carrying capacity (Gardner and Nethercot, 2004), or in the context of the current study, under-prediction of fire resistance.

Based upon tensile tests on material extracted from the corner regions of cold-formed stainless steel cross-sections, expressions for the prediction of the corner material strength have been developed in (Ashraf et al, 2005). It was proposed that the 0.2% proof strength of the corner material $\sigma_{0.2,c}$ for both roll-forming and press-braking may be approximated by Eq. (5.3).

$$\sigma_{0.2,c} = \frac{1.881\sigma_{0.2,v}}{\left(\dfrac{r_i}{t}\right)^{0.194}} \qquad (5.3)$$

where $\sigma_{0.2,v}$ is the 0.2% proof strength of the virgin material, r_i is the internal corner radius and t is the material thickness. Eq. (5.3) has been adopted in the present study to predict the corner properties of press-braked sections.

It was also proposed that the ultimate strength of corner material $\sigma_{u,c}$ may be approximated on the basis of the 0.2% proof strength of corner material, and the 0.2% proof strength and ultimate strength of the virgin material, $\sigma_{0.2,v}$ and $\sigma_{u,v}$ respectively, as given by Eq. (5.4). Eq. (5.4) has been adopted herein to approximate the ultimate strength of corner material $\sigma_{u,c}$

$$\sigma_{u,c} = 0.75\sigma_{0.2,c}\left(\frac{\sigma_{u,v}}{\sigma_{0.2,v}}\right)$$

(5.4)

Test results (Ala-Outinen, 1996) have indicated that the degradation of strength and stiffness associated with cold-worked material is generally similar to that of annealed material. Strength enhancements associated with cold-work are retained up to about 800°C, beyond which such enhancements disappear. Thus, the elevated temperature stress-strain properties of the corners have been determined on the basis of the predicted room temperature corner properties and the measured strength and stiffness reduction factors for the flat material.

In addition to the level of strength enhancement in the corner regions due to cold-work, the degree to which the strength enhancement extends beyond the curved corner portions of the section is also important. Numerical studies at room temperature have indicated that the corner strength enhancements extend beyond the curved corner portions to a distance equal to the material thickness for press-braked sections (Ashraf et al, 2005) and two times the material thickness for roll-formed sections (Gardner and Nethercot, 2004; Ashraf et al, 2005). In the present investigation, sensitivity studies were carried out on models based on the four SCI column tests in order to assess the influence of the extent of the enhanced strength corner regions on the fire resistance of stainless steel columns. All four columns were formed by press-braking. Table 5.3 shows the measured 0.2% proof strengths of the flat material and the calculated 0.2% proof strengths of the corner material for the modelled columns, and summarises the results of the sensitivity study. Finite element models were generated with (1) no corner strength enhancement (FE), (2) corner strength enhancement in the curved corner portions only ($FE_{(c)}$) and (3) corner strength enhancement in the curved corner portions and extending to a distance equal to the material thickness beyond the curved regions ($FE_{(c+t)}$). The models contained a global imperfection of amplitude L/1000, where L is the column length. The results generally indicate a progressive improvement in the prediction of test behaviour as the extent of the corner regions is increased. Over-prediction of the fire resistance of the][200×150×6 (back-to-back channel) section is believed to be due to the poor performance of the tested specimen, as described in (Gardner and Baddoo, 2006), rather than particular modelling deficiencies. Clearly the importance of inclusion of the corner strength enhancements will be dependent on the geometry of the sections considered, and in particular the ratio of the corner area to the total cross-sectional area. However, the comparisons of Table 5.3 indicate that failure

to account for the corner strength enhancements will lead to under-prediction of fire resistance of about 5% - 10%.

Table 5.3: *Comparison of critical temperature of FE under different corner properties with the tests*

Nominal section size (mm)	Measured $\sigma_{0.2,f}$	Calculated $\sigma_{0.2,c}$	Critical Temperature		
			FE/Test	FE(c)/Test	FE(c+t)/Test
RHS 150×100×6	262	524.9	0.86	0.89	0.92
RHS 150×75×6	262	524.9	0.90	0.91	0.93
RHS 100×75×6	262	524.4	0.89	0.93	0.94
][200×150×6	262	524.4	1.03	1.06	1.16
		Mean	0.92	0.95	0.98

Notes: FE - No strength enhancements included in corner regions

FE(c) - Strength enhancements in curved corner regions of the cross-section

FE(c+t) - Corner strength enhancements in curved corner regions of the cross-section and extending to a distance equal to the material thickness beyond the corners

5.3.4 Residual stresses

The primary effect of residual stresses on the response of the structural components is to cause early yielding of parts of the cross-section, and hence a premature reduction of stiffness. For cold-formed sections, the dominant residual stresses are those induced through plastic deformation during the production process and characterised by through-thickness bending distributions. However, studies (Gardner and Nethercot, 2004; Rasmussen and Hancock, 1993) have concluded that if the material properties are established from coupons cut from within the cross-section, the effects of these bending residual stress will be inherently present, and do not need to be explicitly defined in the FE model.

In a study reported by Gardner and Nethercot (2004) the sensitivity of the stainless steel stub column models to membrane (weld induced) residual stresses was assessed. FE simulations were run with and without residual stresses while other parameters remained identical. The results showed that residual stresses caused a small reduction in stiffness of the stub columns but had little influence on their overall behaviour or ultimate load carrying capacity. Similar

conclusions were reached by Ellobody and Young (2005). Given the higher deformations, greater uncertainties and possible stress-relieving effects associated with structural components at elevated temperature, the influences of residual stresses are expected to be negligible and have therefore been ignored in the present study.

5.3.5 Geometric imperfections

All structural members contain geometric imperfections, which can have an important influence on their structural behaviour. Imperfections of the form of the lowest global and local elastic buckling modes were included in the present study. Gardner and Nethercot (2004) modelled a series of stainless steel columns at room temperature with global imperfection amplitudes of L/1000, L/2000 and L/5000, where L is the column length. Comparisons indicated that a global imperfection amplitude of L/2000 provided the best agreement between FE results and test results. In the present elevated temperature study, three global imperfection amplitudes were considered: L/2000, L/1000 and L/500 were used in the numerical models. The results are shown in Table 5.4. For the global imperfection sensitivity study, enhanced strength corner properties were included in the curved corner portions of the section only. The comparisons indicate that, as for room temperature column buckling, a global imperfection amplitude of L/2000 also provides good agreement with tests at elevated temperatures. Thus a global imperfection amplitude of L/2000 was employed for the remainder of this study.

Table 5.4: *Comparison of critical temperature and fire resistant time of FE with tests under different global imperfection amplitude*

| Nominal section size (mm) | FE/ Test | | | | | |
| | δ=L/2000 | | δ=L/1000 | | δ=L/500 | |
	Time	Temp.	Time	Temp.	Time	Temp.
RHS 150×100×6	0.81	0.90	0.78	0.89	0.75	0.87
RHS 150×75×6	0.73	0.92	0.71	0.91	0.69	0.90
RHS 100×75×6	0.78	0.91	0.75	0.90	0.72	0.89
][200×150×6	1.14	1.09	1.14	1.06	0.93	0.98
RHS 100×100×4	0.67	0.89	0.74	0.91	0.74	0.91
RHS 200×200×4	0.58	0.85	0.58	0.85	0.58	0.85
RHS 40×40×4 (T1)	1.00	0.84	1.00	0.84	0.99	0.83
RHS 40×40×4 (T2)	0.90	0.87	0.76	0.72	0.57	0.49
RHS 40×40×4 (T3)	0.94	0.92	0.90	0.87	0.81	0.78
RHS 40×40×4 (T4)	0.94	0.89	0.93	0.88	0.91	0.86
RHS 40×40×4 (T5)	0.92	0.87	0.91	0.85	0.90	0.84
RHS 40×40×4 (T7)	0.85	0.88	0.84	0.87	0.83	0.86
Mean	0.85	0.90	0.84	0.88	0.78	0.84

A local imperfection was also included in the models to ensure that local plate buckling was not inhibited. Following analysis of measured imperfections in stainless steel hollow sections, Gardner and Nethercot (2004) recalibrated a model proposed by Dawson and Walker (1972) to give Eq. (5.5) for the prediction of local imperfection amplitudes w_0.

$$w_0 = 0.023t\left(\frac{f_y}{\sigma_{cr}}\right) \tag{5.5}$$

where f_y is the material 0.2% proof strength and σ_{cr} is the elastic critical plate buckling stress. Sensitivity of the modelled columns to variation in local imperfections was assessed by considering three imperfection amplitudes w_0: $0.01t$, $0.1t$ and Eq. (5.5), where t is the material thickness. The results displayed very little sensitivity to this variation; Eq. (5.5) was employed throughout the remainder of this study.

5.3.6 Protection of column ends

Four columns, RHS 150×100×6, RHS 150×75×6, RHS 100×75×6 and][200×150×6, were protected with a mineral fibre blanket up to 200 mm from each end of the column, leaving an exposed length of 3 m, as indicated in Figure 5.4. The influence of this partial protection on the fire resistance of the columns was assessed numerically. The first step was to conduct a heat transfer analysis with the heat applied to the exposed portions of the column only, allowing heat transfer to the protected ends by conduction. The results of the heat transfer analysis were input into the anisothermal non-linear analysis to determine the elevated temperature response of the columns. Thermal material properties were taken as those recommended in EN 1991-1-2 (2002) and EN 1993-1-2 (2005).

Table 5.5 compares the results of the FE models with and without protection at the column ends. The models included enhanced strength corner properties extending to a distance equal to the material thickness beyond the curved corner portions, and global imperfection amplitudes of L/2000. The results indicate that the effect of the end protection is to provide a marginal (around 4% on average) increase in fire resistance. The columns with protected ends investigated in this study had fixed boundary conditions; such columns would be expected to gain more benefit from end protection than pin-ended columns, where the level of stress at the ends would be lower.
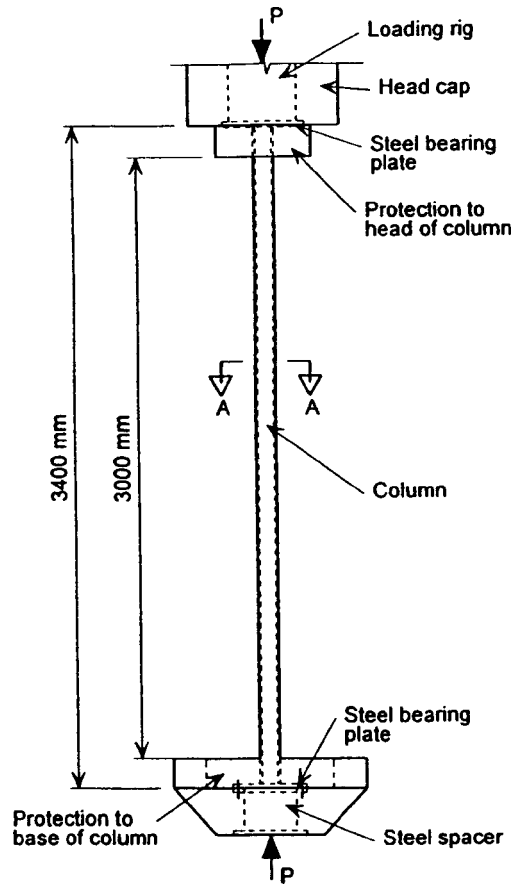
Figure 5.4: *Test arrangement showing extent of protection to column ends*

Table 5.5: *Comparison of critical temperature of FE with and without end protection with the tests*

Nominal section size (mm)	Critical temperature	
	FE/ Test	FE$_p$/ Test
RHS 150×100×6	0.92	0.93
RHS 150×75×6	0.93	0.95
RHS 100×75×6	0.94	0.98
][200×150×6	1.16	1.21
Mean	0.98	1.02

Notes: FE - Model without end protection

FE$_p$ - Model with end protection

5.3.7 Stub column modelling

The six stub columns tested by Ala-Outinen (2005) were modelled numerically, using the parameters described in the previous sections. No global imperfection was included in the models, but local imperfections of magnitude given by Eq. (5.5) and corner strength enhancements extending to a distance of two times the material thickness as predicted by Eq. (5.3) and (5.4) were employed. Boundary conditions were prescribed to replicate those in the tests: all degrees of freedom were restrained at the unloaded ends of the stub columns, whilst all except vertical displacement were restrained at the loaded end. Constraint equations were applied to ensure that the nodes at the loaded end of the stub column moved in unison. A typical stub column model is shown in Figure 5.5. Comparisons between modelled and test results are in Section 5.3.8.
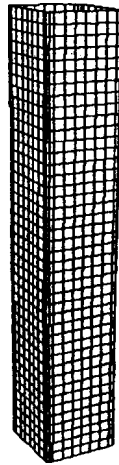
Figure 5.5: *Undeformed shape of finite element stub column model*

Figure 5.6 compare the typical stub column test (200×200×5) and FE column vertical displacement versus temperature behaviour. Overall, good agreement between FE result and test result has been achieved
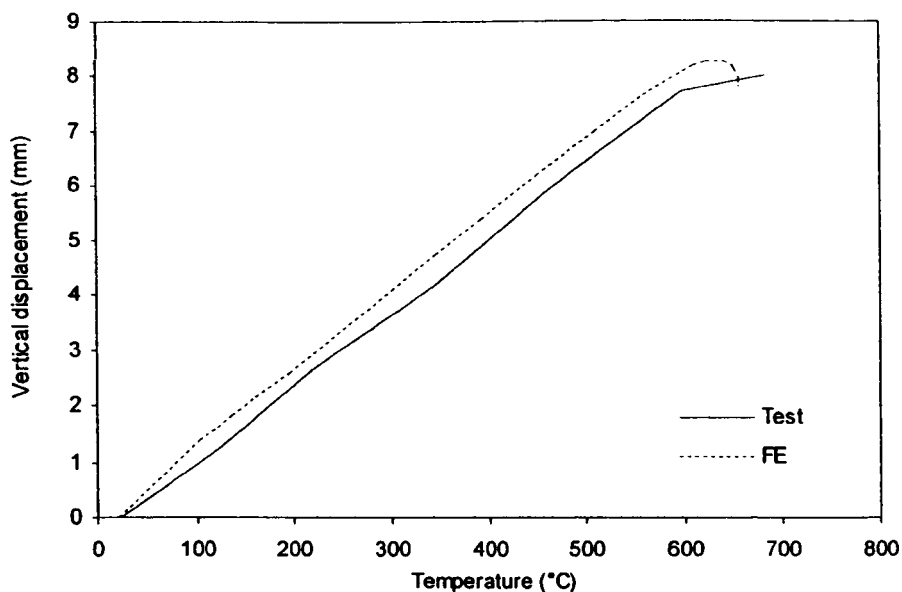
Figure 5.6: *Vertical displacement versus temperature for 200×200×5 stub column*

5.3.8 Results

A total of 12 long columns and 6 stub columns were modelled using the non-linear finite element package ABAQUS (2003). A summary of the comparison between test and FE results for long columns is given in Table 5.6 and for stub columns in Table 5.7. A graph comparing typical test and FE column lateral deflection versus temperature behaviour is shown in Figure 5.7. Overall, good agreement between FE results and test results has been achieved. The general tendency of the FE models to under-predict the fire resistance of the test specimens may be due to the assumption of constant temperature through the wall thickness of the sections, taken as that measured on the surface of the test specimens (representing an upper bound). The FE model of the back-to-back channel section column performed better than the test. As mentioned previously, this is believed to be due to the poor performance of the tested specimen (Gardner and Baddoo, 2006), rather than particular modelling deficiencies. From the comparisons between test and FE results, it may be concluded that the described FE models are capable of replicating the non-linear, large deflection response of stainless steel columns in fire.

Table 5.6: *Comparison of critical temperature between test and FE results for long columns*

Nominal section size (mm)	Test temperature (°C)	FE temperature (°C)	FE/Test
RHS 150×100×6	801	734	0.92
RHS 150×75×6	883	819	0.93
RHS 100×75×6	806	754	0.94
][200×150×6	571	661	1.16
RHS 100×100×4	835	747	0.89
RHS 200×200×4	820	696	0.85
RHS 40×40×4 (T1)	873	736	0.84
RHS 40×40×4 (T2)	579	505	0.87
RHS 40×40×4 (T3)	649	597	0.92
RHS 40×40×4 (T4)	710	633	0.89
RHS 40×40×4 (T5)	832	720	0.87
RHS 40×40×4 (T7)	766	675	0.88
		Mean	0.91

Table 5.7: *Comparison of critical temperature between test and FE results for stub columns*

Nominal section size (mm)	Load level	Test temperature (°C)	FE temperature (°C)	FE/Test
RHS 200×200×5	0.62	610	488	0.80
RHS 200×200×5	0.50	690	657	0.95
RHS 200×200×5	0.41	775	737	0.95
RHS 150×150×3	0.63	590	567	0.96
RHS 150×150×3	0.51	680	710	1.04
RHS 150×150×3	0.42	720	777	1.08
			Mean	0.96
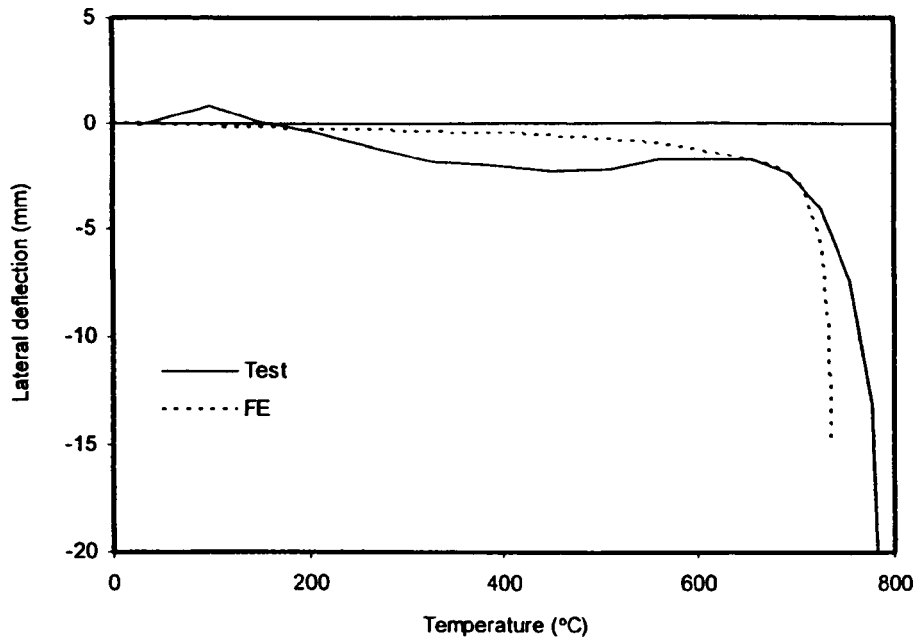
Figure 5.7: *Lateral displacement versus temperature for RHS 150×100×6 column*

5.3.9 Parametric studies

Following satisfactory agreement between the test and FE results, a series of parametric studies was performed in order to investigate the buckling response of stainless steel members at elevated temperatures. The parametric study was based upon the tested RHS 100×75×6 column, and employed the measured material properties throughout the study.

Parametric studies were carried out to examine variation in cross-section slenderness (cross-section classification), overall member slenderness $\bar{\lambda}$ and load ratio. Load ratio was defined as the applied load divided by the room temperature compression resistance, and determined according to EN 1993-1-2 (2005) and EN 1993-1-4 (1996).

Variation in cross-section slenderness was achieved by considering a range of cross-section thicknesses. The results of the cross-section slenderness parametric study are shown in Figure 5.8. Four cross-section thicknesses were considered, with the corresponding section classification given in brackets: 8 mm (Class 1), 6 mm (Class 1), 4 mm (Class 3) and 2 mm (Class 4). Load ratio was also varied from 0.2 to 0.8. The design curve calculated from

Eurocode 3 for Class 1 to 3 cross-sections and that corresponding to the 2 mm section thickness (Class 4) are also shown in Figure 5.8. The results show that all the Class 1 to 3 sections behave similarly, and generally follow the Eurocode 3 design curve. For the Class 4 sections, however, agreement is poor. The reason for this is two-fold. Firstly, the load ratio is determined by normalising the applied load by the room temperature buckling resistance – for Class 4 sections, the room temperature buckling resistance is calculated on the basis of an effective section to account for local buckling; this results in higher load ratios. Secondly, EN 1993-1-2 specifies use of the strength reduction factor corresponding to the 0.2% proof stress $k_{0.2p,\theta}$ for Class 4 cross-sections, whilst Class 1 to 3 sections benefit from the use of a higher 2% strain limit and adopt $k_{2\%,\theta}$. Comparison with test results and development of improved agreement for Class 4 sections are described in Chapter 6.

Variation in member slenderness was achieved by considering a range of column lengths. Results of the study are shown in Figure 5.9. As anticipated, there is a general trend showing that critical temperature reduces with increasing load ratio. The results also indicate that variation of critical temperature with load ratio is slenderness dependent. This would be expected since stocky columns are controlled primarily by material strength and its degradation, whilst slender columns are controlled primarily by material stiffness and its degradation. Since strength and stiffness do not degrade at the same rate with temperature it follows that the critical temperature of columns is slenderness dependent.
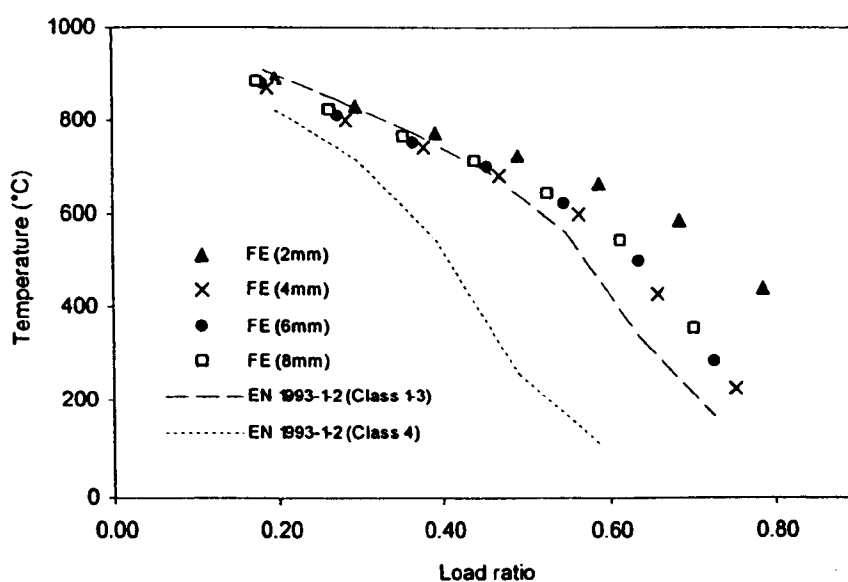
Figure 5.8: *Parametric study results for varying load ratio and cross-section slenderness*
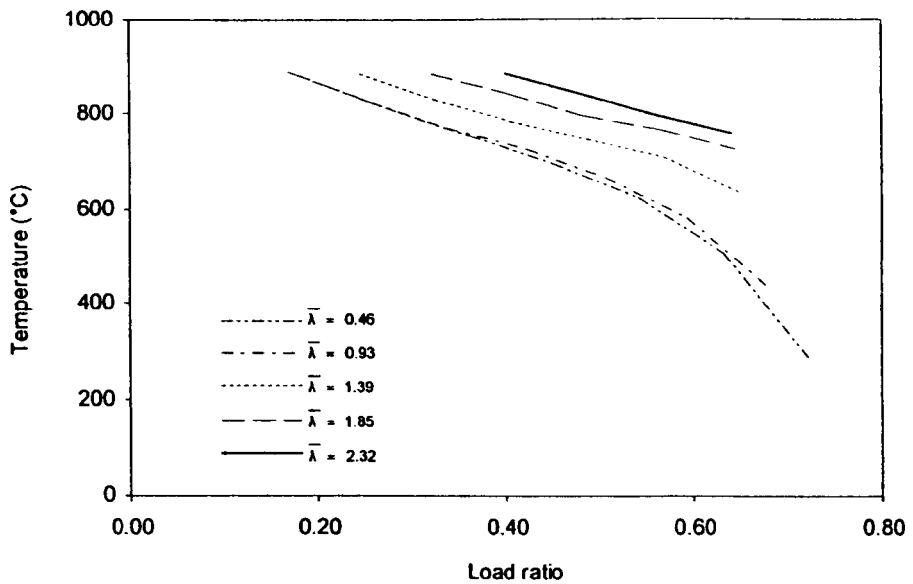
Figure 5.9: *Parametric study results for varying load ratio and member slenderness*

Additional parametric studies were carried out to examine the influence of cross-section slenderness for stub columns. A range of cross-section thicknesses were considered for the two modelled stub column sections, with a range of 1 mm, 2 mm and 3 mm for 150×150×3 section and 3 mm, 4 mm and 5 mm for 200×200×5 section. Load ratio was varied from 0.3 to 0.6.

Figures 5.10 and 5.11 show the results of the cross-section slenderness parametric studies for the 150×150×3 section and 200×200×5 section respectively. The FE results, which were shown to be in good agreement with test results in Table 5.7, are not well predicted by the present design guidance given in EN 1993-1-2 (2005). This is principally due to the determination of the effective section properties, which does not account for the differential rate of loss of strength and stiffness at elevated temperature. This is addressed in Chapter 6.
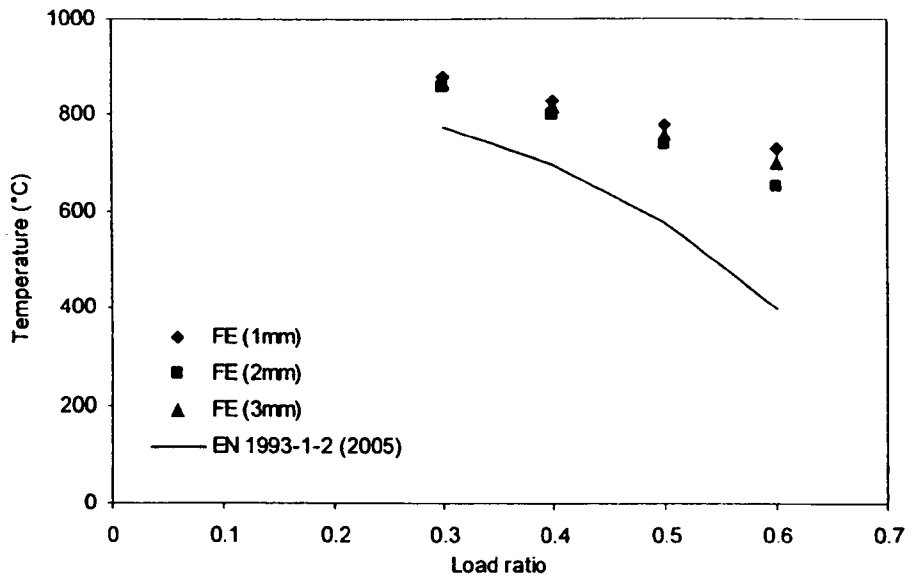
Figure 5.10: *Parametric study results for varying load ratio and cross-section slenderness for stub column section 150×150×3*
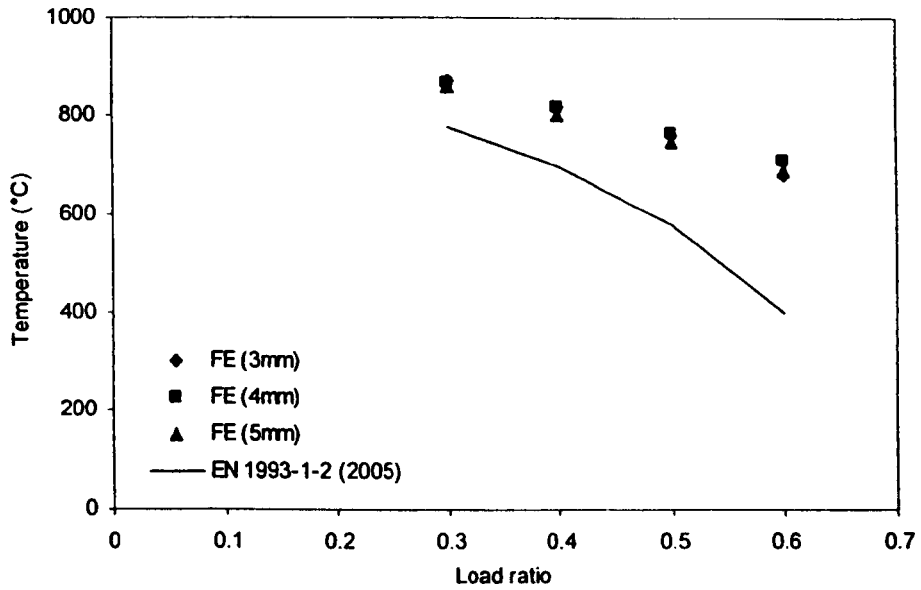
Figure 5.11: *Parametric study results for varying load ratio and cross-section slenderness for stub column section 200×200×5*

5.3.10 Discussion

This chapter has described a numerical study of structural stainless steel members in fire. Twelve column buckling tests and six stub column tests have been replicated numerically and a series of sensitivity and parameters studies to investigate the influence of the key individual parameters have been performed. The principal findings were:

- the non-linear response of stainless steel members in fire can be accurately replicated numerically
- sensitivity to geometric imperfections and residual stresses was relatively low
- inclusion of enhanced strength corner properties increased critical temperatures by about 5%
- the critical temperature of columns is slenderness dependant (for a given load ratio)
- Class 4 models performed considerably better than predicted by Eurocode 3

In Chapter 6, comparisons are made between tests on stainless steel members in fire and existing design guidance. On the basis of the test results, the findings of the numerical study and consideration of the buckling behaviour of structural components, revisions to the existing design guidance are proposed.

CHAPTER 6

DESIGN OF STAINLESS STEEL STRUCTURES IN FIRE

6.1 INTRODUCTION

Design guidance for stainless steel structures in fire is relatively scarce, but there are provisions in Eurocode 3 Part 1.2, the Euro-Inox/SCI Design Manual for Structural Stainless Steel, and some proposals made by CTICM. These will be examined in this chapter, and have previously been analysed by Ng and Gardner (in press) and Ng and Gardner (2006).

In addition to knowledge of the independent degradation of material strength and stiffness at elevated temperatures, the relationship between strength and stiffness is also important, since this defines susceptibility to buckling. For structural stainless steel design, this concept is included in codes for member buckling, though not for local plate buckling (or cross-section classification). This inconsistency is addressed herein.

The test results from Chapter 5 are compared with the current design rules in Eurocode 3: Part 1.2 (2005), the Euro-Inox/SCI Design Manual for Structural Stainless Steel and those proposed

by CTICM. Based on the comparisons, a revised buckling curve for stainless steel in fire, consistent strain limits and a new approach to cross-section classification and the treatment of local buckling are proposed in this Chapter.

6.2 COMPARISON WITH EXISTING DESIGN GUIDANCE

This section presents a comparison of test results from Chapter 5 with existing design rules proposed by EN 1993-1-2 (2005), the Euro Inox/ SCI Design Manual for Structural Stainless Steel (2002) and CTICM (2005). In the comparisons, the measured geometric and material properties are employed and all partial factors are set equal to unity to enable a direct comparison. Calculated Eurocode design resistances in the present paper vary marginally from those given in Gardner and Baddoo (2006) due to use of updated effective width formulations (to reflect code revisions) and measured ultimate strength, in place of the nominal values employed in Gardner and Baddoo (2006). Ultimate strength is required for the determination of the strength reduction factor at 2% strain $k_{2\%,\theta}$.

6.2.1 Compression members

6.2.1.1 Eurocode 3 Part 1.2

From EN 1993-1-2 (2005), the design buckling resistance $N_{b,fi,t,Rd}$ at time t of a compression member with a uniform temperature θ should be determined from Eq. (6.1) for Class 1 to 3 cross-sections and Eq. (6.2) for Class 4 cross-sections.

$$N_{b,fi,t,Rd} = \frac{\chi_{fi} A k_{2\%,\theta} f_y}{\gamma_{M,fi}} \quad \text{for Class 1,2 or 3 cross-sections} \quad (6.1)$$

$$N_{b,fi,t,Rd} = \frac{\chi_{fi} A k_{0.2p,\theta} f_y}{\gamma_{M,fi}} \quad \text{for Class 4 cross-sections} \quad (6.2)$$

where $k_{2\%,\theta}$ is the elevated temperature strength at 2% total strain $f_{2\%,\theta}$, normalised by the room temperature 0.2% proof strength f_y, whilst $k_{0.2p,\theta}$ is the elevated temperature 0.2% proof strength

132

$f_{0.2p,\theta}$, normalised by the room temperature 0.2% proof strength f_y. The reduction factor for flexural buckling in fire χ_{fi} is given by Eqs. (6.3) and (6.4).

$$\chi_{fi} = \frac{1}{\varphi_\theta + \sqrt{\varphi_\theta^2 - \bar{\lambda}_\theta^2}} \tag{6.3}$$

in which

$$\varphi_\theta = 0.5\left(1 + 0.65\bar{\lambda}_\theta\sqrt{\frac{235}{f_y}} + \bar{\lambda}_\theta^2\right) \tag{6.4}$$

where the non-dimensional elevated temperature member slenderness $\bar{\lambda}_\theta$ is defined by Eqs. (6.5) and (6.6). It is worth noting that the buckling curves defined by Eq. (6.3) and (6.4) exhibit no plateau, where design may be based on the cross-section resistance alone.

$$\bar{\lambda}_\theta = \bar{\lambda}(k_{2\%,\theta}/k_{E,\theta})^{0.5} \qquad \text{for Class 1 to 3 cross-sections} \tag{6.5}$$

$$\bar{\lambda}_\theta = \bar{\lambda}(k_{0.2p,\theta}/k_{E,\theta})^{0.5} \qquad \text{for Class 4 cross-sections} \tag{6.6}$$

Cross-sections should be classified as for normal temperature design, but with a reduced value for ε as given by Eq. (6.7).

$$\varepsilon = 0.85\left(\frac{235}{f_y}\right)^{0.5} \tag{6.7}$$

Although it appears to be inconsistent, Annex E of EN 1993-1-2 (2005) states that effective section properties for Class 4 cross-sections should be determined as for room temperature design (i.e. without incorporating the reduced value for ε as given by Eq. (6.7)). Buckling resistance for members with Class 4 cross-sections have therefore been determined on the basis of the room temperature effective section properties.

The value of φ_θ in Eq. (6.4) is dependent on the material yield strength, thus the Eurocode 3 buckling curve cannot be graphically compared directly against the column buckling tests. Figure 6.1 compares the Eurocode 3 buckling curves with $f_y = 300$ N/mm^2 and 500 N/mm^2 with

all available test results (from Table 5.1). A numerical comparison of test buckling loads and predicted buckling resistances at the critical temperature is also given in Table 6.1, revealing a mean Eurocode divided by test resistance of 0.94, with a corresponding scatter (coefficient of variation, COV) of 0.16. Numerical comparison of the stub column test and predicted failure loads is given in Table 6.2, revealing a mean Eurocode divided by test resistance of 0.71, with a corresponding scatter (coefficient of variation, COV) of 0.13.
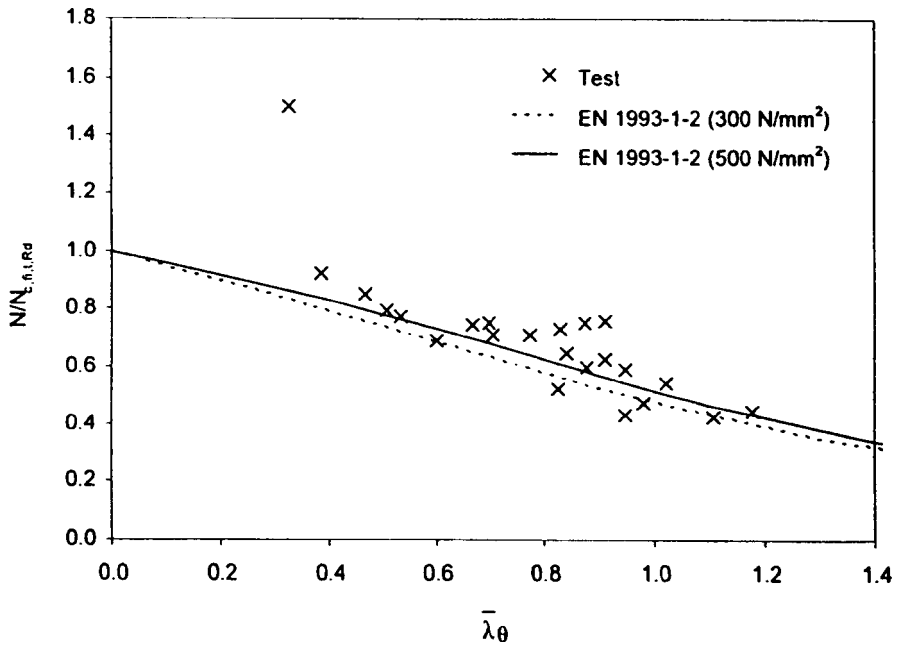
Figure 6.1: *Comparison of EN 1993-1-2 with column buckling fire tests*

Table 6.1: *Comparison of column buckling test results with existing design guidance and proposed approach*

Nominal section size (mm)	Applied Load (kN)	Test critical temperature (°C)	Room temperature classification (EN 1993)	Elevated temperature classification (EN 1993)	Elevated temperature classification (Proposed)	Buckling resistance at critical temperature			
						EN 1993/ Test	Euro Inox/ Test	CTICM/ Test	Proposed/ Test
RHS 150×100×6	268	801	Class 1	Class 3	Class 1	0.85	0.85	0.75	0.97
RHS 150×75×6	140	883	Class 1	Class 3	Class 1	0.88	0.88	0.78	1.00
RHS 100×75×6	156	806	Class 1	Class 1	Class 1	0.91	0.91	0.86	1.03
][200×150×6	413	571	Class 4	Class 4	Class 3	0.91	0.91	1.18	1.06
RHS 100×100×4	80	835	Class 2	Class 3	Class 1	0.83	0.83	0.90	0.91
RHS 200×200×4	230	820	Class 4	Class 4	Class 4	0.55	0.55	0.67	0.83
RHS 40×40×4	45	873	Class 1	Class 1	Class 1	0.96	0.96	1.02	0.96
RHS 40×40×4	129	579	Class 1	Class 1	Class 1	0.77	0.77	0.81	0.76
RHS 40×40×4	114	649	Class 1	Class 1	Class 1	0.80	0.80	0.85	0.79
RHS 40×40×4	95	710	Class 1	Class 1	Class 1	0.85	0.85	0.92	0.85
RHS 40×40×4	55	832	Class 1	Class 1	Class 1	0.96	0.96	1.05	0.98
RHS 40×40×4	75	766	Class 1	Class 1	Class 1	0.92	0.92	1.00	0.92
RHS 40×40×4	102	720	Class 1	Class 1	Class 1	0.94	0.94	1.04	0.93
RHS 40×40×4	73	834	Class 1	Class 1	Class 1	0.99	0.99	1.14	0.99
RHS 40×40×4	63	873	Class 1	Class 1	Class 1	0.95	0.95	1.10	0.95
RHS 30×30×3	41	610	Class 1	Class 1	Class 1	1.00	1.00	1.03	0.95
RHS 30×30×3	33	693	Class 1	Class 1	Class 1	1.12	1.12	1.15	1.09
RHS 30×30×3	21	810	Class 1	Class 1	Class 1	1.31	1.31	1.41	1.31
CHS 33.7×2	26	668	Class 1	Class 1	Class 1	0.92	0.92	1.00	0.92
CHS 33.7×2	12	850	Class 1	Class 1	Class 1	1.17	1.17	1.25	1.17
CHS 33.7×2	20	716	Class 1	Class 1	Class 1	1.10	1.10	1.20	1.10
RHS 100×100×3	52	835	Class 4	Class 4	Class 3[a]	1.02	1.02	1.25	1.31
RHS 100×100×3	52	880	Class 4	Class 4	Class 4	0.92	0.92	1.06	1.33
					Mean	0.94	0.94	1.02	1.00
					COV	0.16	0.16	0.18	0.15

Note: [a] Cross-section classification limited to Class 3

Table 6.2: *Comparison of stub column test results with existing design guidance and proposed approach*

Nominal section size (mm)	Applied load (kN)	Test critical temperature (°C)	Stub column resistance at critical temperature			
			EN 1993/ Test	Euro Inox/ Test	CTICM/ Test	Proposed/ Test
RHS 200×200×5	694	609	0.63	0.63	0.66	0.76
RHS 200×200×5	567	685	0.66	0.66	0.69	0.83
RHS 200×200×5	463	768	0.61	0.61	0.64	0.81
RHS 150×150×3	248	590	0.75	0.75	0.79	0.93
RHS 150×150×3	203	678	0.77	0.77	0.82	1.00
RHS 150×150×3	165	720	0.85	0.85	0.90	1.13
		Mean	0.71	0.71	0.75	0.91
		COV	0.13	0.13	0.14	0.15

6.2.1.2 Euro Inox/SCI design manual for structural stainless steel

The Euro Inox/ SCI Design Manual for Structural Stainless Steel (2002) adopts the room temperature cross-section classification for elevated temperature design, but otherwise follows the Eurocode approach. The ε factor is defined by Eq. (6.8).

$$\varepsilon = \left(\frac{235}{f_y} \frac{E}{210000} \right)^{0.5}$$

(6.8)

Despite the different definition of ε in the Euro Inox/ SCI Design Manual for Structural Stainless Steel, no change in cross-section classification from that of EN 1993-1-2 results for the considered test data, and hence there is no difference in predicted buckling resistances. The graphical comparison of the column buckling test results with the Euro Inox/ SCI Design Manual for Structural Stainless Steel is therefore the same as that given for EN 1993-1-2 in Figure 6.1. The numerical comparisons of test and predicted resistances for column buckling and stub column (cross-section) resistance are shown in Tables 6.1 and 6.2 respectively, and display the same results as obtained for EN 1993-1-2.

6.2.1.3 CTICM proposal

CTICM (2005) has proposed a number of modifications to the EN 1993-1-2 approach in order to simplify calculations by avoiding the need to determine the elevated temperature strength at 2% strain, and to improve agreement with test results. Firstly, it was proposed that cross-section classification at elevated temperature should follow the method laid out the in the Euro Inox/ SCI Design Manual for Structural Stainless Steel (i.e. adopt the room temperature classification, with the ε factor defined by Eq. (6.8). Secondly, it was proposed that the strength reduction factor should always be based upon the elevated temperature 0.2% proof strength for all classes of cross-section. Finally it was proposed to use the room temperature buckling curves from prEN 1993-1-4 (2004) at elevated temperature; this utilises Eq. (6.3), but now φ_θ is defined by Eq. (6.9).

$$\varphi_\theta = 0.5(1 + \alpha \, (\bar{\lambda}_\theta - \bar{\lambda}_0) + \bar{\lambda}_\theta^{\,2})$$

(6.9)

where α is the imperfection factor (determined as for room temperature design) and $\bar{\lambda}_0$ is the limiting slenderness. For hollow sections, α and $\bar{\lambda}_0$ are taken as 0.49 and 0.2, respectively.

Figure 6.2 compares the CTICM buckling curve (with α = 0.49 and $\bar{\lambda}_0$ = 0.2) with the test results. The graph shows that for stocky compression members, the test results are generally under-predicted, whilst for slender compression members, the test results are generally over-predicted. The under-prediction for stocky columns is unsurprising, since the design column buckling resistance is restricted by use of the 0.2% proof strength, whilst the test data indicates that far larger strains can be achieved. The numerical comparisons of Table 6.1 show a mean CTICM divided by test resistance of 1.02, with a corresponding scatter (coefficient of variation, COV) of 0.18. Results of the stub column tests are considered in Table 6.2, showing a mean CTICM divided by test resistance of 0.75, with a corresponding coefficient of variation (COV) of 0.14.

The comparisons between test results and the three design approaches are discussed further in section 6.3 of this paper.
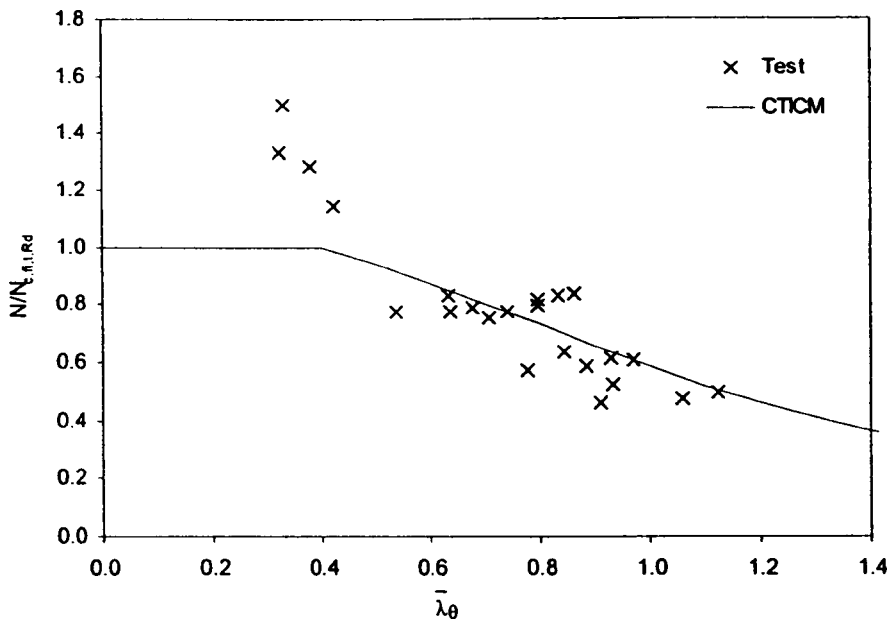
Figure6.2: *Comparison of CTICM design proposal with column buckling fire tests*

6.2.2 Beams

A total of six laterally restrained beams (Baddoo and Gardner, 2000; Gardner and Baddoo, 2006; Zhao and Blanguernon, 2004) have been reported. A summary of the tests provided in Table 6.3. Nominal section sizes, cross-section classifications, boundary conditions, applied loads and critical temperatures have been tabulated.

Table 6.3: *Summary of tests conducted on structural stainless steel beams*

Nominal section size (mm)	Cross-section classification	Boundary conditions	Applied load (kN)	Critical temperature (°C)
RHS 200×125×6[a]	Class 1	Simply supported	52.3	884
][200×150×6[a]	Class 4	Simply supported	32.4	944
][120×64[a]	Class 1	Simply supported	47.0	650
][120×64[a]	Class 1	Continuous	39.9	840
Top hat 100×100×2[d]	Class 4	Simply supported	5.0	880
Top hat 100×100×2[d]	Class 4	Simply supported	9.2	765

Notes: [a] Tests reported in Baddoo and Gardner (2000) and Gardner and Baddoo (2006)

[d] Tests reported in Zhao and Blanguernon (2004)

138

From EN 1993-1-2 (2005), the design cross-section bending moment resistance $M_{fi,\theta,Rd}$ of a beam with a uniform temperature θ_a should be determined from Eq. (6.10) for Class 1 and 2 cross-sections, Eq. (6.11) for Class 3 cross-sections and Eq. (6.12) for Class 4 cross-sections. For Class 1 or 2 cross-sections, plastic section properties are employed with the 2% strain limit (i.e. adopting $k_{2\%,\theta}$), for Class 3 cross-sections, elastic section properties are employed with the 2% strain limit, whilst Class 4 cross-sections utilise the effective section properties (determined as for room temperature design), with the 0.2% plastic strain limit (i.e. adopting $k_{0.2p,\theta}$)

$$M_{fi,\theta,Rd} = k_{2\%,\theta}(\gamma_{M0}/\gamma_{M,fi})M_{pl,Rd} \qquad \text{for Class 1 or 2 cross-sections} \qquad (6.10)$$

$$M_{fi,\theta,Rd} = k_{2,\theta}(\gamma_{M0}/\gamma_{M,fi})M_{el,Rd} \qquad \text{for Class 3 cross-sections} \qquad (6.11)$$

$$M_{fi,\theta,Rd} = k_{0.2p,\theta}(\gamma_{M0}/\gamma_{M,fi})M_{eff,Rd} \qquad \text{for Class 4 cross-sections} \qquad (6.12)$$

The design cross-section bending moment resistance $M_{fi,t,Rd}$ of a beam with a non-uniform temperature distribution at time t is given by Eq. (6.13).

$$M_{fi,t,Rd} = M_{fi,\theta,Rd}/\kappa_1\kappa_2 \qquad (6.13)$$

$M_{fi,\theta,Rd}$ (defined by Eqs. (6.10) to (6.12)) is the design moment resistance of the cross-section for a uniform temperature θ equal to the maximum temperature θ_{max} (generally at the bottom flange of the beam where the beam supports a concrete slab on the top flange) reached in the cross-section at time t. κ_1 and κ_2 are adaptation factors for non-uniform temperature around the cross-section and along the beam length, respectively. For an unprotected beam, exposed to fire on 3 sides and supporting a concrete slab on the fourth, (which was the case for all tested beams considered in this paper), $\kappa_1 = 0.7$. κ_2 is taken as 1.0 for all cases other than at the supports of a statically indeterminate beam. It is recommended that the partial safety factors γ_{M0} and $\gamma_{M,fi}$ both be taken equal to unity. Lateral torsional buckling of stainless steel beams in fire has not been considered herein since all tests have been performed on restrained beams.

As for columns, EN 1993-1-2 proposes that cross-sections should be classified based on the room temperature approach, but employing the modified ε factor given in Eq. (6.7). The Euro Inox/ SCI Design Manual for Structural Stainless Steel adopts the room temperature cross-

section classification for elevated temperature design, but otherwise follows the Eurocode approach. The ε factor from the Design Manual is defined by Eq. (6.8). CTICM (2005) propose no modifications for beams.

A comparison between the design bending moment resistance (at the critical temperature reached in the bottom flange of the beam in the actual fire test) and the applied test bending moment, for each of the beam tests, is given in Table 6.4. Design bending moment resistance is determined according to EN 1993-1-2 and the Euro Inox/ SCI Design Manual for Structural Stainless Steel. In the comparisons, the measured geometric and material properties are employed and all partial factors are set equal to unity. The comparisons shows a mean predicted divided by test bending moment resistance of 0.74 with a coefficient of variation (COV) of 0.23 for both EN 1993-1-2 and the Euro Inox/ SCI Design Manual for Structural Stainless Steel.

Table 6.4: *Comparison of beam test results with existing design guidance and proposed approach*

Nominal section size (mm)	Test moment (kNm)	Test critical temperature (°C)	Room temperature classification (EN 1993)	Elevated temperature classification (EN 1993)	Elevated temperature classification (Proposed)	Bending resistance at critical temperature		
						EN 1993/ Test	Euro-Inox/ Test	Proposed/ Test
RHS 200×125×6	27.8	884	Class 1	Class 1	Class 1	0.85	0.85	0.85
][200×150×6	17.2	944	Class 4	Class 4	Class 3[a]	0.53	0.53	0.55
][120×64	15.2	650	Class 1	Class 1	Class 1	0.97	0.97	0.97
][120×64	8.9	840	Class 1	Class 1	Class 1	0.85	0.85	0.85
Top hat 100×100×2	2.38	880	Class 4	Class 4	Class 3	0.56	0.56	0.82
Top hat 100×100×2	4.37	765	Class 4	Class 4	Class 4	0.71	0.71	0.99
					Mean	0.74	0.74	0.84
					COV	0.23	0.23	0.19

Note: [a] Cross-section classification limited to Class 3

6.3 RECOMMENDATIONS FOR DESIGN GUIDANCE

Results from all available tests on stainless steel columns and beams in fire have been compared to existing design guidance given in EN 1993-1-2(2005), the Euro Inox/ SCI Design Manual for Structural Stainless Steel (2002) and proposed by CTICM (2005). The comparisons given in Tables 6.1, 6.2 and 6.4 generally reveal both conservatism and scatter of prediction in existing design methods, due, in part, to inconsistent treatment of buckling and inappropriate strain limits and member buckling curves. Revised recommendations are made herein.

In addition to knowledge of the independent degradation of material strength and stiffness at elevated temperatures, the relationship between strength and stiffness is also important, since this defines susceptibility to buckling. Currently, this concept is included in EN 1993-1-2 and the Euro Inox/ SCI Design Manual for Structural Stainless Steel for member buckling through the definition and use of an elevated temperature non-dimensional member slenderness $\overline{\lambda}_\theta$. $\overline{\lambda}_\theta$ is defined by a modification of the room temperature non-dimensional slenderness $\overline{\lambda}$, as given by Eqs. (6.5) and (6.6).

The variation of $(k_{E,\theta}/k_{2\%,\theta})^{0.5}$ (where $k_{2\%,\theta}$ is based on the 2% total strain limit) and $(k_{E,\theta}/k_{0.2p,\theta})^{0.5}$ (where $k_{0.2p,\theta}$ is based on the 0.2% plastic strain limit) with temperature for stainless steel and carbon steel is shown in Figure 6.3. Values of $(k_{E,\theta}/k_{2\%,\theta})^{0.5}$ or $(k_{E,\theta}/k_{0.2p,\theta})^{0.5}$ less than unity lead to an increase in the non-dimensional member slenderness and represents greater propensity to buckling (rather than yielding) at elevated temperature than at room temperature. For values of $(k_{E,\theta}/k_{2\%,\theta})^{0.5}$ or $(k_{E,\theta}/k_{0.2p,\theta})^{0.5}$ greater than unity, the reverse is true.

In the treatment of local buckling at room temperature, the ε factor is employed to allow for variation in material yield strength f_y. In fire, ENV 1993-1-2 (2001) modified the ε factor used in section classification to reflect that loss of strength and stiffness at elevated temperatures does not occur at the same rate. Thus, at elevated temperatures ε was modified by the factor $(k_{E,\theta}/k_{2\%,\theta})^{0.5}$ and was defined by Eq. (6.14).

$$\varepsilon = \left[\left(\frac{235}{f_y}\right)\left(\frac{k_{E,\theta}}{k_{2,\theta}}\right)\right]^{0.5} \tag{6.14}$$
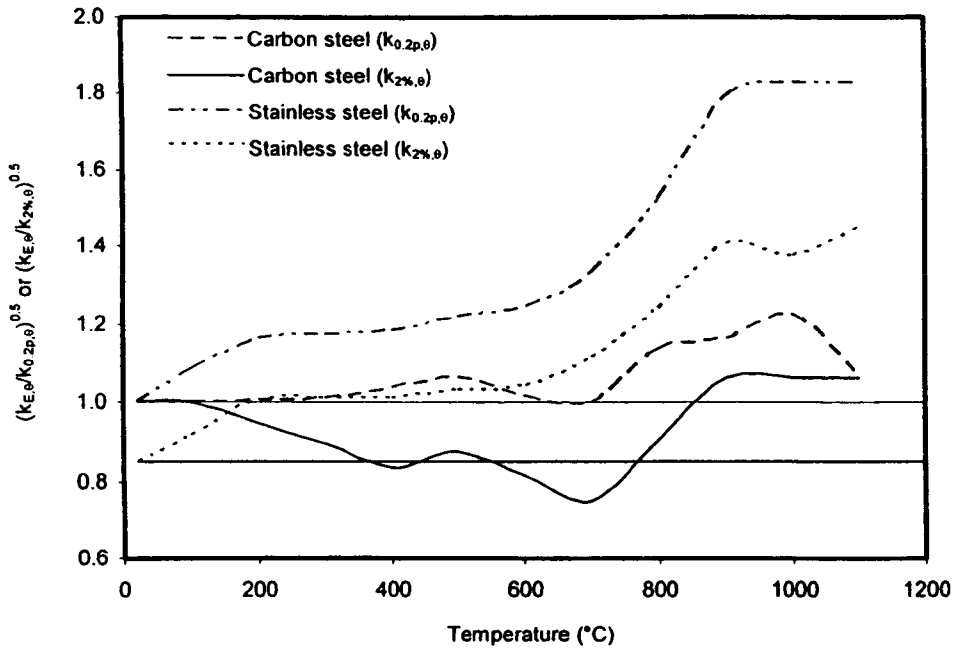
Figure 6.3: *Variation of the modification factor $(k_{E,\theta}/k_{2\%,\theta})^{0.5}$ and $(k_{E,\theta}/k_{0.2p,\theta})^{0.5}$ with temperature*

From Figure 6.3, it may be seen that for the majority of the elevated temperature range, carbon steel has values of $(k_{E,\theta}/k_{2\%,\theta})^{0.5}$ less than unity and is therefore more susceptible to buckling (as opposed to yielding) than at room temperature; neglecting this feature leads to unsafe predictions. To simplify calculations, this factor was set as a constant of 0.85 (which was deemed an acceptably safe average value at fire limit state) in EN 1993-1-2 (2005), for both carbon steel and stainless steel. Clearly from Figure 6.3, however, this factor is inappropriate for stainless steel. The Euro Inox/ SCI Design Manual for Structural Stainless Steel (2002) effectively employs a modification factor of unity by adopting the room temperature classification for elevated temperature. This is more appropriate than the Eurocode 3 treatment, but still, does not correctly reflect the variation of strength and stiffness at elevated temperature exhibited by stainless steel.

It is proposed that the true variation of stiffness and strength at elevated temperature be utilised in cross-section classification and in the determination of effective section properties for stainless steel structures in fire. Thus, the ε_θ factors defined by Eqs. (6.15) and (6.16) should be determined at the critical temperature, and hence used to re-classify the cross-section. Eq. (6.15) may be applied to cross-sections that are Class 1 or 2 at room temperature and utilises

the 2% strain limit, whilst Eq. (6.16) applies to cross-sections that are Class 3 or 4 at room temperature and utilises the 0.2% plastic strain limit. Eq. (6.16) also applies in the determination of effective section properties. The notation ε_θ is introduced to differentiate from the ε factor used for room temperature design.

$$\varepsilon_\theta = \left[\left(\frac{235}{f_y} \frac{E}{210000} \right) \left(\frac{k_{E,\theta}}{k_{2\%,\theta}} \right) \right]^{0.5} = \varepsilon \left(\frac{k_{E,\theta}}{k_{2\%,\theta}} \right)^{0.5} \quad \text{for Class 1 and 2 sections} \quad (6.15)$$

$$\varepsilon_\theta = \left[\left(\frac{235}{f_y} \frac{E}{210000} \right) \left(\frac{k_{E,\theta}}{k_{0.2p,\theta}} \right) \right]^{0.5} = \varepsilon \left(\frac{k_{E,\theta}}{k_{0.2p,\theta}} \right)^{0.5} \quad \text{for Class 3 and 4 sections} \quad (6.16)$$

From Figure 6.3, is may be seen that the factors $(k_{E,\theta}/k_{2\%,\theta})^{0.5}$ and $(k_{E,\theta}/k_{0.2p,\theta})^{0.5}$ for stainless steel are greater than unity at elevated temperatures. The result of cross-section re-classification and the re-determination of effective section properties at the critical temperature will therefore be beneficial, and ignoring this process will be conservative. Cross-sections that are Class 4 at room temperature may become fully effective at elevated temperatures.

Parametric studies were carried out in Section 5.3.9 in order to examine the influence of cross-section slenderness on the response of stub columns. The proposed ε_θ in Eq. (6.16) was adopted in the Eurocode calculation model to compare the proposed design method with numerical results. Figures 6.4 and 6.5 compare the critical temperature of the proposed method with the current design method and FE results for sections 150×150×3 and 200×200×5 (with variations in thickness from parametric studies). Both figures show that use of the proposed ε_θ gives significant improvements in the prediction of critical temperature over the current design method.
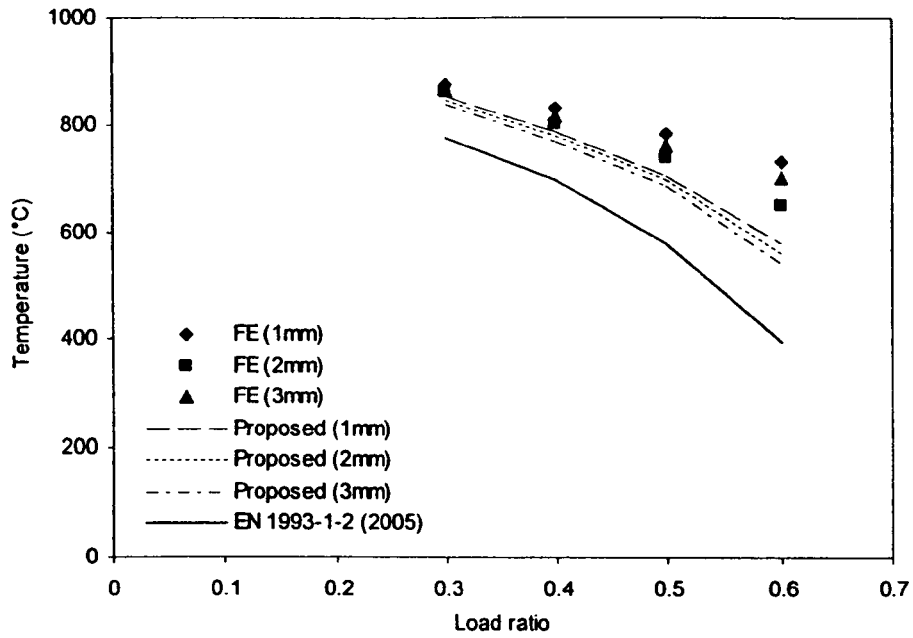
Figure 6.4: *Comparison of critical temperature of proposed method with FE and current design guidance for stub column section 150×150×3 (with variations in thickness)*
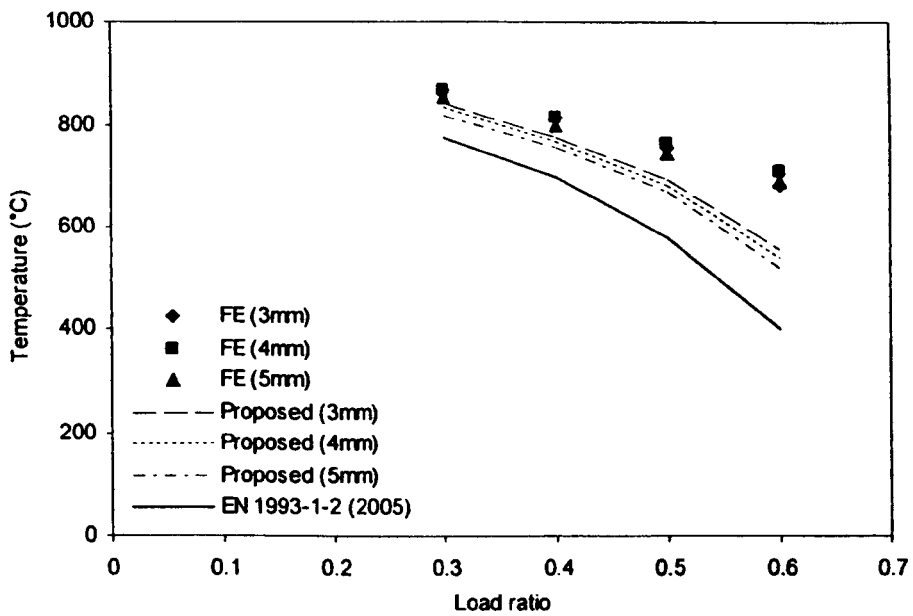
Figure 6.5: *Comparison of critical temperature of proposed method with FE and current design guidance for stub column section 200×200×5 (with variations in thickness)*

Tables 6.5 and 6.6 compare the critical temperatures predicted by the current design guidance and the proposed method, normalised by the critical temperature predicted by the FE models. The proposed method shows better agreement with the numerical results due to proper consideration of the relationship between strength and stiffness at elevated temperature. Improvements of up to 40% are achieved.

Table 6.5: *Comparison of critical temperature predicted by EC 3 and proposed method divided by FE models for section 150×150×3*

Thickness (mm)	0.3 load ratio		0.4 load ratio		0.5 load ratio		0.6 load ratio	
	EC 3 /FE	Proposed /FE	EC 3 /FE	Proposed /FE	EC 3 /FE	Proposed /FE	EC 3 /FE	Proposed /FE
1 mm	0.88	0.97	0.84	0.95	0.74	0.90	0.55	0.79
2 mm	0.90	0.98	0.87	0.97	0.78	0.95	0.61	0.86
3 mm	0.90	0.97	0.86	0.94	0.76	0.90	0.57	0.77
Mean	0.89	0.98	0.86	0.95	0.76	0.92	0.57	0.81

Table 6.6: *Comparison of critical temperature predicted by EC 3 and proposed method divided by FE models for section 200×200×5*

Thickness (mm)	0.3 load ratio		0.4 load ratio		0.5 load ratio		0.6 load ratio	
	EC 3 /FE	Proposed /FE	EC 3 /FE	Proposed /FE	EC 3 /FE	Proposed /FE	EC 3 /FE	Proposed /FE
3 mm	0.89	0.97	0.85	0.95	0.76	0.92	0.59	0.81
4 mm	0.89	0.97	0.86	0.94	0.76	0.89	0.56	0.76
5 mm	0.90	0.96	0.87	0.95	0.77	0.90	0.58	0.75
Mean	0.90	0.96	0.86	0.94	0.76	0.90	0.58	0.77

It is further proposed that in the determination of cross-section and member resistance in fire, the strength reduction factor be based on the 2% strain limit ($k_{2\%,\theta}$) for Class 1 and 2 cross-sections and the 0.2% plastic strain limit ($k_{0.2p,\theta}$) for Class 3 and 4 cross-sections. Use of the strength at 2% strain for Class 3 cross-sections, as is proposed in existing design guidance seems unjustified, since local buckling would be expected before this strain level is reached.

Having established a more consistent basis for the treatment of buckling of stainless steel columns and beams in fire, the test results, which were compared against existing design

proposals in section 6.2, were re-evaluated. The results have been included in Tables 6.1, 6.2 and 6.3. For columns, a revised buckling curve has been proposed to provide a mean fit to the test results, which is acceptable at fire limit state. This was achieved by adopting the general form of the room temperature buckling curves of Eq. (6.3) and (6.9), and selecting appropriate values of the imperfection parameter α and the limiting slenderness $\overline{\lambda}_0$. A comparison of the resulting fire buckling curve with $\alpha = 0.55$ and $\overline{\lambda}_0 = 0.2$ is shown in Figure 6.6. Following analysis of the results it was revealed that one the columns, Class 4 at room temperature, becomes Class 2 at elevated temperature, and its resistance is over-predicted by the proposed method. In the absence of further test results, it is recommended that cross-sections that are Class 4 at room temperature cannot be promoted beyond Class 3 at elevated temperatures.
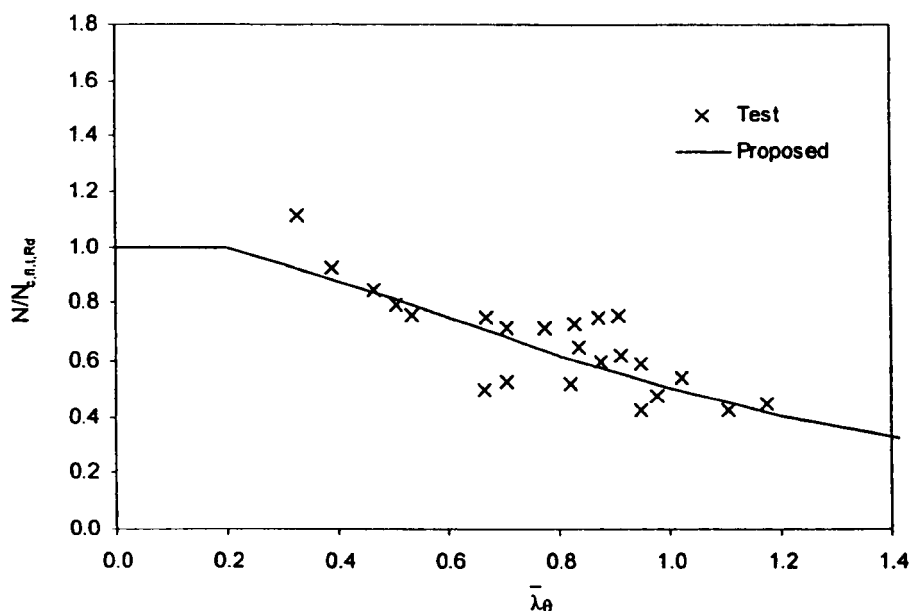
Figure 6.6: *Comparison of proposed design approach with column buckling fire tests*

For column buckling, the mean proposed divided by test resistance is 1.00 with a coefficient of variation (COV) of 0.15. For stub columns, the mean proposed divided by test resistance is 0.91 with a coefficient of variation (COV) of 0.15, whilst for beams, the mean proposed divided by test resistance is 0.84 with a coefficient of variation (COV) of 0.19. The proposed treatment offers a more rational approach to the fire design of structural stainless steel columns and beams, yielding an improvement of 6% for column buckling resistance, 28% for stub

147

column (cross-section) resistance and 14% for in-plane bending resistance over the current Eurocode methods.

6.4 CONCLUDING COMMENTS

At elevated temperatures, stainless steel offers better retention of strength and stiffness than structural carbon steel, due to the beneficial effects of the alloying elements. This behaviour is reflected in EN 1993-1-2 (2005). However, in addition to knowledge of the independent degradation of material strength and stiffness at elevated temperatures, the relationship between strength and stiffness is also important, since this defines susceptibility to buckling. This concept has been recognised in EN 1993-1-2 for member buckling by the use of an elevated temperature non-dimensional member slenderness, but for local buckling of stainless steel sections, current codified treatment is inappropriate.

A revised buckling curve for stainless steel in fire, consistent strain limits and a new approach to cross-section classification and the treatment of local buckling are proposed. These revisions have led to a more efficient and consistent treatment of buckling of stainless steel columns and beams in fire. Improvements of 6% for column buckling resistance, 28% for stub column (cross-section) resistance and 14% for in-plane bending resistance over the current Eurocode methods are achieved.

CHAPTER 7

THERMAL EXPANSION

7.1 INTRODUCTION

All metals expand when heated, but stainless steel expands up to 50% more than carbon steel. Figure 7.1 shows a comparison of the thermal expansion of carbon steel and stainless steel as given in EN 1993-1-2 (2005). The figure shows that stainless steel expands to a greater extent, up to 50% more than carbon steel. The effect of the higher thermal expansion has not been observed directly since no tests have been conducted on restrained stainless steel members or frames in fire. However, given the greater thermal expansion and the ability to retain strength and stiffness to higher temperatures, additional forces will be experienced by restrained stainless steel structural members. The severity of the additional member forces will depend on the applied loading arrangement and on the degree of rotational and translational restraint. Although stainless steel offers better retention of strength and stiffness at elevated temperatures, this greater thermal expansion may be detrimental to fire resistance and therefore requires investigation. When a building is subjected to fire, the unexposed parts remain relatively cool. The fire-affected part of the structure receives significant restraint from the cooler areas surrounding it. Greater thermal expansion rates could lead to excessive thermal deformation, higher member forces due to restraint or may affect the stability of a structural frame which may contribute to collapse at the time of a fire.
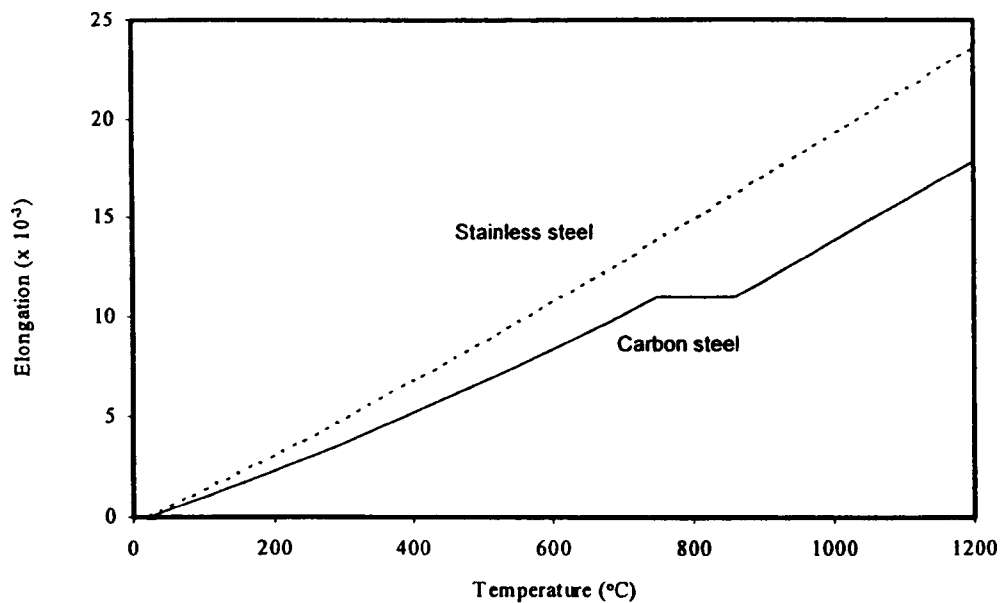
Figure 7.1: *Thermal elongation of carbon steel and stainless steel as a function of temperature*

The Building Research Establishment (BRE) and Corus in the UK carried out full scale fire tests on an eight-storey steel-framed building at Cardington. The effects of thermal expansion were clearly evident in the Cardington tests. For example, thermal expansion of beams introducing bending moments into adjacent columns, as described by Wang and Davies (2003) and Wang (2000). In general, a steel beam subject to a local fire in the interior of a multi-bay floor will bear relatively higher axial forces due to the higher degree of axial restraints provided by neighbouring members than for the same beam near the edge of the floor. Thus different axial restraining conditions may induce significantly different design actions. These generated axial forces in the steel beams in fire could be so significant that a flexural buckling failure may occur.

In this Chapter, the importance of thermal expansion in restrained stainless steel columns and beams in fire is investigated. Numerical comparisons are made with equivalent carbon steel members.

7.2 RESTRAINED COLUMNS

7.2.1 Introduction

Unlike during a standard fire test, where a column is generally free to expand against the load, in a building, a column is axially restrained during a fire due to the presence of the surrounding structure. Axial restraints may induce significantly different design actions at elevated temperature from those calculated at ambient temperature, mainly due to thermal restraining reactions. Greater thermal expansion rates could therefore lead to excessive thermal deformation and increased member forces. As a result, the critical temperature may be reduced.

Many researchers (Valente and Cabrita Neves, 1999; Cabrita Neves et al, 2002) have stated that the critical temperature of steel columns under axial compression with thermal restraint is lower than the critical temperature of the same columns free to elongate in numerical simulations; this is due to the fact that the analysis may not be able to continue beyond the local failure, in which case the temperature that causes buckling of the column will be considered as the failure temperature. During this study, it is shown that even though the column buckles, it is still able to continue to support more than the load it supported before the fire ($N/N_{initial} > 1$), therefore the structure is still not in danger and can still be heated, as previously observed by Franssen (2000).

Correia Rodrigues et al (2000) indicated that load transfer from the heated column to the cold surrounding elements can be accepted as long as these elements are capable of supporting it without producing collapse of the structure. This is believed to be true as in reality, the load supported by a structure before a fire is usually far from its ultimate load-bearing capacity, and so there exists a safety margin in the unexposed columns and these ones can normally support a significant increase of loading (Franssen, 2000).

7.2.2 Previous modelling of restrained columns in fire

Franssen (2000) applied the arc-length technique to the case of restrained columns. Figure 7.2 represents a simple thermally restrained column with pinned joints at both end and a spring is located at the top of the column. P is the applied load, K_s is the spring stiffness and L_c is the length of the column.

151
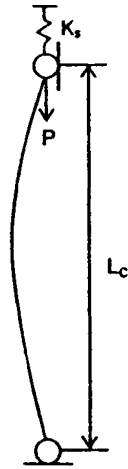
Figure 7.2: *Simple model of a restrained column*

The simple model shown in Figure 7.2 was analysed with the following values:

- Section HEA 100
- Length of the column 4 m
- Yield strength, f_y = 235 MPa
- Young modulus, E = 210 000 MPa
- Buckling resistance $N_{b,fi,Rd}$ = 129 kN, load ratio of 0.39 (i.e. P = 50 kN)
- Area of the section, A = 2120 mm²
- Buckling about the major axis
- Material model from EN 1993-1-2 (2005)
- R (degree of stiffness) varies from no restraint to full restraint.

The stiffness of the spring K_s is given by Equation (7.1):

$$R = \frac{K_s}{K_{co}} \Rightarrow K_s = R \times K_{co} \tag{7.1}$$

where K_{co} is the stiffness of the column at room temperature,

$$K_{co} = \frac{E \times A}{L} \tag{7.2}$$

The value of P is varied from one simulation to another as a function of the restraint in order to induce in the column an initial axial load $N_{initial}$ of 50 kN in all cases. Figure 7.3 demonstrates the results of Franssen's model with six different degrees of restraint, showing the evolution of axial force in the column as a function of the temperature. Growth in axial force is due solely to restrained thermal expansion.
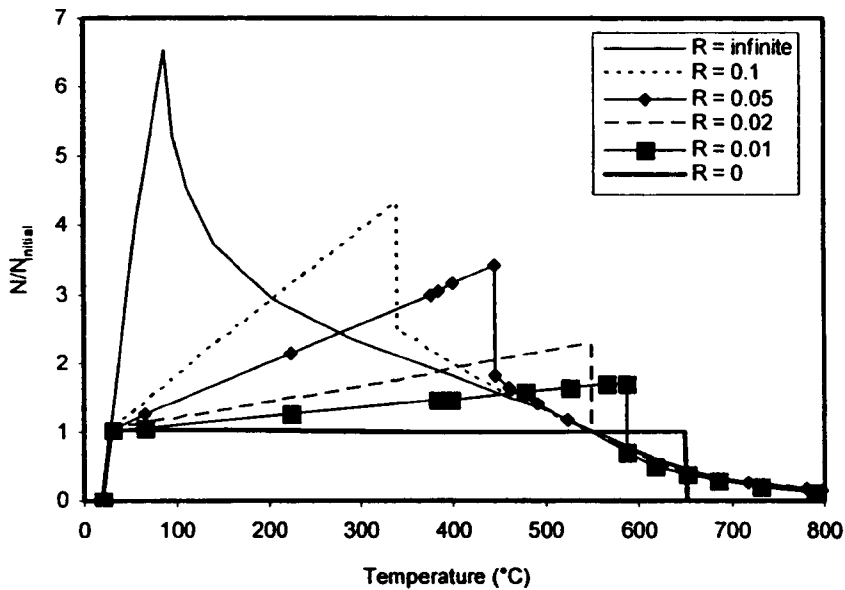
Figure 7.3: *Evolution of the axial force in columns as a function of temperature (Franssen, 2000)*

The critical temperature was defined as when the column could no longer support the initial axial load of 50 kN. The first simulation was made with no restraint, R = 0. The axial force remained constant and the critical temperature was obtained at 652°C. For a degree of restraint of 1% and 2%, the axial force in the column increased progressively when the temperature rose. Buckling occurred at 590°C and 550°C respectively.

For degree of restraint higher than 2%, the buckling of the column occurred at a lower temperature. In any analysis that will not allow the simulation to calculate beyond the local failure, this temperature causing the buckling of the column will be considered as the critical temperature of the structure and the resulting influence of axial restraint on the stability of the structure becomes very severe. However, it is shown in Figure 7.3 that the column is still able to support more than the initial axial load when it buckles, thus the structure is not in danger at this temperature and the temperature can be increased further. Critical temperatures (when the

axial resistance falls below $N_{initial}$) for the various levels of restraint R according to Franssen's models, are therefore given as:

For R = 0, critical temperature = 652°C

For R = 1%, critical temperature = 590°C

For R = 2%, critical temperature = 550°C

For R = 5% critical temperature = 550°C

For R = 10%, critical temperature = 550°C

For R = infinite, critical temperature = 550°C

It can be summarised that for any degree of restraint, the column considered was able to support the initial load of 50 kN as long as the temperature in the column did not reach 550°C. Typical column restraint that exists in structural frames has been estimated to be 2-3% (Wang and Moore, 1994).

7.2.3 Numerical modelling

A numerical modelling study was performed to gain further insight into the influence of thermal expansion of carbon steel and stainless steel compression members in fire. Initially, comparisons were made against the findings of Franssen (2000). The finite element software package ABAQUS was employed throughout the study.

The carbon steel and stainless steel members were modelled using the beam element type of B31, which is a 2-node linear beam. An element size (length) of 20 mm was used throughout the study. Pin-ended boundary conditions were replicated by restraining suitable displacement and rotation degrees of freedom at the column ends.

Franssen's modelling was performed anisothermally. This was reflected in the numerical modelling herein by performing the analyses in two steps: in the first step, load was applied to the column at room temperature, and in the second step, temperature was increased gradually until failure.

The relationship between thermal expansion and temperature for carbon steel and stainless steel given in EN 1993-1-2 (2005) was included in the models. However ABAQUS requires the thermal expansion to be expressed as given by Equation (7.3):

$$\alpha = \frac{\varepsilon^{th}}{(\theta - \theta_0)} \qquad\qquad (7.3)$$

where α is the coefficient of thermal expansion, ε^{th} is the thermal elongation at temperature θ, and θ_0 is the room temperature.

A lateral load of 1.6% of 50 kN was applied at the mid-height of the column, to represent imperfections in the member.

7.2.4 FE models with carbon steel properties

The initial step was to replicate Franssen's models using ABAQUS. Figures 7.4 and 7.5 compare the results of Franssen with those obtained herein (which are labelled FE). Overall, the results are in good agreement for all degrees of restraint, with buckling occurring at marginally lower temperatures in the present study.
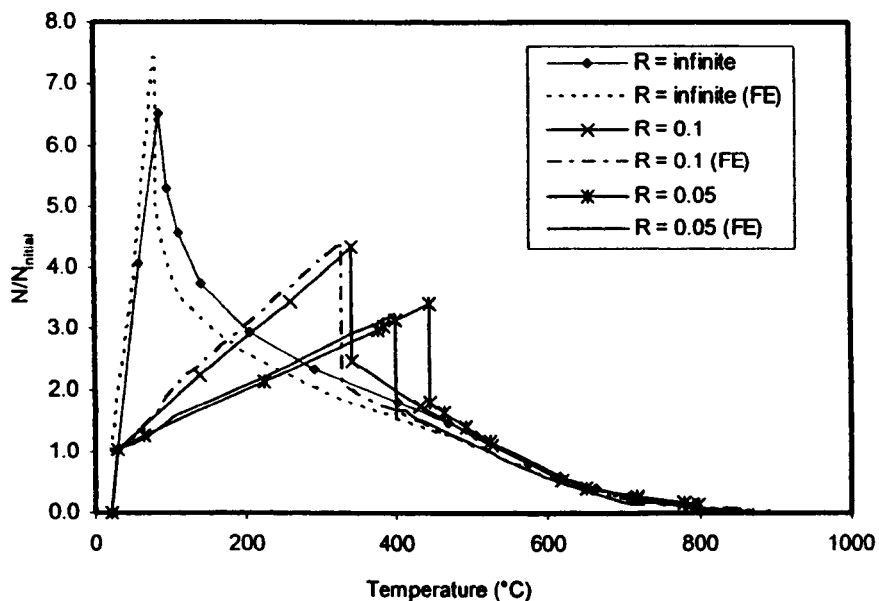
Figure 7.4: *Evolution of axial force with temperature for carbon steel column (R = 0.05, 0.1 and infinite)*
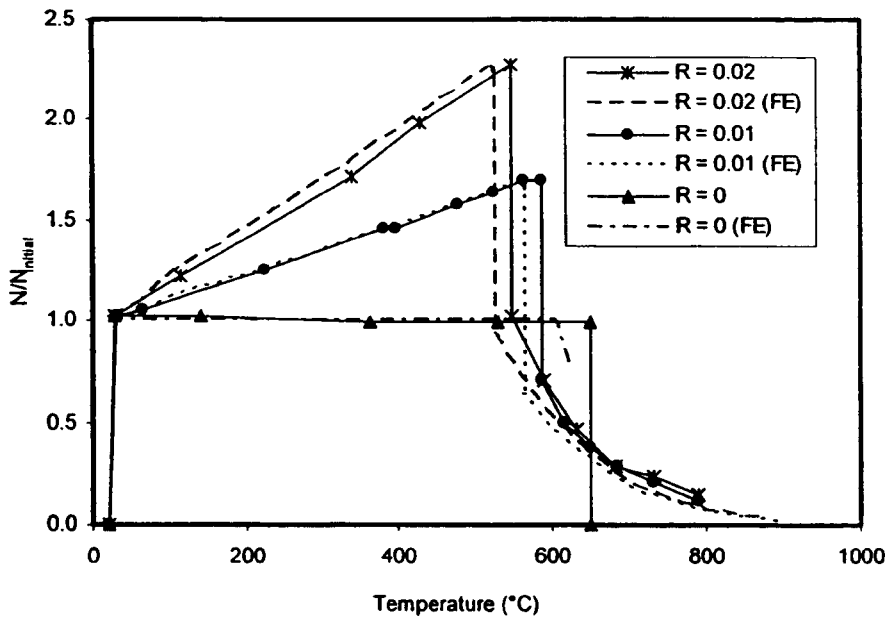
Figure 7.5: *Evolution of axial force with temperature for carbon steel column (R = 0.02, 0.01 and 0)*

7.2.5 FE models with stainless steel properties

Stainless steel models were analysed with the following parameters:

- Grade 1.4301

- Length of the column 4 m

- Yield strength, $f_y = 210$ MPa

- Young modulus, E = 200 000 MPa

- Material model for stainless steel from EN 1993-1-2 (2005)

- Buckling resistance $N_{b,fi,Rd} = 121$ kN, load ratio of 0.41 (i.e. P = 50 kN)

Figures 7.6 and 7.7 compare the evolution of axial force with temperature for carbon steel and stainless steel columns. It may be seen that the rate of increase in axial load with temperature is greater for stainless steel than for carbon steel, as a result of the higher thermal expansion. The peak load reached is controlled by two opposing and temperature-dependant effects – thermal expansion and buckling. With increasing temperature, the column expands, resulting in greater axial force in the member. However, this increase in axial force and the reduction in material

stiffness (and strength) due to increasing temperature, both promote the onset of buckling. The effect of buckling is to relieve the axial force in the member due to the associated lateral deflections.
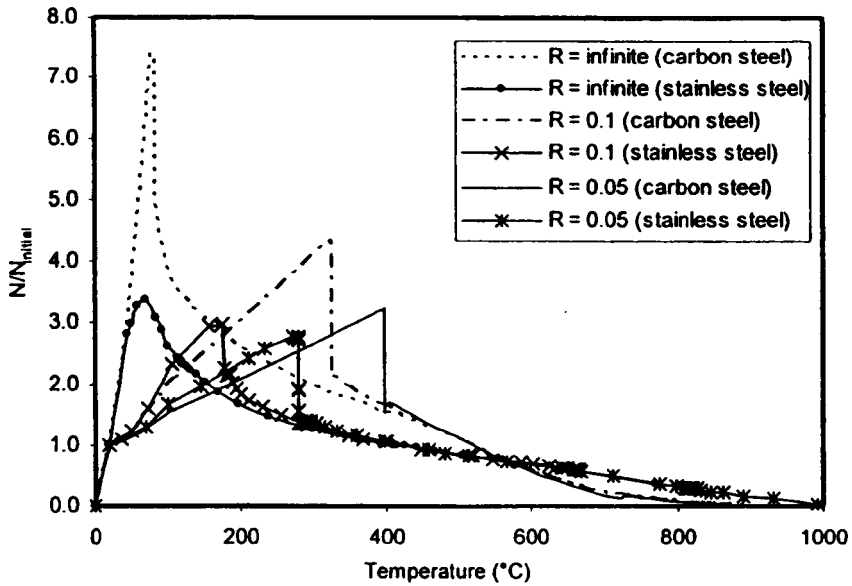
Figure 7.6: *Comparison of evolution of axial force with temperature between carbon steel and stainless steel columns (R = infinite, 0.1 and 0.05)*
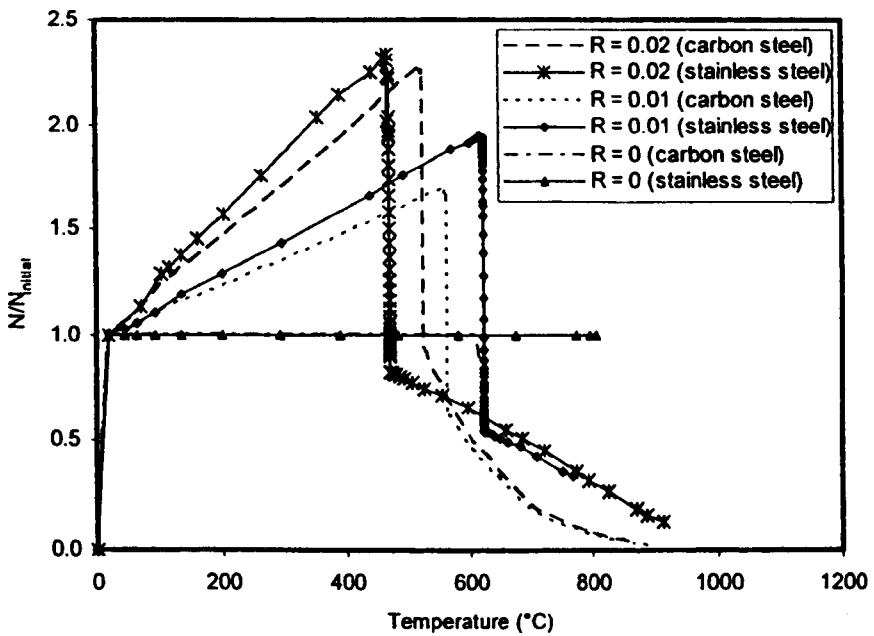
Figure 7.7: *Comparison of evolution of axial force with temperature between carbon steel and stainless steel columns (R = 0.02, 0.01 and 0)*

Figures 7.8 and 7.9 show how the lateral deflection of the carbon steel and stainless steel columns varied with temperature for different axial restraint conditions. In Figure 7.6, the peak generated axial force under full axial restraint occurred at 80°C for carbon steel and 60°C for stainless steel. As explained above, the drop in axial force beyond the peak is associated with buckling of the columns, signalled in Figure 7.8 by rapid increases in lateral deflections at approximately 80°C for carbon steel and 60°C for stainless steel. For high restraint conditions, the effect of restrained thermal expansion is very significant, causing rapid increases in axial force at relatively low temperatures. At these temperatures, the carbon steel columns have greater resistance to lateral deflections (due to the greater low temperature stiffness and strength) and therefore exhibit higher peak loads. However, for high temperatures, the reverse is true (see Chapter 3), and the stainless steel columns exhibit higher peak loads. Figure 7.9 shows that for 10% restraint, the stainless steel columns buckles before the carbon steel column (at approximately 180°C and 330°C, respectively), whilst for the lower 1% restraint, the carbon steel column buckles at the lower temperature (570°C, as compared to 610°C for the stainless steel column).
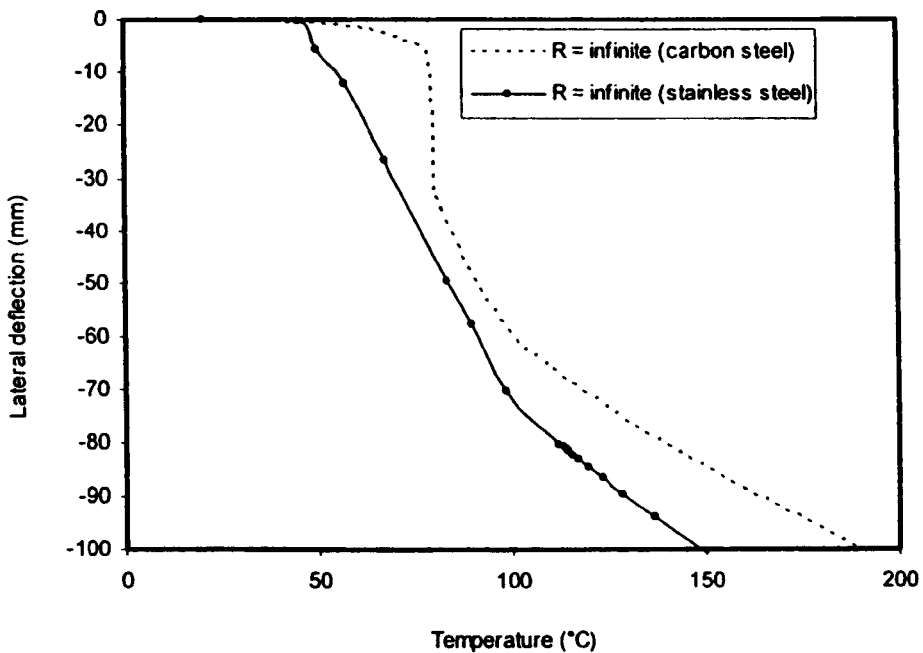
Figure 7.8: *Comparison of lateral deflection between carbon steel and stainless steel columns (R = infinite)*
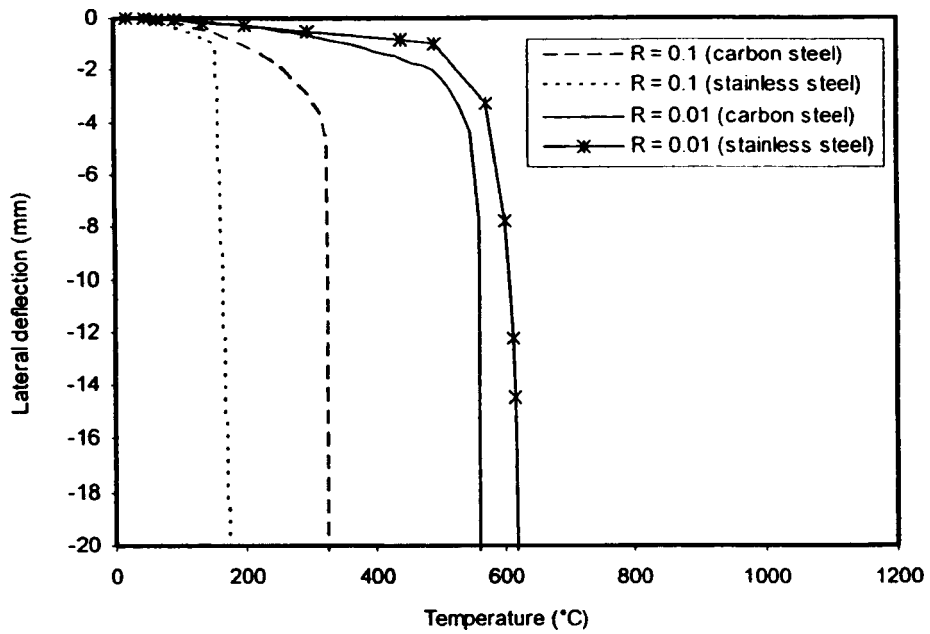
Figure 7.9: *Comparison of lateral deflection between carbon steel and stainless steel columns (R = 0.1 and 0.01)*

Figure 7.10 shows the end shortening (vertical deflections) of the carbon steel and stainless steel columns with 1% and 10% axial restraint stiffness. The evolution of vertical deflections exhibit a similar trend to that of the axial force as shown in Figures 7.6 and 7.7 (since they are closely linked before significant lateral deflection occurs). The vertical deflection initially increases due to the effect of thermal expansion, but shows a sudden drop after the peak is reached due to the rapid growth in lateral deflections associated with buckling.
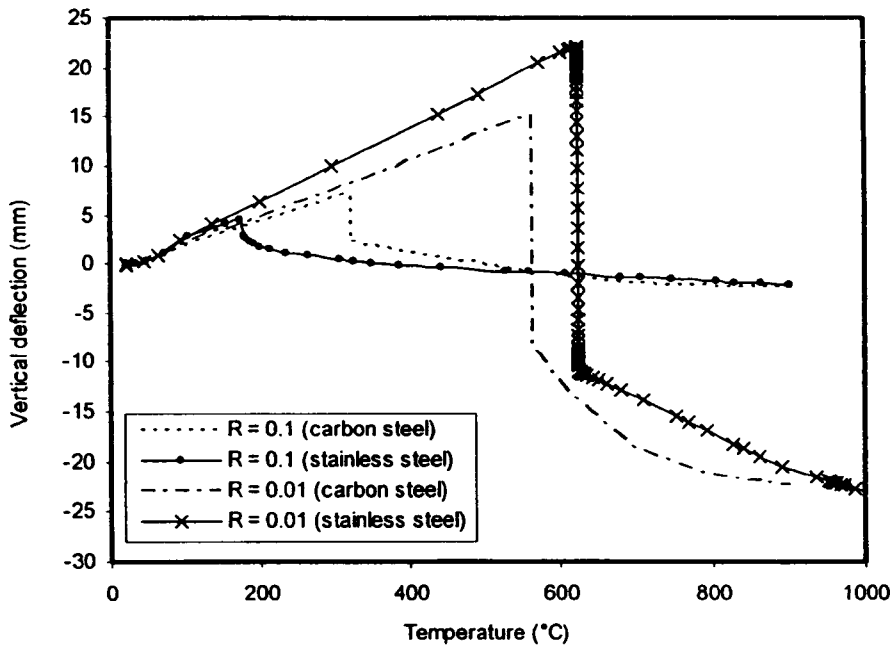
Figure 7.10: *Comparison of vertical deflection between carbon steel and stainless steel columns (R = 0.1 and 0.01)*

Table 7.1 compares the predicted critical temperatures (defined as the point where the resistance of the column falls below the initially applied load $N_{initial}$) from Franssen's method with those predicted in the current study using FE models with carbon steel and stainless steel properties and different degrees of restraint. As anticipated, the stainless steel column has a lower critical temperature under high restraint conditions due to its greater thermal expansion. For low restraint (0 and 1%), stainless steel has a greater critical temperature due to its higher retention factor of strength and stiffness.

Table 7.1: *Comparison of critical temperature with Franssen's method and FE models with carbon steel and stainless steel properties*

R	Critical Temperature (°C)		
	Franssen's model	Carbon Steel	Stainless steel
infinite	550	519	418
0.1	550	518	418
0.05	550	519	420
0.02	550	519	471
0.01	590	563	625
0	652	607	807

7.2.6 Parametric studies

The influence of load level and non-dimensional column slenderness $\bar{\lambda}$ was investigated to assess the general applicability of the results.

7.2.6.1 Load ratio

Figures 7.11 and 7.12 compare the evolution of axial force with temperature for carbon steel columns with three different load ratios: 0.3LR, 0.39LR (initial load ratio) and 0.5LR. As anticipated, when the load ratio is low, the critical temperature of the column is greater. Another observation from the figures is that, for any level of restraint (except no restraint), the value of generated axial force is greater (due to the effect of thermal expansion) when the load level is low.
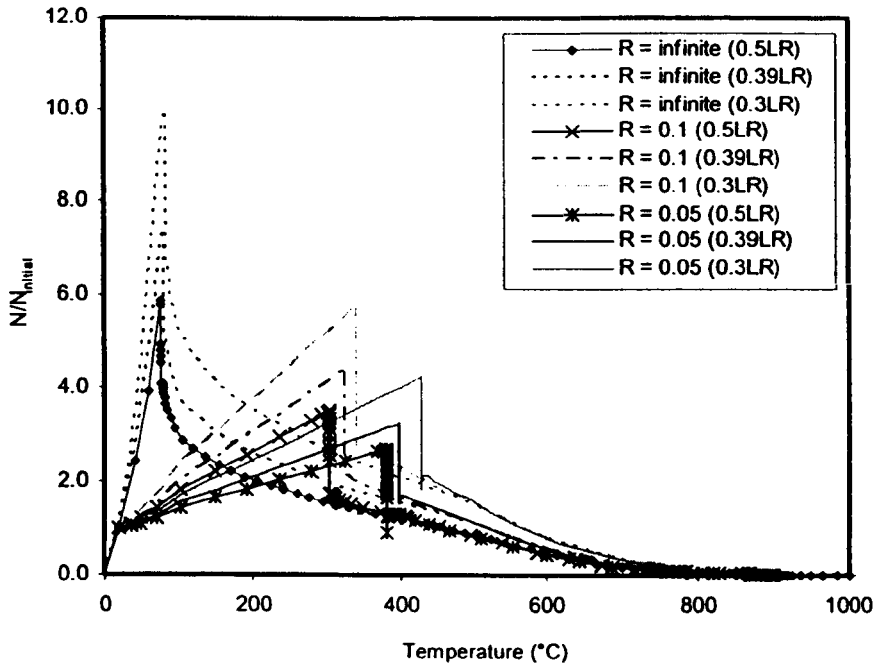
Figure 7.11: *Evolution of axial force with temperature for carbon steel column with three different levels of load ratio (R = infinite, 0.1 and 0.05)*
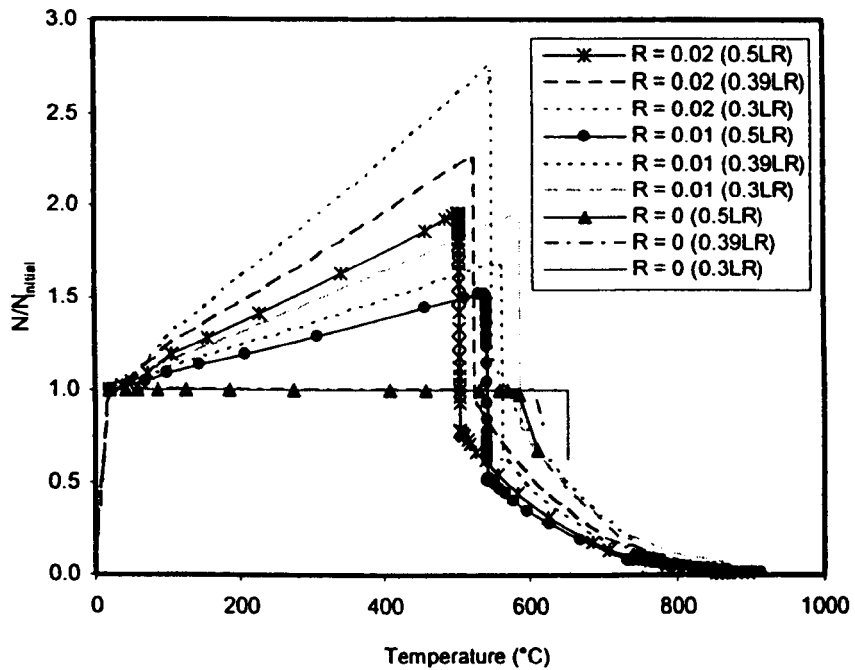
Figure 7.12: *Evolution of axial force with temperature for carbon steel column with three different levels of load ratio (R = 0.02, 0.01 and 0)*

Figures 7.13 and 7.14 compare the evolution of axial force with temperature for stainless steel column with three different load ratios: 0.3LR, 0.41LR (initial load ratio) and 0.5LR. The trend in the results is similar to carbon steel: low load ratios in the column resulting in higher critical temperatures. Figure 7.13 shows unusual results for R = 0.1 (0.5LR) attributed to numerical deficiencies, where high generated axial force is obtained even though the applied load is high (0.5LR).
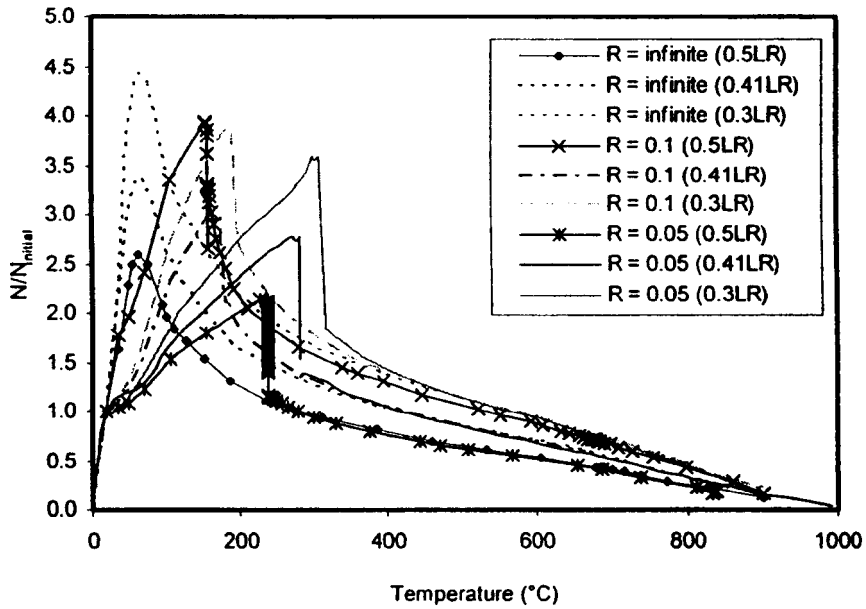
Figure 7.13: *Evolution of axial force with temperature for stainless steel column with three different levels of load ratio (R = infinite, 0.1 and 0.05)*

Figure 7.14: *Evolution of axial force with temperature for stainless steel column with three different levels of load ratio (R = 0.02, 0.01 and 0)*

Table 7.2 compares the predicted critical temperatures from FE models with carbon steel and stainless steel properties for different degrees of restraint and load levels. The results show that the load ratio significantly affects the critical temperature for both materials (more influence on stainless steel than carbon steel). As found earlier, the stainless steel columns have a lower critical temperature under high restraint conditions. For low restraint (0 and 1%), stainless steel has a greater critical temperature due to its higher retention factor of strength and stiffness.

Table 7.2: *Comparison of predicted critical temperature from FE models for carbon steel and stainless steel properties under different level of load level and restraint conditions*

	Critical Temperature (°C)					
	Carbon Steel			Stainless steel		
R	0.3LR	0.39LR	0.5LR	0.3LR	0.41LR	0.5LR
infinite	565	519	455	520	418	267
0.1	560	518	452	560	418	*
0.05	560	519	445	552	420	270
0.02	567	519	503	547	471	*
0.01	587	563	542	680	625	557
0	653	607	587	851	807	637

* Numerical difficulties caused premature termination of analysis

7.2.6.2 Non-dimensional slenderness

Column lengths of 3 m and 5 m have been modelled with a load ratio of 0.4 in order to compare with the initial column length, which is 4 m, and hence to assess the importance of non-dimensional member slenderness.

Figures 7.15 and 7.16 compare the evolution of axial force with temperature for carbon steel column lengths of 3 m, 4 m and 5 m under different restraint conditions. There is a general trend showing that the generated level of axial force (normalised by the column buckling resistance) increases with increasing the column length.
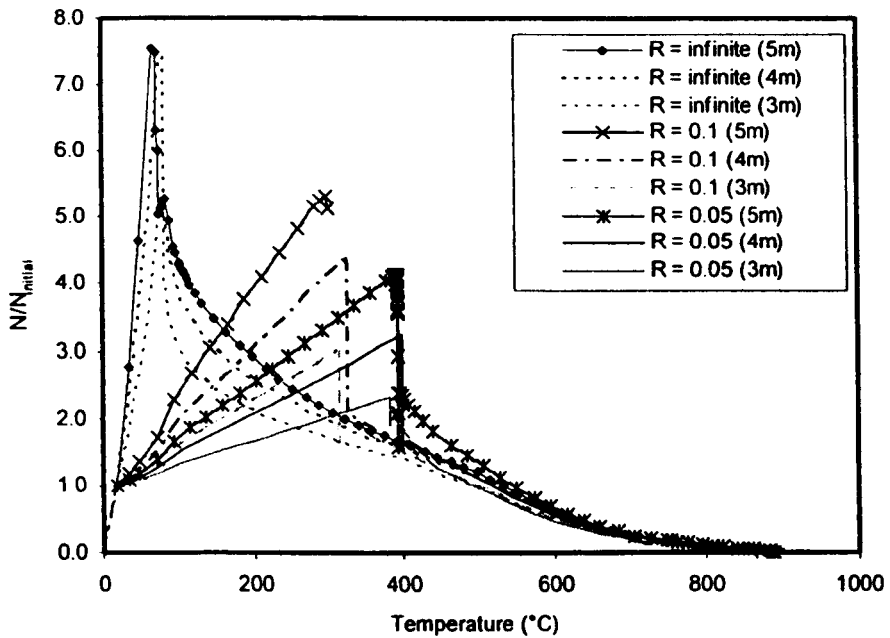
Figure 7.15: *Evolution of axial force with temperature for carbon steel column with three different column lengths (R = infinite, 0.1 and 0.05)*
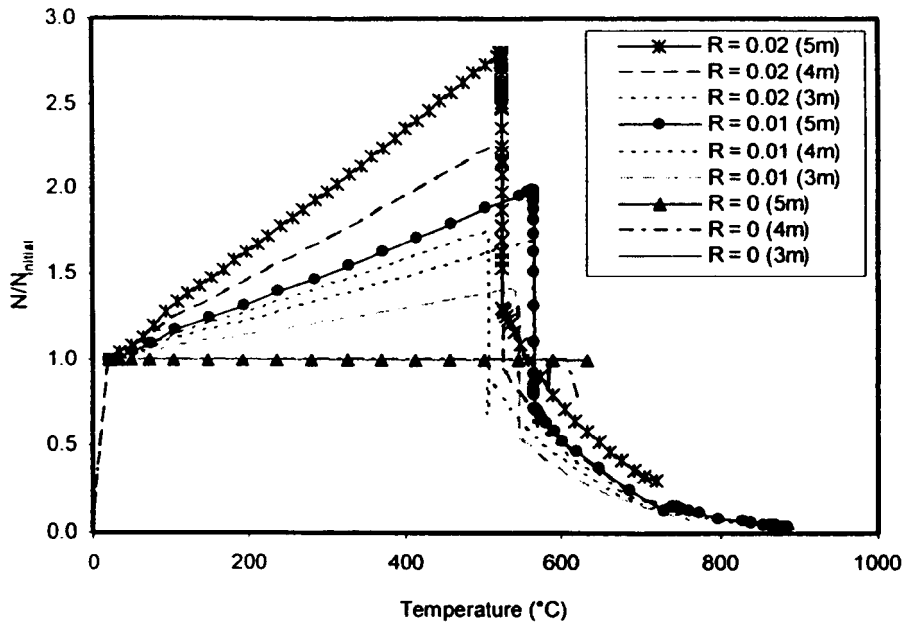
Figure 7.16: *Evolution of axial force with temperature for carbon steel column with three different column lengths (R = 0.02, 0.01 and 0)*

Figures 7.17 and 7.18 compare the evolution of axial force with temperature for stainless steel columns of length 3 m, 4 m and 5 m under different restraint conditions. Both figures show that the more slender stainless steel columns experience greater levels of normalised axial force than the stocky columns.
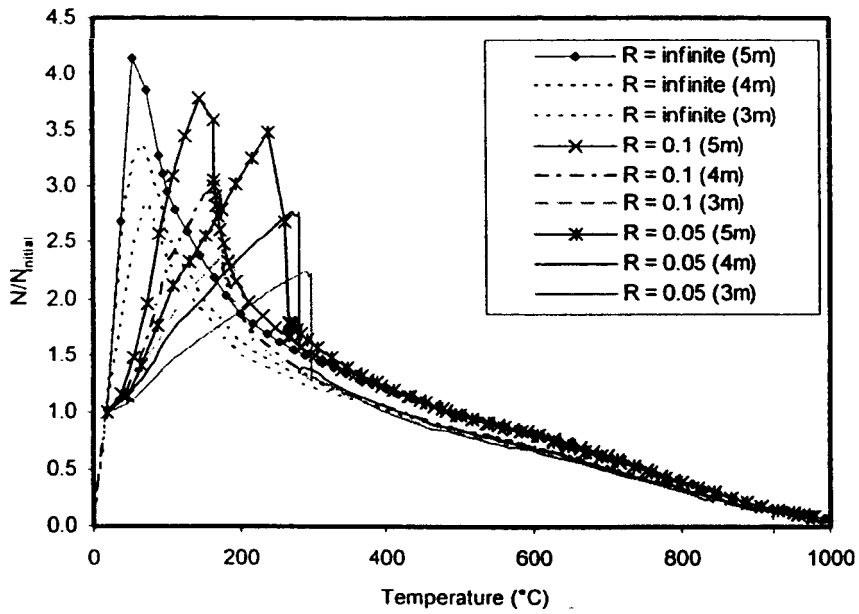
Figure 7.17: *Evolution of axial force with temperature for stainless steel column with three different column lengths (R = infinite, 0.1 and 0.05)*

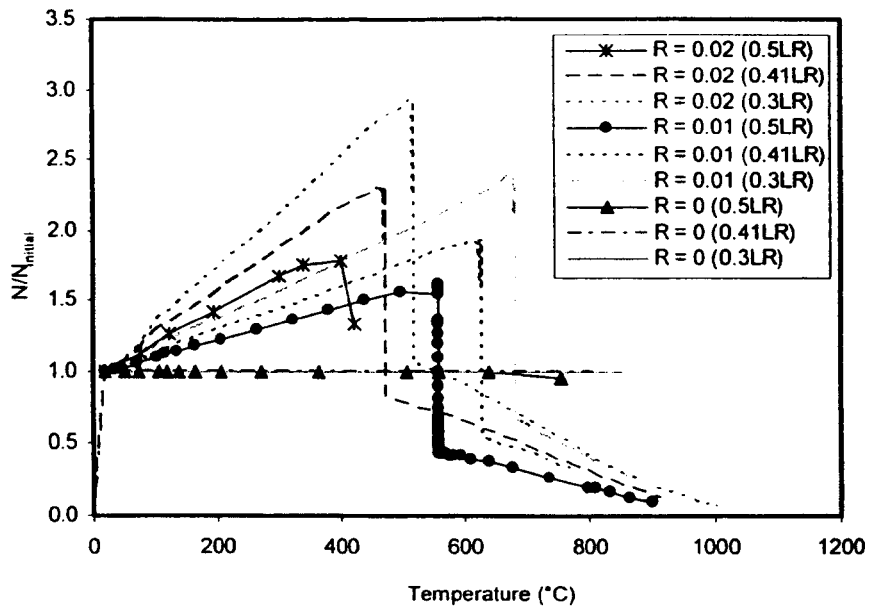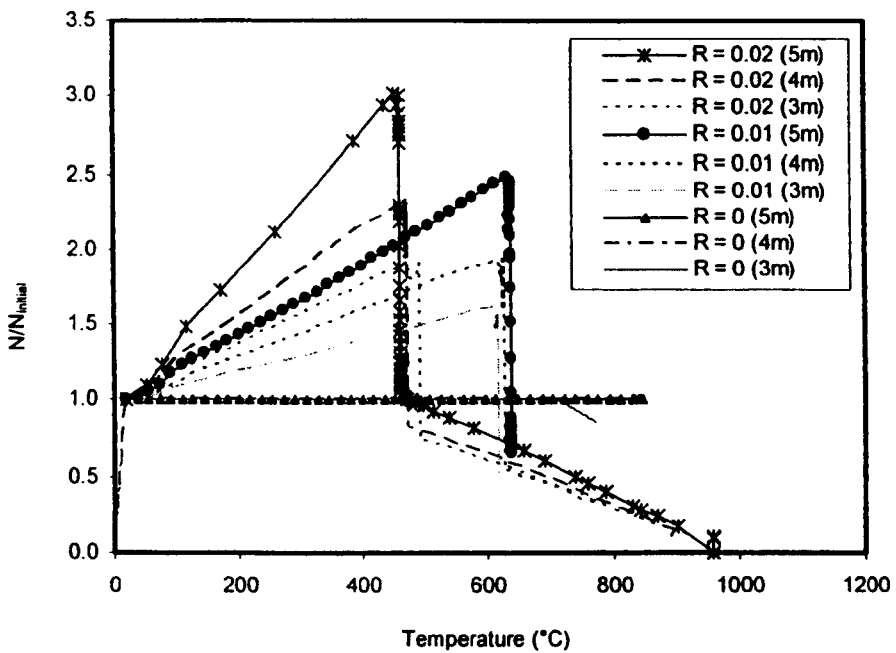**Figure 7.18:** *Evolution of axial force with temperature for stainless steel column with three different column lengths (R = 0.02, 0.01 and 0)*

Table 7.3 compares the predicted critical temperatures from FE models with carbon steel and stainless steel properties with different column lengths and different degrees of restraint. The

critical temperature is increased with increasing column length at any level of restraint for both carbon steel and stainless steel. The overall trend that stainless steel performs better at low levels of restraint and carbon steel performs better where high restraint is present remains to be the case.

Table 7.3: *Comparison of predicted critical temperature from FE models for carbon steel and stainless steel properties under different column length and restraint conditions (load ratio = 0.4)*

R	Critical Temperature (°C)					
	Carbon Steel			Stainless steel		
	L = 3 m	L = 4 m	L = 5 m	L = 3 m	L = 4 m	L = 5 m
infinite	490	519	517	399	418	490
0.1	473	518	*	394	418	491
0.05	510	519	533	401	420	480
0.02	507	519	559	490	471	476
0.01	546	563	567	616	625	638
0	581	607	634	718	807	848

* Numerical difficulties caused premature termination of analysis

7.2.7 Concluding comments

From the comparisons between Franssen's models and the generated numerical results, it may be concluded that the described finite element models are capable of replicating the axial force generated by thermal expansion of structural carbon steel and stainless steel members in fire.

The development of axial force in the columns has been shown to be controlled by two opposing and temperature-dependant effects – thermal expansion and buckling. With low levels of axial restraint, stainless steel columns have higher critical temperatures than carbon steel columns due to the superior strength and stiffness retention at high temperature. However, for high levels of axial restraint, the greater thermal expansion that stainless steel exhibits results in greater axial forces and lower critical temperatures. The actual level of axial column restraint that exists in structural frames has been estimated to be 2-3% (Wang and Moore, 1994). Clearly, both low levels of axial restraint and low load ratios enable the most effective exploitation of the superior high temperature strength and stiffness retention of stainless steel.

7.3 RESTRAINED BEAMS

7.3.1 Introduction

Restrained thermal expansion in beams initially induces axial compression which acts in combination with the bending moments from the vertical loading. However, at large deflections, the beams will pull-in at the supports inducing axial tension in the beam, which may be beneficial in terms sustaining the applied loads.

Fire resistant design of a steel beam based solely on its bending resistance will result in a relatively low survival temperature. This resistance is limited to the cross-section bending moment resistance or lateral torsional buckling resistance and will require expensive fire protection. A more efficient design method is needed in order to eliminate fire protection. Large deflections of steel beams may be tolerated under fire conditions provided a structure can maintain its stability. Provided axial restraint is present, the load-carrying mechanism of steel beams changes from bending to catenary action at large deflections, and this can significantly affect their survival temperature in fire.

7.3.2 Previous testing and modelling

Bailey (2000) reported the results from the Cardington full-scale tests. The results indicated that high moments occurred in the columns during the test. An analytical investigation into the consequence of these column moments on the overall stability of the column was presented. The analyses showed that instability could occur in the column due to the P-δ effect, which was enhanced by the enforced deflected shape of the column caused by the expansion of the connecting beams. It was concluded that column instability was significantly affected by:

- Beam to column heating rates
- Beam cross-section size – increasing beam size has a detrimental effect on the stability of the columns.
- Span of the beams – the longer the span is, the more fire protection required for the column.
- End fixity of the heated column – pinned base causes lower critical temperature on the column.

- Column axial load – the higher load ratio, the lower critical temperature.

The following parameters had a nominal effect on the behaviour of the column:

- Column cross-section size
- Beam-to-column connection rigidity
- Horizontal restraint to the heated beams.

Liu et al (2002) described an experimental programme conducted in the Fire Laboratory at the University of Manchester. The test furnace allowed unprotected or partially protected steel beams to be tested under load whilst restrained between two columns in a structure similar to a rugby goal post (as shown in Figure 7.19). The purpose of the tests was to investigate the structural response and failure of the steel beam under fire. These tests are described in more detail and are replicated in the following sections.

Wong (2005) used a simple technique to model the effect of axial restraints provided to a steel beam by neighbouring members and devised a procedure for determining its limiting temperature in a multi-bay situation in a building. The approach allowed for different end conditions for the columns below and above the beam and also catenary action due to the large deflections associated with beams in fire. The method also took into account the axial restraints provided by the other structural members adjacent to the steel beam. The effect of the axial restraints was modelled by a spring system from which an equivalent stiffness for a semi-rigid connection attached to the end of the beam was calculated. The results showed that if the deflection limit of steel beams was allowed to be relaxed to span/20, limiting temperatures would increase dramatically.

Yin and Wang (2004) replicated an experiment of Liu et al (2002) using ABAQUS to investigate the large deflection behaviour of steel beams in fire with different elastic axial and rotational restraints at the ends. A series of parametric studies were carried out in order to assess the important parameters that affect the development of catenary action in steel beams.

7.3.3 Numerical modelling

7.3.3.1 Introduction

In order to investigate the behaviour of restrained stainless steel beams in fire, numerical models were first developed to replicate the tests conducted by Liu et al (2002) on a restrained carbon steel beam. The same tests were also replicated numerically by Yin and Wang (2004). Once validated against the carbon steel beam tests, the physical and thermal properties of stainless steel are introduced to access the implications of these different properties on structural behaviour in fire.

7.3.3.2 Summary of Liu et al. tests

The goal post arrangement shown in Figure 7.19 provided the beam with an axial restraint stiffness of 62 kN/mm at both ends, while the extended end plate connections were estimated to provide a rotational restraint stiffness of 14,000 kN/rad. This rotational restraint can be modelled by two axial springs, each of stiffness 886 kN/mm, as shown in Figure 7.20. The design bending moment and shear resistance of the beam (UB 178×102×19) are 48 kNm and 156 kN respectively, based on a yield strength of 275 N/mm^2. This gives an expected load-carrying capacity, P of 80 kN load at room temperature (Liu et al, 2002). The experimental study considered two different load levels, having load ratios of 0.5 and 0.7, corresponding to loads equal to 40 and 56 kN respectively. The load ratio was defined as the ratio of applied maximum bending moment in a simply supported beam to the beam's plastic bending moment resistance at ambient temperature.
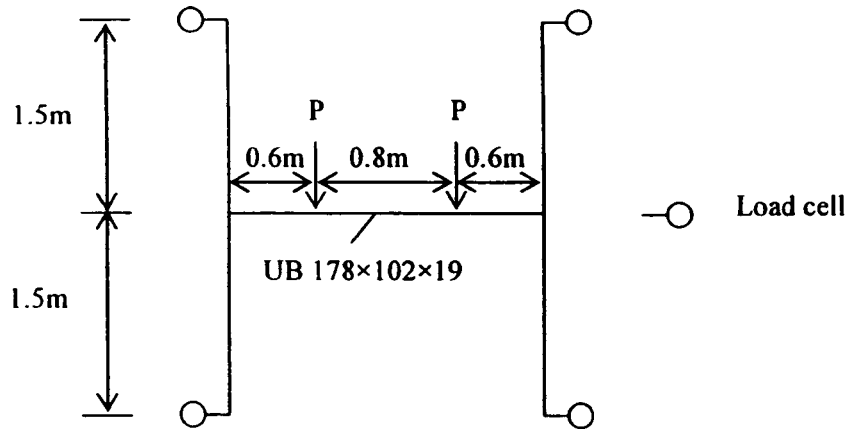
Figure 7.19: *Schematics diagram of the test arrangement of Liu et al (2002)*
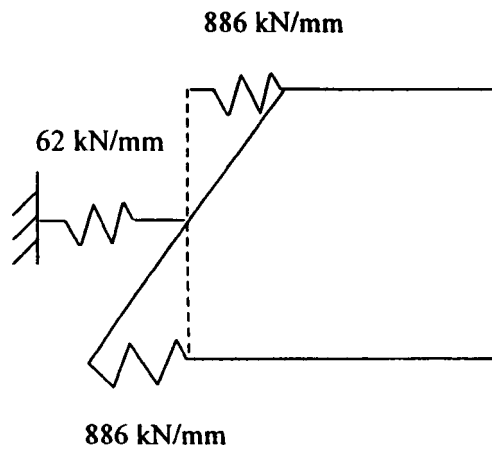
Figure 7.20: *Application of boundary conditions in numerical simulations of Liu et al tests (as employed by Yin and Wang (2004))*

7.3.3.3 Development of numerical modelling

The carbon steel and stainless steel beams were modelled using the shell elements of type S4R, which are suitable for thick and thin shell application (ABAQUS, 2003). An element size of 20 mm was employed throughout the study. All models were performed anisothermally, thus the numerical simulation was divided into two steps: the first step consists of load being applied at ambient temperature while in the second step the temperature is increased at constant load.

The geometrical properties of the steel beam section (UB 178×102×19) were taken from section tables (Corus, 2003). End plates of 10 mm were attached to each end of the steel beam to ensure plane rotation. The end plates were translationally restrained in the vertical and lateral directions. Restraint was provided by means of the linear spring system shown in Figure 7.21. Three axial springs were attached to each end of the beam – one was attached at the level of the neutral axis and fastened to the ground to provide axial restraint, whilst the other two were attached at the level of the flanges, constrained to act as a pair, and represented rotational restraint.
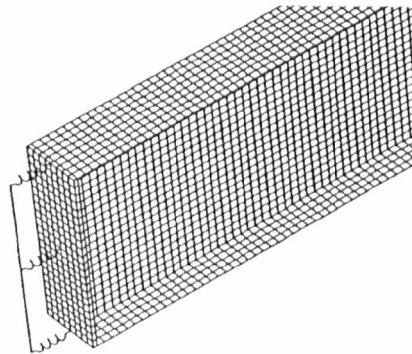
Figure 7.21: *Modelling of axial and rotational restraints*

7.3.3.4 Material modelling and temperature development

Material modelling represents one of the most important aspects of an FE simulation. Inappropriate definition of material behaviour will significantly hinder the ability of a model to replicate observed structural response. The stress-strain properties for the carbon steel beam were obtained by using the reduction factors for strength and stiffness at elevated temperature from EN 1993-1-2 (2005), as shown in Figure 7.22.
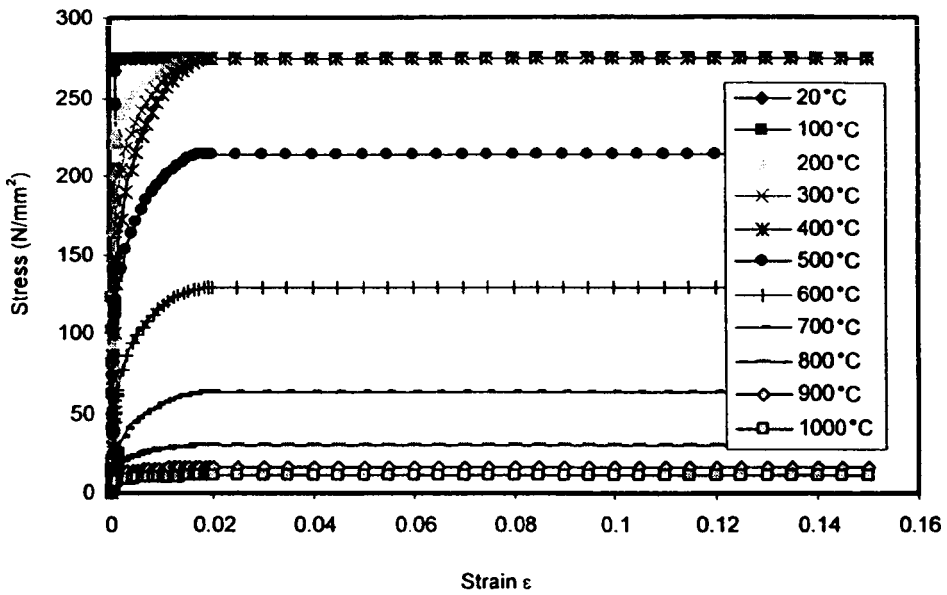
Figure 7.22: *Stress-strain relationship of carbon steel at elevated temperature*

For the stainless steel beam, appropriate properties were defined based on the strength and stiffness reduction factors for stainless steel at elevated temperatures from EN 1993-1-2 (2005). Figure 7.23 illustrates the adopted stress-strain curves for stainless steel at elevated temperature.
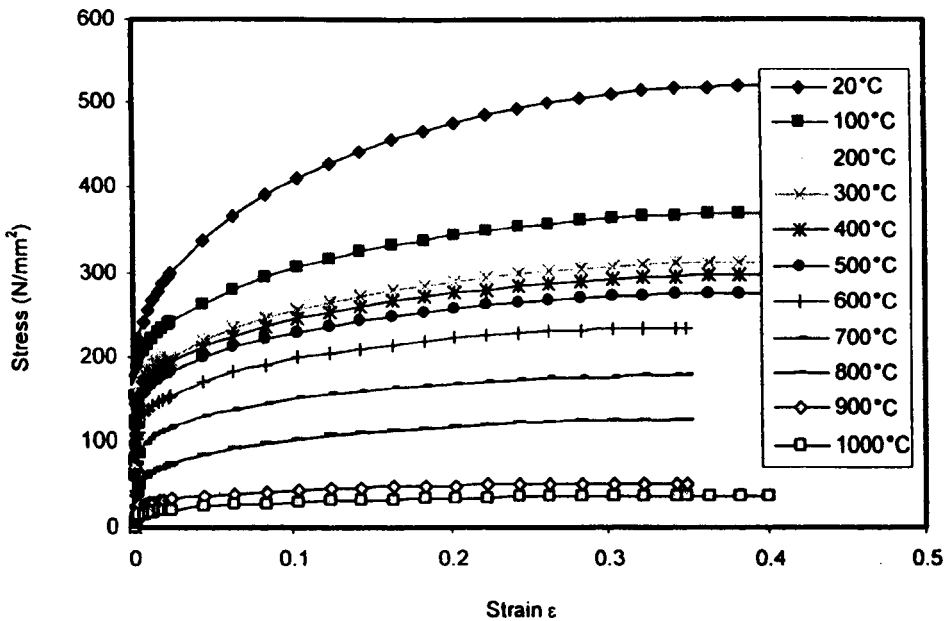
Figure 7.23: *Stress-strain relationship of stainless steel at elevated temperature*

The adopted ambient temperature properties are shown in Table 7.4.

Table 7.4: *Adopted material properties of carbon steel and stainless steel at ambient temperature*

	Carbon steel	Stainless steel
Young's Modulus, E	205000 N/mm²	200000 N/mm²
Yield Strength, f_y	275 N/mm²	210 N/mm²
Poisson Ratio	0.285	0.3

The material stress-strain relationships were defined in ABAQUS as described in Section 5.3.2. The material coefficients of thermal expansion was taken from EN 1993-1-2 (2005) for both materials.

Figure 7.24 shows the measured temperature against time of the bottom flange, web and the top flange, from Liu et al's (2002) tests. These were incorporated directly into ABAQUS to simulate the tests.
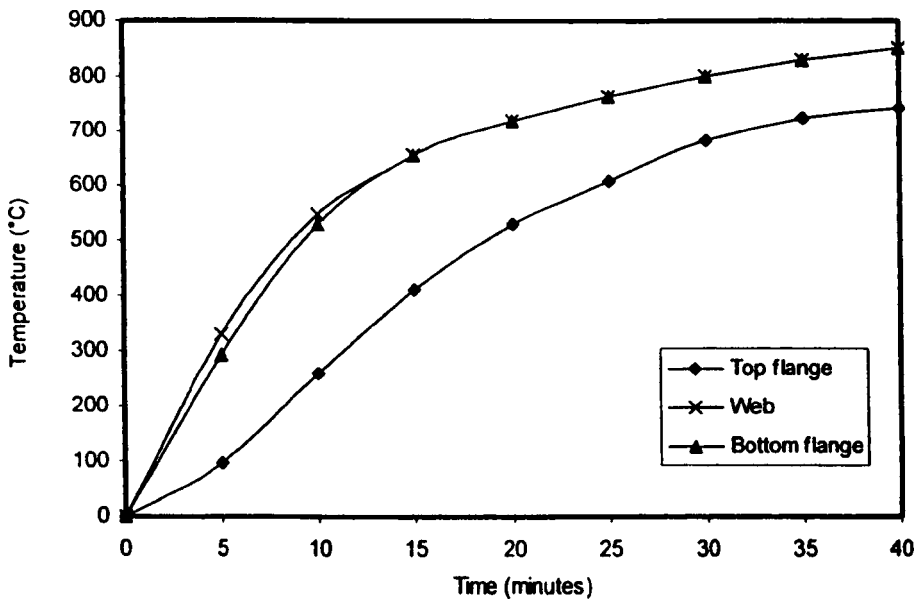
Figure 7.24: *Measured beam temperature-time relationship from Liu's tests.*

7.3.3.5 Comparison of FE models with Liu et al's tests and Yin and Wang's models

Figures 7.25 and 7.26 compare the deflection and axial force against temperature obtained herein (labelled FE) with the test results and those obtained by Yin and Wang (2004). The comparison demonstrates that, in general, the FE simulation follows the same trend as the test and Yin and Wang's model. Differences between FE and test behaviour may relate to differences in material properties (including strength and stiffness reduction factors) and temperature. The initial slower rate of increase in compressive force in the tests compared to the FE model can be explained by the initial low axial stiffness of the end restraint to the test beam before it became fully effective.
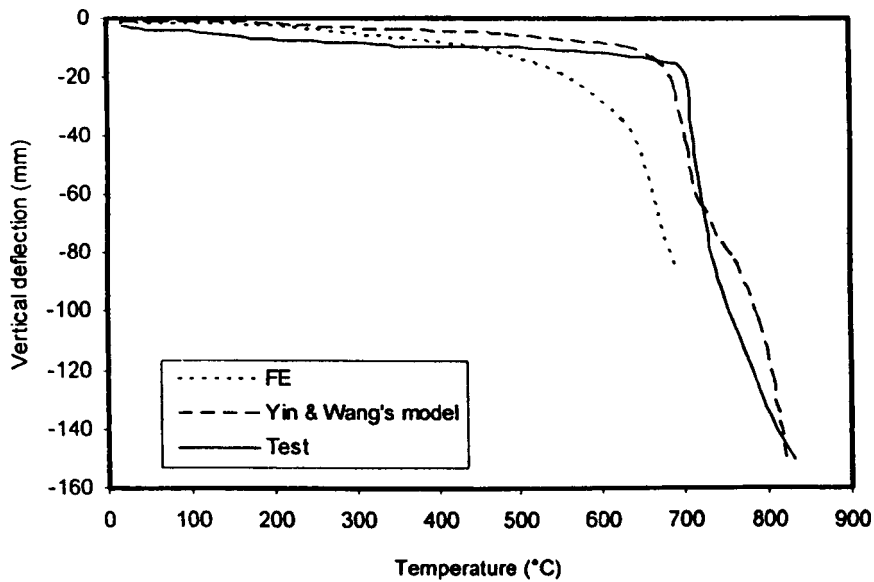
Figure 7.25: *Comparison of experimental and simulation temperature-deflection curves with axial restraint.*
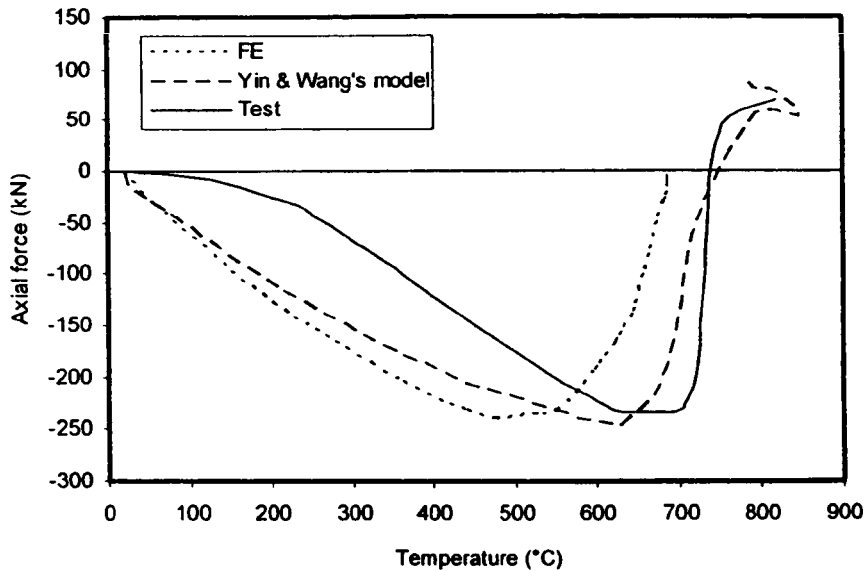
Figure 7.26: *Comparison of experimental and simulation temperature-axial reaction curves with axial restraint.*

After validating the FE models with the test and Yin and Wang's model, it was possible to expand the studies using stainless steel properties. A FE model with an additional level of restraint (low rotational restraint stiffness of 886 N/mm) has been developed to investigate its influence on the behaviour of beams. Figures 7.27 and 7.28 compare the deflection and axial reaction force of stainless steel and carbon steel with two level of rotational restraint stiffness, low and high (corresponding to axial springs of stiffness 886 kN/mm and 886 N/mm). At room temperature, both carbon steel and stainless steel beams deflect more with lower rotational restraint. At 200°C to 600°C, stainless steel beams deflected more than carbon steel beams due to its higher thermal expansion. For temperatures beyond 600°C, the carbon steel beams show a rapid increase in deflection. This can be explained by the fact that carbon steel only retains about 30% of its room temperature stiffness at 600°C. However, stainless steel retains about 75% of its room temperature stiffness at that temperature.

Figure 7.28 shows that the carbon steel beams exhibits catenary action (characterised by tensile axial forces) at approximately 600°C to 700°C whilst the stainless steel beams' catenary action occurs at higher temperatures. The delay in reaching catenary action is due to the lower. deflections at high temperature that results from the superior stiffness retention. From Figure 7.28, it can be seen that although stainless steel exhibits higher thermal expansion than carbon

steel, the stainless steel beam induces significantly lower compressive axial forces than the carbon steel beam for low rotational restraint. The lower axial forces result from the higher deflections that the stainless steel beam exhibits at low temperatures. The deflection will be due to a combination of in-plane bending from the applied vertical loading and buckling due to the axial compression resulting from thermal expansion. High rotational restraint reduces both of these deflection components, leading to higher axial forces.
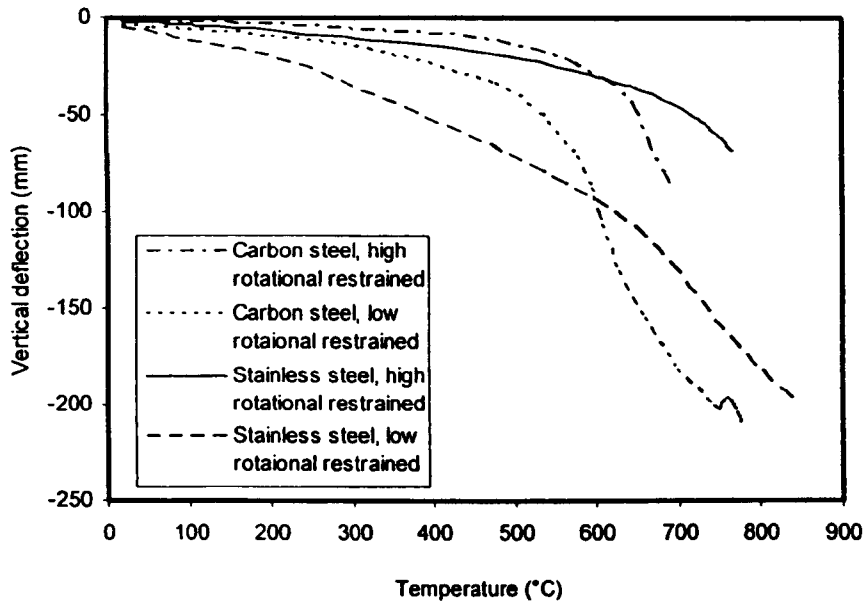
Figure 7.27: *Comparison of experimental and simulation temperature-deflection curves with different levels of rotational restraint*
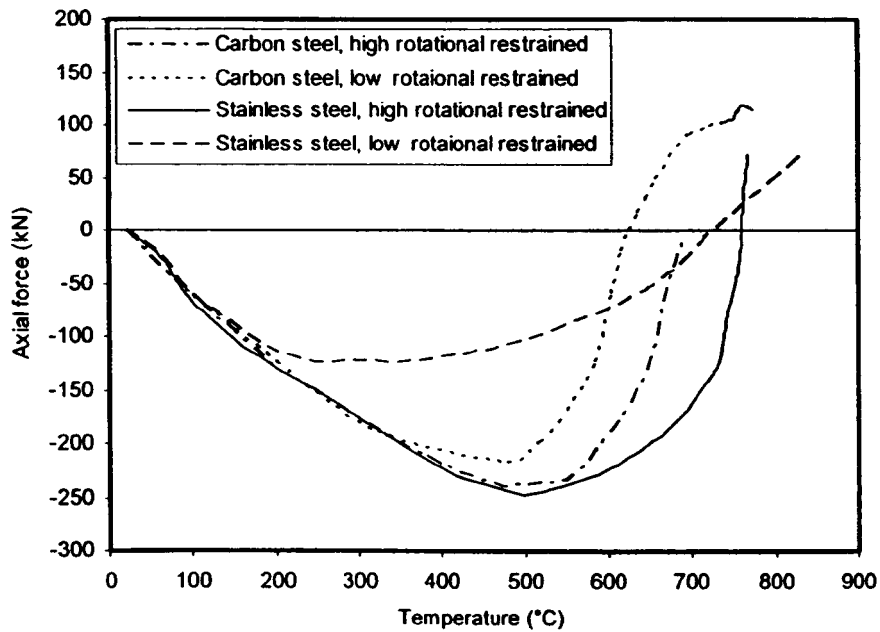
Figure 7.28: *Comparison of experimental and simulation temperature-axial reaction curves with different levels of rotational restraint*

7.3.4 Parametric studies

Following satisfactory agreement between the test and FE results, a series of parametric studies were performed in order to investigate the influence of different levels of restraint to the response of carbon steel and stainless steel beams at elevated temperatures. Yin and Wang (2004) used the beam dimensions of UB 457×152×60 with a span of 8 m for their parametric studies; to allow direct comparisons, the same dimensions have been adopted herein. A central point load was applied at the top flange and lateral torsional buckling of the beam was prevented with lateral restraints. The applied load ratio was 0.7, corresponding to load equal to 62 kN.

7.3.4.1 Laterally restrained beams with different levels of axial restraint

In a real structure, the level of axial restraint to the beams provided by columns or subframes are limited, thus it is not possible to fully restrain the beams from axial movement. A series of different assumed axial restraint stiffness values were considered to investigate the effect of

flexible axial restraints. Table 7.5 shows five different levels of axial restraint, calculated as fixed proportions of the axial stiffness of the beam at room temperature K_B, calculated as $K_B =$

$$\frac{EA}{L} = 195 \text{ kN/mm}.$$

Table 7.5: *Five artificial axial restraint stiffness values.*

Level of restraint	Axial spring stiffness (kN/mm)
0.02 K_B	3.9
0.05K_B	9.8
0.15 K_B	29.3
0.30 K_B	58.5
K_B	195.0
Fully restrained	1000.0

Yin and Wang (2004) stated that the beam is rotationally restrained without giving a numerical value. It was decided to adopt 5% of the rotational stiffness, $0.05K_R$ (achieved with axial springs of stiffness 6.25 kN/mm) as given in Table 7.6. This small value of rotational restraint lead to more stable numerical solutions.

Figures 7.29 to 7.32 demonstrate how the different levels of axial restraint stiffness have a significant effect on both the deflections and axial reaction forces for the carbon steel beam, particularly at low temperatures. The simulations in the present study did not proceed as far as those reported by Yin and Wang (2004), due to convergence problems. However, similar trends in the data may be observed. Steel beams with higher axial restraints encounter more axial compressive force due to the restrained thermal expansion, and the catenary action began almost at the same time for all different levels of axial restraint stiffness, as shown in Figures 7.31 and 7.32.

Figure 7.29: *Deflection curves for different level of axial restraint stiffness for Yin and Wang's model*
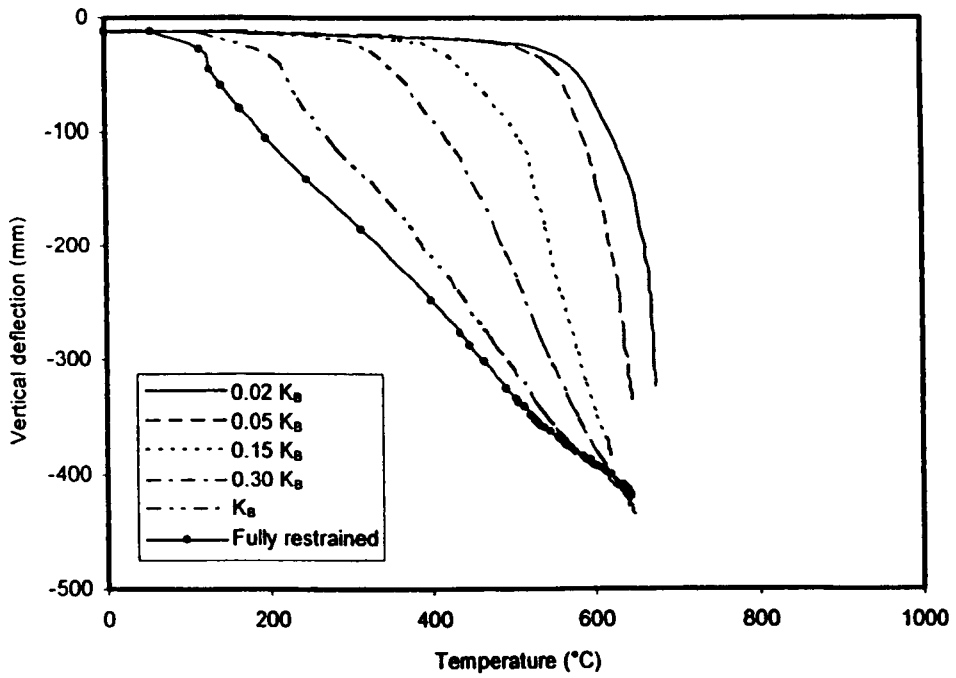
Figure 7.30: *Deflection curves for different level of axial restraint stiffness for FE simulation*
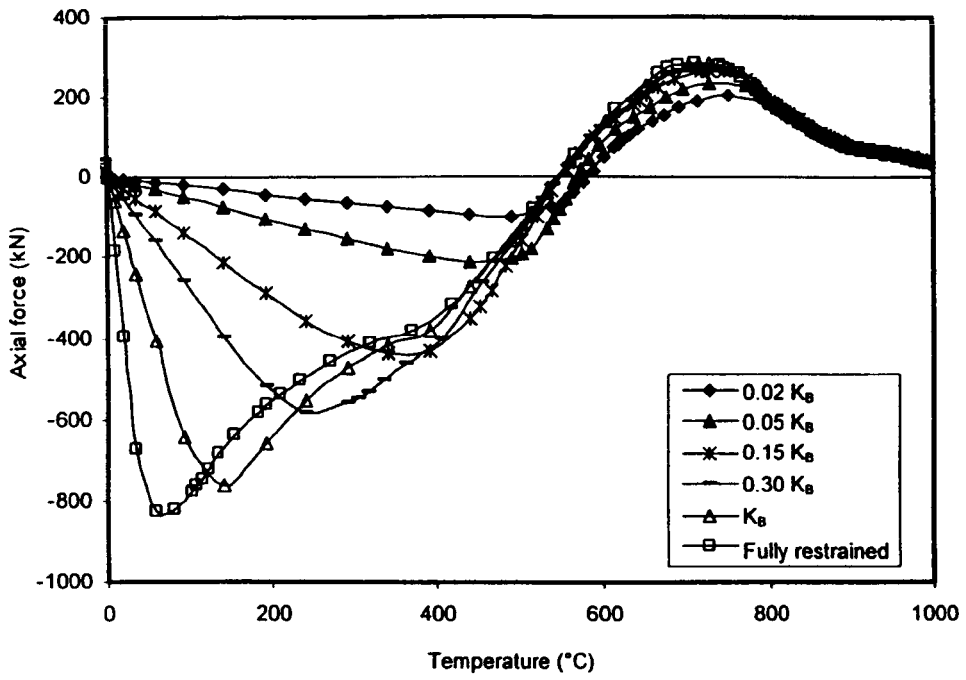
Figure 7.31: *Axial reaction force for different level of axial restraint stiffness for Yin and Wang's model*
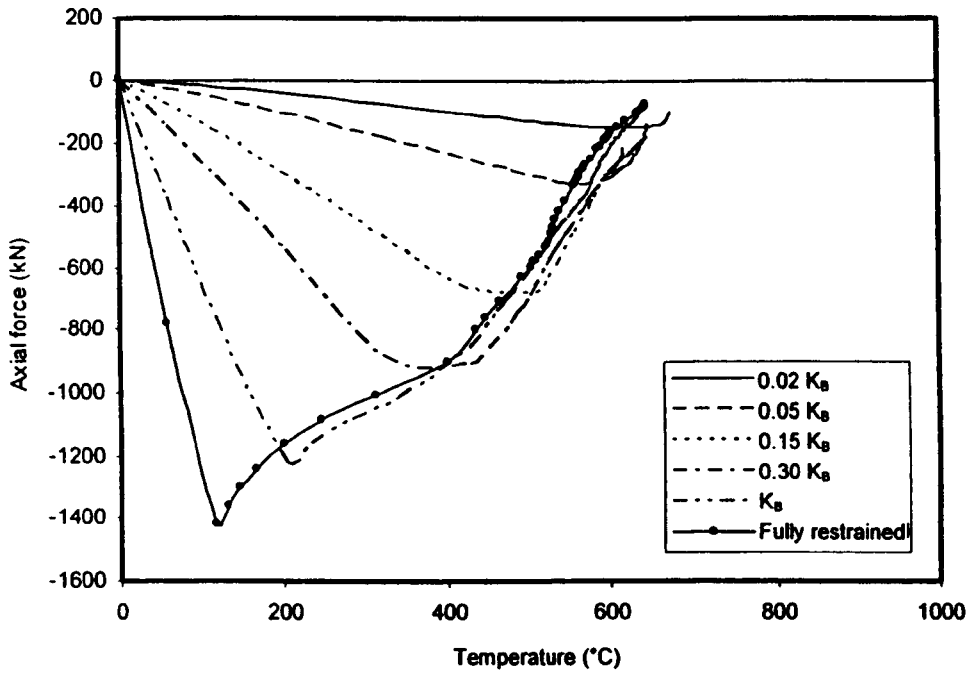
Figure 7.32: *Axial reaction force for different level of axial restraint stiffness for FE simulation*

Figures 7.33 and 7.34 compare the temperature-deflection and temperature-axial reaction force relationships for carbon steel and stainless steel beams. As anticipated, stainless steel deflects more than carbon steel under high axial restraint conditions, due to its higher thermal expansion rate. For low axial restraint, the buckling effect due to restrained thermal expansion is less significant. Thus stainless steel deflects less than carbon steel due to its better retention of stiffness at elevated temperature.

Figure 7.34 shows that the higher the axial restraint, the higher the axial compressive forces that are generated and also the larger the deflections that occur at low temperature. However, at high temperature, higher axial restraints reduce beam deflections. Figure 7.34 shows higher peak axial forces occurring for the carbon steel beams.

Figure 7.33: *Comparison of temperature-deflection curves for carbon steel and stainless steel beams with different levels of axial restraint.*

Figure 7.34: *Comparison of temperature-axial reaction curves for carbon steel and stainless steel beams with different levels of axial restraint.*

7.3.4.2 Laterally and axially restrained beams with different levels of rotational restraint

A beam may also receive rotational restraint from the surrounding structure. Five levels of rotational restraint, including fully restrained as shown in Table 7.6, were applied. The value of K_R is the rotational rigidity of the beam at room temperature, with a value of 13000 kN/rad. An equivalent rotational restraint by using two axial restraint springs acting at the flanges and an adjoining rigid element. The axial restraint used was 100 kN/mm per spring.

Table 7.6: *Six different levels of artificial rotational restraint.*

Type	Rotational restraint (kNm/rad)	Equivalent axial restraint (kN/mm)
Free rotation	0	0
$0.05K_R$	650	6.3
$0.3K_R$	3900	37.8
$0.5K_R$	6500	62.9
K_R	13000	126.0
Fully restrained	Large value	1000.0

Figures 7.35 to 7.38 show that the developed FE models have similar deflection and axial reaction force as Yin and Wang's models. As anticipated, when increasing the rotational restraint, the beam's flexural buckling length is reduced and the beam's axial buckling capacity is increased. Both models agree that, at low temperature, an increase in the rotational restraint gives a reduction in the beam deflection. However the rate of increase in the compressive force in the beam is the same for all levels of rotational restraint since the same cross-section is used. Yin and Wang's models demonstrate that the beam behaviour is controlled by catenary action at high temperature. In general, it may be stated that the level of rotational restraint has relatively little effect on the beam's overall behaviour.
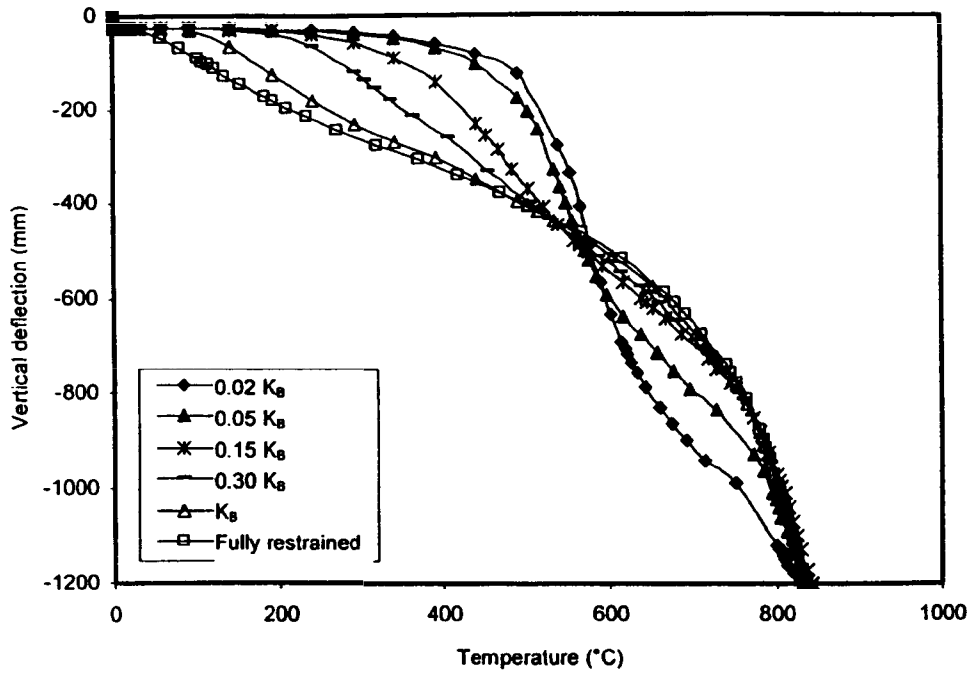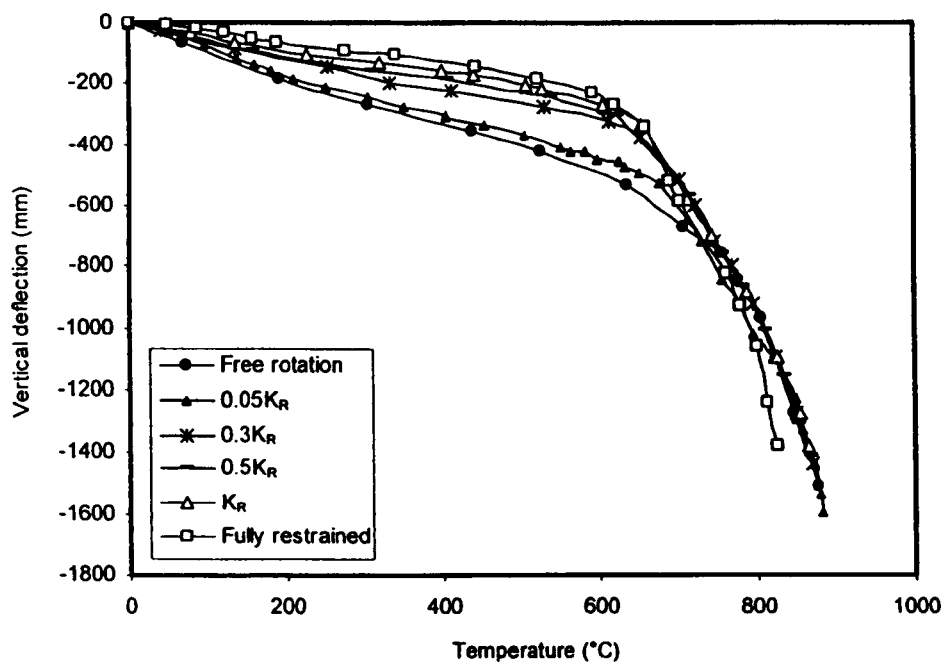

Figure 7.35: *Deflection curves of different level of rotational restraint for Yin and Wang's model*
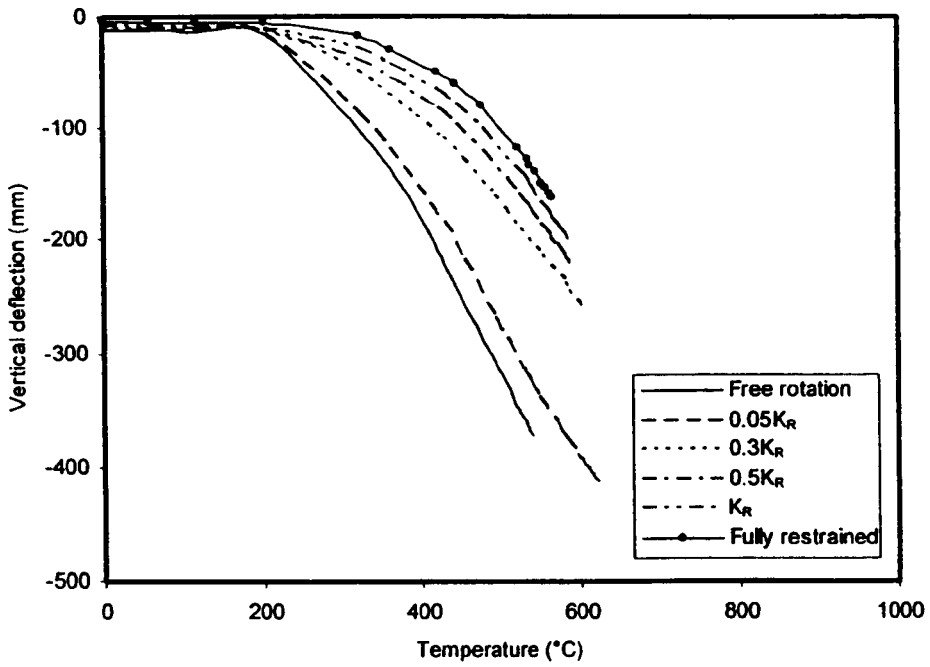
Figure 7.36: *Deflection curves of different levels of rotational restraint for FE simulation*
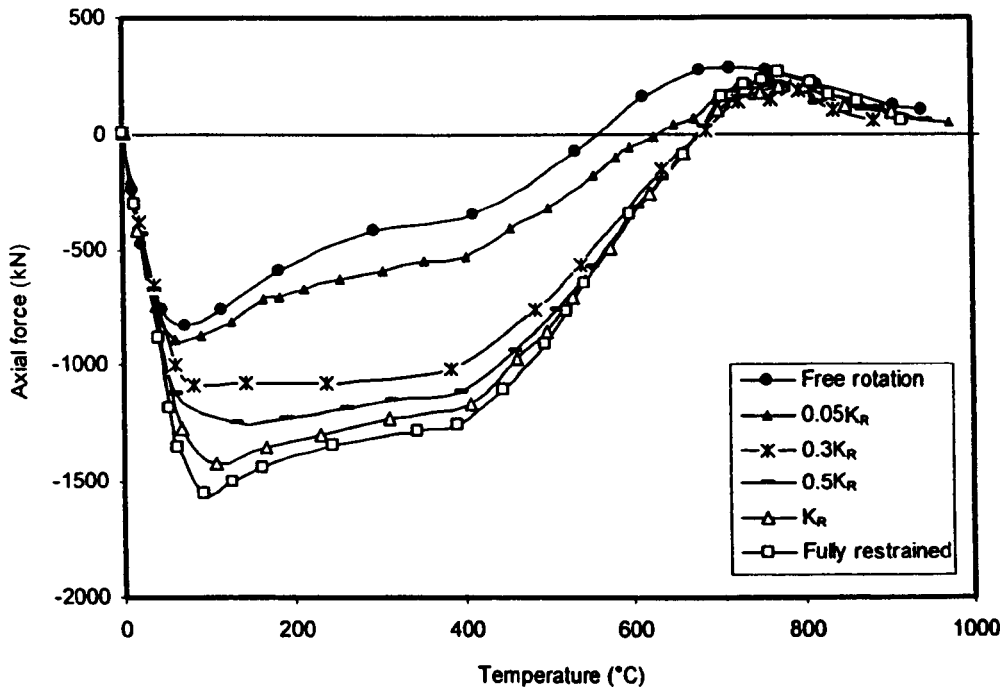
Figure 7.37: *Evolution of axial reaction force of Yin and Wang's model for different levels of rotational restraint*
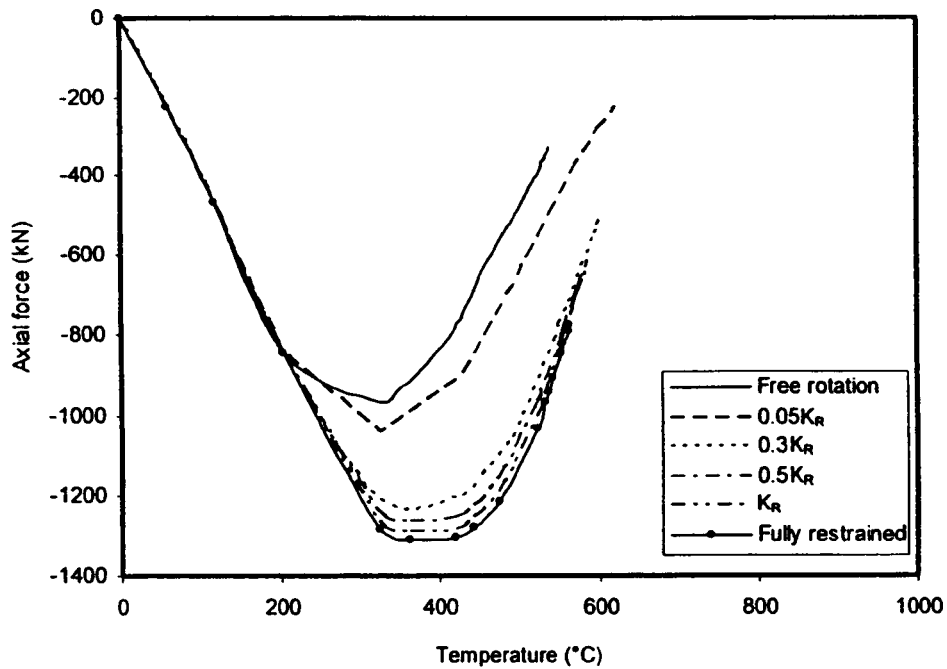
Figure 7.38: *Evolution of axial reaction force of FE simulation for different levels of rotational restraint*

Figures 7.39 and 7.40 compare the temperature-deflection and temperature-axial reaction force relationship of carbon steel and stainless steel beams. At low temperatures, stainless steel exhibits higher deflection than carbon steel due to its higher thermal expansion. However, if the FE simulations are allowed to continue, it can be seen that carbon steel beams deflect more than stainless steel beams at higher temperature, which clearly shows their differences in stiffness retention at elevated temperature. High deflections reduce the effect of restrained thermal expansion and have subsequently caused stainless steel to achieve lower axial compression force than carbon steel. For $0.3K_R$ and K_R rotational restraint stiffness, both carbon steel and stainless steel beams yield similar deflections and axial compressive forces. Once again, the results indicate that the rotational restraint stiffness does not significantly affect the deflection of the beam or the axial compression force exerted to the adjacent part of the structure.
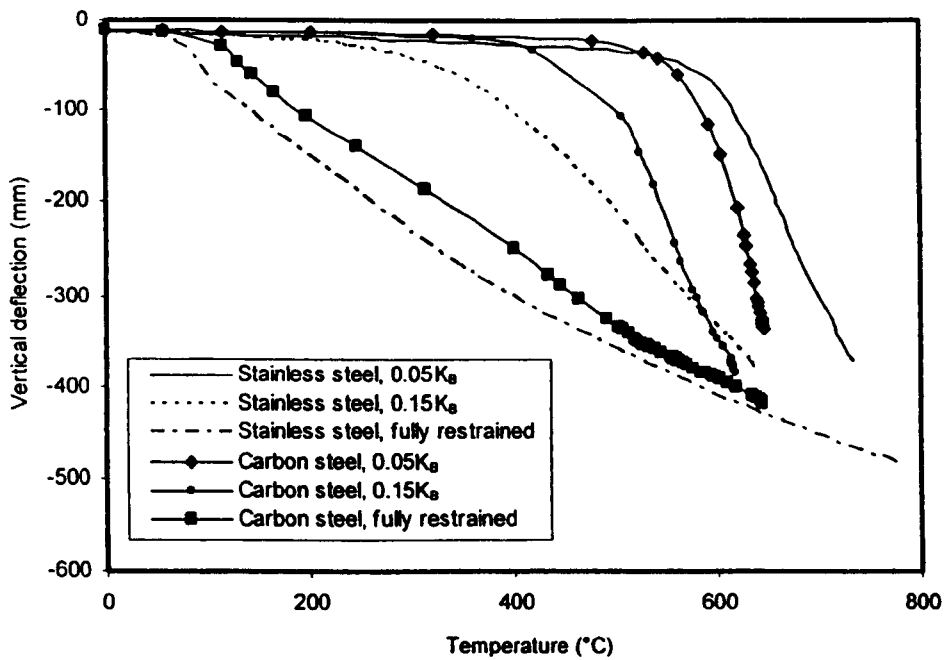
187
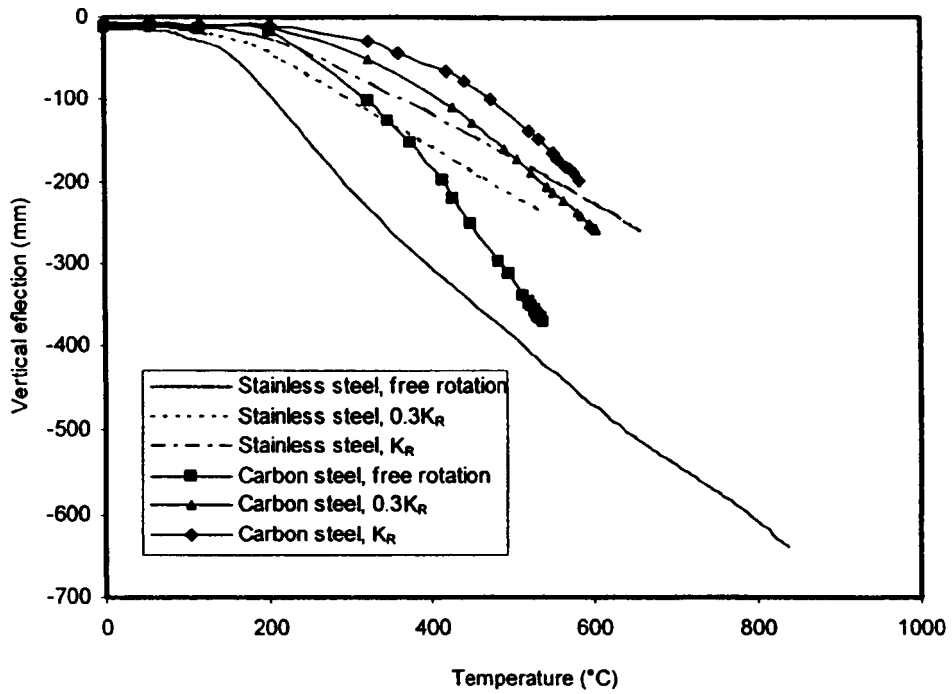
Figure 7.39: *Comparison of temperature-deflection curves for carbon steel and stainless steel beams with different levels of rotational restraint*
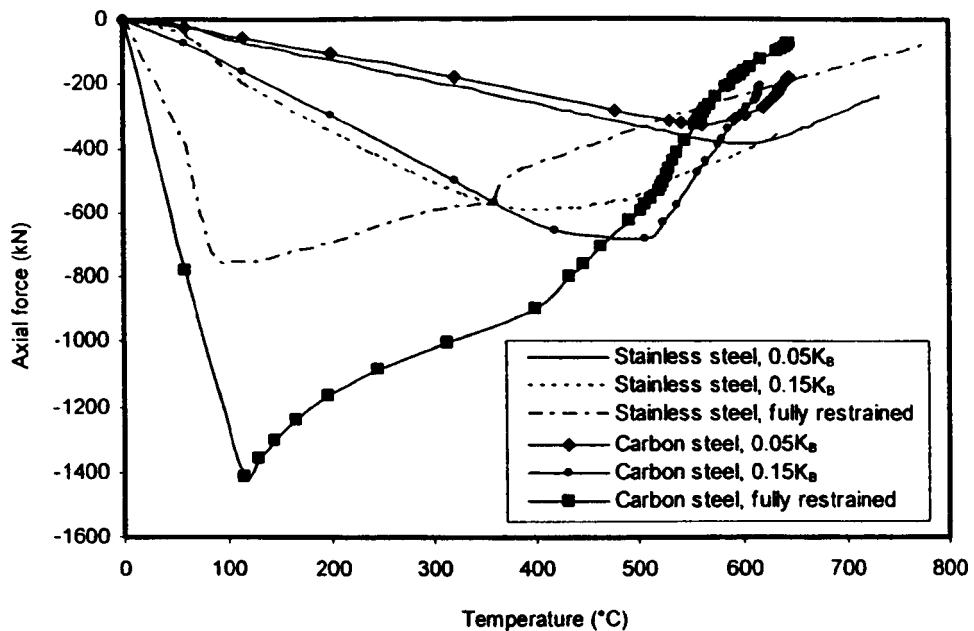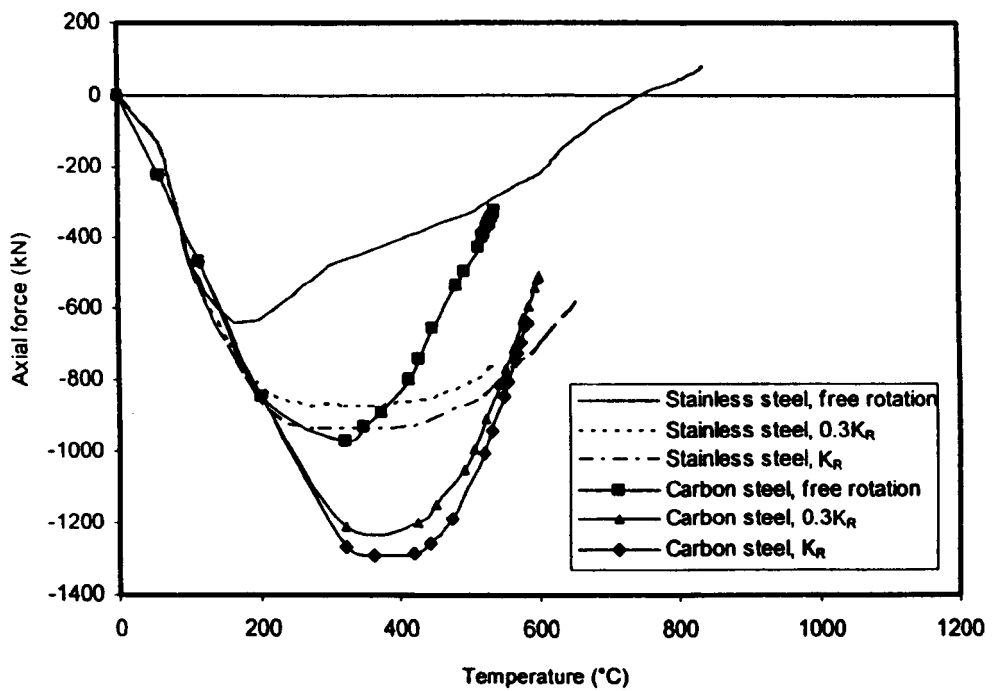

Figure 7.40: *Comparison of temperature-axial reaction curves for carbon steel and stainless steel beams with different levels of rotational restraint*

7.3.5 Concluding Comments

In a real building, steel beams are axially restrained due to the presence of the surrounding structure. The load carrying mechanism of steel beams changes from bending to catenary action at large deflections due to the existence of this axial restraint, which will enable the beam to survive very high temperatures without collapse.

In general, FE results generated herein show good agreement with Yin and Wang's models and Liu et al's test results. The main discrepancy of some FE models with Yin and Wang's simulation is the magnitude of the results due to different restraint. After validating the models with carbon steel material properties, the analyses were extended to include stainless steel material properties in order to compare their beam behaviour with carbon steel at elevated temperature.

Yin and Wang (2004) stated that an axial restraint stiffness of $0.15K_B$ is sufficient to provide similar catenary action to that of a fully axial restrained beam. Figures 7.33 and 7.34 show that a stainless steel beam with an axial restraint stiffness of $0.15K_B$ exerts lower axial compression forces than a carbon steel beam.

The results have shown that the level of rotational restraint has only a minor effect on the large deflection behaviour of restrained beams at elevated temperature. The main factor which affects the beam deflection and the development of catenary forces is the level of axial restraint.

At high temperatures, the higher the axial restraint, the smaller the beam deflection, which is favourable for integrity of the fire compartment in which the restrained beam is located. However it is often unfeasible to provide high axial restraint at connections with the adjacent structure economically. Another drawback for higher axial restraint stiffness is that larger catenary forces will be exerted on the structure adjacent to the beam. Therefore careful consideration and compromise are needed.

CHAPTER 8

CONCLUSIONS AND RECOMMENDATIONS FOR FUTURE WORK

8.1 CONCLUSIONS

Major fires often cause severe structural damage, even in areas remote to the fire area. Fire can, for example, lead to partial or total collapse of an industrial installation or domestic building resulting in loss of lives, as happened in the World Trade Centre Towers collapse in New York in 2001. Careful consideration should therefore be given in the design of the structure and its protection in order to minimize the effects of these events. Hence, an understanding of the behaviour of structures in fire is an important part of structural engineering, with the aim to preserve the load bearing function of the structure and to avoid premature collapse whilst occupants evacuate and fire-fighters operate.

Stainless steel is a relatively new structural material, and although room temperature structural design guidance is now widely available, fire resistant design of stainless steel structures has received less attention. Currently, the only detailed provisions for the design of stainless steel structures in fire are given in EN 1993-1-2 (2005) and the third edition of the Euro-Inox/ SCI Design Manual (2006). Both are based on modifications to the approach for carbon steel,

validated against the limited available fire tests on stainless steel members. The third edition of the Euro-Inox/ SCI Design Manual (2006) includes more recent advances than the Eurocode provisions. The primary objective of this study has therefore been to examine the behaviour of stainless steel structures in fire in detail and to develop a more rational and efficient method for design.

Sophisticated, non-linear finite element modelling has been the principal tool for investigating the behaviour of stainless steel in fire. Models have been developed and carefully validated against existing test results. The developed modelling capabilities now allow the prediction of temperature development in structural sections, the behaviour of isolated stub columns, long columns and beams and the behaviour of restrained columns and beams. All key features associated with structural stainless steel sections have been included, such as the non-linear material behaviour, enhanced strength corners and geometric imperfections. The findings from the numerical models have been used in conjunction with those from the tests to assess existing design guidance and propose advancements.

A broad review of the literature that is relevant to the present research has been presented in Chapter 2. All available laboratory testing programmes, which provided data to validate numerical models and develop design guidance, were introduced. A total of six stub column tests, twenty five pin-ended column tests, four fix-ended column tests and six beam tests on stainless steel in fire have been performed. In addition, temperature development tests on fourteen specimens of different shapes and dimensions were introduced and are examined in detail in Chapter 4. Previous finite element modelling studies of a similar nature to those performed herein were discussed.

The differences of material properties and thermal properties at elevated temperature between carbon steel and stainless steel are described in Chapter 3. Fire design allows use of the 2% strain limit since deformations under fire conditions is less of a concern. This allowance of 2% strain limit at the Fire Limit State is advantageous to stainless steel due to its higher degree of strain hardening. Stainless steel also displays superior behaviour to carbon steel in terms of strength and stiffness retention at elevated temperature. Stainless steel retains 5 times more of its room temperature stiffness than carbon steel at 700°C and up to 2 times more of its room temperature strength than carbon steel above 500°C.

EN 1993-1-2 (2005) provides a single series of strength reduction factor for carbon steel. However, EN 1993-1-2 (2005) and Euro-Inox/ SCI Design Manual (2006) provide a total of eight sets of different strength reduction factors for nine different stainless steel grades, which is not practical for structural engineers. These nine stainless steel grades were firstly divided into 4 groups: duplex, ferritic and 2 groups of austenitic. Revised strength reduction factors for 4 groups, based on all available test data, were then proposed. The proposed curves give good agreement with the current design guidance and the test results.

Accurate and efficient determination of the temperature development within a structural member upon subjection to fire is paramount. In Chapter 4, comparisons of temperature development in structural stainless steel sections were made between existing test results, numerical simulations and the simple calculation model of Eurocode 3: Part 1.2. Based on these comparisons, revised values for the heat transfer coefficient and the emissivitiy of structural stainless steel members exposed to fire were proposed. In the temperature development calculation model of EN 1993-1-2 (2005), it was proposed that emissivity be taken as 0.2 (in place of the currently adopted value of 0.4) and the heat transfer coefficient be taken as 35 w/m²K (in place of the currently adopted value of 25 w/m²K). The significance of such revisions to the fire resistance and critical temperature was assessed. Application of the revised values in the predictive models for member resistances at elevated temperature in Eurocode 3: Part 1.2 also revealed improved agreement with the test results on axially loaded stainless steel columns in fire, and average enhancements in fire resistance of 10%.

Chapter 5 examines existing test results and presents the results of a numerical parametric study, using ABAQUS on stainless steel columns in fire. The developed FE models include accurate material modelling, enhanced strength corner properties, residual stresses and initial geometric imperfections (local and global). Twelve column buckling tests and six stub column tests have been replicated numerically and a series of sensitivity and parameters studies to investigate the influence of the key individual parameters have been performed.

The numerical models were proven to be able to replicate accurately the non-linear response of stainless steel members in fire. The sensitivity to geometric imperfections and residual stresses was relatively low. The mechanical properties of stainless steel are sensitive to the level of cold-work, resulting in the corner regions of cold-formed sections having 0.2% proof strengths significantly higher than the 0.2% proof strengths of the flat regions. Inclusion of these corner strength enhancements increased the critical temperatures by about 5%.

The influence of variation in overall member slenderness and load ratio was investigated. The results indicated that the critical temperature was slenderness dependant (for a given load ratio). This is due to the fact that stocky columns are controlled primarily by material strength and its degradation, whilst slender columns are controlled primarily by material stiffness and its degradation. Class 4 models performed considerably better than predicted by Eurocode 3.

Revised design rules were developed in Chapter 6. The relationship between strength and stiffness is important as this defines susceptibility to buckling. For structural stainless steel design, this concept is included in codes for member buckling, though not for local plate buckling (or cross-section classification). Thus it was proposed that the true variation of stiffness and strength at elevated temperature be utilised in cross-section classification and in the determination of effective section properties for stainless steel structures in fire. The test results from Chapter 5 were compared with design rules from EN 1993-1-2, the Euro-Inox/SCI Design Manual for Structural Stainless Steel (2002) and those proposed by CTICM. Based on the comparisons, a revised buckling curve for stainless steel in fire, consistent strain limits and a new approach to cross-section classification and the treatment of local buckling were proposed. These revisions have led to a more efficient and consistent treatment of buckling of stainless steel columns and beams in fire. Improvements of 6% for column buckling resistance, 28% for stub column (cross-section) resistance and 14% for in-plane bending resistance over the current Eurocode methods were achieved.

All metals expand when heated, but stainless steel expands up to 50% more than carbon steel. In a building, structural members are axially and rotationally restrained during a fire due to the presence of the surrounding structure. Although stainless steel offers better retention of strength and stiffness at elevated temperatures, this greater thermal expansion may be detrimental to fire resistance and therefore restrained columns and beams were examined in Chapter 7.

Many researchers have stated that the critical temperature of steel columns under axial compression with thermal restraint is lower than the critical temperature of the same columns free to elongate in numerical simulations; this is due to the fact that the analyses often terminate prematurely, in which case the temperature that causes buckling of the column will be considered as the failure temperature. It is shown in Chapter 7 that even though the column buckles, it is still able to continue to support more than the load it supported before the fire ($N/N_{initial} > 1$), therefore the structure is still not in danger and can still be heated. At low levels

of axial restraint, stainless steel columns have higher critical temperature than carbon steel columns due to the superior strength and stiffness retention. However, for high levels of axial restraint, the greater thermal expansion that stainless steel exhibits results in greater axial forces and lower critical temperatures.

Fire resistant design of a steel beam based solely on its bending resistance will result in a relatively low survival temperature. Therefore a more efficient design method is needed in order to eliminate fire protection. At large deflections, the load carrying mechanism of steel beams changes from bending to catenary action where axial restraint exists, which will enable a beam to survive very higher temperatures without collapse. Numerical results show that a stainless steel beam with an axial restraint stiffness of $0.15K_B$ exerts lower axial compression forces than a carbon steel beam. The level of rotational restraint has only minor effect on the large deflection behaviour of restrained beams at elevated temperature. The main factor which affects beam deflection and the development of catenary forces is the level of axial restraint.

The primary objective of evaluating and improving the current design guidance for stainless steel structures in fire was achieved. The proposed modifications include revised values for emissivity and the heat transfer coefficient for stainless steel, rationalised material strength reduction curves, a revised buckling curve for stainless steel in fire, consistent strain limits and a new approach to cross-section classification and the treatment of local buckling. Resulting guidance is now more consistent and rational than current stainless steel design methods in fire. It is recommended that these be considered for incorporation into future revisions of Eurocode 3, bringing greater efficiency to structural stainless steel design in fire. In addition to the superior strength and stiffness retention of stainless steel, this study has demonstrated the importance of also considering its higher thermal expansion. It has been shown that both low levels of axial restraint and low load ratios enable the most effective exploitation of the superior high temperature strength and stiffness retention of stainless steel.

8.2 RECOMMENDATIONS FOR FUTURE WORK

8.2.1 Further studies of the structural behaviour of stainless steel frames

In this thesis, significant modelling capabilities have been developed enabling the accurate prediction of the temperature development and non-linear structural response of stainless steel

structural elements in fire. These two capabilities have also been used in combination in Chapter 5, and hence it is possible to examine the structural response of stainless steel elements under any imposed temperature-time regime. The models may therefore be employed to assess the structural stainless performance in natural fire conditions. Previous tests and modelling of stainless steel in fire have also been limited to isolated members. However, in this study, the behaviour of restrained members has also been investigated by the application of appropriate boundary conditions to individual members. Insight into the importance of restrained thermal expansion has therefore been achieved, but a more detailed investigation would require full frame analysis. This is a possible area for future research.

8.2.2 Structural performance data

Laboratory testing schemes of stainless steel in fire are relatively limited. The proposed modifications to design guidance are mainly based on stainless steel hollow sections and limited I-sections. Therefore more testing for stainless steel in fire with different types of structural cross-sections is desirable. However, this thesis has also demonstrated the ability of numerical models to accurately reflect the large deflection non-linear behaviour of stainless steel components in fire, so this may clearly be used as a supplementary tool.

8.2.3 Hybrid systems and concrete filled stainless steel tubes in fire

The importance of using stainless steel efficiently is clear. Two approaches to achieve this, whilst still utilising the strength and stiffness retention of stainless steel in fire are hybrid systems (employing a combination of carbon steel and stainless steel) and concrete filled tubes, utilising corrosion resistance with minimum material use. The numerical capabilities developed herein enable such investigations into the performance of such systems to be carried out. The room temperature behaviour of concrete filled tubes have already been examined (Young and Ellobody, 2006; Ellobody and Young, 2006), but the additional benefits of the concrete including reducing the rate of temperature development in the stainless steel have not been investigated.

8.2.4 Other ideas

The use of stainless steels in structural and architectural applications is increasing due to its attractive appearance, corrosion resistance, ease of maintenance, low life cycle costs and good fire resistance. However the material cost of stainless steel is about 4 times of carbon steel, and the important arguments for selecting stainless steel as a constructional material need to be emphasised. Efficient design guidance will bring material cost savings, and a more detailed study to demonstrate the level of whole-life cost savings typically attainable for stainless steel structures could be conducted.

REFERENCES

ABAQUS (2003). ABAQUS/ Standard User's Manual Volumes I-III and ABAQUS CAE Manual. Version 6.4. Hibbitt, Karlsson and Sorensen, Inc. Pawtucket, USA.

AISI (1979). High-Temperature Characteristics of Stainless Steels, Handbook Series No. 9004, American Iron and Steel Institute/ Nickel Institute.

Ala-Outinen, T. (1996). Fire resistance of austenitic stainless steels Polarit 725 (EN 1.4301) and Polarit 761 (EN 1.4571). VTT Research Notes 1760, Espoo, Finland.

Ala-Outinen, T. (1999). Fire resistance of stainless steel structures. Proceedings of the Second European Conference on Steel Structures (Eurosteel 1999). Prague, Czech Republic, 26th-29th May, 1999. pp. 165-168.

Ala-Outinen, T. (2000). Fire Resistance of Stainless Steel Structures, VTT Building Technology, Finland.

Ala-Outinen, T. (2005). Members with Class 4 cross-sections in fire: Work package 3. ECSC project 'Stainless steel in fire (SSIF)'. Contract No. RFS-CR-04048. VTT. (Confidential).

Ala-Outinen, T. And Myllymaki, J. (1995). The local buckling of RHS members at elevated temperatures, VTT Research Notes 1672, Espoo, Finland.

Ala-Outinen, T. and Oksanen, T. (1997). Stainless steel compression members exposed to fire, VTT Research Notes 1864, Espoo, Finland.

Ala-Outinen, T., Viherma, R. and Nilimaa, H., (2004). Structural Design of Cold Worked Austenitic Stainless Steel. Work package 6: Elevated Temperature Properties. ECSC project 'Structural design of cold-worked austenitic stainless steel'. Contract No. 7210-PR-318. The Steel Construction Institute, UK.

Ali, F. and O'Connor, D. (2001). Structural performance of rotationally restrained steel columns in fire. Fire Safety Journal 36, pp. 679-691.

ASCE (2002). Specification of the Design of Cold-Formed Stainless Steel Structural Members, (SEI/ASCE 8-02) (Standards No. 02-008). American Society of Civil Engineers. New York.

Ashraf, M., Gardner, L. and Nethercot, D. A. (2005). Strength enhancement of the corner regions of stainless steel cross-sections. Journal of Constructional Steel Research. 61(1), pp. 37-52.

Ashraf, M., Gardner, L. and Nethercot, D.A. (2005). Numerical modelling of stainless steel open sections. Proceedings of the Fourth European Conference on Steel and Composite Structures – Eurosteel. 8th-10th June 2005. Maastricht, The Netherlands. 1.2, pp. 197-204.

Aust/NZS. (2001). Cold-formed stainless steel structures. Australian/ New Zealand Standard AS/NZS 4673:2001. Sydney, Australia: Standards Australia.

Baddoo, N. R. and Burgan, B. A. (1998). Fire resistant design of austenitic structural stainless steel, Journal of Constructional Steel Research, Vol. 46, No. 1-3, Paper No. 243.

Baddoo, N. R. and Gardner, L. (2000). WP5.2: Member behaviour at elevated temperatures. ECSC project - Development of the use of stainless steel in construction. Contract No. 7210 SA/842. The Steel Construction Institute, UK.

Baddoo, N. R. (2003). A comparison of structural stainless steel design standards, The Steel Construction Institute, Proceedings of the Stainless Steel Structures International Experts' Seminar. Ascot, UK. pp. 131-150.

Bailey, C. G. (2004). Membrane action of slab/beam composite floor systems in fire. Engineering Structures. 26(12), pp. 1691–1703.

Bailey, C. G. (2000). The influence of the thermal expansion of beams on the structural behaviour of columns in steel-framed structures during a fire. Engineering Structures 22, pp. 755-768.

Bailey, C. (2004). Structural fire design: Core or specialist subject?. The Structural Engineer 82 (9), pp. 32-38.

BS 5950-1 (2000). Structural use of steelwork in buildings – Part 8: Code of practice for fire resistant design. British Standards Institution.

Buchanan, A. H. (2001). Structural design for fire safety. John Wiley and Sons Ltd.

Cabrita Neves, I., Valente, J. C., Correia Rodrigues, and J. P. (2002). Thermal restraint and fire resistance of columns. Fire Safety Journal 37, pp. 753-771.

Chen, J. and Young, B., (2006). Stress-strain curves for stainless steel at elevated temperatures. Engineering structures 28, pp. 229-239.

Correia Rodrigues, J.P., Cabrita Neves, I., and Valente, J.C. (2000). Experimental research on the critical temperature of compressed steel elements with restrained thermal elongation. Fire Safety Journal 35, pp. 77-98.

Corus (2003). Structural sections, Corus construction and industry.

CTICM (2005). Stainless steel column buckling behaviour at elevated temperatures – Comparison of Euro-Inox and CTICM methods. Centro Sviluppo Materiali S.p.A.

Dawson, R. G. and Walker, A. C. (1972). Post-buckling of geometrically imperfect plates. Journal of the Structural Division, ASCE. 98(ST1), pp. 75-94.

Drysdale, D. (1985). An introduction to fire dynamics. Second edition. John Wiley and Sons Ltd.

Ellobody, E. and Young, B. (2005). Structural performance of cold-formed high strength stainless steel columns. Journal of Constructional Steel Research. 61(12), pp. 1631-1649.

Ellobody, E. and Young, B. (2006). Design and behaviour of concrete-filled cold-formed stainless steel tube columns. Engineering Structures. 28(5), pp. 716-728.

EN 1993-1-2. (2005). Eurocode 3: Design of steel structures - Part 1.2: General rules - Structural fire design. CEN.

EN 10088-2. (2005). Stainless steels – Part 2: Technical delivery conditions for sheet/plate and strip for general purposes. CEN.

ENV 1993-1-2. (2001). Eurocode 3: Design of steel structures – Part 1.2: General rules - Structural fire design. CEN.

EN 1991-1-2. (2002). Eurocode 1: Actions on structures – Part 1.2: General actions – Actions on structures exposed to fire. CEN.

EN 1993-1-2. (2005). Eurocode 3: Design of steel structures – Part 1.2: General rules - Structural fire design. CEN.

ENV 1993-1-4. (1996). Eurocode 3: Design of steel structures – Part 1.4: General rules - Supplementary rules for stainless steel. CEN.

Euro-Inox/ SCI (2002). Design Manual for Structural Stainless Steel. Second edition. Euro Inox and the Steel Construction Institute. Building series, Volume 3.

Euro-Inox/ SCI (2006). Design Manual for Structural Stainless Steel. Third edition. Euro-Inox and the Steel Construction Institute. Building series, Volume 11.

Feng, M., Wang, Y. C. and Davies J. M. (2002). Thermal performance of cold-formed thin-walled steel panel systems in fire. Fire Safety Journal 38, pp. 365-394.

Feng, M., Wang, Y. C. and Davies J. M. (2003). Structural Behaviour of cold-formed thin-walled short steel channel columns at elevated temperatures. Part 2: Design calculations and numerical analysis. Thin-walled Structures 41, pp. 571-594.

Feng, M., Wang, Y. C. and Davies J. M. (2003). Axial strength of cold-formed thin-walled steel channels under non-uniform temperatures in fire. Fire Safety Journal 38, pp. 679-707.

Franssen, J. M. (2000). Failure temperature of a system comprising a restrained column submitted to fire. Fire Safety Journal 34, pp. 191-207.

Gardner, L. (2002). A New Approach to Structural Stainless Steel Design, PhD thesis, Imperial College of Science, Technology and Medicine.

Gardner, L. (2005). The use of stainless steel in structures. Progress in Structural Engineering and Materials. 7(2), pp. 45-55.

Gardner, L. and Ashraf, M. (2006). Structural design for non-linear metallic materials. Engineering Structures. 28(6), pp. 926-934.

Gardner, L. and Baddoo, N. R. (2006). Fire testing and design of stainless steel structures. Journal of Constructional Steel Research. 62(6), pp. 532-543.

Gardner, L. and Nethercot, D. A. (2004). Numerical modelling of stainless steel structural components – A consistent approach. Journal of Structural Engineering, ASCE. 130(10), pp. 1586-1601.

Gardner, L. and Ng, K. T. (2006). Temperature development in structural stainless steel sections exposed to fire. Fire Safety Journal. 41(3), pp. 185-203.

Hoke, J. H. (1977). 'Mechanical Properties of Stainless Steels at Elevated Temperatures'. In chapter 21 of Handbook of Stainless Steels, McGraw-Hill, pp. 1-20.

ISO-834-1. (1999). Fire-resistance tests - Elements of building construction - part 1: General requirements. International Organization for Standardization, Geneva.

Kay, T. R., Kirby, B. R., and Preston, R. R. (1996). Calculation of the heating rate of an unprotected steel member in a standard fire resistance test. Fire Safety Journal, 26(4), pp. 327-350.

Kirby, B. (2004). Calibration of Eurocode 1: actions on structures – Part 1.2: actions on structures exposed to fire. The Structural Engineer. 82(19), pp. 38-43.

Kruppa, J., Newman, G., Schleich, J-B. and Twilt, L. (1999). ECCS model code on fire engineering. Final Draft.

Lamont, S., Usmani, A.S. and Drysdale, D.D. (2001). Heat transfer analysis of the composite slab in the Cardington frame fire tests. Fire safety journal. 36(8), pp. 815-839.

Lennon, T. and Moore, D. (2003). The natural fire safety concept - full-scale tests at Cardington. Fire Safety Journal. 38(7), pp. 623–643.

Liu, T. C. H., Fahad, M. K. and Davies, J. M. (2002). Experimental investigation of behaviour of axially restrained steel beams in fire, Journal of Constructional Steel Research, 58 (9), pp. 1211-1230

Ng, K. T. and Gardner, L. (2006). Stainless Steel Compression Members in Fire. Proceedings of Stability and Ductility of Steel Structures. 6th-10th September 2006. Lisbon, Portugal. Pp. 789-802.

Ng, K. T. and Gardner, L. (in press). Buckling of stainless steel columns and beams in fire. Engineering Structures.

Parker, A.J., Beitel, J.J., and Iwankiw, N.R. (2005). Fire Protection Materials for Architecturally Exposed Structural Steel (AESS). Structure Magazine, National Council of Structural Engineers Association. February 2005, pp. 33-36.

prEN 1993-1-2. (2003). Eurocode 3: Design of steel structures - Part 1.2: General rules - Structural fire design. CEN.

prEN 1993-1-4. (2004). Eurocode 3: Design of steel structures – Part 1.4: General rules – Supplementary rules for stainless steels. CEN.

Rasmussen, K. J. R. and Hancock, G. J. (1993). Design of cold-formed stainless steel tubular members. I: Columns. Journal of Structural Engineering, ASCE. 119(8), pp. 2349-2367.

Rohrig, I. A. (1973). 'A Nitrogen Grade of Types 304 and 316 Austenitic Stainless Steels; Specification and Code Considerations.' Elevated Temperature Properties as Influenced by Nitrogen Additions to Type 304 and 316 Austenitic Stainless Steel, ASTM STP 522, The American Society for Testing and Materials, pp. 79-85.

SABS, South African Bureau of Standards, (1997). Structural use of steel – Part 4: The design of cold-formed stainless steel structural members. SABS 0162-4. (not seen)

Sakumoto, Y., Nakazato, T. and Matsuzaki, A. (1996). High-temerature properties of stainless steel for building structures, Journal of Structural Engineering, ASCE. Vol 122, No. 4, pp. 399-406.

SEI/ASCE 8-02, (2002). Specification for the Design of Cold-Formed Stainless Steel Structural Members, Standards No. 02-008, American Society of Civil Engineers.

Smith, G. (1969). An evaluation of the Yield, Tensile, and Rupture Strengths of Wrought 304, 316, 321 and 347 Stainless Steels at Elevated Temperatures, ASTM Data Series DS 5S2, American Society for Testing and Materials, Philadelphia, Pa.

SSBJA (1995). The design and construction specifications for stainless steel structures. Stainless Steel Building Association of Japan. (In Japanese, not seen)

Thomson, G. and Preston R. R. (1996). Towards harmonised standard fire resistance testing. Fire Safety Journal, 27(2), pp. 91-112.

Valente, J. C. and Cabrita Neves, I. (1999). Fire resistance of steel columns with elastically restrained axial elongation and bending. Journal of Constructional Steel Research 52, pp. 319-331.

Wang, H. B. (1995). Heat Transfer Analysis of Components of Construction Exposed to Fire. PhD Thesis. Department of Civil Engineering and Construction, University of Salford, Manchester.

Wang, Y. C. (1997). Effects of structural continuity on fire resistant design of steel columns in non-sway multi-storey frames. Fire Safety Journal. 28(2), pp. 101-116

Wang, Y. C. (1998). Composite beams with partial fire protection. Fire Safety Journal. 30(4), pp. 315-332.

Wang, Y. C. (2000). An analysis of the global structural behaviour of the Cardington steel-framed building during the two BRE fire tests. Engineering Structures. 22(5), pp. 401-412.

Wang, Y. C. (2002). Steel and composite structures – Behaviour and design for fire safety. Spon Press.

Wang, Y. C. and Davies, J. M. (2003). Fire tests of non-sway loaded and rotationally restrained steel column assemblies. Journal of Constructional Steel Research 59, pp. 359-383.

Wang, Y. C. and Moore, D. B. (1994). Effect of thermal restraint on column behaviour in a frame. Proceedings of the Fourth International Symposium on Fire Safety Science (IAFSS), Ottawa, Canada. pp. 1055-1066.

Wang, Y. C. and Moore, D. B. (1995). Steel frames in fire: analysis. Engineering Structures 17, No 6, pp. 462-472.

Wang, Y. C. and Yin, Y. Z. (2005). Feasibility of utilising catenary action to eliminate fire protection to steel beams. Proceedings of the Fourth International Conference on Advances in Steel Structures, 13th-15th June 2005, Shanghai, China. Vol. II, pp. 959-964.

Wang, Y. C., Lennon, T. and Moore, D. B. (1994). The behaviour of steel frames subject to fire. Journal of Constructional Steel Research 35, pp. 291-322.

Wong, M. B. (2005). Modelling of axial restraints for limiting temperature calculation of steel members in fire. Journal of Constructional Steel Research 61, pp. 675-687.

Wong, M. B., Ghojel, J. I., and Crozier, D. A. (1998). Temperature-time analysis for steel structures under fire conditions. International Journal of Structural Engineering and Mechanics, 6(3), pp. 275-289.

Yin, Y.Z. and Wang, Y. C. (2004), A numerical study of large deflection behaviour of restrained steel beams at elevated temperatures. Journal of Constructional Steel Research 60 (7), pp. 1029-1047.

Yin, Y.Z. and Wang, Y. C. (2003). Numerical simulations of the effects of non-uniform temperature distributions on lateral torsional buckling resistance of steel I-beams. Journal of Constructional Steel Research 59, pp. 1009-1033.

Young, B. and Ellobody, E. (2006). Experimental investigations of concrete-filled cold-formed high strength stainless steel tube columns. Journal of Constructional Steel Research 62 (5), pp. 484-492.

Zhao, B. (2000). WP5.1: Member behaviour at elevated temperatures. ECSC project - Development of the use of stainless steel in construction. Contract No. 7210 SA/842. The Steel Construction Instititue, UK.

Zhao, B. and Blanguernon, A. (2004). Member Tests in Fire and Structural Fire Design Guidance. Work package 6: Elevated Temperature Properties. ECSC project 'Structural design of cold-worked austenitic stainless steel'. Contract No. 7210-PR-318. The Steel Construction Institute, UK.